Chemical investigation of leaching and electrochemical behaviour of sensor-based pre-concentrated copper ores with alkaline lixiviant.

Submitted by:

Amos Idzi Ambo

To the University of Exeter as a thesis for the degree of
Doctor of Philosophy in Mining and Minerals Engineering.

I certify that all material in this thesis which is not my own work has been identified and that no material has previously been submitted and approved for the award of a degree by this or any other University.

Signature ……

This thesis is dedicated to GOD in heaven the giver of knowledge to whom alone nothing shall be impossible Luke 1:37 and to the memory of my late father Mr Usman Audu who passed away when I was one month old.

Abstract

While the production of copper metal from primary ores is still increasing, the gradual depletion of high-grade ores implies that the recovery of the metal from low-grade ores is presenting a challenge. A major problem associated with processing of low-grade copper ores can be their high calcite content and concentration of other metals such as Fe, Mn, Co, As, Pb, and Ni. These other metals make the processing of such ores expensive due to the high cost of the leaching chemicals. Therefore, in this study a novel, integrated copper processing method is developed to enhance the economic extraction of copper from such ores.

This research investigated the chemical leaching behaviour of porphyry copper ore samples from Chile, South America. Ores were pre-concentrated and classified with near infrared sensing into product, middling and waste fractions. Mineralogical analysis of the ore was conducted using QEMSCAN®, XRD and NIR. The elemental investigation of the ore was carried out using PXRF, ICP-MS and SEM. Analyses revealed that the major copper-bearing mineral is chrysocolla and that the ore is composed mainly of silicate, oxide and carbonate gangue. Calcite in the ore is considered problematic due to acid consumption. In terms of abundance of gangue in the classified ore the order is waste > middling and product. A systematic comparison of the complexometric behaviour of the ore was investigated with Na_2EDTA reagent while the leaching behaviour of the classified ore was investigated in NH_4Cl and $H_2C_2O_4$ lixiviants. The influence of process variables such as lixiviant concentrations, particle sizes, solid-to-liquid ratio, temperature, time and stirring speed on the behaviour of the classified ore were investigated.

The rate of Cu dissolution and formation of Cu-EDTA complex in Na_2EDTA was higher in the product than the middling while that of the waste was found to be insignificant at 0.01 M, even when the concentration of the complexing agent was increased from 0.01 M to 0.05 M. The rate of Cu-EDTA complex formation was found to increase with decreasing particle sizes and solid-to-liquid ratio across the ore categories. Ammonium chloride leaching of the product and middling revealed contrasting behaviour. The rate of Cu extraction was found to increase significantly from 21.5 % to 75.0 % and 27.3 % to 89.0 % when the temperature was increased from 40 ˚C to 90 ˚C, respectively. On increasing the concentration of NH_4Cl from 0.5 M to 5 M, the extraction of Cu was found to increase from 20.0 % to 65.0 % and 26.5% to 83.3 %, respectively. It was found that the leaching yield of Cu increased substantially when the particle size was decreased from –125+90 μm to –90+63 μm and –63+45 μm and with decreasing solid-to-liquid ratio (middling and product), respectively. A steady decrease in Cu extraction was obtained when the stirring speed was increased from 300 rpm to 800 rpm. Similarly, the effectiveness of the leaching process was investigated over an extended time period from 2 h to 4 h with an NH_4Cl concentration range of 0.55 M to 1.65 M, a temperature of 70 ˚C to 90 ˚C, and at a constant stirring speed of 300 rpm, particle size fraction of -64+45 μm and a

solid to liquid volume of 6 g/ 250 mL. It was found that Cu extraction was enhanced by about 90 % during the experiment. The estimated activation energy of the leaching process was characterized using the shrinking core model under the experimental conditions. It was found to range between 45 and 71 KJ/mol in the first and second batch experiments, which is indicative of a chemically controlled leach process. XRD and ICP-MS characterization of mineralogical and chemical composition of residues suggested that the NH_4Cl lixiviant leaching is selective for Cu. Examination of leachate with ICP-MS for co-extraction of Mn, Co, Ni and Zn indicated insignificant solubilisation of the metals during leaching. Comparison of Cu extraction in NH_4Cl and $H_2C_2O_4$ under the same experimental conditions revealed that NH_4Cl is a better extractant than $H_2C_2O_4$.

Furthermore, the electrodeposition of Cu metal was studied with ore leachate containing $Cu(NH_3)_4^{2+}$ complexes and with $Cu(NH_3)_4SO_4$ synthetic electrolyte. Cyclic voltammetric measurements were conducted across a range of cathodic potentials from 0.8 V to – 1.0 V for selected scan rates of 20, 30, 50, 100 and 200 mV/s. Chemical reduction and electrodeposition of Cu from the complexes was found to proceed via two reversible electrochemical processes, each involving the transfer of a single electron. $Cu(NH_3)_4^{2+}$ complexes are first reduced to $Cu(NH_3)_2^{+}$, which is in turn reduced to metallic Cu. The result is compared with the behaviour of synthetic $Cu(NH_3)_4SO_4$ electrolyte. It was observed that the reduction of $Cu(NH_3)_4SO_4$ to metallic Cu proceeds as two sequential, single electron transfer processes. The $Cu/Cu(NH_3)_4^{2+}$ redox reaction was observed to be fast compared to Cu/Cu^{2+} redox reaction in the $Cu(NH_3)_4SO_4$ solution. Investigation of the electrochemical kinetics shows that the cathodic peak current varied linearly with the square root of the scan rate, which is indicative of the $Cu(NH_3)_2^{+}$ and $Cu(NH_3)_4SO_4$ reduction to Cu proceeding through a diffusion-controlled process.

Assessment of the effect of calcite for leaching of copper from classified ore fractions indicated the potential of NH_4Cl lixiviant for the leaching application. Three processing routes to handle the ore fractions on the basis of variation in calcite, gangue and copper content are proposed.

Acknowledgement

I would like to sincerely and gratefully acknowledge my supervisors: Professor Hylke J. Glass who I have great respect for his invaluable support, mentoring and prompt response I received whenever I come knocking throughout the period of this doctoral research. I would like to also thank my co-supervisor Dr Richard Pascoe for his suggestions and contributions. I am indebted to the lab manager Dr Gavyn Rollinson for co-supervising this work and for his invaluable contributions and encouragement. I would like to thank Sharon Uren in the wet chemistry lab where I spent most of my time as a 'lab rat' for her unwavering support. Dr Chuang Peng I thank you for your support also. To other several CSM lab staff thanks for your kind assistance. My most sincere thanks go to Nasarawa State University, Keffi, Nigeria and Nigeria Tertiary Education Trust Fund (tetfund) for given me the opportunity to further my career through this research. Thanks to Anglo American for providing the samples for this study.

I must sincerely thank the following people: Professor L. Lajide who is not only a father figure to me but a role model and a mentor for making me realise this dream. You told me I can do it, I am happy you stood by me and it's done! Alh. Dalhatu O. Mamman the Registrar Nasarawa State University, Keffi who I often call my father for his effort in ensuring that I secured a vital document and did not miss the opportunity of doing the PhD. Big thanks to Dr Iyi Uwadiae Head of WAEC in Nigeria, 2012 for his kind assistance in ensuring that I obtain my corrected certificate at a very short notice which was a requirement for the University. Dr Saratu S. Audu and family, a million thanks for playing a motherly role in my life. I thank my following colleagues and friends in the CSM PhD room some who have since finished their PhD's. Dr Kelvin F.E. Anderson, Dr Iyakwari Shekwoyandu, Dr Przemyslaw B. Kowalczuk, Anthony Granville and family, Safaa Al-Ali, Muhammed Sajid, Igor Vasconcelos Santana and Luke Palmer. I've really enjoyed your company and support. I would like to convey my sincere thanks to David and Yete, Pastor Rogers Watt of Harbour church, Falmouth for their relentless prayers and support.

To my following friends: Victor Danladi Sule, Luka Ogu, Chaku Shammah Emmanuel, Grace Victor Auta and Monday Timothy. Thanks for your sacrifices. Lemun Yatu Nuhu and Christy Abubakar, I thank you for offering me a place to stay during holidays even at short notice. May God bless you all!

Finally, my deepest love and heartfelt gratitude go to my mother Elizabeth, J. Angyu for providing all the necessary support in ensuring that I pursue my education after the death of my father. You're one in a million I am eternally grateful for all the sacrifices you made. I wish to also thank my step father Mr. Joseph Angyu and my grandfather retired Very Rev. Ambo Idzi for always being there despite the challenges I face. To my siblings: Naomi, Victoria, Anupa, Nada, Hwiji, Tsatu and Achun thanks to all of you. I love you all.

Table of contents

List of Appendices

List of Figures

List of Tables

List of abbreviations

A - Frequency factor in Arrhenius Equation

$\boldsymbol{b}$ - Stoichiometric coefficient

β - Stoichiometric coefficient of the reagent in the leaching reaction

BSE – Back scattered electron

C_A – Concentration of lixiviant

CV – Cyclic voltammetry

CVs – Cyclic voltammetry scan

D - Diffusion coefficient in the porous product layer

Ea - Activation energy (J/ mol)

EDS – Energy dispersive spectrometry

EDTA – Ethylenediaminetetraacetic acid

Na_2EDTA – Ethylenediaminetetraacetic acid disodium

$f1$, $f2$ - Average particle radius

ICP-MS - Inductively Coupled Plasma Mass Spectrometry

k and Kc – Rate constant and Liquid-solid mass transfer coefficient (m/s)

Kd - Apparent rate constant for product layer diffusion (s^{-1})

Kr - Apparent rate constant for surface chemical reaction

Ks - Intrinsic reaction rate constant

ln – Natural logarithm

M_S - Molecular weight of the solid copper ore

NIR – Near InfraRed spectroscopy

PS - Particle size and

ρ_s - Density of classified solid copper ore

PXRF - Portable X- Ray Fluorescence Spectrometer

R - Universal gas constant (8.3145 J/(mol.k))

r_0 , r – Initial and final ore particle radius (m)

SEM – Scanning Electron Microscope

SX-EW - Solvent Extraction- Electrowinning

SL - Solid-to-liquid ratio

SS - Stirring speed

t - Time (h or s)

T - Temperature (K)

α - Copper fraction extracted

XRD – X – ray Diffraction

Chapter 1

Introduction

The global increase in population and the expansion of infrastructure in many countries have continued the need for extraction of natural resources. Copper is a strategic metal of importance in the areas of economic, technological and social applications (Gordon et al., 2006; Dorin et al., 2014). The high demand for copper in recent times for economic and social advancement has triggered a surge in supply. However, the mining, processing and transformation of the ore into a multitude of products sometimes require complex processing. Therefore, there is the need for a concerted effort to maintain the processing and supply of the metal through the development and expansion of processing technology (Awe, 2013). Furthermore, integration with recycling of the products requires innovative approaches (Osman et al., 2013).

Copper occurs naturally in a variety of forms in the Earth's crust due to its ability to combine with nearly every element to form minerals such as sulphides, oxides, carbonates, silicates, phosphates, and chlorides. Only a few are economically viable for exploitation. The major sulphide ore deposits typically contain chalcopyrite ($CuFeS_2$), chalcocite (Cu_2S), covellite (CuS), and bornite (Cu_5FeS4). In carbonate deposits, copper is found as azurite ($Cu_3(CO_3)_2(OH)_2$) and malachite ($Cu_2(CO_3)(OH)_2$) and in silicate deposits as chrysocolla ($(Cu,Al)_2H_2Si_2O_5(OH)_4.nH2O$) and dioptase ($CuSiO_2(OH)_2$). Copper can also occur in its native form (Baba et al., 2013 and Awe, 2013).

Nowadays, processing of low-grade ores from many mineralisations hitherto considered uneconomical is now been considered in a bid to boost the supply of the metal. The major problem associated with processing most low-grade copper ores is their high gangue contents, which makes the processing of such deposits costly in view of their complex nature and significant concentrations of other metals such Fe, Co, Mn, Pb, Zn, and Ni. The only way to overcome the high cost of processing is to develop methods capable of reducing the gangue content and concentration of other metals in ores before or during leaching (Meech and Paterson, 1980). The focus is on the development of techniques that are capable of minimising the amount of undesirable materials going to the downstream processing. This can only be achieved through innovative technologies (Wills and Napier-Munn, 2006). It is believed that this will help in increasing the processing capacity of the ores for valuable metal. The overall intention is to maintain copper supply at minimal cost of processing chemicals and energy (Liu et al., 2010; Biswas and Davenport, 2013).

The process of extracting copper metal from ore can be carried out by either smelting with refining, or by leaching, solvent extraction and electrowinning (Antonijević et al., 2008; King et al., 2011). The extraction process from sulphide ores is carried out to a large extent by pyrometallurgical processing techniques while the processing of oxide

ores is enhanced by the hydrometallurgical technique (Baba et al., 2013; Biswas and Davenport, 2013). The decision whether to use pyrometallurgy or hydrometallurgy is determined by balancing various social, environmental and economy considerations. The economic aspect of extraction is dependent on copper content, the ore type, and the processing cost. The environmental aspect is focussed on the emission of certain gases into the environment and waste management practices. For example, the disposal of waste chemicals, like spent sulphuric acid from leaching plants, usually results in additional costs of processing (Stuurman et al., 2014).

For hydrometallurgical treatment, the cost of leaching chemicals is always the major factor for consideration, especially during the processing of high gangue ore minerals (Dixon, 2004; Peacey et al., 2004). Low-grade copper ores with high calcite gangue requires expensive processing to obtain high purity copper because of additional cost of chemicals required for leaching due to acid consumption by calcite (Liu et al., 2010). For instance, the cost of energy used for crushing and grinding is about 25% of the total cost of processing while the reagent cost is typically around 10% (Wills and Napier-Munn, 2006). As such, it is important to consider other factors such as crushing and electrowinning alongside the cost of leaching chemicals. Since the processing involves several stages, minimisation of the cost at every stage of the copper processing chain is sought (Wills, 2011). This has spurred the development of alternative processes that are cheaper and safer. The major objective is maximising the value from the commodity produced, especially the copper extracted from high gangue, high acid consuming ores (Dixon, 2004).

The processing of copper ore requires consideration of environmental regulations regarding the emission of noxious gases to the environment. Stricter regulations are in place with respect to environmental compliance and control of emissions of gasses from copper smelting plants (Shabani et al., 2012). Smelting with pollution control adds cost to the processing of copper (Liu et al., 2012a; Künkül et al., 2013). The hydrometallurgical method is an alternative technique that can be used to extract metal from low-grade ores. It lacks the gaseous emissions of smelting plants and has the ability to handle higher levels of impurities (Peacey and Robles, 2004). Other merits include suitability for processing complex ores with high recoveries, competitive economics and operational feature. The method is acknowledged to be the only accepted way to enhance reduction in environmental pollution (Dreisinger and Abed, 2002).

The hydrometallurgical leaching method requires careful consideration during selection of leaching chemicals. The choice of leaching reagent plays a central role in the extraction of copper metal from gangue. Possible leaching reagents include sulphuric acid, nitric acid, hydrochloric acid, ferric chloride, alkaline media such as ammonia, sodium sulphide and sodium hydroxide (Künkül et al., 2013), or salt media such as sulphate/chloride and chloride type media (Bingöl et al., 2005; Liu et al., 2010; Chmielewski, 2012). Improved recovery is sought through identification of a more effective reagent or by increasing the dosage of an existing reagent. Much

attention is devoted into the research of chemical leaching lixiviants for copper from high gangue silicate and carbonate ores (Liu et al., 2012b).

The presence of high amounts of gangue and other impurities in an ore usually renders the ore unsuitable or unattractive for leaching based on economic considerations. Chemicals that are successful in the leaching of copper metal from these ores invariably leads to co-dissolution of other metals (undesirable metals) into the leachate as impurities. The presence of these impurities in the leachate has negative impact on the quality of copper metal during electrowinning (Fillipou et al., 2007). Therefore the metals have to be removed prior to electrowinning in order to obtain high quality copper cathode. Careful attention is required to avoid poor end product, especially when the leaching process is not selective for copper (Zhao et al., 2004; Walting, 2006; Cao et al., 2009; Youcai et al., 2009; Awe, 2013). The processes for removing these impurities after leaching usually result in high capital expenditure. This development leads to growing interest in the elimination of impurities before leaching and electrowinning (Larouche, 2001; Awe and Sandström, 2010).

The choice of reagent is thus a fundamental factor that will ultimately lead to a successful hydrometallurgical process. The emphasis is on identifying lixiviants that can leach copper within the framework of green chemistry (Stuurman et al., 2014). The choice of lixiviant for leaching depends on the ability to minimise the entry of impurities during leaching, availability, recyclability, non-toxicity, biodegradability, non-flammability and cheap cost (Popescu et al., 2013). It is desirable to explore chemicals with high selectivity for copper during leaching in high gangue ores.

1.1. Economic importance of copper and global production

Copper and its alloys continue to be used in a variety of applications that are essential for improving our standard of living. Presently, copper is used in power generation and transmission, electronic product manufacturing, in building construction and production of industrial machinery and vehicles (Figure 1.1). It has been estimated that an average car contains 1.5 kg of copper wire, and the total amount of copper ranges from 20 kg in small cars to 45 kg in luxury and hybrid vehicles. Innovative applications of the metal for different purposes have continued to rise. The global copper demand is shown in Figure 1.2 (after International Copper Study Group, 2015)

.

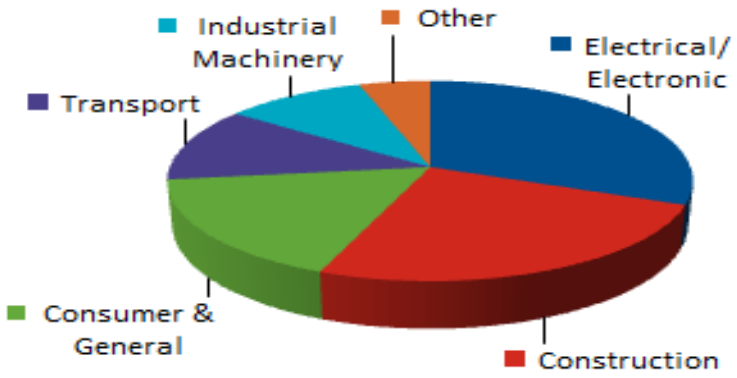

Figure 1.1 Uses of copper

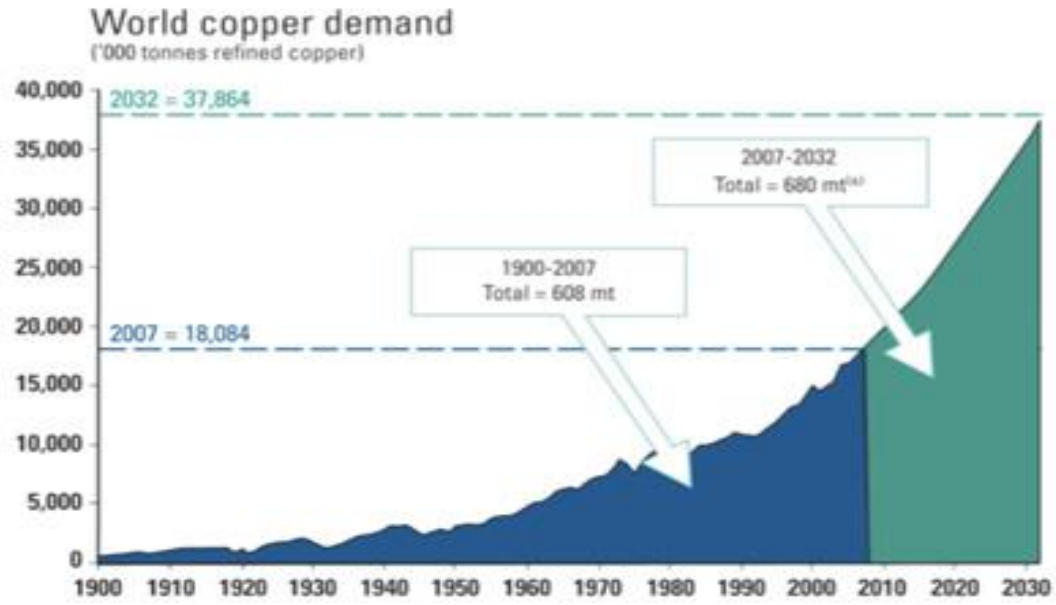

Figure1.2 World copper demand; Source: International Copper Study Group, 2015

The International Copper Study Group (2015) projected that, in 2015, the production of refined copper globally would exceed its consumption (Table 1.1). However, it is expected that a rise in demand will continue beyond 2020 above rates of production. Gordon et al. (2006) and (2007) indicated that the cumulative extraction of copper will not match the cumulative discovery and maintained that due to the high demand the metal will soon be in short supply (Yao and Jiang, 2014, Sawada, 2014).

Chile is the world's largest copper producer with an annual production capacity of about 5,780 thousand metric tonnes in 2014 and a reserve estimated at 209,000 thousand tonnes (Table 1.2). China is the second largest copper producer, with about 1,620 thousand metric tonnes in 2014 and a reserve estimated at 30,000 thousand tonnes.

Table 1.1 World copper demand and supply

World Copper Supply and Demand Forecast (000 Metric Tons)	2013	2014	% Chg. (14/13)	2015	% Chg. (15/14)
Supply 1/:					
Mine Production	18,059	18,904	4.7%	20,283	7.3%
Refined Production (Total)	20,991	22,362	6.5%	23,225	3.9%
Demand 1/:					
Refined Usage	21,273	21,957	3.2%	22,740	3.6%

It is projected that about 2 billion people will live in urban areas by 2025 and 221 Chinese cities are expected to have over one million inhabitants. In Europe, 35 cities will host over 1 million people. This massive increase will require copper for infrastructural development and economic expansion. With 5 million houses projected to be constructed by 2025, and 170 mass transit systems to be built, of which 70 in Europe, the supply of copper needs to cater for the expansion and growth in facilities (International copper study group, 2015).

Table 1.2 World copper producers; Source: U.S Geological Survey on Mineral Commodity, (2015)

Country	Mine production in ('000) metric tonnes		
	2013	2014	Reserves
United States	1,250	1,370	35,000
Australia	990	1,000	93,000
Canada	632	680	11,000
Chile	5,780	5,800	209,000
China	1,600	1,620	30,000
Congo (Kinshasa)	970	1,100	20,000
Indonesia	504	400	25,000
Kazakhstan	446	430	6,000
Mexico	480	520	38,000
Peru	1,380	1,400	68,000
Poland	429	425	28,000
Russia	833	850	30,000
Zambia	760	730	20,000
Other countries	2,200	2,400	90,000
World total	18,300	18,700	700,000

China accounts for about 36% of the global consumption of copper, which is twice the consumption of Europe (Figure 1.3).

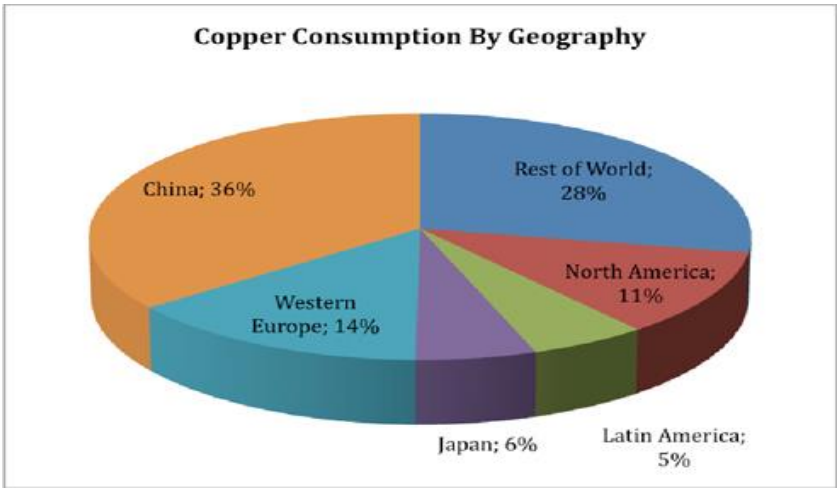

Figure 1.3 Copper consumption patterns by geography; source: Raw Materials Group, 2015

The increased utilisation of copper by China is a result of an annual economic growth rate of 9.9% in the past 10 years (Liu et al., 2011). It is forecasted that China's economy will expand at an annual rate of 9.7% for the next 5 years. With China setting a goal of 65% urbanization rate by 2050, this translates to 20% growth per year over 40 years. By this projection, about 300 million rural communities will be turned into urban residents. The huge demand by China and other countries on copper-intensive power infrastructure will continue to propel demand. Consequently, copper production capacity and expansion is expected to continue to rise (Figure 1.4).

Figure 1.4 Production trend for copper metal (metric tonnes); source: International Study Group, (2015)

The supply of copper will depend on its efficient recovery from copper ore resources, advancement in technology and discovery of new deposits (Wills and Napier-Munn,

2006). It is expected that the use of integrated innovative approaches targeted at optimal copper recovery at a reduced processing cost, with minimal environmental consequences, is the way forward.

1.2. Statement of the problem

In view of the global demand for copper and shrinking copper resources, the aim to increase production capacities from the already lean, low-grade complex ore resources at a competitive lower cost presents a challenge. The economic recovery of copper from an ore depends on the process cost and variable leaching techniques. For example, high gangue containing copper oxide ores require large amounts of sulphuric acid for leaching. The consumption of acid by the carbonate gangue ranges from 0.4 to 0.7 tonnes H_2SO_4 per tonne copper recovered (Bingöl and Canbazoğlu, 2004; Peacey et al., 2004; Habashi, 2009). A leaching technique that is capable of processing copper from high gangue ore presents an opportunity to grow the supply of copper.

Most hydrometallurgical leaching processes are not selective, resulting in co-dissolution of impurities into the leachate solution (Walting, 2006; Künkül et al., 2013). Impurities in ore leachate can increase the cost of solvent extraction and electrowinning of copper from the leachate solution, especially if the thermodynamic and electrochemical behaviours and properties are similar to that of copper (Larouche, 2001; Fillipou et al., 2007; Awe and Sandström, 2010). A selective leaching reagent allows for more efficient recovery of copper.

1.3. Aims and objectives of the research

The aims and objectives of this research are as follows:

1. To determine the mineralogical and chemical composition of porphyry copper oxide ores from a mining district in the Coastal Range of the Atacama Region, Northern Chile.
2. To evaluate the copper content in the NIR sensor-based pre-concentrated classified ore (product, middling and waste).
3. To investigate the dissolution kinetics of the NIR pre-concentrated copper ore in selected lixiviants and also determine the factors controlling the leaching process.
4. To investigate the parameters affecting the leaching process.
5. To explore the possibility of enhancing the economic processing of the ore in the different categories.
6. To examine the leach residue for extent of extraction and effectiveness of the leaching process.

7. To carry out electrochemical analysis of the ore leachate to understand the electrodeposition behaviour of copper from the copper complexes.

8. Develop a model that allows the dimensioning of the leaching process

1.4 Outline of research

Based on results of mineralogical and chemical analysis of the near infrared sensor-based pre-concentrated and classified copper ores, the hydrometallurgical leaching method is considered suitable for processing of the ores. Figure 1.5 is a simplified flow diagram of the hydrometallurgical leaching strategy in the present study.

For optimal extraction of copper from the low grade complex ore by this method, the pre-concentrated and classified ores will be leached with alkaline lixiviant. An alkaline selective leaching process with NH_4Cl is chosen as a preferred reagent in this study because chloride is a well-known aggressive chemical reagent. The reagent does not accumulate copper in an organic phase after leaching and is effective in the leaching of copper due to the complexation ability with NH_3 and chloride ions. There is adequate supply of chloride and ammonium ions from NH_4Cl during leaching which allows for the formation of highly stable copper complexes. During the leaching process, pH of the solution is usually within the range of 6 and 7. Impurities such as Fe_2O_3, SiO_2, CaO and MgO are therefore not dissolved during the process and remain in the residue, thus minimising the dissolution and concentration of associated metals in the leachate.

Due to the nature of the ore, which is composed of readily soluble Cu and gangue, an agitated leaching process is considered advantageous because of its good leaching kinetics. Presence of calcite in the ore usually leads to high sulphuric acid consumption. Thus the choice of alkaline reagent and agitation leaching process in this research is considered effective for treating the ore. There is no literature about the leaching of pre-concentrated copper ores with oxalic acid. This present work will therefore examine the possibility of the application of this reagent for leaching and compare the performance with that relating to NH_4Cl. The effect of some important parameters (temperature, stirring speed, reagent concentration, particle sizes, solid to liquid ratio) on the leaching process will be determined.

The kinetic aspect of the leaching process will be characterised using the shrinking core model due to its suitability for analysing non-catalytic fluid-reaction. This will be done to ascertain the mechanisms controlling the leaching process for optimum plant design and application. This is because the review of the literature showed that the kinetic aspect of sensor-based pre-concentrated copper ore has not been reported. The choice of the model for interpreting the leaching data, especially the leaching kinetics of pre-concentrated ores, was because of it being the best description of the rate expression of reaction between fluid and solid copper ore. Thus, according to the model the reaction is said to take place on the outer surface of the solid which shrinks toward the centre as the reaction proceeds, leaving behind an inert solid

layer, called ‘’ash layer’’ around the unreacted shrinking core. The assumptions are that the copper particles to be leached are spherical and of equal size while the concentration of the reagent is constant during leaching.

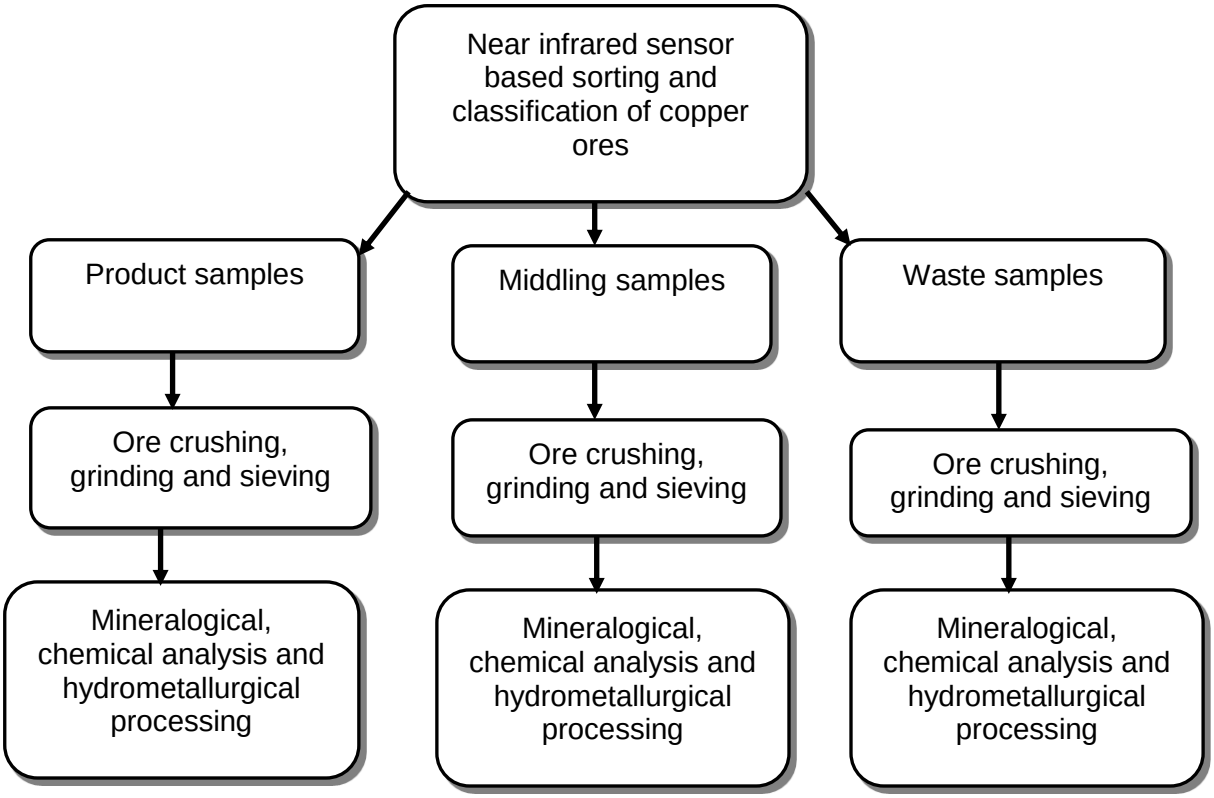

Figure 1.5 Flow diagram of the preparatory steps for processing in this study

Similarly, no literature was found on the electrowinning of Cu ore leachate obtained from NH_4Cl leaching of pre-concentrated copper ores. In view of the importance of electrowinning in hydrometallurgical leaching of copper ore, the leachate obtained from selective alkaline leaching will be analysed for electrochemical behaviour. In this present study, Cyclic Voltammetry (CV) will be utilised for analysing the electrochemical reactions occurring during the electro reduction and electrodeposition of Cu for investigating the electrowinning of the metal from copper-ammonia complexes. For more insight on the electrochemical behaviour of the leachate a comparison will be made with copper ammonia sulphate synthetic solution. This technique is chosen because it reveals electro-reduction, electrodeposition, and electrochemical kinetics occurring in solutions.

1.5. Structure of the thesis

This thesis is divided into ten chapters and a number of appendices. This first chapter introduces the research topic, processes of extracting copper from ores, economic and environmental considerations as well as choice of leaching reagents. Economic importance of copper and global production is discussed. Clear statements of the problems are outlined and the aim and scope of the thesis justified.

Chapter 2 is a review of related literature from several areas which include copper occurrence, compounds and reactions and processing methods. Emphasis is placed on the leaching techniques including various lixiviants, operating parameters and leaching kinetics. The review continues to focus on processes of copper removal from solution, electrolytic processes and electrochemical deposition of copper from alkaline solution.

Chapter 3 outlines the different analytical techniques employed for mineralogical and chemical analysis of the samples throughout the thesis and then the reagents and detailed experimental procedures followed during analysis, and in some instances the instrumental specifications, choices and their limitations.

Chapter 4 focusses on the mineralogy and chemistry of the ore samples used in this research. Quantitative and qualitative compositional analyses (mineralogical and elemental) of the ore are discussed with respect to implications for chemical leaching. The discussion of data is on the basis of QEMSCAN® and near infrared spectroscopy pre-concentration and ore classification carried out by Iyakwari (2014). Contribution of minerals in the ore by volume and concentration on the basis of functional groups in the classified ore are analysed. This is followed by classification of minerals in the ore according to gangue, acid consumption and reactivity toward chemical reagents, elemental analysis of particle samples and size fractions using different techniques in the classified ore and correlation of data of some instruments discussed.

Chapter 5 is a pilot study on the NIR classified ore ultimately to determine the elemental concentration in different size fractions of the classified ore and the effect of some parameters in order to develop a leaching strategy and electrochemical study of leachate. Each category of ore size fractions was tested for copper dissolution and suitability or otherwise for further study. A proposed plan for further study is drawn after comparing each sample's behaviour.

Chapter 6 is a follow up to chapter 5; the chapter continues with the extensive study of the leaching behaviour of the classified ore. This chapter explains batch leaching experiments, effect of different parameters on leaching, optimization of the process, validation of the leaching process, kinetic analysis and determination of activation energy. The comparison of the leaching potential of ammonium chloride and oxalic acid, evaluation of leachate and ore residue for leaching effectiveness is also stated. Relationship between copper extraction and relative extraction of other metals from the ore after leaching in ammonium chloride reagents are discussed.

Chapter 7 outlines detailed procedures for electrochemical analysis. Further analysis of ore leachate to assess the metal concentration present as a measure of determining their influence during copper electrodeposition in the study is stated. The chapter is aimed at establishing the possibility and processes of copper electrodeposition from ore leachate containing copper ammonia complexes and a

synthetic solution of copper ammonium sulphate complex. The kinetic analysis to establish the mechanism controlling copper electrodeposition in the two solutions is described.

Chapter 8 discusses the potential of the practical application of a new hydrometallurgical flowsheet for processing copper from NIR pre-concentrated classified ore. The benefits of using three routes for processing of the classified ore fractions on the basis of copper and gangue content are considered. The chapter is concluded by analysing the effect of Mn, Fe, Ni, Co and Zn in the leachate for electrowinning. The advantages and limitations of the hydrometallurgical processes are highlighted.

Chapter 9 discusses the result and the main findings of the research, and how this compares to the results of previous studies.

Chapter 10 summarises the findings from the work performed and conclusions are presented. Key findings and contributions to knowledge are outlined and recommendations for further study are made.

Chapter 2

Literature review

2.0. Introduction

This chapter reviews the literature on the mineralogical and chemical affinities of copper and transitional properties such as complex formation. It describes the different processes involved and methods of processing copper from ores ranging from ore crushing to copper recovery, various leaching techniques and the types of lixiviants used for copper leaching with emphasis on alkaline leaching processes. Complexometric analysis for copper determination is discussed. The chapter also reviews the kinetics of the copper leaching processes, electrolytic processes including metal electrodeposition processes, electrochemical deposition of copper from alkaline solution and the conventional electrowinning process of copper.

2.1. Copper chemical and mineralogical affinities

Copper occurs in nature in different forms due to its ability to combine with so many metals in the Periodic Table to form minerals such as carbonates, silicates, hydroxides, oxides, chlorides, sulphates, phosphates and sulphides. Out of the numerous copper minerals only a few are economically viable for processing (John, 1999). The metal has a crustal abundance of 60 ppm (Awe, 2013) and is commonly mined as sulphide, oxide, or silicate ores. Copper belongs to the group of metals in the Periodic Table referred to as transition elements; these display distinct chemical behaviour. Interesting properties of these metals are their ability to exist in various oxidation states and their ability to form stable complexes with halides, ammines, azo compounds, cyanides and other complexing media (Habashi, 1998). In terms of chemical properties, copper has an atomic number of 29, with electrons being distributed according to the oxidation state of copper (+1 and +2). The [Ar] $3d^{10}$ $4s^{1}$ electronic configuration applies for copper metal. Cu(I) or Cu^{+} ion indicates the +1 oxidation state, in which the $4s^{1}$ electron is released, leaving the [Ar]$3d^{10}$ electronic configuration. For Cu(II) or Cu^{2+} ion, a further electron is shed from the d-orbital, to reveal a [Ar] $3d^{9}$ electronic configuration. Although Cu (0) and Cu (III) have also been identified in nature, they are not presently of commercial importance (Habashi, 1997).

2.2. Copper ore processing methods

The economics of processing depends on many factors such as the presence of acid soluble minerals in the ore. John (1999), Bingöl and Canbazoğlu (2004), Wang et al. (2009), Liu et al. (2012a and 2012b) and Künkül et al. (2013) indicated that carbonate gangues such as limestone and dolomite ($CaCO_3$ and $CaMg(CO_3)_2$), respectively, in ores are mostly responsible for high acid consumption during leaching. These high acid-consuming gangues pose not only economic problems during mineral processing, but can also lead to severe environmental problems. Mathew (2013) indicated that leaching of ores and other materials containing high

levels of carbonates lead to carbon dioxide generation and emission into the atmosphere. It is estimated that a tonne of sulphuric acid produces approximately 450 kg of carbon dioxide when it reacts with carbonate gangue material (Mathew, 2013). This can be inferred from the following reaction (Bingöl and Canbazoğlu, 2004):

$$CaCO_3 + H_2SO_4 + H_2O \leftrightharpoons CaSO_4.2H_2O + CO_2 \quad (2.1)$$

The consumption of acid by gangue affects the efficiency of leaching. According to Bingöl and Canbazoğlu (2004) and Bingöl et al. (2005), there may be insufficient free lixiviant to leach copper ore minerals.

According to Liu et al. (2012b), most copper oxide ores respond poorly to flotation reagents and, making use of their hydrophilic nature, copper has to be leached from such ores. On the other hand, hydrophobic copper sulphide ores are suited for concentration using flotation methods.

Processes for copper refining from ores, concentrates and other sources are classified as 'conventional' pyrometallurgy or hydrometallurgy methods (Ramatsa, 2012). The choice of process is influenced by key issues such as economic recovery of copper and efficiency of the processing technology, as well as environmental friendliness (Haque et al., 2012; Liew, 2015). For either process, the ore has to be subjected to preparatory steps. According to Lamya (2007), copper processing comprises of several steps: comminution step (crushing, grinding and sieving), followed by either concentration before pyrometallurgical processing (smelting of the ore concentrate) or hydrometallurgical processing (leaching, solvent extraction and electrowinning).

2.2.1. Comminution

This first step to prepare the ore before the main processing method involves the reduction of particle size prior to feeding these into the milling circuit for grinding. Milling liberates or separates the copper particles from the ore mineral matrix and gangue. The liberated ore is then subjected to screening or particle size analysis to obtain desired fractions. As stated in section 2.2, the mineralogy of an ore determines the choice of a particular processing method.

2.2.2. Pyrometallurgy

The pyrometallurgical copper processing technology involves smelting and roasting of the ore (Moskalyk et al., 2003). The heating temperatures used could be as high as 1500 ˚C, making a large consumption of energy necessary (Liew, 2015). Sulphide minerals which are the form of most copper in the Earth's crust, mostly occur either as chalcopyrite ($CuFeS_2$), bornite (Cu_5FeS_4) or chalcocite (CuS) (Awe, 2013). As a result, most of the sulphide ores are usually treated using the pyrometallurgical route. The technique accounts for about 80% copper production while the copper oxide

ores accounts for the remainder (Haque et al., 2012). According to Stevanovic et al. (2009), the majority of copper production is by means of concentration, smelting and refining of sulphidic copper ores. Despite the huge production of copper by this method, the technique has continued to suffer a lot of setbacks (Vračar et al., 2003). Unless flue gasses are treated, pyrometallurgical operations are a major source of SO_2 gas emissions into the atmosphere (Aydogan et al., 2005). Liew (2015) indicated that SO_2 emission may range from less than 4 kg per metric ton (kg/t) of copper to 2,000 kg/t of copper. Emissions of particulate materials are estimated from 0.1 kg/t of copper to as high as 20 kg/t of copper. Awe and Sandström (2010) and Haque et al. (2012) found that, where sulphide ores contained harmful elements such as antimony, arsenic and mercury, these often render the processing of the ores by this method less appropriate due to serious environmental concerns. Authors such as Wang et al. (2009), Haque et al. (2012), Liu et al. (2012b) and Parada et al. (2014) suggest that the hydrometallurgical leaching process has huge potential to process high gangue-complex ore in a more efficient manner than the pyrometallurgical process.

2.2.3. Hydrometallurgy

Hydrometallurgy for extracting copper from ore uses reagents in aqueous solution for the selective dissolution of metals (leaching) from an ore at lower temperatures compared to pyrometallurgy. A metal product such as cathode copper is recovered from the pregnant leach solution by a separation step such as adsorption, precipitation, Solvent Extraction (SX) and/or ElectroWinning (EW) (Wang et al., 2009). Arbiter and McNulty (1999) and Mathews (2013) stated that the hydrometallurgical process was first used for the processing of copper by Rio Tinto in Spain in 1670 as an alternative technology for the production of copper present in mine water by natural oxidation of copper, involving the cementation of $CuSO_4$ using iron. Liu et al. (2012a) indicated that the hydrometallurgical method of copper extraction is usually very efficient when treating lean and low-grade or complex copper ores, with an increase of copper recoveries. Haque et al. (2012) and Liew (2015) indicated that the method leads to a higher recovery rate of copper due to the ease of leaching ores with the possibility of recirculating solid waste to achieve higher recovery rates through electrowinning.

With the gradual depletion of high-grade copper ore deposits, hydrometallurgy holds the key to resolving a future shortage in copper supply. However, Peacey and Robles (2004) maintain that only limited technical successes have been achieved to date. Stuurman et al. (2014) suggested new hydrometallurgical techniques need to be developed to replace pyrometallurgical processes due to some inherent disadvantages such as high capital cost, emission of noxious gases, and impurities entering the downstream processing of copper ores. In a recent development, sulphide ores such as chalcocite are starting to be processed using hydrometallurgical techniques (Davenport et al., 2002; Baba et al., 2013; Aydogan et al., 2005; Liu et al., 2012; Künkül et al., 2013). New approaches in hydrometallurgy

include sensor-based pre-concentration and classification (Iyakwari et al., 2013; Iyakwari, 2014), selective alkaline leaching and the use of mixed reagents (Awe, 2013).

Cost can be an important advantage of hydrometallurgy over pyrometallurgy. For some ores, costs are reported to be at US$ 0.09 per unit pound of copper for hydrometallurgy versus US$ 0.24 per unit pound for conventional smelting and refining. Research aims to maintain this cost advantage in the development of efficient hydrometallurgical treatment of high-gangue, low-grade copper ores.

2.3. Leaching processes

According to Chmielewski (2012), leaching is a chemical or electrochemical process for the extraction of valuable metal(s) from ores, in order to obtain by-product or concentrate in solution. During the leaching process, the lixiviant dissolves soluble materials contained in a rock. In the case of copper ore, metallic copper is recovered through processes like precipitation and electrowinning (Gupta, 2006). The process can also be used for the upgrading of concentrate minerals by dissolving the acid-soluble components of the ore, resulting in a higher grade or purer concentrate (Arbiter and McNulty, 1999).The leaching of the ore can be carried out using different methods such as chemical, electrochemical, electrolytic and galvanic leaching (Mathew, 2013).

2.3.1. Chemical leaching

This is the leaching of metals or metal compounds in alkaline or acidic solutions in the presence or absence of complexing agents. It does not require charge transfer during the process.

2.3.2. Electrochemical leaching

With this method of leaching, metal sulphides or conductive metal oxides are dissolved under oxidative or reductive conditions in either acidic or alkaline solutions, possibly in the presence of complexing agents.

2.3.3. Galvanic leaching

This involves the use of galvanic interaction for leaching of metal sulphides or conduction of oxide metals by galvanic contact of various minerals (Gupta, 2006). The process is based on different potentials of two minerals in contact. In the process the mineral with the more positive potential is reduced while the one with a negative potential is oxidised. Havlík (2014) suggested that the potential difference is the driving force of galvanic corrosion of minerals.

2.3.4. Electrolytic leaching

Gupta and Mukherjee (1990) suggested this type of leaching process depends on conducting metal oxides which effect anodic or cathodic digestion. This is achieved by imposing a potential from an external current source.

2.4. Leaching techniques

A decision on the leaching technique to be adopted for processing a particular metal from an ore such as copper depends on economic and environmental factors. Other important considerations are ore grades, mineralogy and available techniques. Most of the common leaching techniques for copper oxide leaching include: heap, dump, in situ, vat and agitation leaching.

2.4.1. Heap leaching

Heap leaching has been extensively practiced during the past 500 years (Kappes, 2002). This leaching technique involves the stacking of crushed copper-bearing ores into a ‘’heap’’ up to 15 m high on an impermeable pad. The heap is then irrigated for an extended period of time (weeks, months or years) with a chemical solution to solubilise the sought-after metals, and collecting the pregnant leach solution as it percolates out from the base of the heap. When sulphide ores are leached with bacteria, the activity of the bacteria is stimulated by aerating the heap with air emanating from perforated pipes at the foot of the heap. This also helps to maintain the permeability of the heap. The efficiency of the process is difficult to evaluate due to unknown variables such as tonnage (Ramatsa, 2011). According to Gupta (2006), the concentration of copper in the pregnant leach solution is in the range of 2 to 8 litre, with a recovery between 85 to 90 % depending on the leaching time. The advantages of the use of heap leaching stem from its cost effectiveness, based on reduction of the milling cost; the ore only has to be crushed to 20 to 25 mm.

2.4.2. Agitation leaching

Agitation leaching involves placing milled ore or concentrate into a pneumatic or mechanical agitation tank containing copper ore with chemical reagents. The resultant slurry is separated in a solid/liquid separation stage, usually in a Counter Current Decantation (CCD) unit. The solution is upgraded in a Solvent Extraction (SX) circuit and the copper recovered through Electrowinning (EW) (Osman et al., 2013). The agitation tank is typically equipped with agitators, baffles and gas introduction equipment designed to maintain the solid in suspension in the slurry in order to achieve optimum leaching. The process can be conducted under the conditions of ordinary or elevated temperatures and atmospheric pressure. Some authors, Padilla et al. (2007) and (2008), Sokić et al. (2009) and Padilla et al. (2010) have explored conditions such as high temperature and pressure leaching especially for sulphide ores and concentrate that require prior oxidation before leaching and found that the process led to improved copper leaching. Agitation leaching plays a central role in the processing of copper and other metals. It has been found that

agitation leaching and copper recovery using SX-EW technology is more viable than heap leaching, especially if the copper content in the ore is significant (Agitation leaching, 2015). The concentration of copper in the pregnant leach solution can be from 1 to 80 gram per litre, with recoveries approaching 100 % over periods of 4 days or more (An et al., 2009). Effective mixing during agitation leaching promotes heat transfer resulting in higher leaching kinetics when compared to heap leaching which typically takes several weeks to months. The reactions taking place during agitation are heterogeneous and occur faster compared to heap leaching which varies from top to bottom with reaction conditions less heterogeneous. Besides agitation leaching is significantly rapid as compared to heap leaching, however it is more costly.

2.4.3. Vat leaching

With vat leaching, crushed ore is placed in large enclosed vessels (approx. 6 m deep) and flooded with a leaching solution. The method is only suitable for treating high-grade copper ores (> approx. 0.8 %), where readily leached ore maintains some integrity during leaching. Recoveries are usually over 90 % for copper within a short period of time (Mathew, 2013). Vat leaching is uncommon due to its double handling costs for placing the ore in the vat and removing it after leaching.

2.4.4. Dump leaching

Dump leaching involves leaching of ore directly from the mine and stacked on leach pads without crushing. The method is mostly carried out using low-grade mineralised waste rock containing only a small fraction of large rocks. The height of the dumps can be up to 200 m. The ore is irrigated with chemical reagents to leach the copper in the ore. The solution containing the dissolved copper exits the base of the dump and is collected for metals extraction. Copper recovery is generally in the range of 25 to 65 %. The primary concern is its slow kinetics; it usually takes a long period of time of between 1 and 2 years to extract 50 % of the desired metal. As such, it cannot be considered as a short-term leaching process.

2.4.4.1. In situ leaching

This uncommon type of leaching process involves drilling holes into the ore deposit in old underground mines, creating open pathways for the passage of leaching solutions in the deposit through the use of explosives or hydraulic fracturing. The pregnant leach solution is pumped to the surface for processing. Although the solution grade is variable and recovery from the solution is difficult, the method promises significantly lower costs compared to other leaching techniques.

2.5. Selection of leaching reagent

During the selection of chemicals for leaching, properties of the reagents and mineralogical nature of the ore should be taken into consideration. Peacey (2004), Gupta (2006), and Popescu et al. (2013) suggest that the criteria for selection of chemicals depends on various factors which include both chemical and physical

character of the material to be leached, selectivity, cost of the chemical reagent and the reagent amenability for recycling or regeneration. Other criteria are non-flammability, low consumption of the solvent by gangue minerals, biodegradability, availability, and corrosiveness to materials used in plant equipment. Thus, the selection of suitable leaching reagents and the stream of the process to use as well as raw material are the most important considerations in hydrometallurgy (Limpo et al., 1992).

2.6. Alkaline leaching

Several authors such as Arbiter and Fletcher (1994), Oudenne and Olson (1983), Ekmekyapar et al. (2012), and Künkül et al. (2013) have investigated the suitability of alkaline lixiviant for leaching of copper ores. As a result, the alkaline leaching process is gradually becoming acceptable for leaching of copper ores. Alkaline leaching can be carried out with ammonia and its chloride, carbonate, sulphate and hydroxide salts. The conditions under which these leaching systems dissolve copper from ore are either mildly acidic or basic. In each case, the ammonia lixiviant can be recovered by evaporation at the end of the process (Limpo, 1992). Other perceived advantages of alkaline leaching process are the ease of purification of the lixiviant, amenability to regeneration, low cost of production (Liu et al., 2012b; Künkül et al., 2013), reduced dissolution of impurities like iron (Chmielewski et al., 2009) and reduced reagent consumption by carbonate gangues (Bingöl et al., 2005; Künkül et al., 2013). Some components can be removed during the leaching steps as insoluble oxy/hydroxyl compounds, allowing for a more selective extraction of the valuable metals, such as Cu, Ni and Co. These are capable of forming soluble amine complexes through a reaction with the nitrogen-containing group (Meritxell, 2009).

Various authors state that ammoniacal leaching is selective for copper leaching from high gangue copper ores because the reactivity of the lixiviant toward carbonate and siliceous gangues is minimal (Liu et al., 2012b; Künkül et al., 2013). Selective extraction of Cu from high gangue ores also supports downstream recovery of high-purity copper during electrowinning. The tendency for the formation of complexes during the alkaline leaching process differs with the copper and reagents. Copper (II) salts form complexes of the type $[Cu(NH_3)_n]^{2+}$ where n is between 1 to 6. The penta-ammine of the complex is formed when concentrated ammonia solution is used. The hexa-ammine complex is favoured in anhydrous ammonia solution, while the tetra-ammine complexes of the Cu (II) are usually favoured at low ammonia concentration. For the Cu (I) complex of ammonia, only di-ammine complex formation is favoured (Habashi, 1999).

2.6.1. Ammonia leaching

Ammonia has proven to be an effective and widely used metal extractant in hydrometallurgical processes for many years due to its benefits over other reagents (Meng and Han, 1996). The Arbiter/Escondida process was developed in 1970's for

leaching chalcocite in ammonia solution to extract copper from copper-rich ores (Meritxell, 2009). The use of NH_3 for alkaline leaching of low grade-complex copper ores is considered to be efficient. The lixiviant has been used in the following copper treatment plants: Kennecott; Bwana M'kubwa, Zambia; Alaska and Poseidon Limited, Australia (Chase, 1980, François-Xavier, 2013). More recently, the reagent has been applied in the Leon project in Argentina with copper recovery well above 80 % (François-Xavier, 2013). Ochromowicz et al. (2014), Ekmekyapar et al. (2012) and Liu et al. (2010) state that alkaline NH_3 leaching allows for selective extraction of copper. According to Künkül et al. (2013), the NH_3 lixiviant reacts with copper ions to form complexes, which further increases the leaching rate. Limpo et al.(1992) observed the formation of $Cu(NH_3)_2^{2+}$ and $Cu(NH_3)_3^{2+}$ complexes which further react with the ore in the presence of more NH_3 ligands to form stable $Cu(NH_3)_4^{2+}$ complexes. The intermediates are known to be responsible for increased copper extraction rate during leaching.

2.6.2. Ammonium acetate

Ammonium acetate has also been found to be effective for copper leaching. Kinetic studies of the leaching of malachite ore by Künkül et al. (2013) with the lixiviant led to about 99 % Cu extraction and the reaction found to occur through a mixed kinetic control model after the activation energy was determined to be 59.6 KJ/mol. Demirkiran (2008) suggested that the weak acid (acetate) and weak base (ammonia) buffer the pH during the leaching process. A high purity pregnant leach solution is obtained due to minimal dissolution of other metals such as iron, which are precipitated in the form of hydroxides. The high leaching rate is believed to be due to NH_4^+ ions, which contribute to protons generated by the dissociation reaction. The process is summarised in Equations 2.2 - 2.4 (Demirkiran, 2008):

$$NH_4CH_3CO_2 \rightarrow NH_4^+ + CH_3COO^- \quad (2.2)$$

$$NH_4^+ + H_2O \rightleftharpoons NH_3 + OH^- \quad (2.3)$$

$$CH_3COO^- + H_2O \rightleftharpoons CH_3COOH + OH^- \quad (2.4)$$

Ammonia formed in Eq. (2.3) is the main reactant responsible for Cu extraction. The copper ions are first released into the solution in water-soluble form. The reaction of the lixiviant with malachite is shown in Equations 2.5 – 2.8 (Künkül et al., 2013):

$$CuCO_3.Cu(OH)_2 + 2H_3O^+ \rightarrow Cu^{2+} + CO_2 + 3H_2O + Cu(OH)_2 \quad (2.5)$$

$$Cu(OH)_2 + 2H_3O^+ \rightarrow Cu^{2+} + 4H_2O \quad (2.6)$$

$$Cu^{2+} + 4NH_3 \rightleftharpoons Cu(NH_3)_4^{2+} \quad (2.7)$$

$$CuCO_3.Cu(OH)_2 + 4NH_4CH_3CO_2 \rightarrow 2Cu^{2+} + 4NH_3 + 4CH_3COO^- + CO_2 + 3H_2O \quad (2.8)$$

2.6.3. Ammonium nitrate

The use of NH_4NO_3 for extracting Cu from malachite ore has been investigated by Ekmekyapar et al. (2012). Leaching is essentially carried out at a constant pH. Dissociation of NH_4^+ ions produces protons, which increases the H_3O^+ concentration, and NH_3, which forms stable complexes with copper ions. The presence of the complexes in solution led to increasing dissolution rate of the copper minerals; reaching about 88 % extraction of Cu. Ekmekyapar et al. (2012) indicated that the reagent has great potential for copper ore leaching because NH_4NO_3 is a salt of a strong acid (HNO_3) and a weak base (NH_3). The reagent has a weakly acidic character and ionises in aqueous medium according to the reactions in Equations 2.9 and 2.10 (Ekmekyapar et al., 2012):

$$NH_4NO_3 \rightarrow NH_4^+ + NO_3^- \quad (2.9)$$

$$NH_4^+ + H_2O \rightleftharpoons NH_3 + H_3O^+ \quad (2.10)$$

The reactions occurring during the leaching of malachite ore and NH_4NO_3 is shown in Equations 2.11 – 2.14:

$$CuCO_3.Cu(OH)_2 + 2H_3O^+ \rightarrow Cu^{2+} + CO^2 + 3H_2O + Cu(OH)_2 \quad (2.11)$$

$$Cu(OH)_2 + 2H_3O^+ \rightarrow Cu^{2+} + 4H_2O \quad (2.12)$$

$$Cu^{2+}\ 2NH_3 \rightleftharpoons Cu(NH_3)_2^{2+} \quad (2.13)$$

$$Cu(NH_3)_2^{2+} + 2NH_3 \rightleftharpoons Cu(NH_3)_4^{2+} \quad (2.14)$$

2.6.4. Ammonia/ammonium carbonate

Mixtures of NH_3 and $(NH_4)_2CO_3$ have previously been used for the pressure leaching of oxidic uranium ore without achieving much recovery. As such, it was not adopted for commercial use (Merritt, 1971). Bingöl et al. (2005) found that the extraction of copper reached 98 % after they studied the dissolution kinetics of malachite ore using a combination of $NH_3/(NH_4)_2CO_3$. They also suggested that the lixiviant appears to be selective with the dissolution of copper by the NH_3 ligand. Whereas gangue minerals were unreactive toward the reagent, this is an indication that the reagent could be efficient for leaching high gangue ore minerals. The mechanism controlling the dissolution process was said to occur via diffusion across the product layer. The calculated activation energy of the process was found to be 15 kJ/mol, which is lower than that observed for ammonia/ammonium chloride leaching by Yartaşi and Çopur (1996) and Ekmekyapar et al. (2003). This indicates that the dissolution kinetics in the former were faster than the latter, suggesting that two leaching reagents can be beneficial.

2.6.5. Ammonia/ammonium sulphate

Leaching of copper from ore containing calcium-magnesium carbonate in a $NH_3/(NH_4)_2SO_3$ solution with persulfate was carried out by Liu et al. (2012a). The extraction efficiency of Cu was about 87.6 % suggesting that the use of the mixture of the alkaline lixiviants was suitable for ore containing carbonate gangue. The authors noted that the extraction rate was enhanced by increasing the leaching temperature from 293 K to 323 K. This temperature-dependence suggests that the process is chemically controlled.

2.7. Ammonia concentration balance and process recovery in leach liquor

The importance of controlling the concentration of NH_3 in the leach circuit has been investigated by Mathews (2013). A high concentration of NH_3 in a leaching circuit can lead to higher NH_3 losses and lower efficiencies at the Solvent Extraction (SX) stage. They recommend that the NH_3 concentration in the Pregnant Leach Solution (PLS) is maintained in the range of 40 to 60 g/ litre. Matthews (2013) indicated that copper can be recovered from dilute ammoniacal PLS liquor using a solvent extractant such as LIX 54-100 followed by electrowinning of the solution. The process of recovering stripped PLS is carried out by incorporating scrubbing bags in the SX process. The aim is to remove both entrained and co-extracted ammonia, thereby reducing the influx and transfer of ammonia from the PLS to the electrolyte. Bleeding out a portion of the electrolyte can be used to achieve the desired target. The authors suggested a lower value of 2 gram per litre of ammonia in the electrolyte as ideal for good quality of copper cathode.

The inclusion of a recycling unit for ammonia is considered a vital process component. Frantz and McNulty (1973) highlighted three stripping techniques of recovering the lixiviant: sparing and submerged combustion evaporation, direct steam sparing, and indirect steam evaporation. Mathews (2013) pointed out that steam stripping has a high throughput but is energy-intensive.

2.8. Inorganic acid copper leaching

Extraction of Cu from ores can be carried out using many inorganic acids such as H_2SO_4, HNO_3 and HCl (Habbache et al., 2009). Ntengwe (2010) and Baba et al. (2013) found that H_2SO_4 acid is the most common reagent used in leaching of copper from ores. The ability of the reagent to dissolve Cu quicker than metals such as Zn, Co, and Fe is the reason for its popularity. According to Gupta (2006) and Bingöl and Canbazoğlu (2004), most copper ores are soluble in sulfuric acid, which is cheap and readily available. The reactions involving H_2SO_4 and some copper ores is shown in Equations 2.15 to 2.18 (Bingöl and Canbazoğlu, 2004):

$$Cu_3(OH)_2(CO_2) + 3H_2SO_4 \rightarrow 3CuSO_4 + 2CO_2 + 4H_2O \quad (2.15)$$

$$Cu_2(OH)_2CO_3 + 2H_2SO_4 \rightarrow 2CuSO_4 + CO_2 + 3H_2O \quad (2.16)$$

$$CuO + H_2SO_4 \rightarrow CuSO_4 + H_2O \quad (2.17)$$

$$CuSiO_3.2H_2O + H_2SO_4 \rightarrow CuSO_4 + SiO_2 + 3H_2O \quad (2.18)$$

Even the limited presence of impurities such as iron and other metals from ore leached with sulfuric acid is problematic during the SX-EW process (Badilla and Haussmann, 2013). Other issues are corrosion of leaching equipment.

The use of H_2SO_4 acid in combination with other reagent has been found to improve leaching kinetics of copper. Seo et al. (2013) found that the maximum extraction of copper using H_2SO_4 acid was 80 % while a mixture of the acid with hydrogen peroxide led to enhanced copper recovery of about 90 % and concluded that the use of H_2O_2 and H_2SO_4 acid mixture could be a potential source of lixiviant for improving the dissolution of Cu and Co in a copper-cobalt ore. Habashi (1999) and Vračar et al. (2003) indicated that the use of nitrate with H_2SO_4 acid for leaching gave better result than when the acid was used alone. Vračar et al. (2003) investigated the leaching of Cu (I) using H_2SO_4 acid and $NaNO_3$ and found that the leaching process without $NaNO_3$ as an oxidant could not take place as the acid failed to react with chalcocite (Cu_2S). Similarly, Sokić et al. (2009) examined the leaching of chalcopyrite concentrates with H_2SO_4 acid and $NaNO_3$ and found that the oxidant had significant influence on copper extraction. The copper leaching increased from 43 % to 75 %.

The use of H_2SO_4, HCl, and HNO_3 for leaching of copper oxide by Habbache et al. (2009) indicated that over 90 % Cu extraction rate was attained. Similar results were obtained by Alafara et al. (2015) for quantitative leaching of a Nigerian chalcopyrite ore. The authors found that the dissolution of copper was fastest with HCl and the slowest with HNO_3. Baba and Adekola (2010) determined the leaching efficiency of copper using HCl acid to be 91.8 % suggesting that the reagent could also be applied for copper leaching. A lower dissolution rate of 91.3 % was obtained using the same acid to leach a Nigerian chalcopyrite by Baba et al. (2013).

2.9. Organic acid leaching

Unlike the alkaline bases and inorganic acids, leaching with organic acids such as oxalic acid, acetic acid and citric acids is not very popular (Habbache et al., 2009; Gharabaghi et al., 2010; and Stuurman et al., 2014). Their weak acidity, possible decomposition and low boiling capacity constitute inherent setbacks. However, the use of organic acids for copper leaching is increasingly considered as a safer leaching agent due to environmental problems of waste acid disposal. Stuurman et al. (2014) observed that the extraction of metal by the reagent occurs through the formation of complexes. Humar et al. (2004) suggested that oxalic acid reacts with copper to form insoluble complexes. Habashi (2009) determined the extraction of copper using citric acid and obtained a high dissolution rate of 76 % at elevated temperature. The ranking of copper extraction rate was: HCl > H_2SO_4 > HNO_3 > $C_6H_8O_7$ (Habbache et al., 2009). The use of organic acid in combination with oxidizing agent such as H_2O_2 has been undertaken to leach cobalt from ores.

Ntengwe (2010) obtained between 72 and 93 % copper recovery when leaching dolomitic-copper ore, but observed the co-dissolution of other metals in significant quantity.

2.10. Acid consumption rates for sulphuric acid and ammonia

The acid consumption capacity of ores or Acid Neutralising Capacity (ANC) is often established in conjunction with the cost of chemicals and grinding cost. According to AmmLeach (2009) and Mathews (2013), the consumption of gangue by ammonia lixiviant is typically less than 5 kg/t ore. Liu et al. (2002) reported that the consumption of NH_3 by gangues is between 102 and 250 kg/t and that of H_2SO_4 ranged between 400 to 700 kg/t ore. John (1999) determined that 1 kg of calcite usually consumes about 0.98 kg of acid. The presence of calcite in ore is a major disadvantage for the use of H_2SO_4 due to its fast leaching kinetics. There are concerns that, with dwindling copper ore grades, the continued use of sulfuric acid for leaching may not be economical in a future of low copper prices.

2.11. Complexometric determination of copper in ores

Because copper is soluble in most aqueous solvents, its determination by complexometric titration is possible. Since copper ores usually contain other metals such as As, Pb, Zn, and Fe, these can interfere with the determination of copper. Interfering elements should be removed or masked prior to copper determination (Christian, 2004). Junar (2014) indicated that selective determination of copper by complexometric titration can be achieved by controlling the pH of the solution through the use of an auxiliary complexing or masking agent, proper titrant, and/ or by controlling the differential rates of the reaction. Complexometric determination of metals like Fe, Cu, Co, Mn, Pb, Zn, Cd, and Al at pH 4 to 7 can be enhanced by controlling the pH using a suitable buffer solution, such as an auxiliary agent (Junar, 2014). Ethylene Diamine Tetra Acetic acid (EDTA) is the most widely used titrant for determination of copper in ores because it is able to form complexes with copper ions in the presence of murexide indicator (Rao et al., 1969; Rao et al., 1994; Ni and Wu, 1997; Roldan et al., 2005).

2.12. Copper recovery from leach solution

The resulting leach solution is usually treated by either precipitation with scrap iron (cementation) for concentrated leach solutions containing 40 kgm^{-3} Cu^{2+} ions, or by electrowinning after solvent extraction. Biswas and Davenport (2013) stated that the copper obtained by cementation process is usually contaminated with iron and is retreated in the smelting furnace or converter. However, the electrowinning process has witnessed improvement in the quantity and quality of copper produced due to development of the solvent extraction process (Kordosky, 2002). Solvent extraction reagents like LIX 64 were superseded by better reagents such as LIX64N, LIX65, LIX84-1, LIX54-100, ketoxime and aldoxime. These display greater selectivity for copper, fast phase separation, stability and good physical performance (Kordosky,

2002). Several authors like, Fu et al. (2011), Wieszczycka et al. (2012) and Ochromowicz et al. (2014) report the successful efficient solvent extraction of copper from copper ammonia complexes using different solvents. According to Soldenhoff (1989), the problems often encountered during solvent extraction include the separation of Fe and Cu from solutions. Chmielewski et al. (2009) and Ochromowicz et al. (2014) found that selective leaching can be used to reduce the presence of Fe in the leachate. The removal of impurities and other undesirable metals from the pregnant leachate solution is usually based on the elemental concentration of metals co-dissolved with copper. For effective recovery of copper from the pregnant leach solution after selective leaching, the solvent extraction and purification processes should be carried out separately.

2.13. Leaching kinetics

Since leaching is a key stage in copper ore hydrometallurgy, kinetic analysis to characterize the mechanism of leaching reaction is a fundamental requirement for effective design of leaching reactors (Ekmekyapar et al., 2012). The parameters often considered during leaching are the overall reaction rate and the variation in reaction rate with time (Awe, 2013). The leaching rates are usually studied on a pilot scale in the laboratory, and the kinetic data obtained from the investigation are subjected to the scaling-up process (Awe, 2010). The influence of experimental variables such as operating rate, temperature, stirring rate, reagent concentration on copper extraction are all relevant. Selection of the best model for interpreting experimental data obtained from laboratory experiments is important for scale-up to pilot scale trials and, ultimately, to full-scale implementation.

2.13.1. Selection of kinetic model for leaching

The requirement for a good engineering model is one that provides the closest representation of reality which can be applied without mathematical complexities. Here, kinetic data is interpreted with a model expressing the leaching rate. The following step processes are distinguished:

1. Diffusion of reacting species to the interface,

2. Adsorption at the interface,

3. Reaction at the interface,

4. Desorption of the products, and

5. Diffusion of the product from the interface.

Any of the steps 1 to 5 may be rate-controlling, depending on the relative velocity with respect to others. The most widely used kinetic model for copper leaching is the heterogeneous kinetic model by Levenspiel (1999), where the reacting materials are found in more than one phase. For non-catalytic reaction of particles with

surrounding fluid, two models frequently encountered are the progressive conversion model and the shrinking unreacted-core model. For expressing the rate of non-catalytic fluid-solid reaction involving copper and a reagent, the shrinking core model is the most popular. According to this model, the reaction of solid-fluid systems takes place on the outer surface of the solid, and this surface shrinks toward the centre of the solid as the reaction proceeds, leaving an inert solid layer called the “ash layer” around the unreacted core (Liu et al., 2010). According to Ekmekyapar et al. (2012), it is assumed that the initial radius of the solid does not change while leaching is in progress.

2.13.1.1. Chemically controlled kinetic model

If the leaching rate is controlled by the surface chemical reaction, then the rate of chemical reaction is much slower than the rate of diffusion and therefore the integrated rate can be determined using Equation 2.19:

$$\text{Rate} = -\frac{dw}{dt} = kAC \qquad (2.19)$$

Where dw is the change in the mass w of the mineral particle, dt is as time increment, k is the reaction rate constant, A is the area of the particle with radius r (=πr^2), ρ is the density and C is the reagent concentration.

The fraction of leached copper, α, is given by:

$$\alpha = \frac{Wo - W}{Wo} \qquad (2.20)$$

where w_o is the initial mass of the particle. Assuming that the particle is spherical, we can substitute $w_o = \frac{4}{3}\pi r_o^3 \rho$ and $w = \frac{4}{3}\pi r^3 \rho$ into Eq. 2.20. By rearranging, we obtain:

$$r = r_0\,(1-\alpha)^{1/3} \qquad (2.21)$$

Noting that $A = \pi r^2$ and $W = \frac{4}{3}\pi r^3 \rho$, we find:

$$\frac{dw}{dt} = \frac{dw}{dr} \times \frac{dr}{dt} = 4\rho\pi r^2 \frac{dr}{dt} \qquad (2.22)$$

Substituting $\frac{dw}{dt}$ in Equation 2.19, we obtain:

$$-4\rho\pi r^2 \frac{dr}{dt} = 4\pi r^2 KC$$

On integration and substituting α, the rate equation becomes:

$$1-(1-\alpha)^{1/3} = \frac{kC}{\rho ro}\, t = kct \qquad (2.23)$$

The mechanism of the leaching process can be determined from experimental data obtained from leaching. For a chemically-controlled process, a plot of $1-(1-\alpha)^{1/3}$ vs

time t, should give a straight line. This type of process is independent of the agitation speed since the rate of mass transfer from the solution to the surface is always sufficient. The chemically controlled process is characterised by strong dependence on temperature because the rate of the chemical reaction increases exponentially with increasing temperature (Awe, 2013, Baba et al., 2013, Parada et al., 2014).

2.13.1.2. Diffusion-controlled kinetic model

Diffusion-controlled kinetic processes are said to be responsible for leaching of a particle when the rate of chemical reaction at the interface is much faster than the rate of diffusion reactant to interface. Thus the concentration of the reactant (C_s) at the interface tends to zero.

Denoting P as the number of the reactant molecules diffusing in time t through a product layer, the diffusion rate can be expressed according to Fick's law:

$$P = AD\frac{dc}{\mathrm{dr}} = -4D\pi r^2\frac{dc}{dr} \qquad (2.24)$$

Where A is the average particle area per copper particle in a given reaction zone, D is the diffusion of the particle through pores to the reaction zone, $\frac{dc}{dr}$ is the concentration gradient, r_0 and r are the initial and final radii of the particle. From the preceding equation, the expression below is obtained:

$$\int_{Cs}^{C} dc = -\frac{P}{4\pi D}\int_{r}^{ro}\frac{dr}{r^2}$$

On integration with the boundary condition $C_s = 0$ at $r = r_0$, an expression for diffusion-controlled leaching is obtained:

$$P = 4\pi D\left(\frac{r_0 r}{r_0 - r}\right)C$$

Where C is a constant. Recalling that the fraction of the copper particle reacted or dissolved is expressed by Equation 2.22:

$$r = r_0\,(1-\alpha)^{1/3}$$

Denoting N as the number of moles of unreacted copper solid present at any time t, M as the molecular weight of the reactant solid and ρ the density of the reactant, the expression below is obtained:

$$N = \frac{4}{3}\pi r^3\,\frac{\rho}{M}$$

so that $$\frac{dN}{dt} = \frac{dN}{dr}\times\frac{dr}{dt} = \frac{4\pi\rho r^2}{M}\,\frac{dr}{dt}$$

From the above expression, the rate of N is proportional to the flux of the material P diffusing through the spherical ore material of thickness, $ro - r$. Therefore,

$$P = -4\pi D \left(\frac{ror}{ro-r}\right) C = 4\pi \frac{\rho}{M} r^2 \frac{dr}{dt}$$

When the above expression is rearranged, we have

$$-\frac{MDC}{x\rho}\, dt = \left(r - \frac{r^2}{ro}\right) dr$$

Where, x is the stoichiometry factor. Integrating the above expression gives the expression below:

$$-\frac{MDC}{X\rho} \int_0^t dt = \int_{ro}^{r} (r - \frac{r^2}{ro})\, dr \text{ and}$$

$$-\frac{MDC}{x\rho} t = \frac{r^2}{2} - \frac{ro^2}{6} - \frac{r^3}{3ro}$$

If Equation 2.22 is substituted into this expression, Equation 2.25 is obtained:

$$1 - \frac{2\alpha}{3} - (1-\alpha)^{2/3} = \frac{2MDC}{x\rho r_0^2} t = kdt \qquad (2.25)$$

In order to determine the mechanism of a diffusion process, a plot of $1 - \frac{2\alpha}{3} - (1-\alpha)^{2/3}$ vs time t is used. A straight line indicates that the leaching process is diffusion-controlled. Diffusion-controlled processes are strongly influenced by the agitation speed since agitation decreases the thickness of the boundary layer. Contrary to a chemically-controlled process, it is only slightly dependent on temperature (Awe, 2013).

2.13.1.3. Determination of activation energy

The Arrhenius equation is used to determine the temperature dependence of chemical reactions. The main parameter of the Arrhenius equation is the activation energy, E_a, which can be used to understand the mechanism controlling a leaching process. According to Awe (2013) and Baba et al. (2013), a leaching reaction is regarded to be diffusion-rate controlled through the porous layer when the activation energy of the process is between 4 and 12 kJ/mol while a chemical-rate controlled through the particle surface reaction is obtained when the activation energy of the process is greater than 40 kJ/mol. Activation energy between 20 and 40 kJ/mol suggests a mixed control mechanism. The Arrhenius equation can be expressed using Equation 2.26:

$$lnk = lnA - \frac{\boldsymbol{Ea}}{\boldsymbol{RT}} \qquad (2.26)$$

Where k is the rate constant, A is the frequency factor, R is the universal gas constant (8.3144 J/mol.K), T is the temperature (K) and Ea is the activation energy. The activation energy is determined graphically by plotting lnk versus $1/T$ with the slope of the graph being equal to $-\frac{Ea}{R}$.

Several authors have determined the activation energy of leaching different copper ores using different lixiviants and found that the leaching mechanism depended on the temperature and type of copper ore undergoing leaching. Relatively little has been published on the activation energy of leaching different grades of copper ore in the presence of chelating reagent and the corresponding leaching mechanism. Liu et al. (2010) investigated the leaching of low grade copper ore in ammonia-ammonium chloride solution and found that the mechanism controlling the process was diffusion through the product layer based on the value of the activated energy determined to be 23.279 kJ/mol^{-1}. You-Cai (2013) obtained a value of 32.3 kJ/mol for malachite ore leaching in $(NH_4)_2CO_3$. Bingöl et al. (2005) obtained a value of 15 kJ/mol^{-1} with $NH_3/(NH_4)_2CO_3$ but indicated that the mechanism controlling the leaching process was diffusion across the product layer. The value of activation energies depends on the nature of the ore and experimental conditions. For instance, Liu et al. (2010) found that in the leaching of low-grade copper ore containing calcium-magnesium and carbonate gangues in ammonia-ammonium sulphate proceeded through two mechanisms: diffusion across the product layer and mixed control based on the kinetic energy of 22.91 kJ/mol obtained. Künkül et al. (2013) found that the activation energy of the alkaline leaching of malachite was 59.6 kJ/mol^{-1}. They suggested that the leaching process followed a mixed kinetic model. Ekmekyapar et al. (2012) investigated the leaching kinetics of malachite in NH_4NO_3 and determined values of 95.10 and 29.50 kJ/mol during the initial stage (surface chemical reaction) and later stage (diffusion through the porous layer), respectively.

A literature search for work on kinetic analysis of copper ore leaching revealed studies on the dissolution kinetics of malachite, chalcopyrite, and other copper sulphide and carbonate ores, while with much less on chrysocolla. None was found on the leaching kinetics of sensor-based pre-concentrated copper ores. Since the kinetics of any chemical process is considered to be of great importance for reactor design, it is against this backdrop that this current work investigates the leaching and kinetics of pre-concentrated classified ore in alkaline and organic lixiviants in order to generate data for leaching application.

2.14. Electrochemistry

Electrochemistry is the most widely used technique for acquiring quantitative information about electrochemical reactions (Parker, 2005). The dissolution of minerals in oxidising media may occur through electrochemical processes (Holliday and Richmond, 1990). Electrochemical techniques such as Cyclic Voltammetry (CV) have been used to investigate the quantities of active chemical species undergoing

oxidation and passivation in solution containing metal ions. The power of this technique lies in its ability to reveal mechanisms and potentials of electrode reactions (Lu et al., 2000). The electrodeposition and dissolution of metals may be through a slow or fast process. The precise cause or mechanisms associated with this phenomenon could be difficult to understand in some instances (Elsherief, 2002). This has led to investigation of the electrochemical behaviour of metals in solution, metal deposition processes, and reactions of electroactive substances to understand the nature and rate of the reactions taking place.

2.14.1. Cyclic voltammetry

Lamping and O'Keefe (1976) indicate that Cyclic Voltammetry (CV) can be conducted to determine the mechanism of metal deposition and electrowinning of metals from solutions. Cyclic voltammetry is based on the measurement of current (i) as a function of voltage (E) (Chander, 1991, Parker and Yoo, 2003), revealing the electrochemical behaviour of metals in solutions over a wide potential range (Majidi et al., 2009; Popescu et al., 2013; Filik et al., 2013). It provides insight into in situ mass transfer of metal ions, including mechanistic and kinetic characteristics. Nacer and Lanez (2013) indicated that the analytical method is a powerful tool for evaluating the diffusion of redox-active reagents in many solutions. Their technique utilises a three-electrode configuration for the electrochemical measurements, involving a non-polarisable reference electrode, a counter electrode and a polarisable working electrode (Parker, 2005). The electron flow in the external circuit is measured and related to the electrochemical reactions. The measurements indicate that the potential at which a redox current commences relates to the onset of a chemical reaction in the system. For a better and clear interpretation of cyclic voltammetry results, Holliday and Richmond (1990) stated that the analysis has to be carried out over different electrode potentials and values calculated based on established thermodynamic data.

Parker (2005) indicated that the rate current is governed by the following fundamental processes:

1. Electron transfer at the electrode surface,
2. Mass transport or transfer (such as oxidant from the bulk solution to the electrode surface),
3. Surface reactions such as adsorption, desorption, precipitation and crystallisation, and
4. Chemical reactions preceding electron transfer (homogenous or heterogeneous)

The potential indicates the rate constant for processes such as electron-transfer at the electrode surface or desorption. Parker et al. (2003) and Parker and Hope (2010) state that, if a redox system remains in equilibrium throughout the potential scan, the

electrochemical reaction is said to be reversible. This implies that the rate of electron transfer is rapid compared to the voltage sweep rate. Thus, if the surface concentrations of oxidised species and reduced species are kept at the values predicted by the Nernst equation, then equilibrium is achieved. The Nernst equation is given by:

$$E = E^{o} + \frac{R.T}{n.F}\, ln\left(\frac{[O]}{[R]}\right) \qquad (2.27)$$

Where E is the applied potential, E^{o} is the standard redox potential, R, T, n and F are the ideal gas constant, temperature, number of electrons transferred per molecule, Faraday's constant, O are oxidised forms of species and R is the reduced form of species respectively. While the Nernst equation describes the concentration changes occurring near the electrode, Parker (2005) states this may not always be the case for all electrochemical processes: A different situation arises when redox reactions are not reversible. The latter occurs when chemical reactions are coupled to the redox process or when adsorption of either reactants or products occurs. This rare situation is usually of greatest chemical interest and for which the diagnostic features and properties of cyclic voltammetry are of particular interest and suited.

2.15. Electrodeposition processes

2.15.1. Copper electrodeposition

Haarberg and Keppert (2009), Majidi et al. (2009) and Popescu et al. (2013) showed that voltammograms generated from cyclic voltammetric scans are useful in understanding the electrodeposition of Cu in solutions. They suggested that the voltammetric curves recorded at different potential scan rates and the corresponding peaks obtained at the cathodic and anodic directions are proportional to the shift in potentials with increasing scan rate. The number of electrons transferred during the reduction and oxidation process corresponds to the electrodeposition of the metal, and can be calculated from the half-peak width. The metal deposition proceeds according to Faraday's laws, which state that the rate of deposition of a metal depends solely on the electric current applied. The Faraday current depends on the kinetics of electron transfer and the rate at which redox species diffuses to the surface. Deposited metal is always crystalline and varies from coarse large-grained deposit to fine-grained powder. It was found that nucleation and crystal growth are the processes occurring during Cu electrodeposition (Grujicic and Pesic, 2005). The nucleation and growth depends on the substrate onto which the electrochemical reduction is performed, its chemical nature and structural state (Chander, 1991). When the rate of nucleation is much larger than the rate of crystal growth, the metal deposited will be fine powder. However, when the rate of crystal growth is much larger than the rate of nucleation, then the deposit will be coarse-grained (Popov et al., 2002; Majidi et al., 2009; Habashi, 2009). According to Grujicic and Pesic (2005), the nucleation process can be observed from current-time transients in a voltammogram due to its sensitivity to nucleation and growth. So many factors are

responsible for the metal deposition processes. For example, powder formation during electrodeposition occurs when the electrode process is diffusion-controlled and coarse grain deposits occur when the process is chemically controlled. The above processes of metal deposited are influenced by current density, electrolyte concentration, stirring, temperature and colloidal substances present in the electrolyte (Awe et al., 2013).

2.15.2. Copper electrowinning

Electrowinning was developed in the 19th century and since then it has become a key component of copper processing technology (Beukes and Badenhorst, 2009). In order to develop the copper electrowinning stage, it is necessary to study the behaviour of copper deposition at the cathode and electrolytic oxidation at the anode. In view of the importance of the process for hydrometallurgical leaching of copper, cyclic voltammetry is applied in the present study. This aimed at understanding all the electrochemical processes occurring during electrowinning of Cu from leachate solution and to explore the large scale application of the process. Copper electrowinning is expected to conform to Faraday's law, Nernst equation and mass transport.

2.15.3. Copper electrolytic processes

2.15.3.1. Faraday's law

As stated in section 2.15.1, Faraday's law states that the mass deposited or discharged at an electrode is proportional to the quantity of electricity passed. In mathematical terms:

$$m = \frac{M.I.t}{v.F} = \frac{Z.I.t}{F} = \frac{Z.Q}{F} \qquad (2.28)$$

Where m is the mass (g) of substance of atomic mass M (g/mol) deposited by the passage of a current I (A) for time t (s), v is the valency of the substance, F is the Faraday constant (96,485 C), Q is the quantity of current flow (coulomb) through the solution and z is the mass of the given element liberated.

For the electrowinning of copper by the addition of electrons, the expression is shown in Equation 2.29:

$$Cu(aq)^{2+} + 2e^{-} \rightarrow \quad Cu(s) \qquad (2.29)$$

During the electrowinning process, cations migrate towards the cathode, and anions go to the anode. Oxidation of a substance takes place at the anode or counter electrode and reduction occurs at the cathode or working electrode. The general expression for oxidation/reduction (Ox/Red) electrochemical reaction can be written according to Equation 2.30:

$$Ox^{n+} + ne^{-} \rightarrow \quad Red \qquad (2.30)$$

Where Ox is the oxidised species and Red the reduced species. From Faraday's law, the total amount of charge spent to reduce M mol of Ox (Q) is:

$$Q = n.F.M \qquad (2.31)$$

Thus, the charge spent per unit time depends on current (I) as follows:

$$\frac{dQ}{dt} = I = n.F.\frac{dM}{dt} \qquad (2.32)$$

Normalising with unit area, the current density, i, can be written as:

$$i = \frac{I}{A} = n.F.\frac{I}{A}.\frac{dM}{dt} \qquad (2.33)$$

When the above expression is related to the Faraday's law, it follows that the current flowing in an external circuit is proportional to the reaction rate at the electrode (Beukes and Badenhorst, 2009).

2.15.3.2. Mechanism of electron transfer

Two main mechanisms are primarily responsible for controlling elementary electron transfer reactions at an electrode. The reactions are either mass transfer-controlled or kinetically controlled.

2.15.3.3. Mass transfer controlled

The diffusion of copper cations from the bulk solution phase to where the reaction occurs at the surface is controlled by mass transfer as expressed in Equation 2.34:

$$Cu^{2+}(bulk) \overset{kd}{\rightarrow} Cu^{2+}(surface) \qquad (2.34)$$

2.15.3.4. Kinetically controlled

This involves the transfer of electrons from the solid electrode to the copper cation at the surface of the electrode as shown in Equation 2.35:

$$Cu^{2+}(surface) + 2e^{-} \overset{kr}{\rightarrow} Cu^{0}(surface) \qquad (2.35)$$

Other phenomenon such as adsorption and formation of phases, coupled with other chemical reactions may also play vital roles in the electron transfer mechanism. Grijicic and Pesic (2002, 2005) suggested that the formation of phases is relevant to the plating of copper on the cathode and involved nucleation and crystal growth steps. Adsorption and nucleation process steps are relevant and also considered in the heterogeneous electron transfer reaction rate mechanism. It is known that copper atoms can diffuse through the solid phase to an appropriate site of the crystal lattice. The overall rate controlling the reaction is the slowest step, which is either mass transfer or reaction kinetics (Parker, 2005). As such for effective copper electrowinning, it is always necessary to determine the rate limiting steps for

optimization in order to maximise conditions for both capital and operating ability of the process (Beukes and Badenhorst, 2009).

2.16. Heterogeneous electron transfer

Heterogeneous electron transfer reactions involve electrons moving from an atom or molecule to another atom or molecule (Bhatti et al., 2006). During the process of electron transfer, the oxidation states of both reactants change. Parker (2005), Schwartz (1994) and Beukes and Badenhorst (2009) suggest that the main reactions governing the reduction and electrodeposition of copper are heterogeneous in nature. The rate constants can be determined by voltammetric and impedance-based methods with respect to the redox species. A smooth polished surface is considered indispensable as a medium for providing fast and easy transfer of electrons between the electrode and the analyte solution containing the redox species (Feeney and Kounaves, 1999).The reactions occurring are usually charge-transfer between individual particles and chemical species in the analyte and is dependent on electrical conductivity, size of particles and distance between them. The rate-limiting step of the electron-transfer reaction process is the charging of the particles. Therefore, most heterogeneous electron transfer reactions are connected with activation energy (Tasior et al., 2008; Alamary et al., 2008; Torma et al; 2003). Many techniques have been used for determining mechanism of heterogeneous, quasi-reversible reactions at electrode surface which include A.C polarography, cyclic voltammetry and other similar techniques (Marcus, 1968, Bhatti et al., 2006).

The rate of electron transfer reactions at the electrode electrolyte solution interface is of great importance in electrochemistry (Bhatti et al., 2006). Since electrode processes are said to occur commonly through a reaction pathway involving specifically adsorbed intermediates, gaining an understanding of the kinetics governing chemical reactions at the surface of the electrode is important.

First order reactions can be used to infer the various heterogeneous electron transfer processes. According to Setterfied-Price (2013) the degree of reversibility can be observed using CV by evaluating the potentials as well as currents. Increase of peak separations of a redox couple with scan rate, is indicative of quasi reversible kinetics. The peaks associated with forward and backward electrochemical process (k_f and k_{rev}) can be represented by rate Equations 2.36 and 2.37:

$$k_f = k_o.\exp(\frac{-\alpha.n.F.(E-Eo')}{R.T}) \qquad (2.36)$$

$$k_{rev} = k_o.\exp(\frac{(1-\alpha).n.F.(E-Eo')}{R.T}) \qquad (2.37)$$

Where ko is the standard heterogeneous rate constants for the redox couple, E is the potential applied on the electrode/solution interface, Eo' is the formal electrode potential different from the standard electrode potential by the activity coefficients, T

is the temperature, R is the gas constant, n is the number of electrons transferred, F is the Faraday constant, and α is the transfer coefficient.

Assuming the net current at the electrode is the sum of the currents in the forward (cathodic current) and backward directions (anodic current), then the total current density for the electrode can be represented as follows:

$$i = ic - ia = n.F.\frac{1}{A}.\left(k_f.Cox_{(surface)} - k_{rev}.Cred_{(surface)}\right) \quad (2.38)$$

Where A (m^2) is the surface area of electrode, $[Cox]$ and $[Cred]$ are the concentrations of oxidant and reductor. Substituting for k_f and k_{rev} from Equations (2.36) and (2.37), the Bulter-Volmer Equation (B-V) describing the rate of electron transfer between the electrode and analyte k_f evaluated based on potential dependence is obtained:

$$i = n.F.\frac{1}{A}.KO.\left(Cox_{(surface)}.\exp\left[\frac{-\alpha.n.F.(E-EO')}{R.T}\right] - Cred_{(surface)}.\exp\left[\frac{(1-\alpha).n.F.(E-EO')}{R.T}\right]\right) \quad (2.39)$$

The Butler-Volmer Equation of current-potential relationship governs all fast and single step heterogeneous electron transfer reactions. This is an indication that k_f and k_{rev} changes rapidly when the potential differs significantly from the standard potential E_0. Thus, when the standard rate constant k_o is very large, the current changes rapidly near the standard potential and the system is in a reversible state. When k_o is small, the system is in irreversible state (Setterfield-Prince, 2013, Noren and Hoffman, 2005; Park and Yoo, 2003; Rubi and Kjelstrup, 2003; Engelken and Doren, 1985).

2.16.1. Mass transport

The movement of chemical species from the bulk solution to the electrode surface occurs through three possible mechanisms: (a) convection also called conveyance, which can be forced or natural (free), is described by hydrodynamics or density/temperature differences. This is the main transport mechanism in the bulk of electrolyte and becomes in efficient in the vicinity of the cathode where the electrolyte movement is restricted by combine viscous force; (b) Diffusion described by a gradient in concentrations; and (c) ionic migration described by a gradient in electrical potential (Pletcher and Walsh, 1993; Zoski, 2007; Awe, 2013).

Experimental conditions of the electrode reactions are generally adopted to minimize the effects of migration in the system. This is achieved by providing a large quantity of inert electrolyte that does not interfere with the electrode reaction, thus allowing only diffusion and convection mechanisms for consideration.

The ionic migration is the movement of charged species through the electrolyte due to an electrical potential gradient. The current of electrons through the external circuit must be balanced by the passage of ions through the solution between the electrodes (at both electrodes, anions to the anode and cations to the cathode). The

process of mass transport is only significant if the potential gradient is sufficiently large. It has been found that, in most electrowinning practices, diffusion usually dominates ionic migration since most of the solutions used in electrochemistry system are too conducting (Ettel et al., 1975; Pletcher and Walsh, 1993; Awe, 2013).

In the case of diffusion, mass transport of species occurs whenever there is a chemical change at the surface. An electrode reaction converts starting material to product (O → R). Close to the electrode surface, there is a boundary layer in which the concentration of O is lower than in the bulk. While the opposite is true for R, O will diffuse towards the electrode and R away from the electrode. Diffusion is concentration-gradient dependent. Due to the nature of the discharging process at the cathode, the decrease of the metal ion concentration at the electrode interface is usually compensated by diffusion of a fresh supply of metal ions from the bulk of the solution. The rate of the diffusion is given by the expression:

$$Rate\ of\ diffusion = \frac{DA}{\delta}.\Delta C \qquad (2.40)$$

The expression for the rate at which ions are discharged when current is applied is shown below:

$$Rate\ of\ discharge = \frac{I}{nF} \qquad (2.41)$$

Where, I is the current applied, n is the valency of the metal, F is the Faraday's constant, A is the surface area of the electrode, D is the diffusion coefficient, δ the thickness of the boundary layer and $\Delta C = C - Ci$ is the difference between the chemical species concentrations at the bulk of the solution (C), and the electrode interface (Ci). It then follows that at a steady state, the diffusion and discharged rates of the metal are equal. Assuming that at the steady state there is no change in concentration with time and that the conveyance inside the diffusion layer is significantly smaller than the diffusion component, the following expression in Equation 2.52 is obtained (Beukes and Badenhorst, 2009 and Awe, 2013):

$$\frac{I}{A} = \frac{nFD}{\delta}.\Delta C \qquad (2.42)$$

The rate of consumption (or regeneration) is equal to the rate change of concentration difference across the diffusion layer. During electroplating of metal, increasing the current density, $\frac{I}{A}$, will ultimately lead to an increase in concentration difference ΔC of metal ions, principally due to the rapid depletion of metal ions at the interface as a result of metal deposition.

2.17. Electrodeposition of copper from alkaline solution

For efficient electrowinning of copper, it is necessary to understand its behaviour and deposition at the cathode and electrolytic oxidation at the anode from ammonia based solution used for leaching copper ore. Electrodeposition of Cu involves the

reduction of the metal ions from the electrolyte solution. Hayes (2003) showed that the reaction occurring in the aqueous medium at the cathode can be expressed using Equation 2.43:

$$M^{n+} + ne^- \rightarrow M \qquad (2.43)$$

The electrodeposition of high purity copper cathode by electrowinning process requires copper rich electrolyte. A high copper concentration is very important in the electrowinning process because it ensures that enough copper ions are available for deposition at the cathode surface without applying a high overvoltage, in addition a better smooth high purity and readily marketable cathode copper can be recovered (Koyama et al., 2006; Oishi et al., 2007). According to Hayes (2003) and King and Davenport (2011), the copper electrodeposition process at the cathode is given by the following reaction:

$$Cu^{2+} + 2e^- \rightarrow Cu \quad E^0 = + 0.34V \qquad (2.44)$$

Hayes (2003), Lou and Huang (2005), Cifuentes et al. (2014) and King and Davenport (2011) found that some metallic impurities (Fe, Mn, Pb, and Zn) can also be deposited at potentials close to that of copper. According to Cifuentes et al. (2014) and Ntengwe et al. (2010), iron is an impurity deposited at the cathode relative to the other metals:

$$Fe^{2+} + 2e^- \rightarrow Fe \quad E^0 = - 0.44V \qquad (2.45)$$

$$Fe^{3+} + 3e^- \rightarrow Fe \quad E^0 = - 0.037V \qquad (2.46)$$

The anode material can be either a sacrificial anode or an inert anode. If a sacrificial anode is used, the electrode reaction is electrodissolution that continuously supplies the metal ions. During electrodeposition with an inert electrode, both the cathode and anode are immersed in an alkaline electrolyte with the formation of oxygen gas at the anode (Lou and Huang, 2005; King et al., 2011):

$$H_2O \rightarrow H^+ + OH^- \rightarrow \frac{1}{2}O_2 + 2H^+ + 2e^- \quad E^0 = - 1.23V \qquad (2.47)$$

Those electrodeposition systems based on ammonia chemistry are known for their diverse speciation of aqueous cuprous and cupric ions (Grujicic and Pesic, 2005, Popescu et al., 2013). Many researchers have studied copper electrodeposition processes from a solution containing Cu(I), Cu(II) and NH_3, $(NH_4)_2CO_3$, NH_4Cl, Cu(I)-Cu(II)-NH_3-$(NH_4)_2SO_4$. There is evidence that the cathode current efficiencies could be up to 100% (Koyama et al., 2006). Koyama et al. (2006) carried out analysis on the electrodeposition of copper using solutions containing copper ions at different current densities and agitation speed. They showed that copper is deposited on the cathode from ammoniacal solutions containing Cu(I). They also suggested that Cu ion activity is the sum of the concentrations of NH_3 and NH_4^+ in the electrolyte containing the copper metal. The authors suggested that Cu(I) and Cu(II) are

respectively stable as either $Cu(NH_3)_2^+$ and $Cu(NH_3)_4^{2+}$ in neutral and alkaline solutions. They showed that the redox reaction of Cu(I)/Cu can be expressed as:

$$Cu(NH_3)_2^+ + e^- \rightarrow Cu + 2NH_3 \qquad (2.48)$$

The expression in Eq. (2.63) can be written as:

$$E = E^O - \frac{RT}{F} ln \frac{aNH3^2}{aCu(NH3)2^+} \qquad (2.49)$$

According to Koyama et al. (2006) and Oishi et al. (2007), the relationship between the Cu(I) and Cu(II) concentrations, the equilibrium equation among Cu, $Cu(NH_3)_2^+$ and $Cu(NH_3)_4^{2+}$ and the equilibrium constant can be expressed as shown in Equation 2.50:

$$Cu(NH_3)_4^{2+} + Cu \rightarrow 2Cu(NH_3)_2^+ \text{ where } k = 10^{3.38} \qquad (2.50)$$

Popescu et al. (2013) found that copper electrodeposition can be carried out using different electrodes with solutions of NH_4Cl, $(NH_3)_4SO_3$ and NH_4NO_3 containing copper ion. The presence of chloride and nitrate ions does not prevent the copper electrodeposition, but the nitrate tends to react with the newly deposited copper. Oishi et al. (2007) suggested that it is possible to carry out electrowinning of copper at a lower cell voltage by using NH_4Cl and NH_4NO_3. Majidi et al. (2009) showed that the electrodeposition process of copper occurs via a two stage electrochemical reaction:

$$\text{Stage 1} \quad Cu^{2+} + e^- \rightarrow Cu^+$$

$$\text{Stage 2} \quad Cu^+ + e^- \leftrightharpoons Cu$$

Dachen et al. (1997) and Brown and Wilmot (1985) investigated the electrodeposition of copper from ammoniacal cupric complexes by cyclic voltammetry. They found out that Cu (I) and Cu (II) exist as their ammine complexes in aqueous solutions containing dissolved ammonia. The cyclic voltammograms obtained comprised two cathodic and two anodic peaks at different scan rates. This suggests that the cathodic reduction and electrodeposition of copper (II) ammine complex proceed in a stepwise from Cu(0) through Cu(I) ammines with the reduction occurring in two stages where each stage of the reduction corresponding to a single electron transfer. This corroborates the findings by Majidi et al. (2009). It has been shown that the Cu(II)/Cu(I) redox couple is a reversible system and takes place at the cathode according to Equation 2.51:

$$Cu(NH_3)_4^{2+} + 1e^- \leftrightharpoons Cu(NH_3)_2^+ + 2NH_3 \qquad (2.51)$$

The second step is the reduction and electrodeposition of copper. The Cu(I)/Cu(0) deposition process proceeds as follows:

$$Cu(NH_3)_2^+ + 1e^- \leftrightharpoons Cu + 2NH_3 \qquad (2.52)$$

Darchen et al. (1997) and Aravinda et al. (2000) indicated that the difference in the number of ammonia ligands co-ordinated to Cu(I) and Cu(II) complex ions suggest that the redox reaction (Eq. 2.66 and 2.67) consists of several steps and the overall reactions involve the decoordination of ammonia ligands. Brown and Wilmot (1985) concluded that the actual reduction of the copper from the complex occurs on the triammine complex

$$Cu(NH_3)_3^{2+} + 1e^- \leftrightharpoons Cu(NH_3)_3^{+} \qquad (2.53)$$

Darchen et al. (1997) found that, for ammoniacal copper (II) complexes, electrodeposition of copper metal from the solution occurs at the cathode. During the anodic electrochemical process, the cuprous complex undergoes oxidation in order to regenerate the starting cupric complex. Darchen at al. (1997) showed the oxidation is also a two-step thermodynamic process:

$$Cu(0) + Cu(NH_3)_4^{2+} \rightarrow 2Cu(NH_3)_2^{+} \qquad (2.54)$$

$$Cu(NH_3)_2^{+} + \frac{1}{2}O_2 + 2NH_4^{+} + 2NH_3 \rightarrow 2Cu(NH_3)_4^{2+} + H_2O \qquad (2.55)$$

During electrochemical oxidation, various coordinating species (NH_3, Cl^-, and H_2O) in the solution are involved in the process. Giannopoulou et al. (2009) indicated that the reduction of copper from ammonia complexes can be carried out by potentiometry. Pecequilo and Panossian (2010) suggested that cyclic voltammetry can be used to understand the electrodeposition mechanism of copper from a strike alkaline bath. Schwartz (1994), Majidi et al. (2009), Ntengwe et al. (2010) and Popescu et al. (2013) showed that the deposition of Cu from Cu-ammonia complexes consists of steps, each involving the transfer of electrons. The process depends on factors like the concentration of electrolyte, applied voltage and agitation.

Chapter 3

Materials and methods

3.1. Introduction

Accurate mineralogical and chemical analysis is required for the understanding of ore mineralogy and gangue content in an ore for process control and optimization (Neighbour, 2010; Anderson, 2014; Iyakwari, 2014). In copper ore, elements such as As, Mn, As, Co, Mn, and Fe could be a concern for processing. This chapter describes different analytical techniques employed for mineralogical and chemical analysis of samples throughout the thesis. A description is given of the reagents used, experimental procedures followed and, in some instances, the instrumental specifications and reasons for adopting some experimental approaches are stated. The pre-concentration strategy for ore samples used in this research is discussed under the materials section.

All instrumental analyses were carried out at Camborne School of Mines (CSM), Penryn Campus, Cornwall, United Kingdom. The laboratories are equipped with many analytical instruments that enabled the successful study of the mineralogy, geochemistry and mineral chemistry within ore samples. Mineralogical analyses were conducted using QEMSCAN®, X-Ray Diffraction (XRD), Scanning Electron Microscopy (SEM) and Near Infrared Spectroscopy (NIR). The bulk elemental analyses were conducted using Portable X-Ray Fluorescence Spectrometer (PXRF), and Inductively Coupled Plasma Mass Spectrometry (ICP-MS).

3.2. Materials

Near infrared sensor-based pre-concentrated and classified porphyry copper ore samples were used in this study. Samples were obtained from a copper mine in the Atacama district, northern Chile. A total of 32 samples (size between 5 and 10 cm) were considered for mineralogical characterization.

3.2.1. Ore pre-concentration

Each sample was subjected to different analytical methods of analysis before near infrared sensor-based pre-concentration. Samples were classified into three main groups: product, middling and waste, after Iyakwari et al. (2013), (Figure 3.5). The NIR pre-concentration strategy employed is aimed at eliminating both calcite and clay (muscovite/kaolinite) rich particles as gangue (Iyakwari and Glass, 2016). Hence, the classification was carried out as follows:

1. Product: are samples with all NIR spectra showing chrysocolla and or hematite, chlorite, biotite pattern. This group includes featureless NIR spectra.

2. Waste: are samples with all NIR spectra showing calcite and or muscovite characteristics.

3. Middlings: are samples with NIR spectra containing individual spectra of both waste and product category. This is likely since individual mineral grains are smaller than the pixel size of 2.9 by 9 mm, and particles scanned consisted of at least two pixels (which may be distinct). This group may require further liberation to a size not less than the pixel size and rescanned.

3.2.1.1. NIR spectra mapping

The NIR line scanner at Camborne School of Mines (CSM) measures each spectrum at a dimension of 0.29 by 0.9 cm. Each sample was an average of between 2 and 2.7 cm. In order to properly map each sample, individual samples were divided into three sectors measuring 0.9 cm each, corresponding to NIR spectrum height, with width measuring 0.29 cm (Figure 1). The number of spectra produced by individual samples per sector depended on particle size and shape. Details on NIR background, procedure of NIR data acquisition, instrumentation and data pre-treatment are described in Iyakwari et al. (2013) and Iyakwari and Glass (2015). Typical NIR-active minerals fieldscan are shown in Figures 3.2 to 3.4.

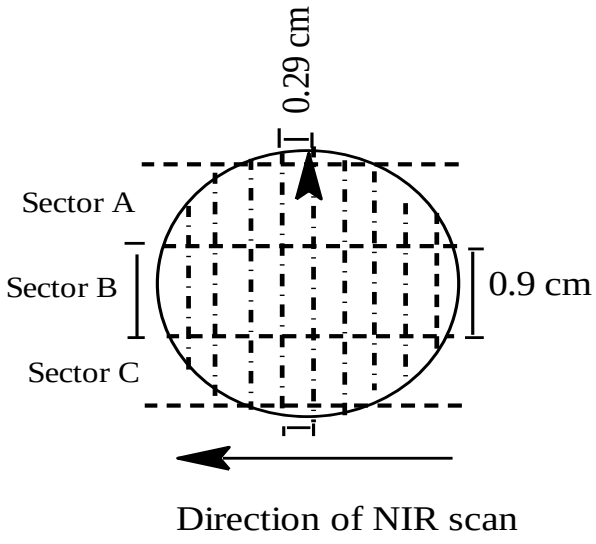

Figure 3.1 Samples marked for directional scanning and spectra/mineral mapping (after Iyakwari et al., 2016)

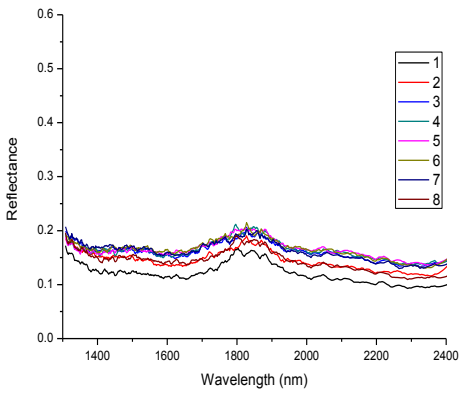

Sector a

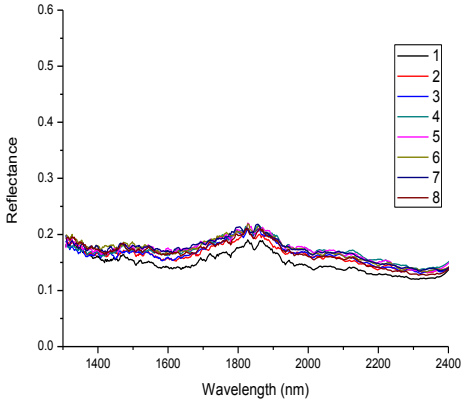

Sector b

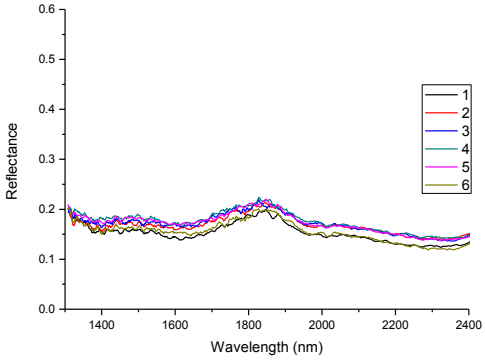

Sector c

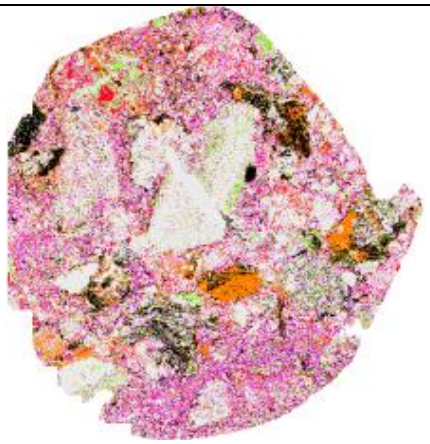

Sector d

Figure 3.2 (sectors a, b and c) – NIR spectra of product sample. While d is the QEMSCAN® fieldscan image of sample at 10 µm X-ray resolution, showing only NIR active minerals present in the sample

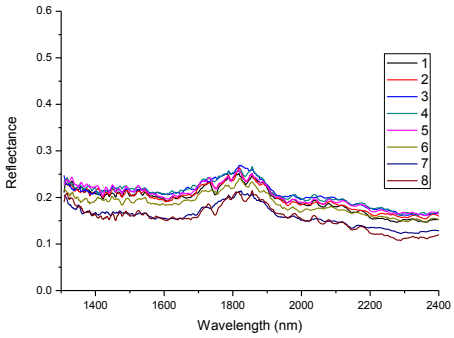

Sector a

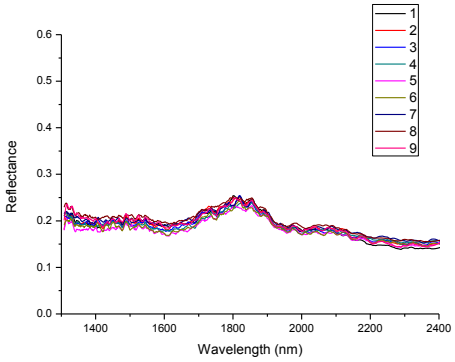

Sector b

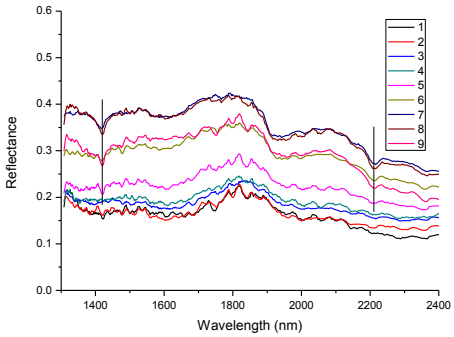

Sector c

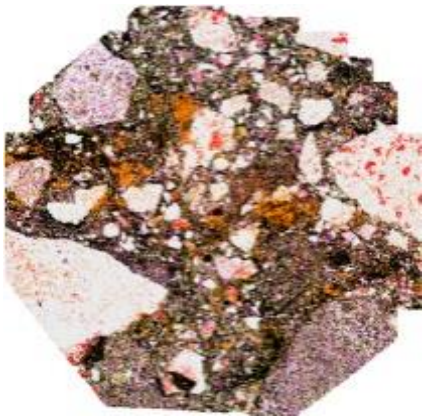

Sector d

Figure 3.3 (sectors a, b and c) – NIR spectra of middling While d is the QEMSCAN® fieldscan image of sample at 10 µm X-ray resolution, showing only NIR active minerals present in the sample

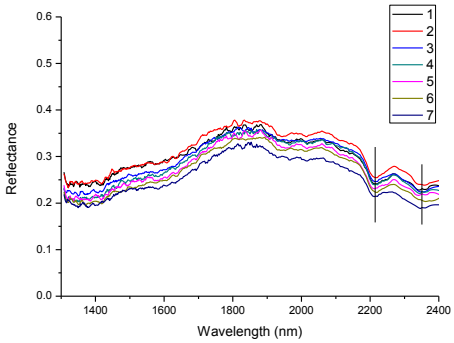

Sector a

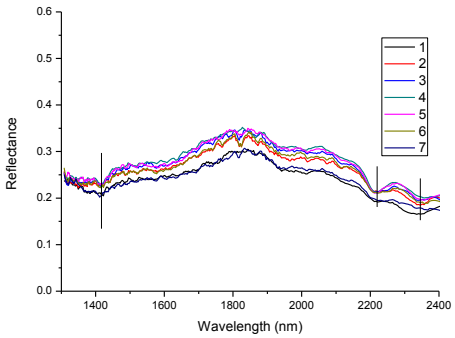

Sector c

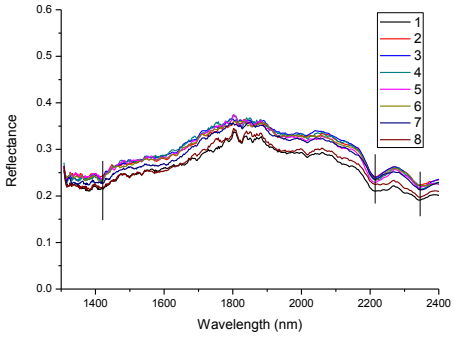

Sector b

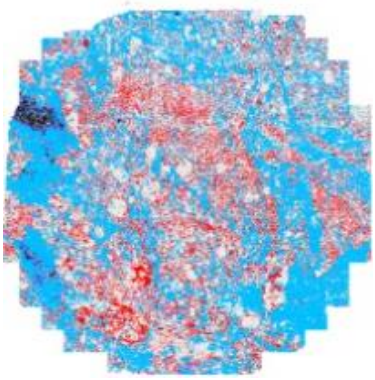

Sector d

Figure 3.4 (sectors a, b and c) –NIR spectra of waste While d is the QEMSCAN® fieldscan image of sample at 10 µm X-ray resolution, showing only NIR active minerals present in the sample

Details of the pre-concentration strategy can be found in Iyakwari (2014) while the analytical techniques used in this work are presented in the sections below.

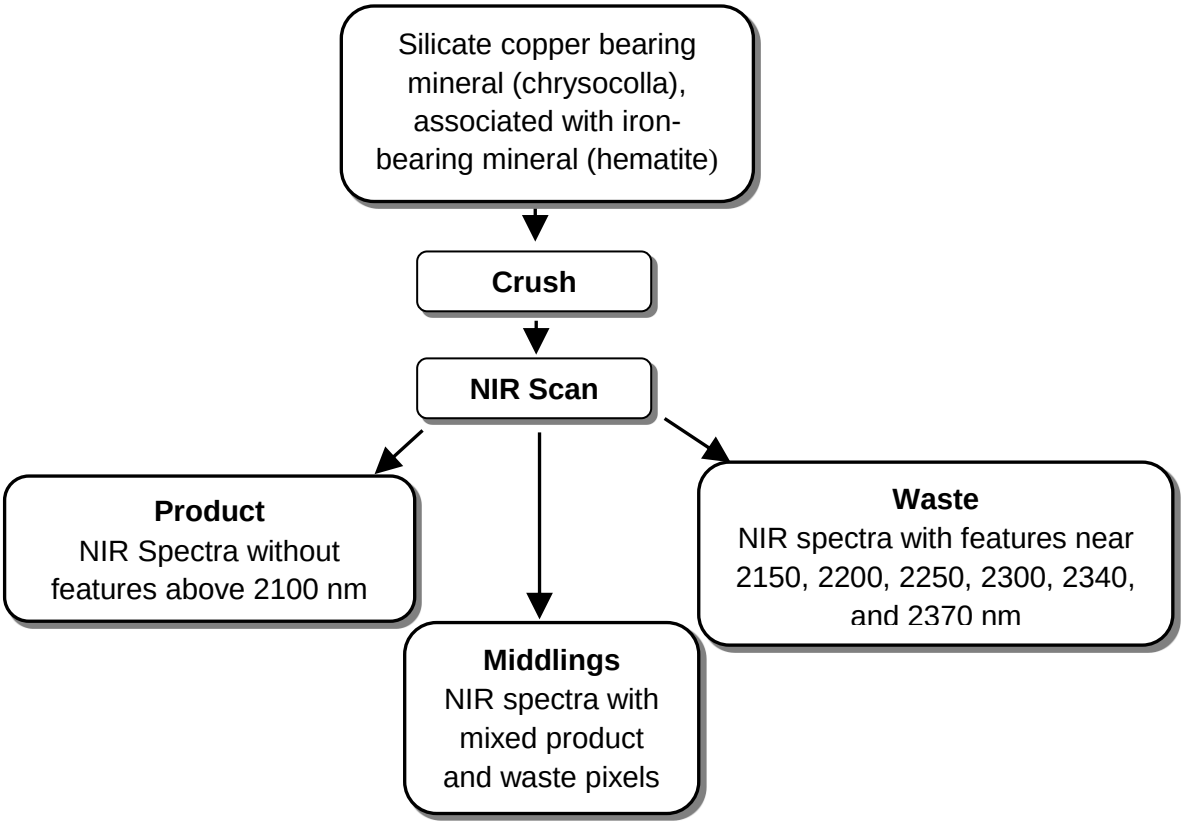

Figure 3.5. NIR Classification strategy of Chilean copper ore (after Iyakwari et al., 2013)

3.3. Particle size analysis

3.3.1. Comminution

The crushing and grinding of the ore samples to liberate the minerals and gangue was carried out on both individual samples and classified ore samples (product, middling and waste) separately. Samples were crushed using a Retsch steel jaw crusher (to -3mm), milled using a tungsten–carbide Tema pot, and then homogenised and milled prior to sieving to the desired size fractions. Machine particle size analysis was used to classify the samples into the multiple desired size fractions using stack sieves called a nest. To avoid plugging, trapping and collecting undersized particles in each sieve, which could lead to undesired results, the stacked sieves were not overloaded with the feed sample. The stacked sieves were shaken automatically with a machine sieve stack shaker. The shaker used for the sieving analysis at Camborne School of Mines was manufactured by Pascal Engineering. It has an inbuilt digital timer and is designed to accommodate 12 sieve stacks at a time. The timer is used to set the shaking time. During this, the time was set to 20 minutes. To mitigate noise arising from vibration of the machine, the shaker is enclosed in a sound insulation box or cabinet capable of reducing sound levels by 20 dB. The table of the shaker only moves in gyratory motion at a speed rotation of 2 rpm, thus allowing for materials to be spread over the entire surfaces of the mesh of each

sieve. The table of the shaker lifts and falls at 300 jolts per minute over short distances such that each copper-bearing particle on the mesh is given maximum chance of passing through the aperture of the mesh. The machine shaker is presented in Figure 3.6. To minimise cross-contamination of samples, cleaning of the tungsten-carbide grinder between samples by pulverising with barren quartz was done. Thereafter, sieves were cleaned with compressed air and brushes between every sample and then washed with acetone before the next set of analyses. The Pascal number 1 Inclyno test sieve shaker is 640 mm tall and 200 mm wide. The machine has the following features:

Electrics: 110 V to 230 V

Weight: About 69 kg

Recommended sieve diameter: 100 mm diameter × 15 or 200 mm diameter × 12

Figure 3.6 Pascal Engineering machine sieve shaker at CSM (CSM, 2015), A) Stacked sieves, B) timer C). Acoustic enclosure it's about 640 mm tall and 200 m wide.

3.4. Mineralogy

3.4.1. X-Ray Diffraction (XRD)

XRD was used to generate data on the bulk mineralogy of the samples. The analysis was based on the qualitative identification of minerals and estimation of their abundance on the basis of crystalline structure and peak height (Moore and Reynolds, 1989). X-rays emanating from a source are scattered by the crystal lattice in the minerals, with the diffraction of the X-rays creating both constructive and destructive interferences at a distance between the samples and the detector

(Neighbour, 2010; Anderson, 2014; Iyakwari, 2014). The patterns generated by the XRD scan are smoothed and interpreted using the JCPDS PDF-2 (2004) database and Bruker EVA software V.10.0.1.0.0 to match known diffraction patterns stored within a database (www.bruker.com). Results are presented in section 4.3.1. For further details see Iyakwari (2014).

Figure 3.7 XRD Siemens D5000 at CSM (CSM Laboratory, 2015).

3.4.2. QEMSCAN®

Mineralogical composition of samples was determined by QEMSCAN®, after Iyakwari (2014). The QEMSCAN® is an automated SEM instrument that provides quantitative mineralogy of mineral samples through EDS analysis and data processing using associated software (Anderson, 2014). The principle of operation of QEMSCAN® is based on a scanning electron microscope, capable of examining mineralogical and textural parameters. Samples to be determined were prepared as epoxy resin mounts with Epofix resin and polished to a 1 μm finish before carbon coating. Each sample, having an average size of between 2 and 2.7 cm, was mapped using the fieldscan measurement mode in order to obtain a full image of the sample being measured. A beam step interval of 10 μm was used across the sample surface (i.e. an X-ray was acquired every 10 μm across the surface grid). This resulted in the acquisition of typically more than 3,500,000 individual X-ray analysis points per sample and is dependent on the size/area of the sample as resin is ignored.

The QEMSCAN® instrument is an automated technique for rapid mineralogical assessment, including the spatial mapping of minerals, via combined Scanning Electron Microscopy and Energy Dispersive X-ray Spectrometry (SEM-EDS) (Gottlieb et al., 2000; Pirrie and Rollinson, 2011). Mineralogical determinations are based on a comparison of sample spectra from each point of analysis with a library of mineral

spectra. The detection limit of elemental analysis, from which minerals are identified, is around 3 wt.% (Anderson et al., 2009; Iyakwari, 2015).

Since the QEMSCAN® instrument has a 3 wt.% lower limit of detection for individual elements, XRD was used to validate the QEMSCAN® data. Levels of minor and trace minerals found by QEMSCAN® have been shown to be significantly below the detection limit of XRD (Rollinson et al., 2011; Iyakwari et al., 2016). The instrument was used to resolve quantitative modal mineralogy, evaluate the distribution of trace minerals; additionally it was used to provide data for minerals that had not previously been identified by XRD. Despite drawbacks such as poor detection of elements with atomic numbers less than 6 and weak signals obtained with N, O and F elements (Williamson et al., 2013), the QEMSCAN® technique gave good precision in the analysis of samples in this work.

In each case the results obtained are presented in mineral wt. % and/or vol. % (Chapter 4). Mineral mass (wt. %) which is density weighted, was calculated using the density taken from the primary mineral list, which is input by the operator (average for the mineral) while mineral volume (vol. %) of the different minerals in the ore was calculated by the number of pixels allotted to that mineral divided by the total number of pixels in the samples (area %, like a point count).

3.5. Mineral chemistry

3.5.1. Portable X-Ray Fluorescence Spectrometer (PXRF) elemental analysis

XRF is a non-destructive analytical technique used to identify and determine the concentration of elements in a sample (Gill, 2014). The non-destructive process is independent of the chemical form of the element or material composition (Glanzman and Close, 2007; Neighbour, 2010; El-Taher, 2012). XRF analysis is based upon the generation of characteristic X-rays from sample irradiated by an energetic beam which is capable of measuring the concentrations of different elements in the sample.

Qualitative elemental analysis of samples was carried out using a Portable Thermo Scientific Niton FXL 950 FM-XRF analyser (PXRF), on loan to CSM for 1 week during 2013 (Figure 3.8). The equipment did not require any form of sample preparation before performing analyses, depending on the material been analysed. The desktop PXRF analyser employs the Energy Dispersive Spectrometry (EDS) method. X-rays penetrate samples at depths of approximately 1 to 2 mm. The PXRF analyser has an 8 mm diameter scanning window, with integrated camera which shows the surface being scanned. It consisted of a sample mount (stage), which could be set to rotate when scanning. PXRF was used principally to determine the elemental composition of minerals containing Cu and associated metals in the samples. Samples were ground to powder and sieved to different size fractions before analysis. A 10 to 20 g portion of powdered particle size fraction was taken and placed on the sample chamber and the “mining Cu/Zn” mode selected from the method set up. The equipment was set to scan for 150 seconds per sample while rotating. For large non-

ground fragments of ore samples the stationary mode was used to scan. Results are presented in (Chapters 4 and 5) while a summary of the samples determined is shown in Table 3.1. It should be noted that the PXRF analysis in this work is only qualitative due to uncertainty in calibration of the instrument.

Table 3.1 Summary of PXRF analysis of samples (p = product, m = middling, w = waste, + = determination)

Number	Ore category	Nature of ore determined		
		Particle fragment	Powder fraction	Sieved particle size fractions
1	P	+	+	+
2	P	+	+	+
3	P	+	+	+
4	P	+	+	+
5	M	+	+	+
6	M	+	+	+
7	M	+	+	+
8	M	+	+	+
9	W	+	+	+
10	W	+	+	+
11	W	+	+	+
12	W	+	+	+

Figure 3.8 PXRF Niton FXL 950 FM-XRF analyser at CSM (CSM Laboratory, 2013)

The PXRF analysis is qualitative and was aimed at estimating the concentration of available metals. The detection limit of the instrument ranged from an estimated

value of 1 % for most trace elements. The detection limit is usually counting-time and sample matrix dependent (Glanzman and Close, 2007).

3.5.2. Inductively Coupled Plasma Mass Spectrometry (ICP-MS)

ICP-MS is an analytical technique used for elemental analysis of samples in solution. The ICP-MS has superior detection capabilities for trace elements compared with XRF, and can potentially measure elements down to parts per trillion (ppt) levels, under standard and accurate calibration. The instrument has advantages over atomic absorption and atomic emission spectroscopy (ICP-AES) (Townsend et al., 1998), in that it can handle both simple and complex matrices with minimum interferences and has superior detection limits.

Samples for ICP-MS analysis were first digested in aqua regia by weighing 1g of sample into a 50 ml polyethylene tube and 6 mL HCl and 2 ml HNO_3 was added. Samples were left for 15 minutes at room temperature before heating in a block digester at 90 ˚C for 60 minutes. After cooling the samples were made up to 50 ml with de-ionised water and filtered. A further dilution (1:50) was made in 5% HNO_3 and the solutions were run on the ICP-MS, Agilent Technology, Model 7700 for determination of elemental concentrations (Figure 3.10).

Within the ICP-MS, argon plasma is first generated by the collision of the argon gas with oscillating electrons, the latter produced by a strong alternating current of radio frequency with a copper coil outside the gas flow. Electrons are continually stripped off from the argon as a result of collisions between electrons and argon atoms. The process continues until the rate at which electrons are lost is equal to the rate of electron gain (Gill, 2014). The process causes immense heat, with temperatures approximately reaching those of the surface of the sun. Thus, at equilibrium the following takes place (Gill, 2014):

1. The sample solutions for ICP-MS analysis are typically introduced into the ICP plasma as an aerosol, by aspirating a liquid sample into a nebulizer (Ikehata et al., 2008; Gill, 2014). Intense heat causes dissociation of chemical compounds
2. The absorbed energy gives rise to excitation and ionization transitions
3. Spectral lines are emitted characteristic to their elements
4. Each spectral line generated is analysed by the ICP’s spectrometer
5. The information from the ICP is translated to output of specific elements in ppm, ppb, ppt, depending on the input. The data from the ICP-MS analyses is presented in chapters 5 and 6.

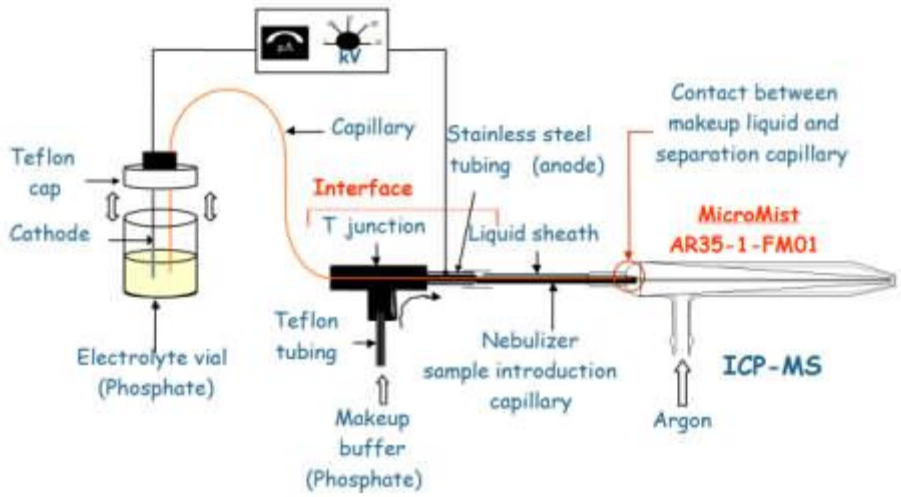

Figure 3.9 ICP-MS flow diagram (Agilent, 2015)

Figure 3.10 ICP-MS Agilent technologies, 7700 at CSM (CSM Laboratory, 2015)

Due to high concentration of metals in solution above the detection limits for the ICP-MS, samples were diluted for accurate results. For every set of analyses a blank solution was run in duplicate to assess the precision of the data. Experimental results obtained revealed that the ICP-MS produces very good precision with variability of 1.2 % between sample batches with a maximum standard deviation of 0.1 % for the metals (Cu, Mn, Co and Ni) determined. Details of the step-by-step method of sample preparation and analysis can be found in Appendix 3.1.

3.5.3. Scanning Electron Microscope (SEM)

The Scanning Electron Microscope (SEM) was used to provide images of the surfaces of polished blocks of residue samples and elemental determination. The SEM uses a high voltage beam of focused electrons to obtain high levels of

magnification using a Back-Scattered Electron (BSE) detector to produce high quality images. The greyscale of BSE images is based on average atomic number to help identify mineral phases (Reed, 2005). This enabled the quantitative and semi-quantitative chemical analysis. The interaction of electrons with atoms in samples generates signals that give information on the sample topography and compositions. The SEM equipment used for the analyses was a JEOL JSM-5300LV Low Vacuum SEM equipped with EDS ISIS software (Figure 3.11).

Figure 3.11 JEOL JSM-5300LV at CSM (CSM Laboratory, 2015)

The pre-concentrated ore samples (product and middling) were first crushed, ground, homogenised and sieved to -63 + 45 µm fraction. Details of the crushed particle size fraction can be found in Table 5.2 (chapter 5). Samples consisted of ground particles embedded in 30 mm diameter blocks which were prepared into polished epoxy resin blocks. The polished blocks were coated with a 25 nm conductive coating of carbon to prevent charging under electron bombardment which can reduce image quality and affect EDS analysis.

Analyses were undertaken in a high vacuum mode and images captured at an acceleration voltage of 25 kV. The EDS X-ray detector was linked to an Oxford ISIS system for quantitative chemical analysis (Reed, 2005). The analyses were carried out on the basis of morphology and grain composition using both secondary electron and BSE mode. The SEM photomicrograph in Figure 4.21a to c and elemental data obtained provided information on the examined surface texture and chemistry of the minerals in the blocks. The SEM operating parameters and conditions are presented in Table 3.2 while results are shown in section 4.3.3.

Table 3.2 Scanning electron microscope specifications (JEOL, 1993).

Operating parameters	Machine conditions
Accelerating voltage:	25 kV
Electron gun:	Tungsten filament
Vacuum modes:	High pressure 7×10^{-4} pa, 5×10^{-6} torr
Detectable elements:	^{6}C to ^{92}U. X-ray analysis detection to 1%
Imagery modes:	SEI, BEI (BSE)
Specimen stage:	Eucentric goniometer x = 80 mm, y = 40 mm, Z = 5 to 48 mm, T = -10 to 90, R = 360

3.5.4. Leaching experiments

Leaching experiments were conducted in batches in a 500 ml reactor with a four-neck split flask in a thermostatic heating mantle with a temperature control unit (Figure 3.12). The temperature of leaching was adjusted using the thermostatically-controlled electric heating mantle. Agitation was provided by a mechanically overhead stirrer, which could be set to any required stirring speed. For all leaching experiments, 250 ml of the leaching solution was placed into the glass reactor. The leaching solution was prepared by dissolving ammonium chloride (NH_4Cl) powder or oxalic acid dihydrate ($H_2C_2O_4.2H_2O$) powder in de-ionised water. After the desired reaction temperature is attained and required stirring speed is reached, a known weight of solid sample was introduced into the reactor and leached over a period of time. At regular predetermined time intervals, 5 ml of leachate was withdrawn from the reactor and filtered using Whatman 540 filter paper for analysis of leached metal concentration with ICP-MS, unless otherwise stated. At the end of the experiment, the leached slurry was filtered and the residue dried in a UNITEMP drying cabinet at an approximate temperature of 30 ˚C for 7 days. Finally, both the dried residue and filtrate were analysed for chemical and mineralogical compositions using ICP-MS and XRD methods described in sections 3.4.1 and 3.5.2. Filtrates obtained from ore leachates and residue samples were diluted before ICP-MS analysis. Three different tests were performed on the classified ore particle size fractions which include: analysis of head grade for available copper for leaching, leachates obtained after ore leaching and digested residue for determination of extraction efficiency. A summary of samples tested is shown in Table 3.3 while the step by step method of the analyses can be found in Appendix 3.1. All reagent chemicals used were freshly prepared and purchased from VWR Chemicals International Ltd, UK and were used without further purification.

Table 3.3 Summary of analyses of samples with ICP-MS (+ = sample type determination, p = product, m = middling)

Ore category and particle size fractions		Analyses		
		Head grade	leachate	residue
P	-63 + 45 μm	+	+	+
P	- 90 + 63 μm	+	+	+
P	-125 + 90 μm	+	+	+
M	-63 + 45 μm	+	+	+
M	- 90 + 63 μm	+	+	+
M	-125 + 90 μm	+	+	+

Figure 3.12 Leaching experiment set up; A) Overhead mechanical stirrer, B) reactor, C) pH probe, D) heating mantle, E) sampling pipette, F) measuring cylinders

3.5.5. Cyclic voltammetry

The Cyclic Voltammetry (CV) analyser instrument is a computerised general purpose potentiostat/galvanostat select model. It has a fast digital function generator and high-speed data acquisition circuitry. The system has a potential control range of ± 10V and a current range of ± 250 mA. The instrument has the capability of measuring current down to pico Amperes, with a dynamic range of experimental time scales. The potentiostat/galvanostat in the analyser has four-electrode configurations which can be used for liquid/liquid interface measurement.

The electrochemical analyser used in the study is CHI Electrochemical Analyser Model 660D. It consists of a 100 ml polarographic cell fitted with a three-electrode configuration. The working electrode consisted of 0.08 cm^2 and 0.5 cm^2 coiled platinum wire, the counter electrode was made of platinum, and the reference electrode was Ag/AgCl in a 3 M KCl solution. All potentials are quoted with reference to the standard hydrogen electrode. Potentiodynamic experiments were conducted across a range of cathodic and anodic potentials over selected scan rates. All the experiments were carried out at room temperature with 100 ml of leachate or synthetic solution (Figure 3.13). The leached ore slurry was filtered prior to CV while the synthetic solution of tetra-ammine copper (II) sulphate [$Cu(NH_3)_4SO_4$] was prepared using copper sulphate pentahydrate ($CuSO_4.5H_2O$) and de-ionised water. All chemicals were purchased from VWR Chemicals International Ltd, UK, and used as received without further purification. The solutions used for the experiments were high purity reagent grade chemicals freshly prepared before each experiment.

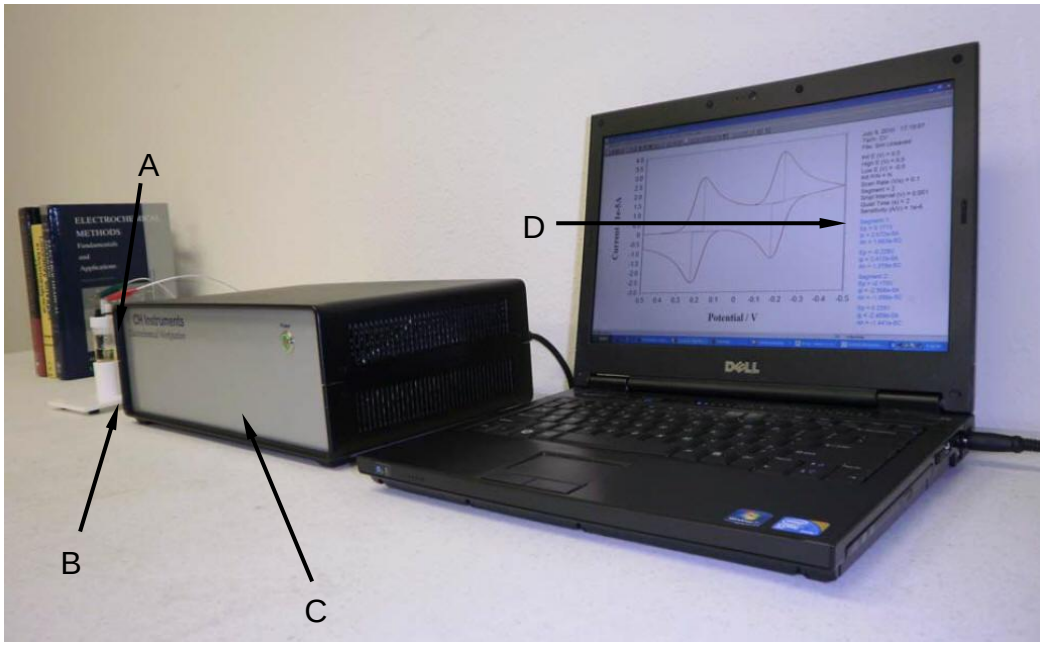

Figure 3.13 The CHI 660D electrochemical analyser at CSM (after Electrochemical analyser, 2015), A) Electrodes, B) polarographic cell, C) analyser , D) computer

The CV technique is considered efficient because it can be carried out on small portions of solution. Other perceived advantages include: Versatility, non-destructive nature and relatively quick ease of information generation. Chapter 7 contained the result of electrochemical analysis.

3.5.6. Complexometric analysis

The technique involves titrating metal ions with a complexing agent (ligand) commonly referred to as complexometric titration. It involves transferring ions into complex ions and the equivalence point determined using metal indicators.

For complexometric determination of copper, a known weight of the size fraction was transferred into a 250 ml Erlenmeyer conical beaker. 20 ml of a mixture of concentrated sulphuric acid and hydrochloric acid (1:1) was added and gently heated on a hot plate until the ore was digested. The content was cooled to room temperature, 100 ml of de-ionized water was added, and the solution was rewarmed gently until all the salt that had formed was dissolved. The solution was filtered using Whatman 540 filter paper. 25 ml aliquots of the solution were taken and ammonium chloride-ammonia buffer (pH 7-9) was added until the solution turned completely blue and the precipitate that formed had dissolved. 2 to 3 drops of murexide indicator were added to the aliquot solution and the copper in the solution was determined by the titrimetric method until the colour changed from yellow (green) to deep violet. In each case, the analysis was carried out in triplicate. Complexometric tests were carried out on three particle size fractions of classified ore using Na_2EDTA concentrations of 0.01 M and 0.05 M at solid-to- liquid ratio of 1 g/100 mL and 2 g/100 mL (Table 3.4) while a step-by-step method of the analysis is outlined in appendix 3.2. The choice of the particle sizes in Table 3.4 was aimed at finding optimum particle sizes for leaching studies. This is because the dissolution of copper particles have been shown to increase with decreasing particle sizes with better extraction rates (Baba et al., 2013).

Table 3.4 Summary of complexometric analysis of samples (+ = measured)

Sample category	Effect of particle size			Effect of Na_2EDTA con.		Effect of solid-to-liquid ratio	
	-90+63 μm	-125+90 μm	-180+125 μm	0.01 M	0.05 M	1 g/ 100 mL	2 g/ 100 mL
Product	+	+	+	+	+	+	+
Middling	+	+	+	+	+	+	+
Waste	+	+	+	+	+	+	+

The effect of Na_2EDTA concentration, solid-to-liquid ratio and particle size were varied to ascertain their influence during the analysis. The Na_2EDTA was prepared using de-ionised water and standardised using zinc chloride solution prepared from zinc chloride pellets of known weight. The percentage copper extracted or dissolved in the ore was calculated using the value of molarity of Na_2EDTA found using the relationship:

Concentration of EDTA = EDC_A

Volume of EDTA = EDV_A

Concentration of given solution of Cu ore = CuC_B

Volume of given solution of Cu ore = CuV_B

Thus, $EDC_A \times EDV_A = CuC_B \times CuV_B$

$$CuC_B = \frac{EDCA\ X\ EDVA}{CuVB}$$

Cu in ore (Y) = CuC_B X 63.54 g/L

Amount of copper in given sample (%) = Y X $\frac{100}{1000}$

De-ionised water was used during all experiments. Table 3.5 contained the list of all the chemical reagents used, which were sourced from VWR Chemical International Ltd, UK.

Table 3.5 List of chemical reagents, purity (%)

Reagents	Purity
NH_4Cl	> 99%
Na_2EDTA	99%
$H_2C_2O_4.2H_2O$	99%
$CuSO_4.5H_2O$	-
NH_3	> 28%
H_2SO_4	98 %
HCl	38 %
HNO_3	> 68%
Murexide	Passed test
NH_3/NH_4Cl buffer	-
Coiled platinum wire	> 99.9%

Chapter 4

Ore mineralogy and chemistry

4.1. Introduction

In order to have a clear understanding of the behaviour of different minerals and gangue in the leaching test, this chapter focusses on the mineralogy and elemental composition of the ore studied in this research. Quantitative and qualitative analyses were carried out with the following instrumental techniques: Data from PXRF, XRD, SEM, QEMSCAN® and near infrared analysis of pre-concentrated copper ore samples after Iyakwari (2014) were collated. The minerals determined in the ore were grouped according to the following mineral divisions: silicates, oxides, carbonates and phosphates while gangue in the ore was further re-classified into three gangue types. The different gangues type was further considered on the basis of their reactivity toward chemical reagents and their implications to leaching. The ores were assessed in terms of properties according to ore particle mineralogy and size fraction. The data obtained using QEMSCAN®, PXRF and SEM for either particle samples and/ or size fractions of the pre-concentrated ore analyses were correlated.

4.2. Ore mineralogy

Complex copper ore minerals are increasingly expensive to process and require detailed analysis of the ore component to establish the most viable techniques and methods for recovering copper. The analysis should include all the minerals present and gangue that could lead to consumption of chemicals and energy resulting in additional cost in the processing chain. Poor interpretations of mineralogy may lead to poor recoveries and huge capital processing cost (Neighbour, 2010).

A total of 32 samples labelled 1-32 were analysed using QEMSCAN® and NIR by Iyakwari (2014) and results obtained are presented in Appendix 4.1 and 4.2. The analyses indicated the presence of a variety of minerals (Table 4.1).

Table 4.1 Minerals present in the classified ore (after Iyakwari, 2014)

No.	List of minerals	Chemical formula
1	Chrysocolla	$(Cu, Al)_2H_2Si_2O_5(OH)_4.n(H_2O)$
2	Cuprite	Cu_2O
3	Malachite	$Cu_2CO_3(OH)_2$
4	Biotite	$K(Mg,Fe^{3+})_3AlSi_3O_{10}(OH,F)_2$
5	Ankerite	$Ca(Fe^{3+},Mg,Mn)(CO_3)_2$
6	Hematite	Fe_2O_3
7	Calcite	$CaCO_3$
8	Muscovite	$KAl_2(AlSi_3O_{10}(F,OH)_2$
9	Kaolinite	$Al_2SiO_5(OH)_4$
10	Chlorite	$(Mg,Fe^{2+})_5Al(AlSi_3O_{10})(OH)_8$
11	Quartz	SiO_2
12	Plagioclase	$(Na,Ca)(Si,Al)_4O_8$
13	K-feldspars	$KAlSi_3O_8$
14	Tourmaline	$(NaFe_3^{2+})Al_6(BO_3)_3Si_6O_{18}(OH)_4$
15	Apatite	$Ca_5(PO_4)_3(OH,F,Cl)$

Other mineral phases found in low concentrations were zircon, rutile and ilmenite. The percentage of copper in each sample was calculated from the copper bearing minerals in the ore. QEMSCAN® modal mineral data showed that, of the three copper-bearing minerals present, chrysocolla constitutes about 94.4 wt. % and malachite and cuprite 5.3 wt. % and 0.4 wt. %, respectively.

The cumulative mineral data presented in Table 4.2 is a reflection of the total concentration of each mineral in the classified ore. For the purpose of leaching the samples were considered according to each category shown in Table 4.2 and not as individual samples. Cumulative values (wt. %) obtained infer that the concentration of copper is product > middling > waste. Thus, the data revealed that some minerals have significant copper concentrations when considered individually (Appendix 4.1), however their concentration in the whole rock is insignificant, as shown in Table 4.2. The pattern of mineral concentration of chrysocolla and K-feldspar followed a systematic order from product to middling to waste. The inverse pattern, where the waste ranked higher than the middling and product, was observed for muscovite, and ankerite. A different pattern, where the waste, middling or product ranked high in certain minerals was observed for kaolinite, biotite, tourmaline, chlorite, plagioclase, cuprite, malachite, calcite, quartz and apatite. Amongst all the minerals, apart from chrysocolla, the cumulative values of muscovite, biotite, chlorite, quartz, K-feldspar, hematite, and calcite were well above 1.3 wt. % in the pre-concentrated ore samples.

However, K-feldspar, chlorite, quartz, and hematite all have significantly higher values than the rest of the minerals in the ore. Incidentally some of them are considered gangues. Gangue content is discussed under the section 4.3.2 implication of minerals for leaching.

The minerals in the ore are considered under the following classes: silicates, oxides, carbonates and phosphates. Each mineral class was further divided into subclasses, according to its mineralogical content and susceptibility to leaching (Appendix 4.1 and 4.2). The silicate class consisted of the following minerals in the ore: chrysocolla, muscovite, kaolinite, biotite, tourmaline, chlorite, quartz, K-feldspar and plagioclase. Of all the silicate minerals, the major copper-bearing silicate is chrysocolla (Iyakwari and Glass, 2015). Amongst the silicate minerals group, three of them are iron-bearing (biotite, tourmaline and chlorite) while the non-iron bearing are chrysocolla, muscovite, kaolinite, quartz, K-feldspar and plagioclase (Iyakwari, 2014). The oxide mineral classes in the ore include: hematite and cuprite while cuprite is a copper-bearing mineral, hematite is iron-bearing. The carbonate mineral class in the ore includes: malachite, calcite and ankerite. Malachite is copper-bearing whilst ankerite is iron-bearing and calcite contains pure carbonate (Iyakwari, 2014). The only phosphate mineral in the ore is apatite, a non-iron bearing mineral (Appendix 4.1). Thus, the total percentage by volume of all the different classes of the minerals in the ore varies with the different classes. Silicates account for the highest content in the ore at about 76.3%, oxides at 15.1%, carbonates at 8.3% and phosphates only 0.3% by volume (Appendix 4.1). It was found that of the three copper bearing minerals in the ore, chrysocolla constitutes about 94.4%, and malachite and cuprite are 5.3% and 0.4% by volume, respectively (Figure 4.1).

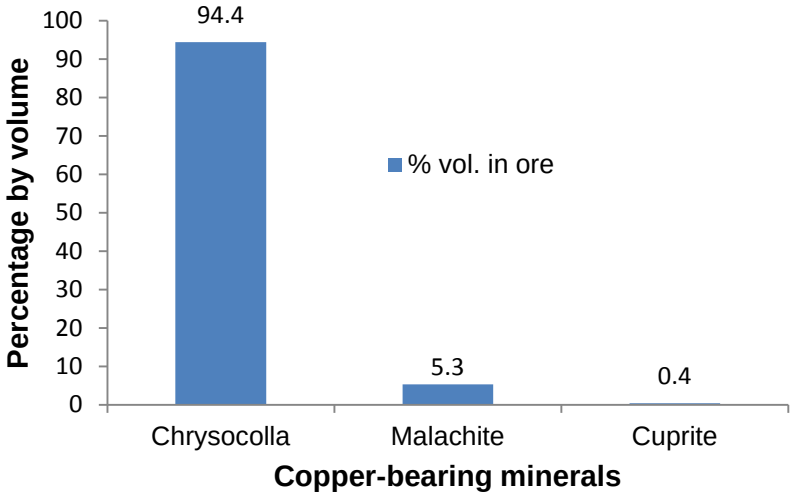

Figure 4.1 Volume % of copper-bearing minerals in the ore samples

Table 4.2 Cumulative mineral data for product, middling and waste samples (wt. %) (modified from Iyakwari, 2014)

NIR Classification	Silicates									Oxides	Carbonates			Phosphates	Others (Trace phases)	Total
	Cu-bearing	Non-Cu-bearing									Cu-bearing	Non-Cu-bearing				
	Non-Iron-bearing			Iron-bearing			Non-Iron-bearing			Iron-bearing	Non-Iron-bearing			Iron-bearing	Non-Iron-bearing		
	Chrysocolla	Muscovite	Kaolinite	Biotite	Tourmaline	Chlorite	Quartz	K-feldspar	Plag-feldspar	Hematite	Cuprite	Malachite	Calcite	Ankerite	Apatite		
Products	7.95	2.86	0.08	9.36	0.32	9.36	14.77	23.20	0.17	28.58	0.02	0.32	1.91	0.34	0.20	0.57	100
Middlings	4.36	3.07	0.49	5.10	0.73	6.14	14.71	15.75	0.31	47.35	0.00	0.00	1.30	0.52	0.00	0.20	100
Waste	0.68	3.75	0.01	7.33	0.45	21.54	34.85	14.35	1.07	1.65	0.01	0.15	11.49	0.62	0.35	1.70	100

4.2.1. Volume % of minerals in the ore samples

In terms of contribution by volume from different minerals, quartz ranked very high with about 27 %, as shown in Figure 4.2. The concentration of quartz varied in the samples cutting across the different mineral classes (silicate, oxide, carbonate and phosphate). Most of the high values were recorded from the middling and waste samples (Iyakwari, 2014), as shown in Appendix 4.1. After quartz, the most abundant mineral is K-feldspar, with about 17.2 vol. %. Hematite and chlorite constitute 15.1 vol. % and 16.4 vol. %, respectively. The most significant hematite content is in the middling samples (Appendix 4.1). Samples 11 to 14 have higher values than the rest while samples 16, 17, 19, 28, 31, 25, 21, and 23 have the highest chlorite contents of the ore (Appendix 4.1). Since these two minerals are iron-bearing, they are responsible for the high iron content in the sample (Figure 4.2 and Appendix 4.2). With cuprite, kaolinite, malachite, apatite, ankerite, tourmaline, plagioclase-feldspar, chrysocolla, muscovite, calcite and biotite, the percentage contribution by volume of these minerals is 0.01%, 0.01%, 0.2%, 0.3%, 0.5%, 0.5%, 0.7%, 3.2%, 3.5%, 7.6% and 7.7%, respectively (Figure 4.2). The total contribution from these minerals put together is less than that of quartz even when compared with that from hematite and chlorite. However, three out these minerals are the hosts to the copper content in the ore (Appendix 4.1).

The contribution of iron-bearing minerals (biotite, tourmaline, chlorite, hematite, and ankerite) is shown in Figure 4.3. The calculated iron content in Appendix 4.2 appears to correlate with the presence of these minerals shown in Figure 4.3.

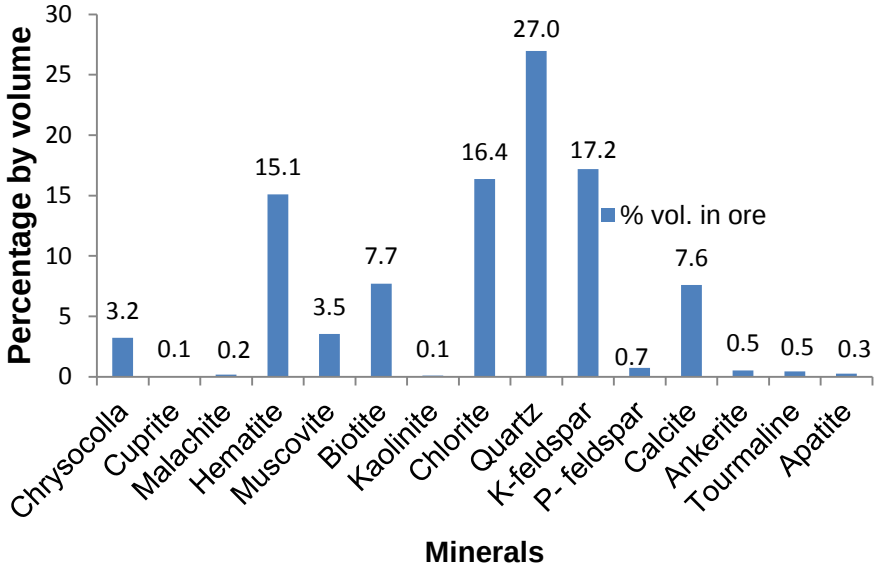

Figure 4.2 Volume % of different minerals in the pre-concentrated ore samples

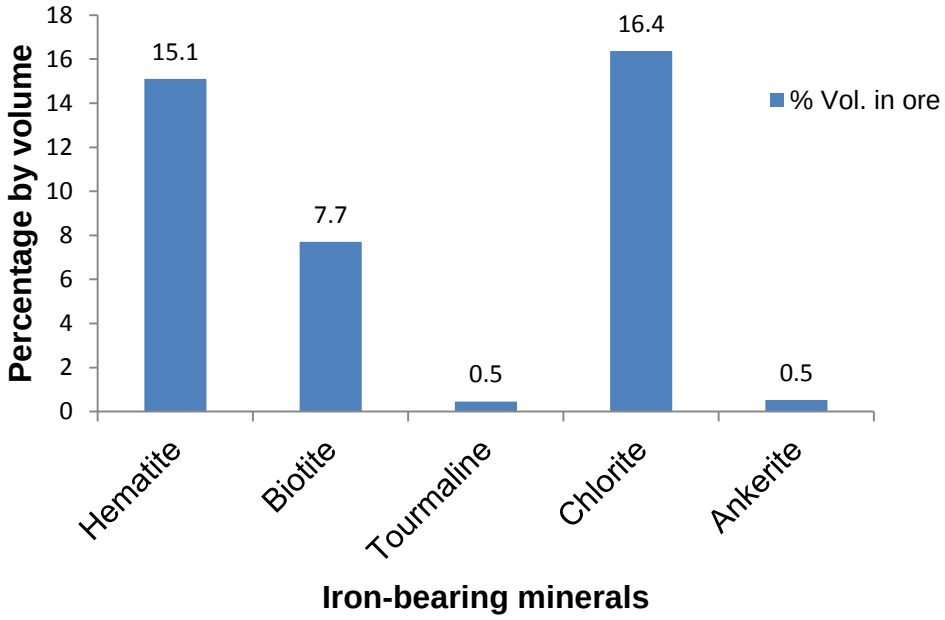

Figure 4.3 Volume % of iron-bearing minerals in the classified ore samples

The calculated value of the contribution of these minerals based on the different categories: product, middling and waste from Appendix 4.1 and Table 4.2, is presented in Figures 4.4 to 4.6. The copper-bearing minerals make up a total of 8.0 % by volume with chrysocolla having the most significant concentration amongst the three copper-bearing minerals. Hematite, K-feldspar and quartz have concentrations of 28.7%, 23.3% and 14.8% by volume in the ore category. Apart from biotite, with a concentration of 9.4%, all the other minerals have concentrations of less than 3.0% by volume. The trend in pattern of concentrations of these minerals is hematite> K-feldspar > quartz > biotite > chlorite > chrysocolla > muscovite and calcite (Figure 4.4).

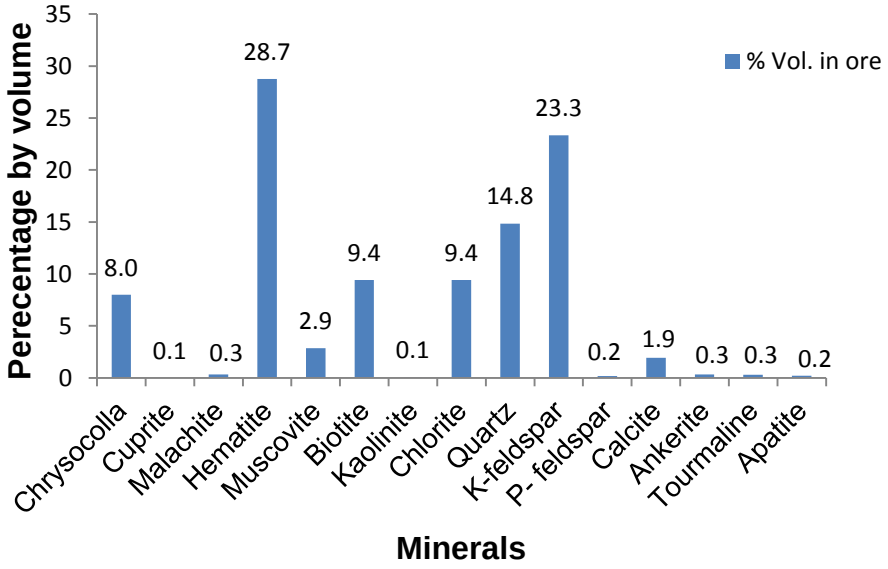

Figure 4.4 Volume % of different minerals in the product sample

The chrysocolla concentration in the middling category is 4.4% by volume while copper concentration in the other copper-bearing minerals is insignificant (Figure 4.5). Hematite has a very high value of 47.5 vol. % by volume, an indication that the middlings are a source of high iron-bearing minerals in the ore in addition to chlorite: the other iron bearing minerals in the samples do not have significant concentrations when compared to hematite (Appendix 4.1 and Table 4.2). Next to hematite in abundance is K-feldspar and quartz with concentrations of 15.8 and 14.7 vol. %. Other minerals present include 6.2 vol. % chlorite, 3.1 vol. % muscovite, 5.0 vol. % biotite, 1.3 vol. % calcite, and less than 1 vol. % by volume of cuprite, malachite, kaolinite, plagioclase, ankerite, ankerite and apatite.

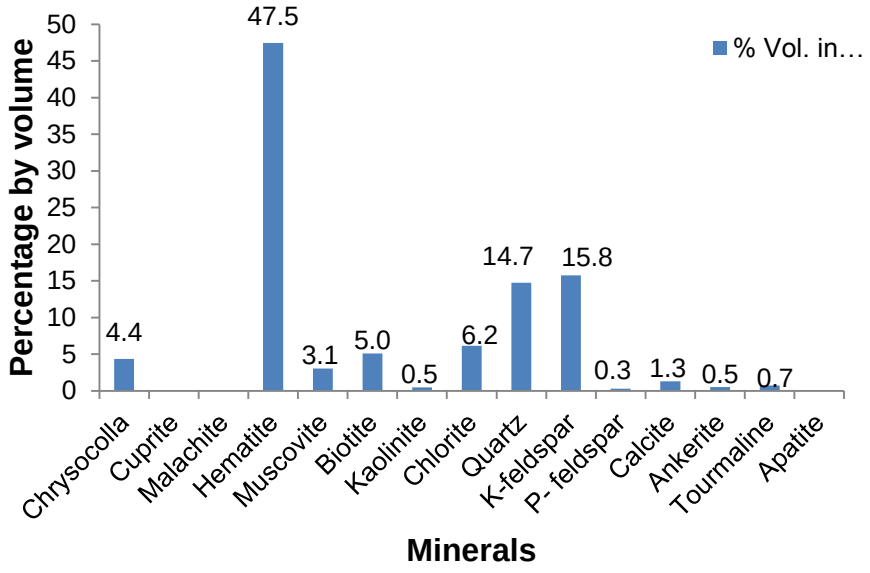

Figure 4.5 Volume % of the different minerals in the middling samples

In the waste fraction, quartz is not abundant, with a value of about 35.5%. Next to quartz is chlorite and K-feldspar with concentrations of 22 and 14.6 vol. %, respectively (Figure 4.6). The concentration of calcite is very significant in the waste category compared to the product and middlings, with a value of 11.7 vol. %. Biotite is 7.5 vol. % while plagioclase, hematite and muscovite have concentrations of 1.1, 1.7 and 3.8 vol. %, respectively. The rest of the minerals, i.e. chrysocolla, cuprite, malachite, kaolinite, ankerite, tourmaline, and apatite, all have concentrations of less than 0.8 vol. % by volume (Figure 4.6). It is also observed that, while hematite accounted for the high iron content of the product and middlings, the case is different with the waste where chlorite is the dominant iron-bearing mineral. Similarly, the concentration of copper bearing mineral is very low, an indication that the waste has less content of the metal.

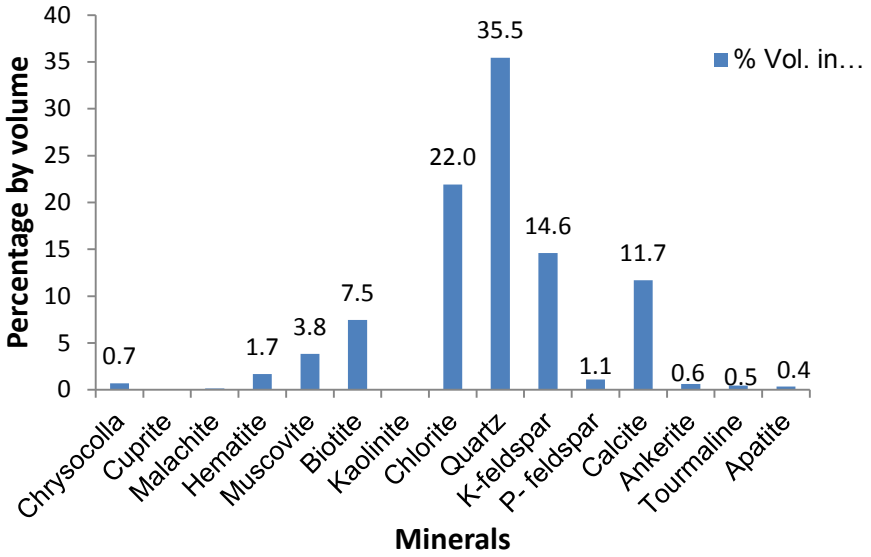

Figure 4.6 Volume % of different minerals in the waste samples

The trend in cumulative concentration of minerals in the ore categories (Table 4.2) appears to correlate with that of the particle samples in Appendix 4.1. Although a slight variation is observed in the pattern in Figures 4.4 to 4.6 due to the varying % of certain minerals in high concentration relative to others in the particle samples shown in Appendix 4.1, the discrepancies are negligible. However, it is observed that a strong positive correlation between the concentration of certain minerals: chrysocolla, chlorite, quartz, hematite, calcite and K-feldspar in Appendix 4.1 and the cumulative data of these minerals in Table 4.2 exist.

4.2.2. Functional group analysis of samples

Analysis of data and discussion in this section is focussed on the classification of the minerals on the basis of their functional groups (CO_3^{2-} and OH^-). This is useful in determining the behaviour of minerals on the basis of chemical activity. Since the near infrared sensor-based sorted ore classification was carried out according to functional group activity, identifying minerals with respect to their activity is essential for leaching application, details can be found in Iyakwari (2014). Appendix 4.2 present the concentration of minerals in ore samples based on the activity of hydroxyl (OH^-) and carboxyl (CO_3^{2-}) functional groups and calculated concentration of iron and copper in ore samples from QEMSCAN® data, after Iyakwari (2014).

The total concentrations of the different minerals in all the samples in terms of OH^- activity were found to be: muscovite, 8.53%, biotite, 7.83%, kaolinite, 26.34%, chlorite, 22.85%, tourmaline, 6.61%, chrysocolla, 20.71%, apatite, 3.34%, and malachite, 15.38% (Appendix 4.2). In comparison with Appendix 4.1, it is observed that kaolinite, chlorite, chrysocolla and malachite showed

more activity toward the OH^- functional group compared to muscovite, biotite, tourmaline and apatite minerals whose concentration are less than 10%.

Only three minerals (malachite, calcite and ankerite) are CO_3^{2-} active with the NIR spectroscopy in view of the presence of carboxyl functional group in the minerals. These minerals contained carbonate in them, as typified by their NIR behaviour. Malachite has a carbonate concentration of 27.13%, while the carbonate concentration in calcite is 59.95% and 58.14% in ankerite (Appendix 4.2). It is observed that malachite exhibits both OH^- and CO_3^{2-} NIR activity. However, calcite is considered the most significant CO_3^{2-} mineral in the ore (Appendix 4.2). Values shown in the Appendix 4.2 indicate that hematite is an oxide mineral and does not show any activity in the NIR spectra (Iyakwari, 2014).

A comparison of the cumulative functional groups and calculated values of iron and copper is presented in Figures 4.7 and 4.8. In the product samples, the calculated cumulative value shows that OH^- and CO_3^{2-} in the minerals is 5.73 and 1.43%, respectively. The middling is 5.07 and 1.08% and the waste is 9.43 and 7.29% (Iyakwari, 2014). It was found also that the high calcite mineral content observed in the wastes samples (Appendix 4.1and Figure 4.6): appear to correlate with the high CO_3^{2-} functional groups in Appendix 4.2. It can be observed that ore category with high concentration of either of this functional group relates to their solubility and reactivity tendencies during leaching. From the cumulative averages shown in Figure 4.8, a strong correlation between iron concentration and iron-bearing minerals in the ore samples is found to be related to their concentrations in the samples shown in Appendix 4.1. The same can be said of the copper concentration in the copper-bearing minerals. For middlings, it was observed that most of the middling samples ranked very high in hematite compared to product and waste while for copper content the product ranked higher with significant hematite content compared to the middling and waste. On the other hand, the waste ranked very high in quartz compared with the middling and product (Appendix 4.1 and Figures 4.4- 4.6).

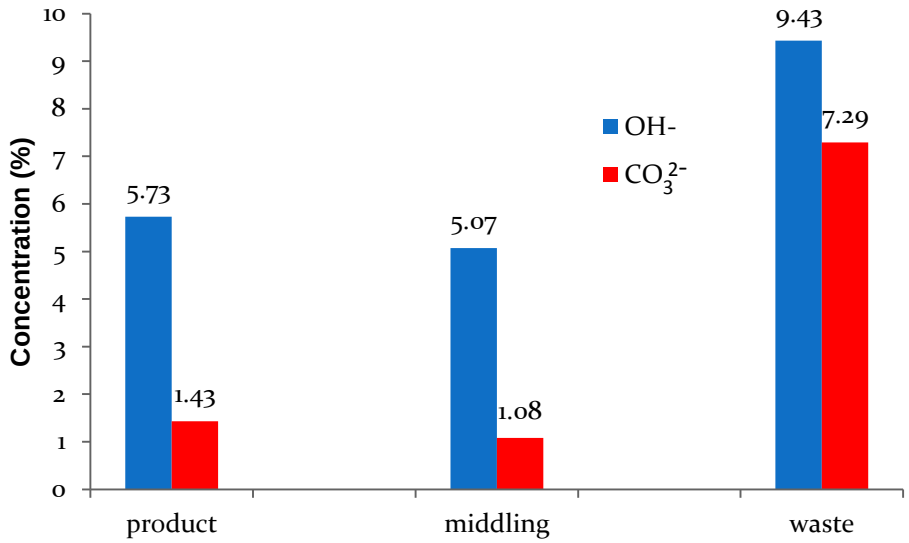

Figure 4.7 Carboxyl and hydroxyl concentrations in the product, middling and waste fractions

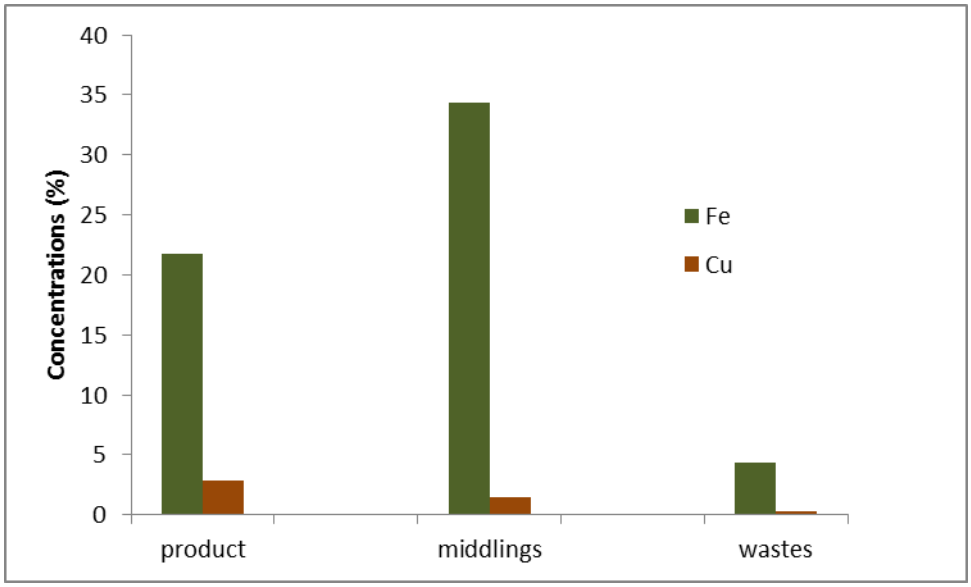

Figure 4.8 Concentration of Cu and Fe in the product, middling and waste fractions

It is to be noted that functional groups of these minerals ore fractions are considered to have significant influence on the solubility and other chemical behaviour of the fractions during leaching. This is because the capacity of the hydroxyl and carboxyl to form hydrogen bonds with chemical reagent is responsible for their solubility, which is what gives the copper oxide ores their hydrophilic property. It is therefore, an important property that differentiates the copper oxide ore minerals in this research from the copper sulphide ores. Thus, the absence of these functional groups is responsible for the poor solubility of the sulphide ore with chemical reagents.

4.2.3. Susceptibility of minerals to leaching

Since this study is aimed at leaching NIR sensor-based sorted ores according to three classifications, a clear understanding of the mineralogy and behaviour of each mineral in each category in relation to acid consumption and leaching is a very useful tool that could help as a guide in predicting their expected behaviour during leaching. The purpose of this section is to establish whether there is a relationship between minerals considered as gangue and acid consumption. This will provide the basis for understanding the behaviour of the different minerals in the ore in order to develop a suitable leaching process. Since leaching is considered as the intended method of processing of the ore minerals, information on gangue minerals in the ore is vital in choosing a chemical lixiviant. This is imperative because the leaching kinetics and acid consumptions of copper ores are dependent on the ore and gangue mineralogy of the different mineral group as presented in Appendix 4.1 to 4.2 and Table 4.2. Focus will be on the three classifications and the implication of the presence of the minerals to leaching.

Analysis of data in Appendix 4.1to 4.2 and Table 4.2 revealed that the ore samples are dominated by three types of gangue minerals (silicates, oxide mineral group and carbonates). The classification of different minerals according to gangue types in the ore is presented in Figure 4.9. It was found that the gangue minerals which fall under the silicates group are muscovite, kaolinite, biotite, tourmaline, chlorite, K-feldspar, and plagioclase feldspar. The second group is made up of iron-bearing hematite and the third group is the carbonate gangue comprising of calcite and ankerite.

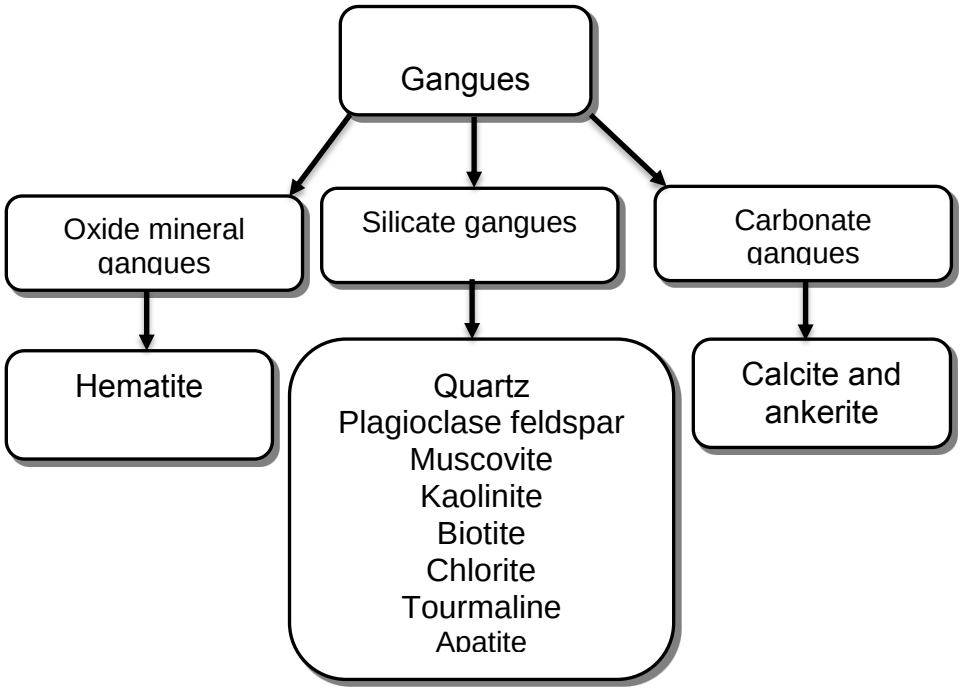

Figure 4.9 Classification of gangue minerals

The ore sample is composed of about 72.7% silicate gangue, 18.2% carbonate and 9.1% iron oxide mineral gangue. The behaviour of gangue minerals during leaching with lixiviants relates to their rates of dissolution and metal-oxygen bond strength (Jansen and Taylor, 2003). Gangue reactivity produces mainly acid consumption, loss of permeability and copper retention (Helle and kelm, 2005). Considering the high percentage of silicates and carbonate gangue in the ore, the anticipated acid consumption during leaching is very high. This is because the reactivity of gangue minerals during leaching lies in its increasing capacity to neutralize the reagent. As such, the higher the gangue content, the higher acid requirement for leaching (John, 1999).

The gangue minerals (oxide, silicates and carbonates) were further considered according to three different categories on the basis of reactivity after John (1999) and Jansen and Taylor (2003), (Figure 4.10). The consideration of minerals on basis of gangue reactivity is due to the fact that the reactivity of gangue mineral during leaching is actually a factor responsible for determining the acid consumption pattern of the gangue with the lixiviant. The proposed gangue classification was done based on leaching kinetics of minerals gangue after John (1999).

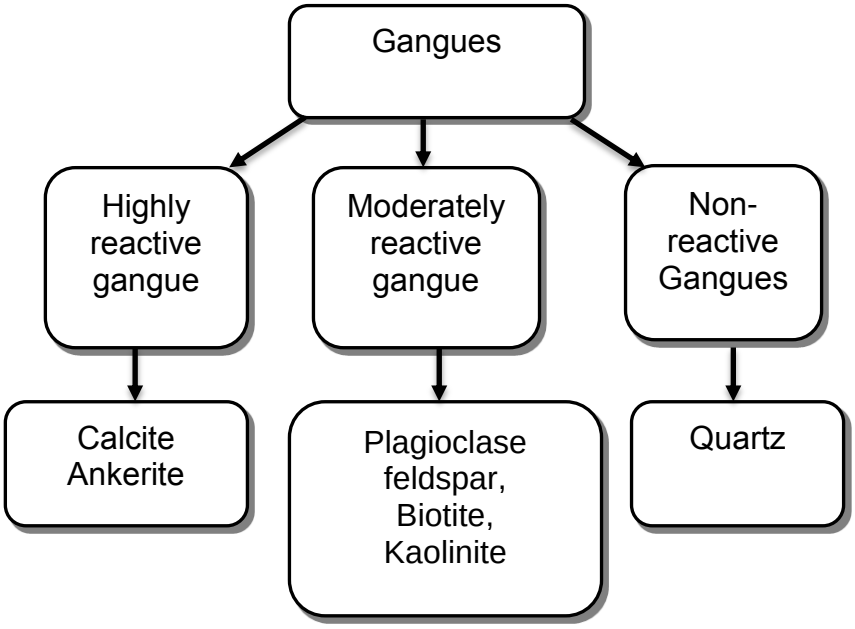

Figure 4.10 Classification of gangue minerals according to acid reactivity (John, 1999)

The leaching kinetics of calcite and ankerite minerals suggests that they can be considered as highly reactive gangue minerals. The reactive behaviour of these minerals with acids was observed by Bingöl and Canbazoğlu (2004) and Bingöl et al. (2005). The presence of the carbonate (CO_3^{2-}) functional group in the

calcite may be responsible for the spontaneity of the reactions with acid (Appendix 4.2). The dissolution of these minerals in acid usually produces cations, water and CO_2 gas. These gangue minerals have been shown to be the major consumer of acid during leaching (Liu et al., 2010; Wei et al., 2010; Liu et al., 2012a). According to Jansen and Taylor (2003) and John (1999), the presence of calcite could lead to tremendous consumption of acid during leaching. For example 1 kg of calcite consumes 0.98 kg of acid thus implying that 1% of calcite consumes about 9.8 kg of acid. This implies that the corresponding acid consumption by 1 % calcite determined in ore during leaching is 9.8 kg. As shown in Table 4.2 the concentration of calcite in the ore fractions differs (product contained 1.91 % calcite, middling contained 1.31 % and waste 11.91%). These suggest that the tendency of acid consumption in the ore fractions varies, with the waste showing very high tendencies toward acid consumption compared with the product and middling. In view of the significant content of gangue mineral and its distribution pattern in the ore, high acid consumption is to be expected. It has been stated that the significant concentration of calcite and ankerite in an ore could render the process of leaching of an ore unsuitable (Bingöl and Canbazoğlu, 2004; Liu et al., 2012b). The moderately reactive gangue leaching kinetics are higher with a substantially lower rate of acid consumptions compared to the highly reactive gangue. The minerals considered under this class can further be classified as reactive, moderately reactive and slightly reactive depending on their relative quick dissolution with lixiviants during leaching (John, 1999).Gangue minerals such as quartz are unreactive to leaching lixiviants. The leaching is usually accompanied by little consumption of acid, with the leaching process progressing uniformly. Hematite was not included in the classification: it is an oxide mineral contained at high concentration in the ore samples. The abundance of hematite will lead to the release of ferric or ferrous ions during leaching into the leachate solution. As such it is expected that its high concentrations will interfere with the leaching if high amount of it is dissolved into the solution which will further complicate the downstream processing stage as such is considered a potential gangue mineral with negative impact of the process.

Analysis of Figures 4.4 to 4.6 indicates that samples classified as products have hematite, calcite and K-feldspars as the most significant gangue with about 28 %, 1.9% and 23% by volume in the total samples. The reactive gangue minerals have 1.9%, and the non-reactive gangue have about 15%. However, most of the gangue fall under the moderately reactive gangue category (Figure 4.10). On this basis it is expected that the reagent consumption during leaching will be lower compared to the other two sample categories. The middlings have higher concentrations of hematite than the product and wastes samples. The percentages of other gangue are biotite 5%, chlorite 6%, quartz 15%, calcite 1.3% and K-feldspar 15.8%. The concentration of the reactive gangue minerals

and moderately reactive gangue is similar to that of the product category. However, the high concentration of hematite will be a source of major concern during leaching. The most notable difference is that the product categories contain more copper compared to the middlings and wastes, while the middlings contain more hematite compared to the product and waste. The concentration of hematite and copper in the waste is insignificant compared to product and middlings. Similarly, it is observed that the waste samples ranked very high in acid consuming gangues which are also considered reactive gangues (Figure 4.6). The concentration of calcite is high at 11.7%. This value is three times higher than that obtained for both the product and middling. The concentrations of gangue minerals: chlorite, quartz, K-feldspar, biotite, and muscovite are also significantly higher (in that order) in the waste (Figure 4.6). Most of the gangue minerals in ore are either silicate, or under the moderately reactive and non-reactive gangue classes. Thus, two gangue minerals have a dominant effect on the waste samples (calcite and quartz). The leaching of the waste fractions will ultimately lead to high acid consumption due to the high concentrations of reactive gangues in the samples category.

Since hydrogen ions released from acid are the drivers in copper leaching and considering the mineralogy of the ore samples, it is expected that the interaction of acid with the mineral gangue will lead to high acid consumption. Chrysocolla is a highly porous mineral that promotes the entry of solution into minerals, and hence will further allow for the dissolution of other metals in associated gangue alongside copper metal (John, 1999).

4.3. Ore mineral chemistry

The chemistry of minerals is useful in understanding their chemical behaviour during leaching. Determining the elemental concentration in ores is important because it provides information that could be used in outlining strategies for processing the minerals from gangue.

4.3.1. X-Ray Diffraction (XRD) analysis

X-Ray Diffraction (XRD) studies of two sample categories of the pre-concentrated ore (product and middling) were analysed using XRD for mineralogical evaluation. Because the XRD detection limit is 5%, the technique cannot be used to determine trace minerals in the ore. Because of this QEMCAN® was used to identify much wider range of minor minerals that are below the detection limit of the XRD equipment. X-ray diffraction patterns are presented in Figures 4.11 and 4.12 while the presence of minerals in all the samples is presented in Table 4.3 after Iyakwari (2014). The results presented in the Figures 4.11 and 4.12 are compared with those of individual particles of the ore after Iyakwari (2014). It was found that some of the minerals identified in the individual particles using XRD and QEMSCAN® were also detected in the

product and middling. Major minerals identified by the XRD analysis of particle samples include: quartz, hematite, clinochlore (chlorite), orthoclase and microcline (K-feldspar), muscovite, calcite and biotite as the eight dominant crystalline mineral constituents present in the ore (Iyakwari, 2014). The XRD pattern shown in Figure 4.11 revealed the presence of quartz, clinochlore, hematite, microcline and calcite. In Figure 4.12, the presence of only four minerals was detected (quartz, hematite, muscovite and calcite). The observed rise in baseline in Figure 4.11 confirms the presence of the amorphous mineral (chrysocolla), which was not visible in Figure 4.12. The rise of the baseline of XRD pattern with increase in the 2-theta value in the product suggests that chrysocolla is the dominant amorphous mineral in the ore. In comparison with middling (Figure 4.12), it can be seen that only the product XRD profile shows a rise in baseline with increase in the 2-theta value indicative of the presence of chrysocolla. This is in line with the earlier observations by Gaydon (2011) and Iyakwari (2014).

Table 4.3 showed that quartz was detected in all the samples (Figures 4.11 and 4.12). With hematite only 7/9 and 3/4 detection in product and middling was obtained. With muscovite only 2/9 and 1/4 samples were detected while with clinochlore 5/9 and 0/4, with calcite 1/9 and 0/4, with microcline 5/9 and 2/4, with orthoclase 4/9 and 0/4, and with amorphous phases 6/9 and 1/4 detections were observed in the product and middling particle samples. The most significant mineral detected in both Figures 4.11 and 4.12 and Table 4.3 was quartz, contained in all samples. Hematite has about 77.7% detection in the product and 75% in the middling, calcite is 11% in the product and 0% detection in the middling, although Appendix 4.1 indicated the presence of most of the minerals in one sample. It appears that the concentration of these minerals within a certain limit is responsible for the observed detection pattern.

Table 4.3 XRD analysis of Chilean ore samples, presence of mineral is marked with + (Note: amorphous phase is inferred from increased height of background in XRD patterns) (after Iyakwari, 2014).

Sample ID	NIR Samples	Quartz	Hematite	Muscovite	Clinochlore	Calcite	Biotite	Microcline	Orthoclase	Amorphous phase
1	Products	+	+		+		+		+	+
2		+	+		+				+	+
3		+	+						+	+
4		+	+					+	+	
5		+		+	+			+		
6		+	+		+	+		+		+
7		+	+					+		
8		+	+		+			+		+
9		+		+						+
10	Middlings	+	+					+		+
11		+								
12		+	+							
13		+	+	+				+		

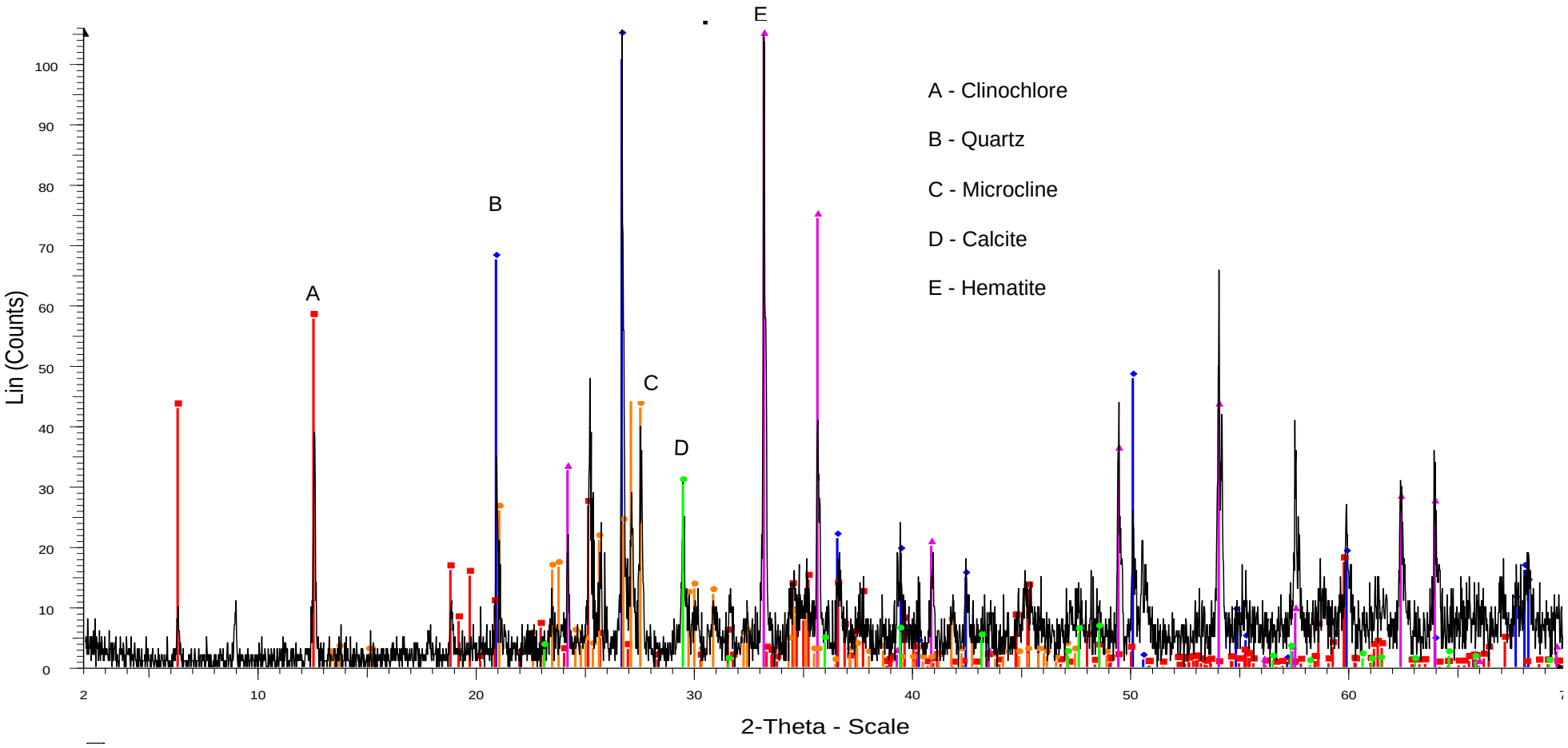

Figure 4.11 X-ray diffraction pattern of NIR product ore sample

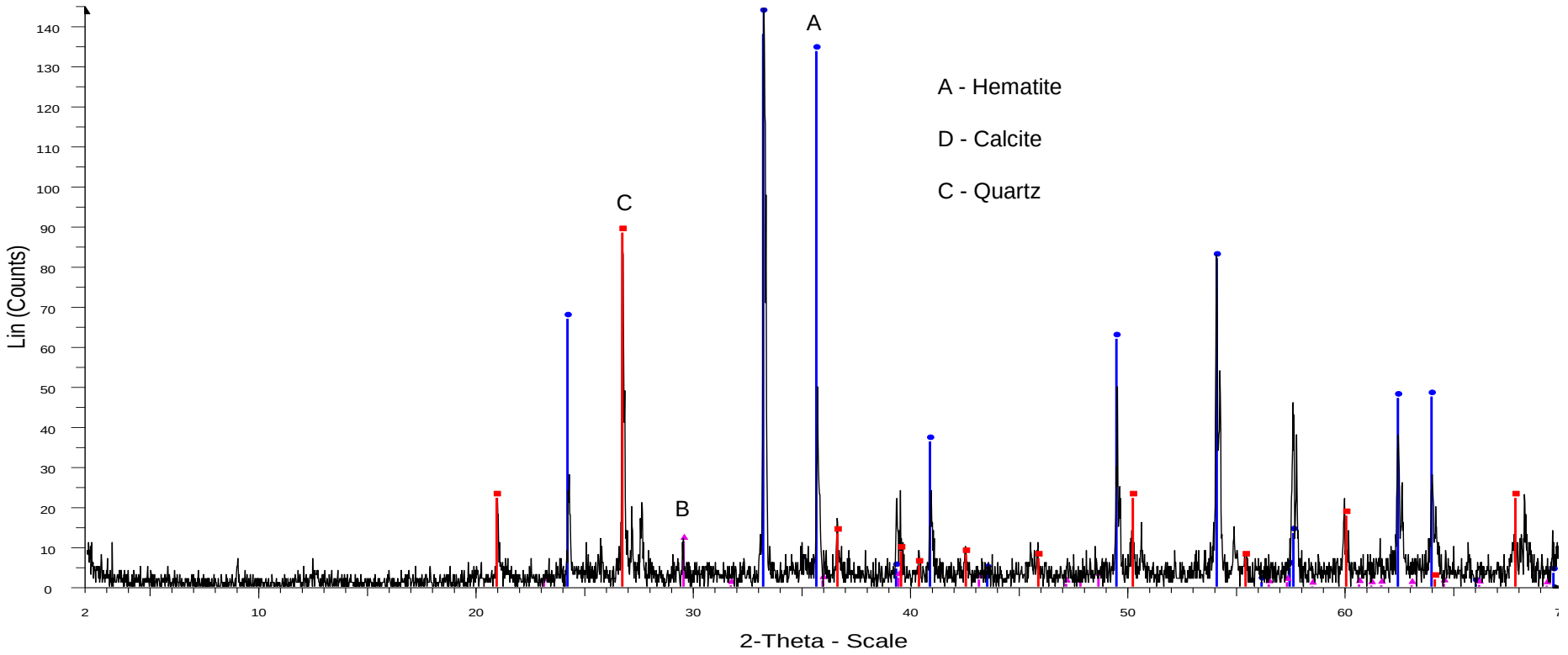

Figure 4.12 X-ray diffraction pattern of NIR middling ore sample

4.3.2. Portable X-Ray Fluorescence Spectrometry (PXRF)

Results of the qualitative elemental analysis of pre-concentrated ore samples in Appendix 4.1 using PXRF shows that the elemental concentration of samples varied from a low value of 0.01% to a high value of 44.0 % for the different elements (Ba, Zr, Rb, Zn, Cu, Ni, Co, Fe, Mn, Cr, V, Ti, Ca, and K). It was found that Fe has the highest concentration in the samples with ranged values of between 2.5% to 44.0 %. The following samples: 3, 4, 7, 8, 9, 10, 11, 12, and 13 have high values of between 21.0 % and 44.0%. This is an indication that the ore is very rich in iron minerals the same could be deduce for the ore deposit. With K none of the samples have concentrations of more than 5.0 %. All the samples had low concentrations, with a few exceptions that ranged between 4.0 and 5.0 % which include samples 6, 7, 8, 14, 24, and 27. With Ca, the highest concentration is in sample 26 with 18.0 %. Other samples have values that ranged between 0.1 to 16.0 %. With Cu the pattern of elemental concentration is different: there seem to be an increase in concentration across the samples from 1 to 32, though in varying proportion. The values are between 0.02 and 7.0 % with samples 1, 2, 3, 4, 5, 9, 10, 11, 19 and 20 having significant Cu content compared to the rest. The following metals, Zr, Rb, Zn and Ni all have similar pattern in elemental concentration throughout the samples. It was observed that all the samples have insignificant values as low as 0.01%. With Co, Mn, Cr and V, their elemental concentrations in the samples are similar with few samples showing disparity in concentration slightly higher than others. None of the metals have values that exceeded 0.6 %. All the elements have values that fall between 0.01 and 0.5 %, of which were only obtained for Ti element.

The observation is an indication that the elemental concentration of certain metals (Cu, Fe, Ca, and K) appear to correlate with their minerals abundance in Appendix 4.1 to 4.2 and Table 4.2. For Cu and Fe the patterns of elemental concentration across some samples appear to correlate with the pre-concentrated ore samples classification (Appendix 4.1and 4.2).

Further analysis of the ore for better understanding of the mineral chemistry was carried out on classified ore particles and grain size fraction using the PXRF technique. The results revealed that the product have high copper content than the middling to waste with values of between 0.04 to 1.0 %, while the middling ranked very high in iron content, followed by the product and the waste, with ranged values of between 4.0 to 30.0 %. The following metals have varying elemental values which ranged: cobalt, 0.02 to 0.03%, manganese, 0.03 to 0.2 %, barium, 0.04 to 0.06 %, titanium, 0.07 to 0.5 %, chromium, 0.01 to 0.03%, vanadium, 0.02 to 0.03%, calcium, 0.1 to 11.0 % and potassium 1.0 to 3.0 % while nickel, rubidium and zircon have the same concentration. Since

the objective of this study is to investigate the chemical leaching of copper in ores, further investigation of the ore is required because the result obtained may not be representative of the entire samples. This is on the consideration that the PXRF depth of penetration varies with concentration, available metal at the point of determination and density of the first surface mineral encountered. Analysis on crushed samples was performed to evaluate the elemental concentration. Results showed significant increase in metal content of all the elements compared to that obtained from particle samples. This is an indication that crushing of the ore led to the liberation of minerals. The result obtained from this analysis with PXRF is only indicated. However, the values obtained for Cu and Fe from the pre-concentrated ore is in line with the classification with the product samples having higher concentration of copper than the middling and waste, respectively.

4.3.3. Scanning Electron Microscope (SEM) analysis

Scanning Electron Microscopy (SEM) was used to determine the elemental composition of the ore and also to observe the ore characteristics such as texture, size, shape and liberation sizes in relation to copper. It is important to understand, for example, if copper minerals are interlocked with other minerals, the recovery process may be slow or sub-optimal.

Results obtained for the pre-concentrated ore samples were similar: the only difference was in the concentration of elements as indicated by the X-ray peaks. Figure 4.21a presents the EDS and X-ray peaks generated. Note that the image shows that the minerals are finely intergrown on a micron scale. For the middling polished block very abundant peaks of Fe with short peaks of Cu peak were obtained with corresponding elements (Al, Si, K, Ca), while for the product polished blocks the Cu peak was very pronounced compared to that of the middling, although the Fe peak was visible but not as pronounced as that of the middling. It is noted that the Fe and Cu peaks appear to correlate with their mineralogical concentrations according to the classification. The SEM image obtained indicated that the copper particles in the crushed ore are finely disseminated, the ore is morphologically characterised by intergrowth with chrysocolla mineral found in close association with hematite and K-feldspars. The observed phenomenon could be due to absorption of elements by chrysocolla. The analysis of pre-concentrated ore revealed spatial variability within the crushed ore with copper ubiquitously distributed within the crushed grain sizes of the chrysocolla, K-feldspar and hematite.

Though the ore is dominated by hematite, which acts as a masking agent for copper located in the grains, the recovery of copper by leaching from the fractions could be carried out. This is based on the mineralogical findings in the preceeding sections. Considering the calcite content in the ore fraction fine grinding will increase surface area for leaching and better copper extraction.

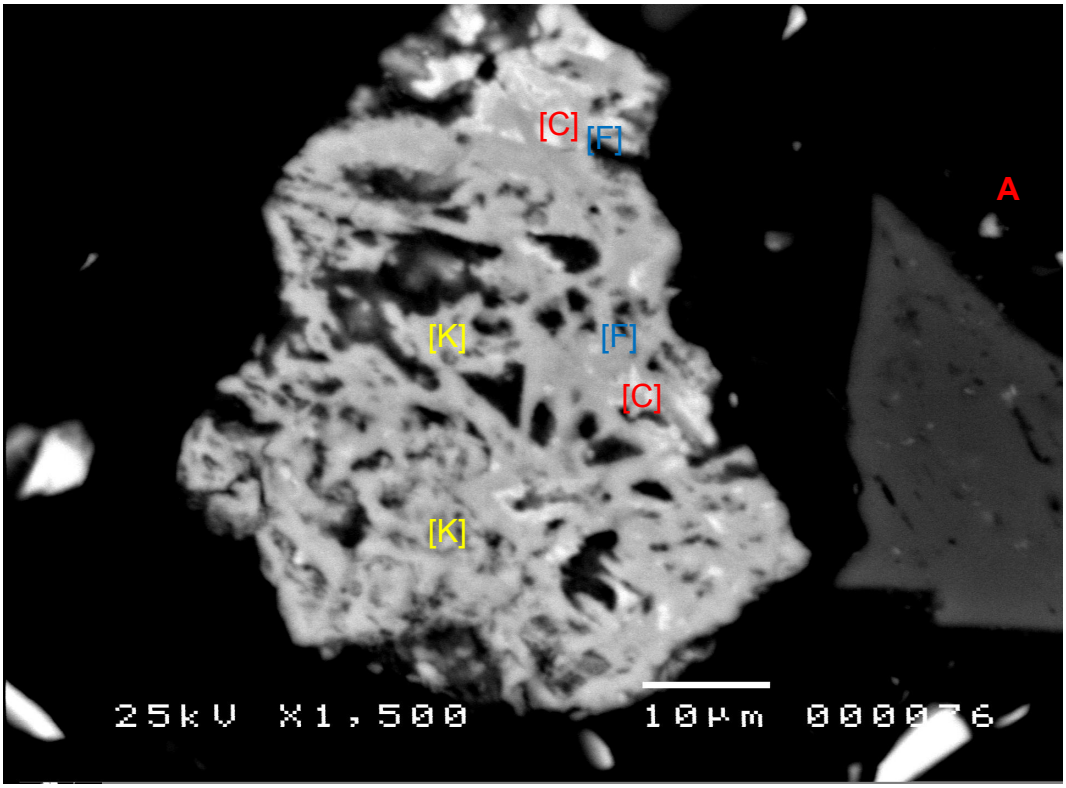

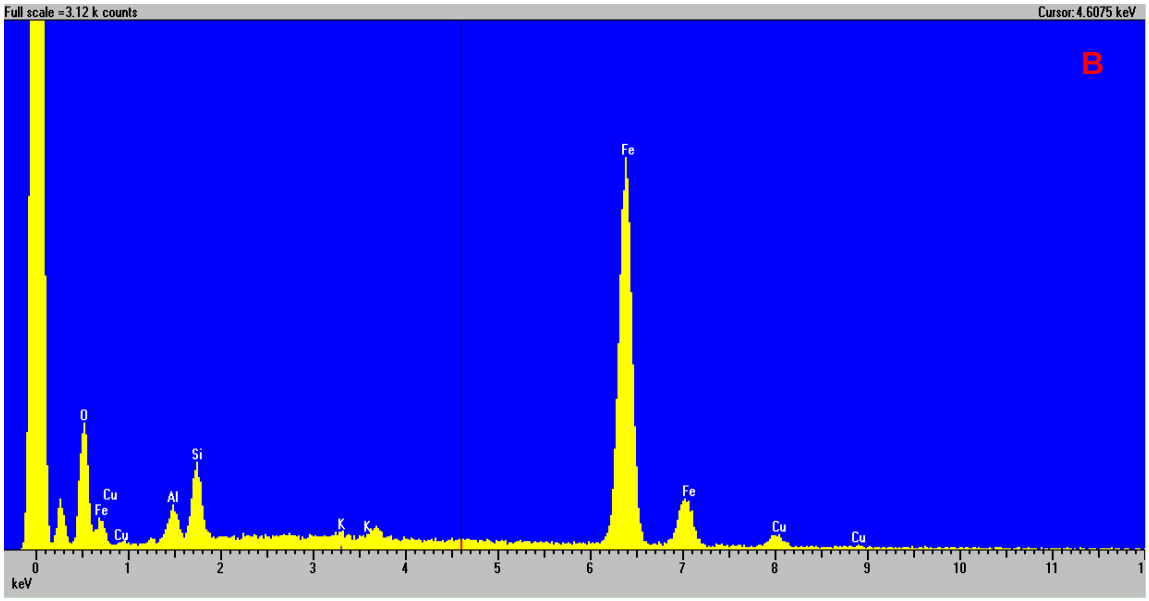

Figure 4.13 A) BEI SEM image of pre-concentrated ore: [C] Cu-bearing particle, [F] Fe-bearing particle and [K] K-feldspar B) EDS X-ray spectrum of the sample revealing the presence of Fe and Cu in the middling.

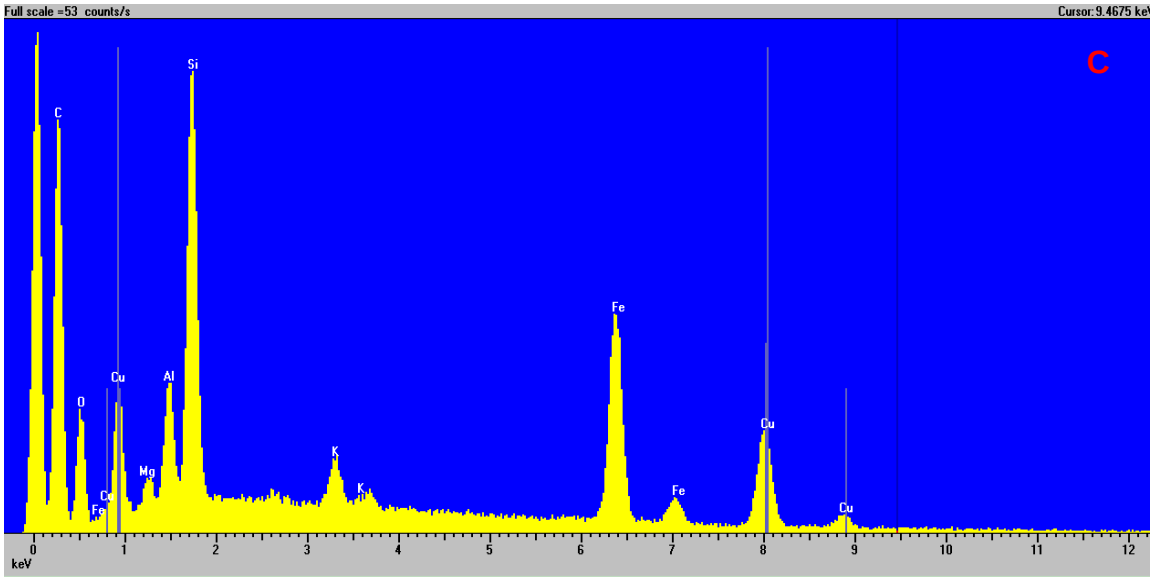

Figure 4.13. C) EDS X-ray of the sample revealing the presence of Fe and Cu in the ore product.

The relative abundance's of elements in the samples were determined from their metal oxides. In each case the determination was carried out in triplicate and averages taken. The values obtained are only qualitative and are based on standard-less analysis, and in each case the values normalized to equal 100 %. Bearing in mind also that the values obtained may not be a true reflection of the entire sample because the determination is based on elements requested on a point location and identified by the instrument, as such the possibility of other elements occurring in appreciable amount which could be measured cannot be ruled out. The result of elemental abundance's is presented in Table 4.7 while the correlation plot for the elemental oxides is presented in Figure 4.22.

Table 4.4 Metals and metal oxides analysis of pre-concentrated ore (product and middling) with SEM (wt. %)

Metal concentration ↓ Sample category→	Product	Middling	Metal Oxides↓ Category →	Product	Middling
Na	0.13	0.13	Na_2O	0.18	0.18
Mg	0.60	0.10	Mg_2O	0.99	0.17
Al	0.21	0.12	Al_2O_3	0.40	0.23
Si	12.10	12.22	SiO_3	26.1	26.14
K	6.18	0.26	K_2O	7.45	0.31
Ca	1.71	0.71	CaO	2.39	0.99
Fe	40.0	48.11	Fe_2O_3	57.19	68.78
Cu	4.23	4.01	CuO	5.30	3.20

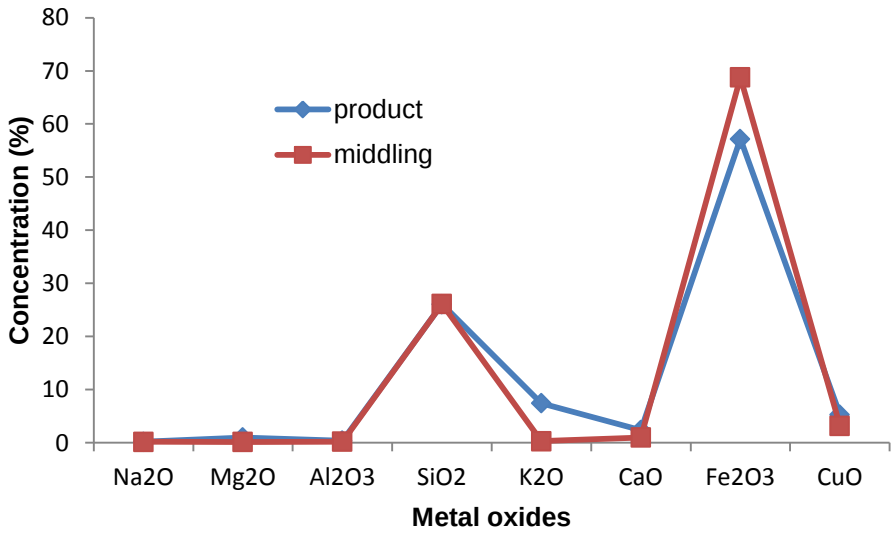

Figure 4.14 Correlation plots of metal oxides obtained with SEM

Values shown in Table 4.7 indicated that some metals (K, Fe, Si, and Cu) determined using the SEM appears to correlate with results of other instrumental techniques (XRD, PXRF and QEMSCAN®). Results obtained by these instruments also indicated the presence of these metals in the classified ore. The elemental abundance's of these elements are a reflection of their background concentrations in the minerals (hematite, K-feldspar, quartz, chrysocolla) hosting them in the samples. Although other minerals such as chlorite, biotite, ankerite and muscovite were also determined with other instruments, the likelihood of their rich sources of the elements is a possibility. It is found that the metal oxides content (wt. %) of SiO_2 and Fe_2O_3 were quite significant than those measured for CaO, K_2O and Mg_2O (Table 4.7). The high concentration of SiO_2 and Fe_2O_3 is from the middling which is in line with results obtained using other instrumental techniques. The correlation result suggests a positive relationship in the analysis of the two samples. Variations in the values obtained may be due to the point of determination as such the elemental abundance is assumed to be indicative.

Since the BEI image revealed that most of the copper minerals are disseminated within the grains of hematite and other minerals, in order for effective leaching of copper the ore requires crushing to fine liberation size to separate copper from the ore matrix and gangues. Although the results shown in Table 4.7 revealed metal concentration in the ore, the result only represents a small amount of data but is very useful in getting information on the samples. For more information on the ore, rigorous test using the SEM has to be extended or samples determined for mineralogy. However, in this case it was not necessary because the result obtained is enough to give clarity on the samples.

4.4. Conclusion

The mineralogy of the classified ore was determined using QEMSCAN®, PXRF, XRD and SEM analytical techniques. The results obtained were related to ensure sufficient understanding of the ore and to avoid bias interpretation of leaching results. It was found that all the results obtained agreed indicating good correlation. The mineralogy of the ore by QEMSCAN® and XRD shows that the copper ore samples consisted of different minerals which are broadly divided into for classes as silicate, oxide, phosphate, carbonate and oxide with each class having a subdivision comprising of different mineral groups. The three main copper-bearing minerals in the ore are chrysocolla, malachite and cuprite. Chrysocolla was determined to be the major copper-bearing mineral and the bulk ore is a silicate oxide. The result presented shows that the copper ore samples considered according to three main categories according to the NIR sensor-based classification strategy as product, middling and waste differ in both mineralogy and chemistry. The concentration of all the minerals in the ore varies with particle samples and NIR classification. The product samples have more copper content than middling to waste. The concentration of hematite is very significant in the middling than the product and waste. The waste ranked very high in quartz and calcite content. The concentration of Cu and Fe appears to correlate with the minerals hosting them. The result of instrumental analysis of the ore for mineral chemistry revealed a positive correlation suggesting good ore analysis. PXRF results of size fractions indicated higher content of metals compared to particle samples: This is an indication that liberation of the classified ore is the only option of achieving better leaching results. SEM analysis of the classified ore indicated that copper is finely disseminated in the ore as such the ore requires crushing and grinding to finer size fractions for efficient contact of lixiviant for better leaching.

Based on the mineralogy and chemistry of the ore, the gangue contents in the ore can be classified as silicate, oxide or carbonate with the latter being the major acid consuming gangue mineral group in the ore. The waste samples have significant concentrations of this gangue mineral compared with middling and product. In terms of reactivity, some gangue minerals fall under highly reactive, moderately reactive and non-reactive depending on their leaching kinetics (after John, 1999).

In view of the significant concentrations of the silicates, oxide and carbonate gangue cutting across the three sample classifications, the leaching of the ores with acid will lead to high consumption. As such, for effective and efficient leaching of the ore samples, lixiviant selective leaching is an alternative process that could lead to high copper recovery. It is hoped that this will not only ameliorate the problem of high gangue content in the ore but will lead to high economic copper recovery. In order to reduce the effect of reactive gangue, crushing of the ore to fine size fraction before leaching will increase the surface

area for thereby reducing the effect of high consumption of the lixiviant during leaching by promoting fast leaching of copper from the ore as well as fast reaction with gangue.

Chapter 5

Pilot study of pre-concentrated ore and method development

5.0. Introduction

The hydrometallurgical leaching process of copper ore depends on many factors such as the mineralogy of the ore, gangue content, available copper content for leaching, concentration of the reagent, particle sizes, solid-to-liquid ratio, leaching time, stirring speed for agitation leaching and temperature, amongst others (Dhawan et al., 2012). The mineralogical results presented in the previous chapter (Figure 4.1) showed that almost 100% of the total copper was acid soluble (chrysocolla 94.3%, malachite 5.3% and cuprite 0.4%). The complexity of the ore is due the presence of high hematite, high calcite and silicate gangue which are considered problematic for leaching and subsequent recovery. This chapter provides a foundation towards better understanding of the leaching behaviour of classified ore samples. In addition, this chapter will serve as the basis for distinguishing categories of ore for studies based on gangue behaviour and drawing up a strategy for processing.

Chapter 5 is focussed on determination of copper dissolved in each ore category and across the different size fractions using complexometric analysis. Details of the complexometric analysis are given in chapter 3. Furthermore, suitable values of leaching parameters are investigated. In order to achieve this, the ore is subjected to a pilot study by conducting series of tests for their appropriateness for leaching, as outlined in the next section.

Elemental concentrations in the different ore size fractions of the pre-concentrated ore were determined using Portable X-ray Fluorescence (PXRF) and Inductively Coupled Plasma Mass Spectrometry (ICP-MS) techniques in order to find out the variation in elemental concentration with size fractions. The following parameters were examined: particle size fractions, reagent concentration and solid-to-liquid ratio for their appropriateness and application for leaching studies. For better understanding of the dissolution of copper and the pattern with respect to these parameters, the crushed, ground and sieved ore fractions were titrated using Na_2EDTA as titrant and the pH maintained at a value of between 6 and 9 using an ammonia-ammonium chloride buffer. The method is based on the determination of the metal ion complex concentration by difference in the amount of copper dissolved in each category. Na_2EDTA has six bonding sites that essentially can form 100% bonds with copper. The amount of copper-EDTA complex available in solution was calculated as a function of copper dissolved in each size fraction using two different Na_2EDTA concentrations while varying the solid-to-liquid ratio as described in section 5.3. The influence of certain parameters on the leaching studies is discussed. The objectives can be summarised as follows:

1. To reduce the ore to different size fractions and to expose copper in the mineral grains for analysis.
2. To determine the effect of parameters such as effect of size fractions, effect of solid-to-liquid ratio, and effect of dissolution behaviour of copper in each category at different reagent concentration.
3. Analyse each size fraction in the ore samples category (product, middling and waste) to determine the liberation sizes for complexometric titrations and size fractions which have the potential to be exploited for chemical leaching and electrochemical studies.
4. Elemental analysis of all the different size fractions using PXRF. The qualitative analysis was aimed at determining the presence of copper and other metals and their variations in the pre-concentrated ore
5. To determine trace and heavy metals in the different size fractions using the ICP-MS technique. This is to determine the available copper amenable to leaching.

The outline of the approach for sample preparation for the analytical determinations and complexometric analysis is presented in Figure 5.1.

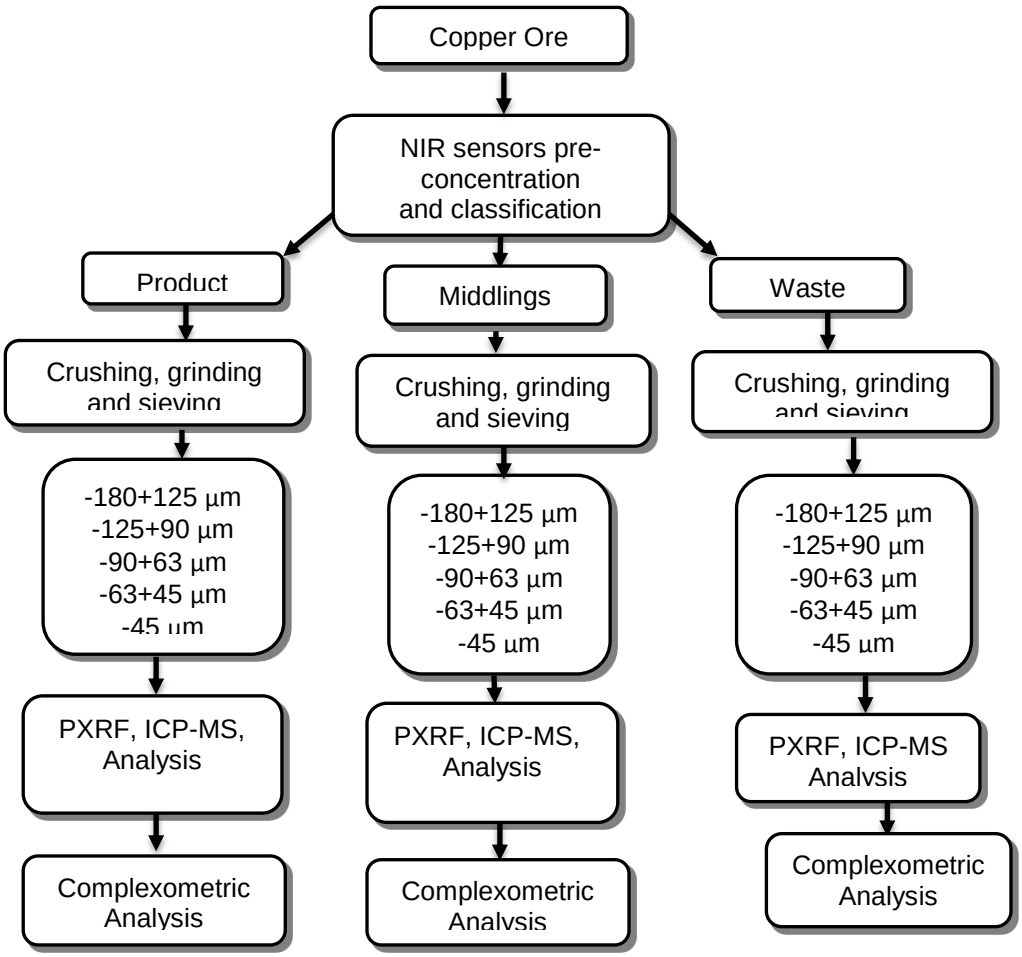

Figure 5.1 Outline flowsheet for preliminary analysis.

5.1. Size-based particle analysis

Size-based particle analysis is important in view of the performance of physical separation techniques (Kilbride et al., 2008). Classified ore samples were separately crushed, ground, and sieved to different size fractions using a stack of sieves as described in chapter 3. The different size fractions obtained are shown in Figure 5.1. Details of the comminution and sieving analysis can also be found in chapter 3. It should be noted that not all the size fractions were further advanced for complexometric analysis because results from the fractions used provided sufficient information.

5.1.1. Elemental analysis of different size fractions with Portable X - Ray Fluorescence (PXRF)

PXRF qualitative analysis of pre-concentrated ore (Table 5.1) indicated that the NIR-sensor based sorting and classification produce fractions with characteristic metal concentrations. It was found that the copper grade increases sharply according to the classification from waste to middling to product. With calcium, the inverse trend was observed: the waste fractions contain the highest calcium concentration while the product fraction contains the lowest calcium. The grades of all the selected elements follow a different pattern. With iron, expectedly the metal dominated the middling fraction as noted in the preceding chapter (49.1 to 55.6% concentration) which is higher than the product fraction (32.9 to 42.2% concentration) which, in turn, is greater than the waste fractions. This pattern is also observed for nickel and cobalt. The inverse pattern, where the middling ranked lowest and the waste grade is highest, occurs for manganese, barium, potassium, silicon, titanium, and the residue fractions. With phosphorus, the product and middling grades are similar with a higher waste grade. The opposite is true for vanadium and chromium. In terms of elemental grade in the different size fractions, it was observed that in the product size fractions, an increase in copper concentration with increasing particle size was the case (from −63+45 µm to −180+125 µm). The same was observed for both the middling and waste fractions. The opposite trend applies to iron, potassium and the residue fractions in the product size fractions.

The trend of increasing iron grade with decreasing particle size is also observed in the middling and waste fractions. Of particular importance is the concentration of calcium and silicon as the major constituent of the minerals hosting the gangue. The concentration of these metals expectedly, is higher in the middling and waste categories, which signifies a difference in metal grade of copper. Therefore, it is observed that there is a positive correlation between elemental concentration and host minerals. For instance, the concentration of copper, iron and calcium is a reflection of their abundances in the following minerals: Cu (chrysocolla, malachite and cuprite), Fe (hematite and chlorite) and Ca (feldspars, calcite and ankerite) as showed in Appendix 4.1to 4.2 and

Table 4.2. Consequently, minerals which were observed to show a certain pattern in concentration in the classified ore (Appendix 4.1 to 4.2 and Table 4.2) have been found to show correlation in elemental abundance determined with PXRF. This pattern is a clear indication that the mineralogy of the ores has influence in determining the outcome of the ore behaviour during leaching.

Table 5.1 PXRF qualitative analysis of the product, middling and waste fractions (Wt. %)

Sample category	Particle size range	Cu	Ni	Co	Fe	Mn	Ba	Cr	V	Ti	Ca	K	Al	P	Si	Residue
Product	−180+125 µm	1.83	0.02	0.02	32.9	0.06	0.05	0.04	0.04	0.26	0.23	2.21	2.1	0.28	7.9	51.9
	−125+90 µm	1.82	0.01	0.03	36.2	0.05	0.05	0.04	0.04	0.26	0.22	2.12	2.3	0.27	7.9	48.5
	−90+63 µm	1.73	0.01	0.03	38.2	0.05	0.03	0.04	0.04	0.27	0.24	2.05	2.2	0.27	7.8	46.9
	−63+45 µm	1.56	0.01	0.04	42.2	0.05	0.02	0.04	0.04	0.25	0.25	1.81	2.1	0.27	7.5	43.7
Middling	−180+125 µm	0.36	0.02	0.02	49.1	0.00	0.03	0.04	0.04	0.09	1.68	1.01	1.5	0.27	5.3	40.1
	−125+90 µm	0.33	0.03	0.05	52.8	0.00	0.02	0.04	0.04	0.08	1.60	0.93	1.5	0.26	5.1	37.1
	−90+63 µm	0.34	0.03	0.06	53.3	0.00	0.02	0.04	0.04	0.09	1.61	0.90	1.5	0.27	5.0	36.6
	−63+45 µm	0.32	0.04	0.06	55.6	0.11	0.03	0.04	0.04	0.09	1.55	0.82	1.6	0.26	4.8	34.7
Waste	−180+125 µm	0.07	0.03	0.00	8.10	0.14	0.09	0.02	0.02	0.27	4.66	3.74	2.3	0.36	11.0	68.8
	−125+90 µm	0.07	0.00	0.00	8.20	0.13	0.10	0.02	0.03	0.27	5.25	3.83	2.2	0.38	10.0	68.4
	−90+63 µm	0.07	0.00	0.00	9.20	0.13	0.09	0.02	0.03	0.28	5.94	3.76	2.1	0.38	10.0	67.2
	−63+45 µm	0.07	0.00	0.00	10.0	0.13	0.09	0.02	0.03	0.30	6.12	3.86	2.3	0.39	10.0	65.9

5.1.2. Inductively Coupled Plasma Mass Spectrometry (ICP-MS)

The result of the determination of some metals (copper, zinc, manganese, cobalt and nickel) with ICP-MS is presented in Table 5.1. The method has the ability to measure elemental quantities down to parts per million (ppm) in this project. The technique was used to determine the quantities of these selected metals in only two categories of the ore (product and middling), based on the outcome of the complexometric analysis of the fractions in section 5.3. The waste category was not considered for leaching as described by the result under section 5.3. Samples for ICP-MS were digested in aqua regia before analysis. Details on the experimental technique and procedures for analysis are discussed in chapter 3. The result of the elemental concentration of the metals indicated a different pattern with that of PXRF. With ICP-MS it was found that, the copper grade increases sharply with a decrease in particle sizes (-45 µm to -125+90 µm) in the product and middling. This is to be expected due to increase in surface area with decreasing particle sizes. This suggests that the higher specific area of finer particles makes these more amenable for dissolution due to effective interaction with chemicals for reactions to occur. Since the technique involves the sample being dissolved in aqua regia before analysis, it is appropriate to state that the observed rate of dissolution depends on concentration of reagent used and particle size fractions. The same trend of increasing metal concentration with decreasing particle fraction was observed in

the middling fractions. With manganese, nickel, cobalt and zinc, the concentration is lower than that observed in the product. Iron was not analysed using this technique due to its significant concentrations in the classified ore (Iyakwari, 2014). Also the concentration of Fe in the ore is above the range limit of the ICP-MS, thus in each case the determination would require huge dilutions which cannot be accurately equated in relation to the concentration of the other metals. The choice of these metals for analysis is based on their concentration in the ore which are considered of interest in the study. It should be noted that the waste category was not analysed with ICP-MS, this follows the result of PXRF and complexometric titration which indicated poor copper content and high gangue content. Thus, subjecting the waste samples to leaching will only lead to poor results and a high cost of chemicals.

Table 5.2 Metal grades determined with ICP-MS

Sample category	Particle size range	Cu (wt. %)	Zn (ppm)	Mn (ppm)	Co (ppm)	Ni(ppm)
Product	−125+90 µm	1.04	0.01	0.04	0.00	0.00
	−90+63 µm	1.70	0.01	0.05	0.00	0.00
	−63+45 µm	1.79	0.02	0.06	0.03	0.01
	−45 µm	1.97	0.02	0.06	0.03	0.01
Middling	−125+90 µm	0.70	0.01	0.01	0.01	0.00
	−90+63 µm	0.72	0.02	0.02	0.01	0.00
	−63+45 µm	1.01	0.02	0.02	0.03	0.02
	−45 µm	1.10	0.02	0.03	0.04	0.02

5.1.3 Comparative assessment of analytical techniques

Comparative assessment of the results of the metals determined by the PXRF quantitative technique of size fractions and aqua regia digestion, followed by ICP-MS metal determination showed that both instruments in some cases either overestimated or underestimated the concentrations of the metals. This suggests that the concentration of metals in copper ores cannot be effectively determined using one particular technique. The observation could be caused by the differences in the methods of sample preparation and or measurement. As shown in the Table 5.1, definitive values for copper were obtained across the entire size fractions in the classified ore. Although PXRF qualitative results for metals concentrations in Table 5.1 show an increasing pattern of the metal concentration from coarse to fine fractions, the opposite was observed for the metals which were evaluated by ICP-MS (Table 5.2). This observation could be due to increasing solubility of the ore with decreasing size fractions. This trend would allow for prediction of solubility and leaching properties of the ore fractions with chemical reagents. PXRF concentration of the rest of the metals

did not follow the same pattern as that of copper, as some metal concentrations were observed to either increase with increasing size fractions or decrease with increasing size fractions and vice versa. For ICP-MS the pattern of metal concentration was consistent across the entire size fraction. Thus, the ICP-MS technique is considered suitable for determination of the metal concentration after leaching. The trend in increase of metal content with decreasing particle size fractions in aqua regia digestion before ICP-MS determination will serve as a guide toward establishing a relationship between particle size fractions and leaching efficiency.

5.2. Complexometric analysis

Since chrysocolla is soluble due to its hydrophilic nature, there is a high chance that the presence of the hydroxyl group will make the classified ore amenable for dissolution with Na_2EDTA reagent and to readily form bonds with the copper in the ore. Thus, the possibility of dissolving the ore is feasible because any material that is hydrophilic in nature often responds to solvent attack with attendant solubility. The analysis was carried out on selected size fractions to determine the dissolution behaviour of each fraction with respect to the different ore categories. The method is based on the technique of masking by reducing the +2 oxidation state of copper to the +1 state (Narayana et al., 2000). The dissolution of copper was made possible by oxidation of the metal in the ore and or by formation of complex copper ions (Habashi, 1997). The result of complexometric analysis is presented in Figures 5.2 to 5.4.

5.2.1. Effect of particle size fractions

The effect of particle size fractions was determined using the following experimental parameters and conditions: 1 to 2 g sample, particle size fraction tested (−180+125 µm, −125+90 µm and −90+63 µm) and Na_2EDTA concentrations (0.01 M and 0.05 M). As shown in the Figures 5.2 to 5.4 the result of the rate of copper dissolution from the ore by the formation of complexes increases significantly according to the classification from waste to middling to product. Similarly, the trend of increasing dissolution is observed with decreasing particle size fractions from -125+90 µm to 180+125 µm and -90+63 µm in all the three classified ores. The sharp increases were more significant in the product size fractions than middling to waste. Expectedly, the pattern of increasing dissolution with formation of copper-EDTA complex is greater in the product sample due to the high copper content in the ore category compared to the middling and waste fractions (Tables 5.1). This is an indication that as the particle size fraction decreases the specific surface area of finer particles increases, which makes them more amenable for interaction with the chelating agent. Thus, the larger the size particle fractions the less the metals in the ore are exposed for chemical attack. The rate of dissolution of copper in a particle can be affected by the distribution of the metal within a mineral grain:

This is referred to as topological effect (Olubambi et al., 2007). The result of the trend in dissolution of copper from the ore is consistent with the near infrared classification strategy in Figure 3.1.

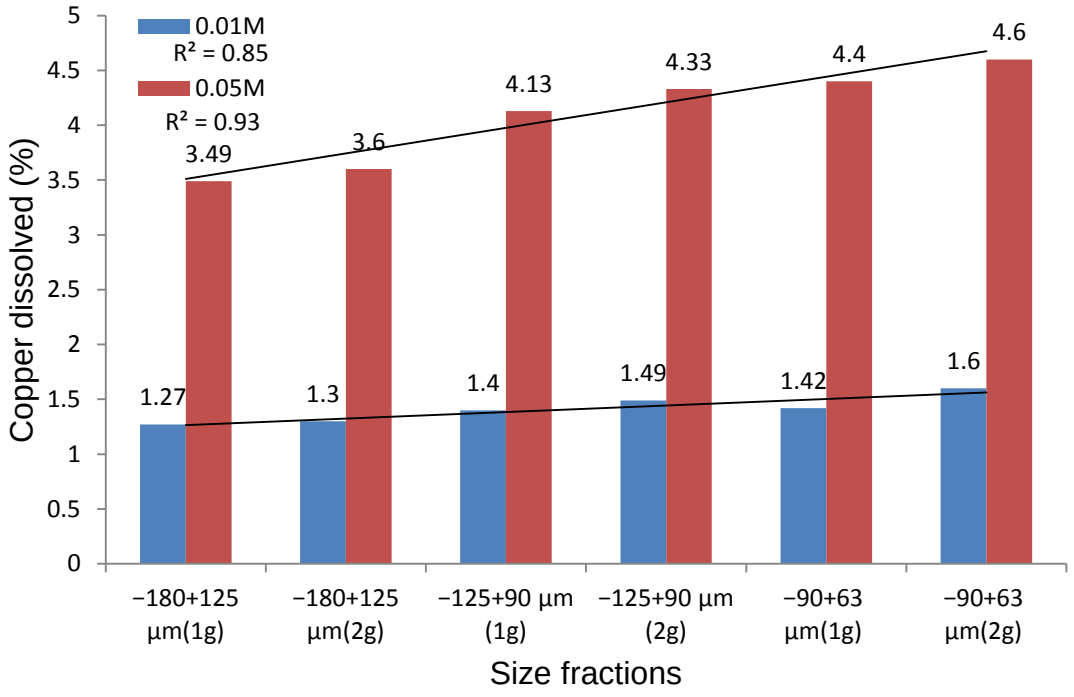

Figure 5.2 Effect of Na_2EDTA concentrations vs. particle size fraction and solid-to-liquid ratio on copper dissolved (product)

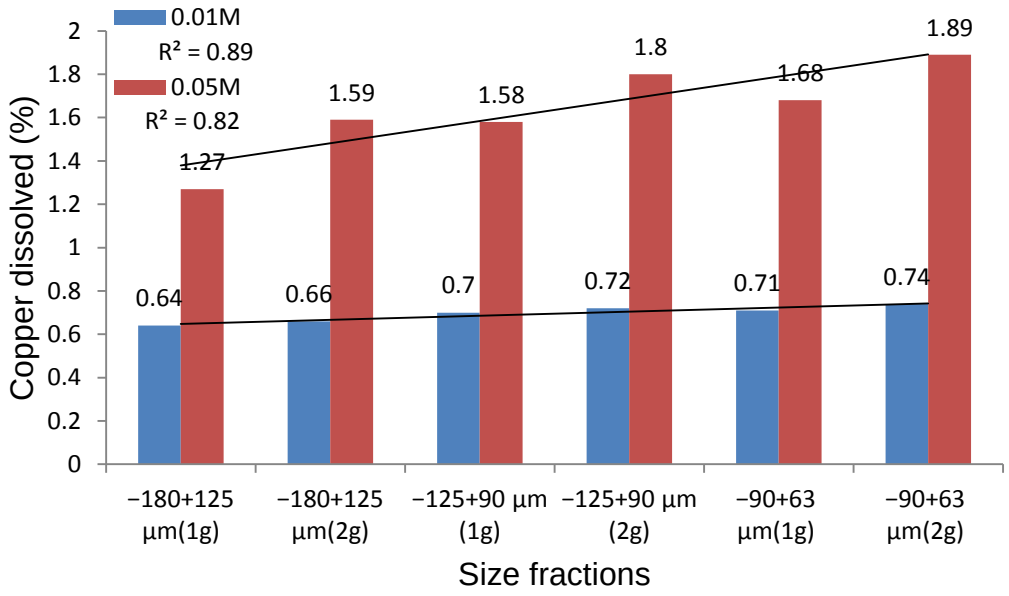

Figure 5.3 Effect of Na_2EDTA concentrations vs. particle size fraction and solid-to-liquid ratio on copper dissolved (middling)

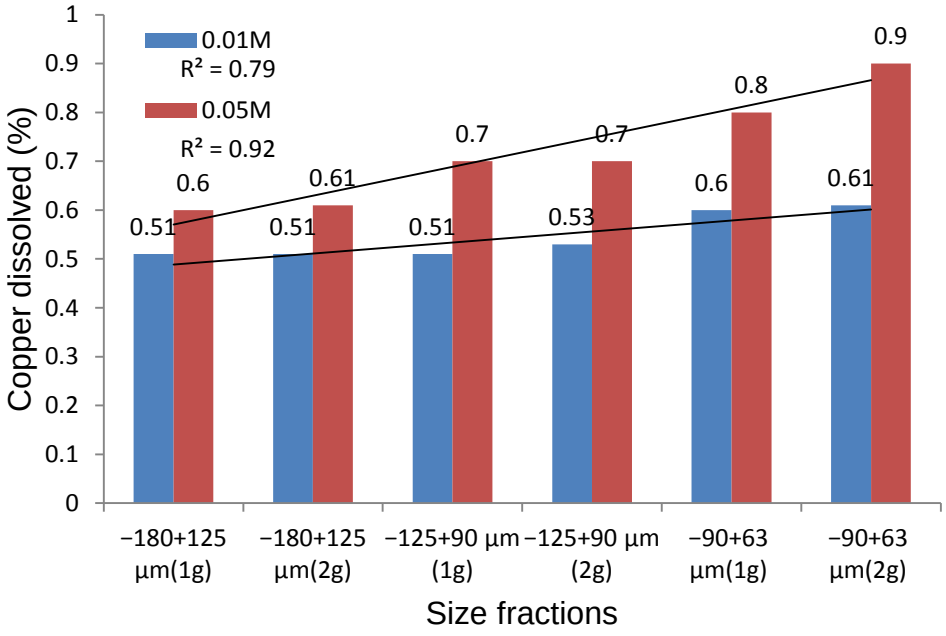

Figure 5.4 Effect of Na_2EDTA concentrations vs. particle size fraction and solid-to-liquid ratio on copper dissolved (waste)

5.2.2. Effect of Na_2EDTA concentration

The effect of Na_2EDTA concentrations on the determination of copper by complexation on the classified ore was carried out using the same experimental conditions stated in section 5.3.1. It was found that the rate of dissolution of copper increases considerably in all the classified ore when the concentration of the Na_2EDTA was increased from 0.01 M to 0.05 M. The trend in increasing dissolution of the metal is from waste to middling to product. The product category indicated a higher rate of dissolution of copper metal than the middling and waste fractions (Figures 5.2 to 5.4). The observed pattern of dissolution by complex formation is dependent on the copper content in the different classified ore and available copper for reagent attack. Thus, in terms of size fraction, the rate of copper complex formation increases with decreasing particle size fraction when the concentration of the reagent was increased due to the availability of finer fractions to the reagent attack. The trend is the same in the classified ore. The solubility of copper in the classified ore is dependent on the concentration of the reagent. This suggests that higher reagent concentration favours the formation of Cu-EDTA complex hence more copper dissolution, and possible recovery. The low Cu-EDTA complex formation in the waste fractions indicated poor copper content in the sample category due to the presence of high gangue content in the system which suppresses the metal solubilisation by preventing the contact between the reagent and the available copper in the mineral (Kelm and Helle, 2005, Daoud and Karamanev, 2006). The complexometric reaction is surface chemical reaction-controlled: thus the category with high gangue content reduces the rate of complex formation.

5.2.3. Effect of solid-to-liquid ratio

The effect of solid-to-liquid ratio on the classified ore indicated that the extent of copper dissolution was significant in all the samples. As shown in the Figures 5.2 to 5.4, at 1 g weight, and concentration of 0.01 M and 0.05 M Na_2EDTA the rate of dissolution in the product ranged between 1.27 and 4.4 %, 0.64 and 1.68 % in the middling and 0.51 and 0.8% in the waste. When the weight was increased to 2 g the rate of dissolution increased from 1.3 to 4.6% in the product, 0.66 to 1.9% in the middling and 0.5 to 0.9% in the waste. In general, the -90+125 µm size fraction indicated a significant rate of dissolution amongst all the size fractions. This is an indication that the finer grain fractions even at high solid-to-liquid ratio are capable of leaching with better output. Similarly, the influence of solid-to-liquid ratio is not independent of reagent concentration and particle size fraction. The significance of this is for effective leaching of the copper ore: measures have to be taken to optimise solid/liquid ratio for the most out of leaching.

5.3. Conclusion

The preliminary tests provided a good insight into the amenability of the classified ore for leaching and provide options for the selection of the appropriate lixiviant. The result of the pilot study also revealed information on the aspect of the lixiviant that will be more suitable for effective electrodeposition of copper from the leachate. The effect of chemical reagent, particle size and solid-to-liquid ratio on the rate of extraction of copper by complex formation, indicated that these parameters are keys to effective leaching of the ore and also provide the basis for the proposed strategy for leaching and other aspects of the research. The use of Na_2EDTA as a complex forming agent for determining the rate of copper dissolution in the ore is a very useful technique for understanding copper dissolution behaviour with size fractions and reagent concentration in the classified ore fractions. The reagent has great potential for selective dissolution of copper by complex formation. Increasing the concentration of the reagent ultimately led to an increase in the rate of dissolution of the metal, hence for effective leaching of the classified ore higher concentrations of the leaching reagent is required for better leaching yield. The rate of dissolution with increasing solid-to-liquid ratio was not pronounced. This may be as a result of excessive increase in solid per unit amount of lixiviant in the reaction mixture. Thus, it's a balance between amounts of material versus reagent. Since particle size fraction has a strong effect on the dissolution rate of copper in the classified ore, it is appropriate to classify them on the basis of amenability to reagent for solubility. On that note, the -180+125 µm fraction is considered to have contributed to the rate of dissolution at least in the early stages of contact with reagent but can only become more involved with more copper dissolution with prolonged contact with the leaching solution as new cracks and fissures will be generated in the ore

particles, thus more accessibility to leach solutions would be possible. The finer particle size fraction produced more copper dissolution and contributed throughout the reaction and so has the highest potential for copper dissolution and recovery during leaching.

Given the nature of the ore and the results of complexometric analysis obtained for effective leaching, the classified ore requires crushing and grinding to finer particle size before sieving to provide sufficient surface area for interaction with the complexing agent. It is likely that the gangue content and mineralogical difference in the classified ore is responsible for the observed trend in behaviour of the particle size fractions in the classified ore (Jansen and Taylor, 2003; Urbano et al., 2007; Liu et al., 2012b; Crundwell et al., 2013). Thus, the extent of dissolution is dependent on three factors: Particle size fraction, reagent concentration, and solid-to-liquid ratio. The EDTA molecules form very strong bonds with copper using six ligands sites that are tighter compared to copper-ammonia bonds (Figure 5.5). A comparison of the stability constant (Ks) in Table 5.3 shows that the value for Cu-EDTA complex is significantly higher (300,000 times greater) than copper-ammonia. This implies that the ligands in Cu-EDTA bonded to the copper metal are held strongly such that they are not easily broken for copper recovery compared to copper-ammonia complex. The larger the value for the stability constant: the less likely that the complex will break up. On this basis ammonia is considered more suitable for copper leaching and electrowinning than Na_2EDTA. This is in line with observation by Allen and Chen (1993), Revathi et al. (2012), and Complex formation (2015)

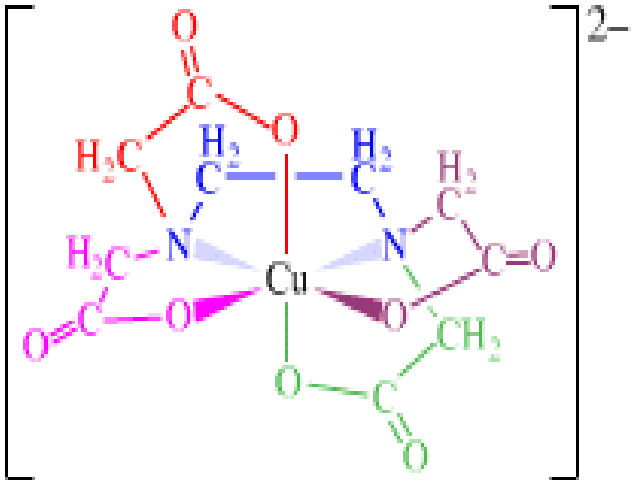

Figure 5.5 Diagram of Cu-EDTA ions (after complex formation, 2015)

Table 5.3 Comparison of the stability constant of Cu-EDTA and Cu-$(NH_3)_4^{2+}$ complexes (after complex formation, 2015)

Metal ion	Ligand	Coordination number	Formation constant
Cu^{2+}	NH_3	4	$2*10^{13}$
Cu^{2+}	EDTA	6	$6*10^{18}$

Experimental difficulties such as heating and readjusting of pH were observed in the determination of copper by complexometric titration which is in line with that obtained by Junar (2014). The prospect of the use of aqueous solutions of complex forming reagents such as ammonia and ammonium salts for copper ore leaching is high (Habashi, 1997). It is therefore, necessary to investigate further, the effect of parameters such as stirring speed, temperature, and concentration, solid-to-liquid ratio and particle sizes on leaching and optimization of the process for better understanding and to further establish the mechanism and kinetics of the reaction process. Further studies will be carried out with other reagents (alkaline and organic reagents) to explore their potential for application as alternative lixiviant for leaching in this work.

Based on the results of pilot studies, a proposed outline for the leaching and electrochemical study is presented in Figure 5.6. The plan includes a series of steps to be adopted ranging from crushing of ore, grinding and sieving, leaching, metal analysis of leachate, kinetic studies of the leaching process, electrochemical study of leachate and hydrometallurgical flow sheet development for copper recovery from the classified ore. The determination of the influence of parameters such as pH, stirring speed, reagent concentration, particle size, temperature and solid-to-liquid effect on leaching and the optimization of these parameters for efficient copper leaching in the classified ore will be carried out. The waste samples are not considered suitable for leaching because it will lead to high reagent consumption due to high gangue content which will invariably lead to poor leaching output.

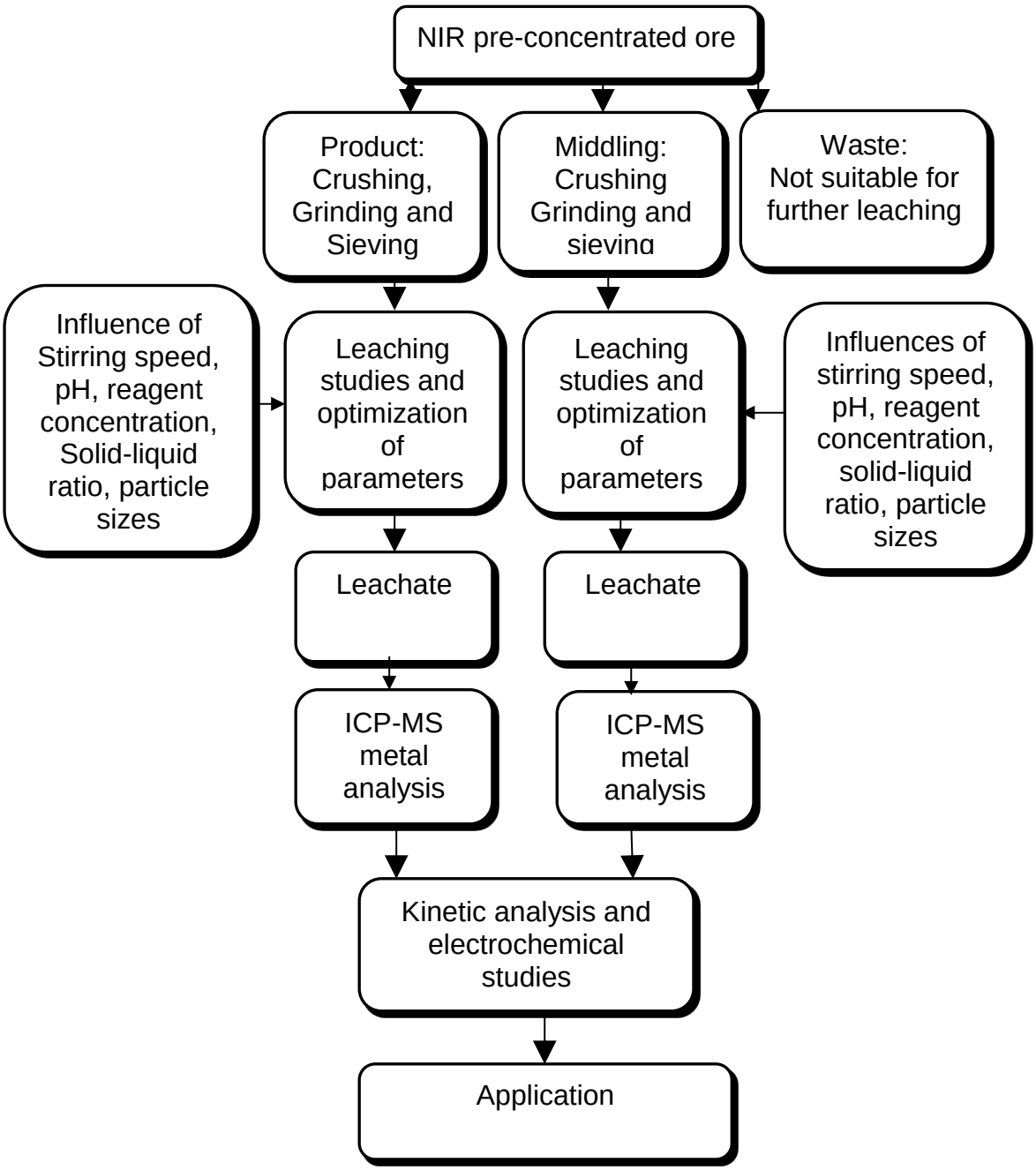

Figure 5.6 Workflow describing the strategy for leaching and electrochemical studies

Chapter 6

Leaching studies

6.1. Introduction

The results of the pilot study in the preceding chapter provided the basis for further detailed experimental analysis on the classified ore. Based on the evaluation of experimental results generated from the pilot study, a strategy for the leaching studies presented in this chapter and electrochemical studies in chapter 7 was developed. For practical considerations variables included higher solid-to-liquid ratio, temperature, reagent concentrations, leaching time and stirring speed. The listed process variables were considered for determination of their effect on leaching. This is informed based on the contrasting results obtained in the pilot study carried out in the preceding chapter. Thus, this chapter is poised at improving the understanding of the leaching of the classified ore by further investigating the influence of these parameters on the leaching process and optimization for improved copper extraction. The results obtained in the preceding chapter were essentially with Na_2EDTA in order to find a suitable leaching approach for the classified ore whereas this chapter will elucidate the effectiveness of Cu extraction using NH_4Cl because the stability constant (Ks) of Cu-EDTA is considered too large. In the case of $Cu(NH_3)_4^{2+}$ the Ks value is more suitable when considered in terms of electrodeposition.

The product and middlings were considered for investigation in this chapter because better results were obtained for these when compared to the waste. The waste fractions will not be considered for leaching due to the poor results obtained which is indicative of the high gangue and low copper content in these fractions. Alkaline and organic acid leaching are now been considered for leaching applications with a high prospect for copper recovery. Although much research work has been done over the last two decades with some degree of success, the technology has not yet attained an optimum level due to the lack of commercial application of the process (François-Xavier, 2013). Perhaps the reason could be poor economic recovery of the process or complex chemistry of the separation process which are found to be very unfavourable or complicated (Mathew, 2013). This may be some of the reasons hampering the slow growth of the process and further exploitation and expansion in the technology. The application of NIR pre-concentration and classification of copper ores before leaching and electrowinning considered in this research is an innovation with great potential for economic copper extraction and recovery from high gangue copper ores. The integrated approach adopted in this study is currently being investigated for economic development. Since this research focuses on the study of sensor-based pre-concentrated ores according to ore classifications, each category is treated separately under the same experimental conditions and result compared on the basis of amount of copper

dissolved (extracted). Therefore much interest is placed on the optimisation of the leaching process, kinetics of the leaching process and selectivity process for copper extraction in the classified ore. The optimisation of leaching parameters is expected to provide an insight into improved conditions for obtaining higher copper dissolution and optimum kinetic conditions of the process. The optimization processes for the operating conditions are presented in appendix 6.1 and 6.2.

The solubility of copper ores in the presence of a chemical lixiviant is well known from literature. However, as earlier stated the rate of copper extraction from the ores varies depending on the interaction of many operating conditions. As was found in the preceding chapter the dissolution of copper is one of the accurate ways to understand its leaching behaviour from ores, especially in ores and concentrates which are considered uneconomic to be treated by sulphuric acid and other inorganic lixiviants (Bingöl et al., 2005; Biswas and Davenport, 2013; Baba et al., 2013; Alafara et al., 2015). The development and optimisation of leaching processes is informed on the understanding that the classified ore have different mineral compositions which may cause differences in the leaching behaviour. Although the mechanism and kinetics of copper dissolution has been studied for different ores by many researchers, there is the need to exploit the leaching of pre-concentrated ore for greater understanding of the mechanism and kinetics governing the leaching rate. This will help to predict the performance of the process for industrial application.

In summary the chapter is focussed on the investigation of the leaching behaviour of pre-concentrated ore and the optimization of the process variables to improve the understanding of the process. Also, to observe the technical feasibility of the use of ammonium chloride and oxalic acid for leaching, and to suggest which is better with respect to operating conditions investigated based on the classified ore feed material. Consequently, this chapter will outline the effect of the concentration of ammonium chloride and oxalic acid, temperature, particle size fractions, solid-to-liquid ratio and stirring speed as important parameters, determining the leaching rate and mechanism controlling the process in this study. The chapter also presents the results of analysis of leachate and residue for determination of selective extraction of copper and efficiency of the lixiviants for application. To achieve this target many experiments were conducted to test the reproducibility. Detailed experimental procedures of the analysis can be found in chapter 3 unless otherwise stated.

6.2. Leaching strategy

The leaching was carried out in three batches with each batch specifically targeted at finding the best option for copper extraction. The first batch is mainly an optimization process to develop optimum conditions for copper extraction. All the process variables were tested by different experiments in order to determine

their effect on the rate of extraction. To achieve this, the sets of experiments were conducted under different conditions shown in Table 6.1.

Table 6.1 Parameters and leaching conditions for first batch experiment

Parameters	conditions
Ammonium chloride	0.5 M to 5 M
Temperature	40 ˚C to 70 ˚C
Stirring speed	300 rpm to 800 rpm
Particle sizes	- 63 +45 μm, - 90 + 63 μm and -125 + 90 μm
Weight of solid	2 g to 4 g
Reagent volume	Constant volume (250 mL)
Leaching time	2 hour

It should be noted that the first experiment batch is preparatory to the second batch. It is expected that the result from the first batch will serve as a model toward achieving best leaching results. Since this batch is concerned with the optimization of the leaching process, the effect of time on leaching was limited to 2 hours. Details of the optimization process and conditions are presented in appendix 6.1.

The second batch of the experiment was conducted to test the effect of the optimised parameters developed during the first batch of experiments. The target was to ascertain the effect of increasing some variables such as leaching time, temperature and solid-to-liquid ratio, on copper extraction at low ammonium chloride concentration. Consequently, the solid-to-liquid ratio was increased from 4 g to 6 g and the leaching time was extended to 4 hours, temperature 70 ˚C to 90 ˚C while the ammonium chloride concentration was varied from 0.55 M to 1.65 M. Table 6.2 and Appendix 6.2 shows the parameters, conditions and optimization process.

Table 6.2 Parameters and leaching conditions for second batch experiment

Parameters	Conditions
Ammonium chloride conc.	0.55 M to 1.65 M
Temperature	70 ˚C to 90 ˚C
Stirring speed	Constant (300 rpm)
Particle size	Constant (- 63 + 45 μm
Weight of solid	4 g to 6 g
Reagent volume	Constant (250 mL)
Leaching time	Constant (4 hour)

The third batch of the leaching experiment was a comparative leaching study between alkaline lixiviant (ammonium chloride) and organic lixiviant (oxalic acid). The experiment was carried out separately in a batch under the same experimental conditions (Table 6.3) to evaluate the leaching efficiency of the two reagents.

Table 6.3 Parameters and leaching conditions for third batch experiment

Parameters	Conditions
Oxalic acid conc.	0.25 M to 0.75 M
Ammonium chloride conc.	0.5 M to 0.75 M
Temperature	Constant (80 ˚C)
Stirring speed	Constant (300 rpm)
Particle size	Constant (- 63 + 45 μm)
Weight of solid	Constant (5 g)
Reagent volume	Constant (250 mL)
Leaching time	Constant (4 hour)

In each case all the experiments were conducted using the same reactor while in each experimental run, 250 mL of the reagent was kept constant. At the end of each experimental run in all the three batches, leachates obtained were filtered to obtain filtrate for ICP-MS analysis. The selected residues obtained after optimum leaching from second batch and third batch were dried according to the method described in chapter 3, Section 3.5.4. The percentage of copper extracted and other metals in the filtrate with ICP-MS is reported as a function

of leaching time, t. To ascertain the amount of copper extracted and the leaching efficiency of the reagents the remaining portion of the residue was examined for mineralogical transformation of the ore phases using XRD. Details of the experimental procedure can be found in chapter 3.

6.3. Effect of leaching parameters

Investigation of the leaching behaviour of the classified ore was carried out by monitoring the effect of variations in the process parameters. Leaching kinetics of the process was evaluated using the shrinking core model (Khang and Levenspiel, 1973, Levenspiel, 1999, Awe, 2013, Baba et al., 2014, Parada et al., 2014). The chemical conversion of leaching particle can be expressed using equations depending on the chemical-physical process controlling the copper leaching. To avoid ambiguity the three kinetic models tested in this work are repeated in this section.

1. For surface chemical controlled process the expression is shown in Equation 6.1:

$$1-(1-\alpha)^{1/3} = \frac{K_c M_B C_A t}{\rho s \beta r o} t = k_r t \quad (6.1)$$

2. For diffusion controlled process the expression is:

$$1-\frac{2}{3}\alpha - (1-\alpha)^{2/3} = \frac{2M_S D C_A t}{\rho_s \beta r^2 O} = k_d t \quad (6.2)$$

3. For mixed control process the expression is:

$$\alpha = k_f t = \frac{3bk_c C_A}{\rho s r o} \quad (6.3)$$

Where α is the fraction reacted, K_C is the kinetic constant, M_S is the molecular weight of the solid, C_A is the concentration of the dissolved lixiviant A in the bulk of the solution, ρ_s density of the classified ore, β is the stoichiometric coefficient of the reagent in the leaching reaction, ro is the radius of the solid particle, t is the reaction time, D is the diffusion coefficient in the porous product layer, k_r and k_d are rate constants

6.3.1. Effect of temperature on the leaching behaviour of pre-concentrated ore

The effect of temperature on the leaching behaviour of the classified ore was investigated on the first batch of the leaching experiment by keeping the other leaching parameters constant while the temperature was varied (Appendix 6.1). The experiments were conducted for the temperature range of 40 ˚C to 70 ˚C with a solid-to-liquid ratio of 1: 250 mL, particle size of −63+45 µm, stirring speed of 300 rpm, and ammonium chloride concentration of 5 M. Results obtained are presented graphically in Figures 6.1a and 6.1b for the product and

middling, respectively. For each experiment the percentage extractions of copper in the classified ore are compared to evaluate the difference in the rate of extraction between the middling and the product. The trend in copper dissolution during the leaching is shown by plotting the rate of copper extraction against leaching time as shown in Figures 6.1a and 6.1b. Details on the extraction of other metals in the leachate solutions after leaching will be discussed under the section of residue analysis. The results shown in Figures 6.1a and 6.1b indicate that temperature had a positive influence on the dissolution behaviour of the classified ore. It was found that increasing the temperature of the leaching system from 40 ˚C to 70 ˚C led to an increase in the rate of copper extraction both in the middling and the product. The improvement on the rate of Cu extraction suggests that the leaching reaction is temperature sensitive. The observed increase in the rate of Cu dissolution clearly reveals the dependence of the process on temperature. The initial rate of extraction was 21.5 % and 27.3 % at a temperature of 40 ˚C which gradually increased to 75 % and 89 % when the temperature was increased from 40 ˚C to 70 ˚C. As can be seen in Figures 6.1a and 6.1b, the rate of Cu dissolution was higher in the product than in the middling. This is a clear indication of the difference in the Cu content. It is worth noting too that the content of gangue in the two classified ores is not the same. This could be another contributing factor. The pattern of Cu dissolution in the classified ore is a further confirmation of the earlier results presented in the preceding chapter where Cu extraction was found to be higher in the product than in the middling and waste. The enhancement of leaching by temperature is attributed to the fact that when copper particles gained more kinetic energy the rate of effective collision between them increases, resulting in the breaking of the ore matrix with the reagent in contact with Cu in the ore. This is in line with the study by Prada et al. (2014).

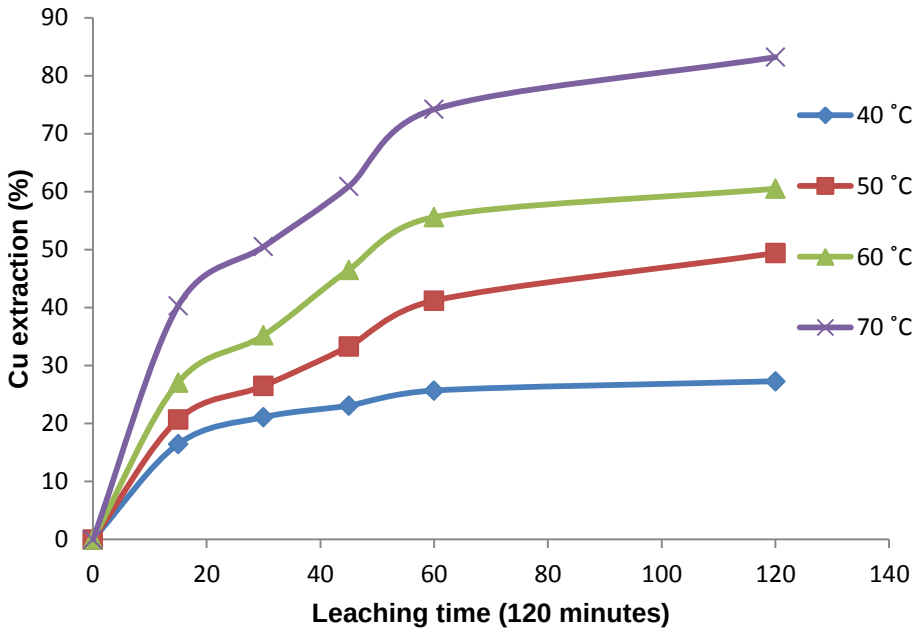

Figure 6.1a: Cu extraction in the product as a function of leaching time (t), temperature range 40 ˚C to 70 ˚C, stirring speed 300 rpm, - 64 + 45 µm, NH_4Cl concentration 5 M, solid-to-liquid ratio 1: 250 mL

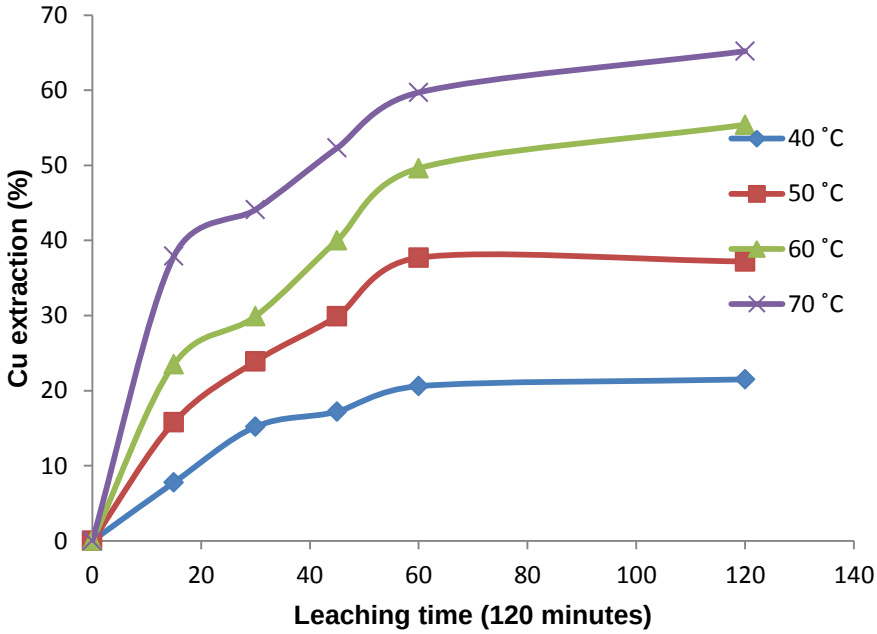

Figure 6.1b: Cu extraction in the middling as a function of leaching time (t), temperature range 40 ˚C to 70 ˚C, stirring speed 300 rpm, - 64 + 45 µm, NH_4Cl concentration 5 M, solid-to-liquid ratio 1: 250 mL

6.3.1.1. Kinetic analysis

As earlier stated, the chemical kinetics of the conversion of copper particles during the leaching process can be described using the shrinking core model (Levenspiel, 1999). The fluid-solid heterogeneous reaction of the shrinking copper particle with ammonium chloride reagent can be expressed using Equation 6.4:

$$a\,(A\ NH_4Cl) + b(B\ \text{solid Cu ore}) \rightarrow \text{product} \qquad (6.4)$$

To determine the rate controlling the kinetic process during leaching, the experimental data in Figures 6.1a and 6.1b were tested using all the three Shrinking Core Models (SCM) outlined in equations 6.1 to 6.3. Temperature-dependence of a rate equation has been discussed in chapter 2, it was reported that the Arrhenius type equation (Equation 2.26) can be used to represent the temperature dependence of the leaching process. The procedure for determining the parameter revealed that the fractions reacted can be plotted against time to obtain the rate constants. So the frequency factor Ao and the activation energy Ea of the leaching process can be calculated by finding K of the reaction at different temperatures. This was obtained by plotting the fraction of copper reacted α, against time, t for all the experimental data. The result obtained is shown in Figure 6.2a and 6.2b for the product and middling, respectively. By fitting the data into all the SCM models, where higher correlation coefficient values are obtained with a particular model is considered the best fit. The Arrhenius equation is presented in equation 6.5 for clarity after Awe (2013) and Baba et al. (2013).

$$k_r = A\exp\left[{}^{-Ea}/_{(RT)}\right] \qquad (6.5)$$

Where A is the frequency factor, Ea is the apparent activation energy, R is the universal gas constant, and T is the absolute temperature.

The activation energy for the leaching process of the classified ore was calculated from the apparent rate constants, k_r obtained from slopes of the straight lines in Figure 6.1a and 6.1b. The result of the Arrhenius plots of (ln k_r) versus the reciprocal of temperature ($1/T$) is presented in Figures 6.3a and 6.3b. It should be noted that of all the SCM models tested better fits (higher correlation coefficient) were obtained using the chemically controlled model on account of higher correlation coefficient values obtained. This suggests a good agreement between experimental results and the model.

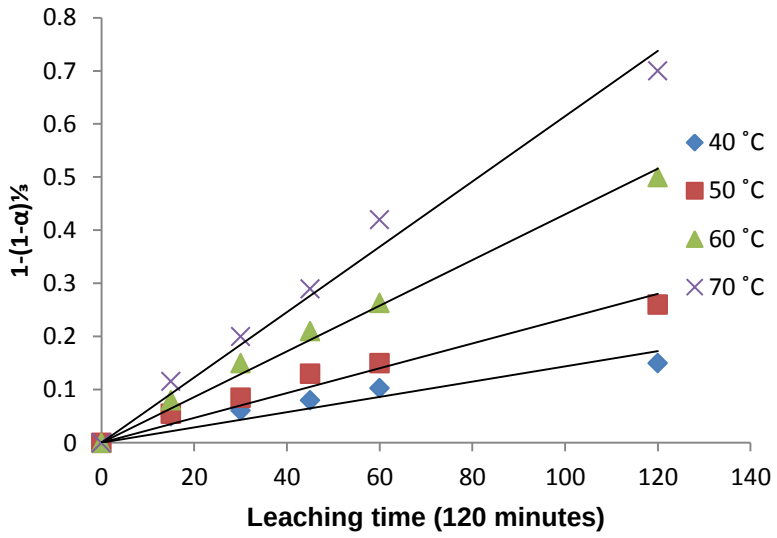

Figure 6.2a: Plot of $1-(1-\alpha)^{⅓}$ versus leaching time, t for product at different temperatures

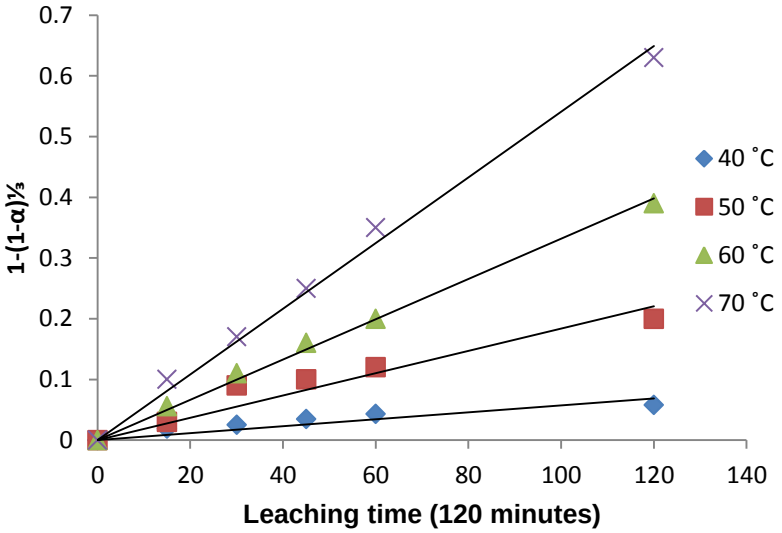

Figure 6.2b: Plot of $1-(1-\alpha)^{⅓}$ versus leaching time, t for middling at different temperatures.

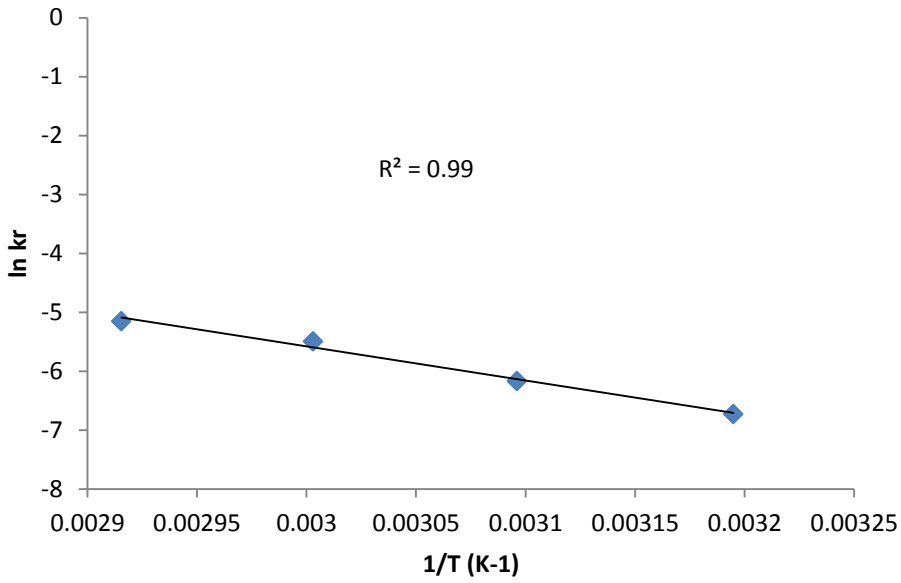

Figure 6.3a: Arrhenius plot of ln k_r versus 1/T for product

The activation energy is calculated using the relationship:

Ea = - (slope) (8.314) J/mol

= - (-5803.2) (8.314)/1000

Ea = 48 kJ/mol

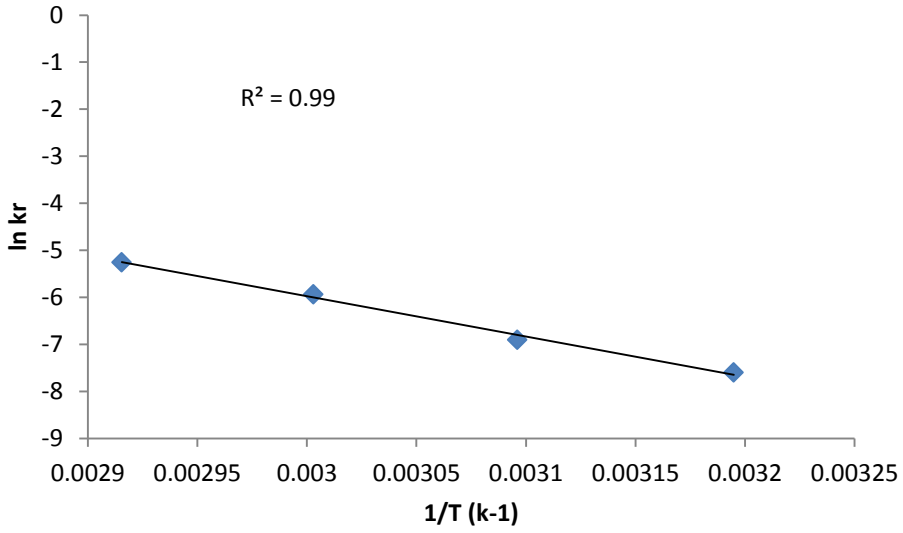

Figure 6.3b: Arrhenius plot of ln k_r versus 1/T for middling

The activation energy is calculated using the relationship:

Ea = - (slope) (8.314) J/mol

= - (-8571.8) (8.314)/1000

Ea = 71 kJ/mol

Figures 6.3a and 6.3b suggest that, the activation energy of the reaction (Ea) was 48 kJ/mol and 71 kJ/mol according to the Arrhenius relationship (Equation 6.5). These values indicate that the leaching behaviour of the classified ore (product and middling) fractions proceeds according to the surface chemical reaction control. Chemically-controlled reactions are temperature-dependent, independent of the agitation speed and characterised by activation energy usually greater than 12 kJ/mol (Awe and Sandström, 2010; Awe, 2013; Baba et al., 2013; Baba et al., 2010; Ekmekyapar et al., 2008). The variations in Ea values between the product and the middling fractions may be related to the variation in mineralogical concentration. This implies that more energy and or chemicals are required for Cu extraction from the middling. Van der Merwe and Kasaini (2011) found that the sensitivity of copper leaching to change in temperature is an indication of surface-controlled reaction. The observation in this study may probably be due to the location of copper minerals in the ore which was found to be locked up and disseminated within the ore matrix. Hence temperature is required to breakdown the matrices of the ore minerals for effective contact of the leaching chemical and copper mineral.

6.3.2. Effect of ammonium chloride concentration

The effect of ammonium chloride concentration was determined on the leaching behaviour of the classified ore. The concentration of the lixiviant was varied from 0.5 M to 5 M while the other experimental parameters; temperature, stirring speed, particle size, solid-to-liquid ratio and leaching time, were kept constant (Appendix 6.1). Results indicated that the variations in NH_4Cl did affect the leaching process. The rate of copper dissolution increases considerably in both samples when the concentration was increased from 0.5 M to 5 M. The rate of copper extraction after 2 h was observed to increase from 20 % and 26.5 % to 65.0 % and 83.3 % in the middling and product, respectively. Apparently the rate of Cu dissolution in the classified ore increases steadily with increasing NH_4Cl concentration. The result is an indication that the leaching of the ore depends strongly on concentration of the lixiviant. The leaching process was initiated by ionization of the lixiviant in aqueous medium and the hydrolysis of NH_4^+ to produce the NH_3 ligand in the leaching solution for the reaction to occur. It has been found that the hydrolysis reaction is a vital requirement for releasing the ligand required for Cu extraction from the ore (Ekmekyapar et al., 2012). The NH_3 ligand undergoes a complexometric reaction with Cu to form many intermediates of copper-ammonia complex species $[Cu(NH_3)_2^+]$ and $[Cu(NH_3)_3^{2+}]$ which are further converted to the stable copper-ammonia $[Cu(NH_3)_4^{2+}]$ complexes in the leachate solution (Liu et al., 2010, Ekmekyapar et al., 2012). Electrochemical studies of the leachate to understand the copper ammonia complex species formed during leaching and the electrodeposition of

copper from the complexes in solution is presented in the next chapter. The result of the rate of Cu extraction in the classified ore is presented in Figures 6.4a and 6.4b, for the middling and product respectively.

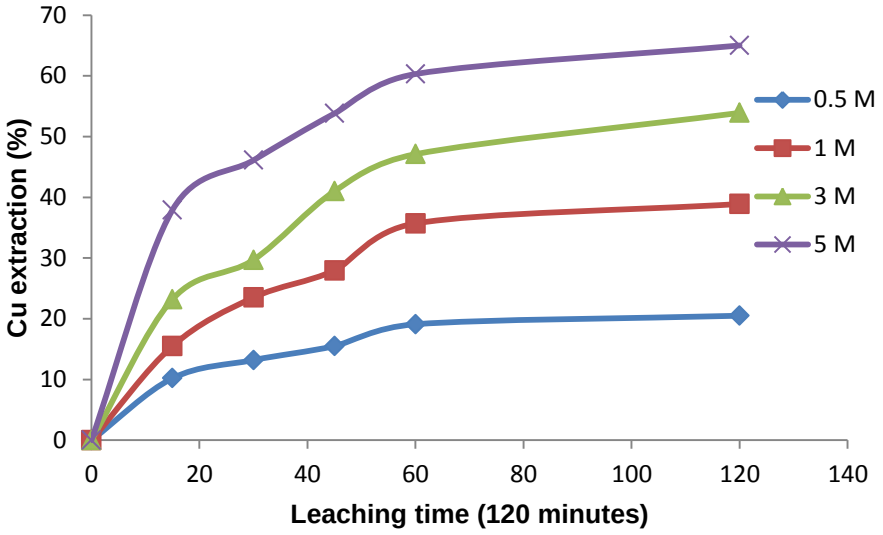

Figure 6.4a: Cu extraction in the middling as function of leaching time, t, NH_4Cl concentration range 0.5 M to 5 M, stirring speed 300 rpm, particle size - 64 + 45 µm, temperature 70 ˚C, solid-to-liquid ratio 1: 250 mL

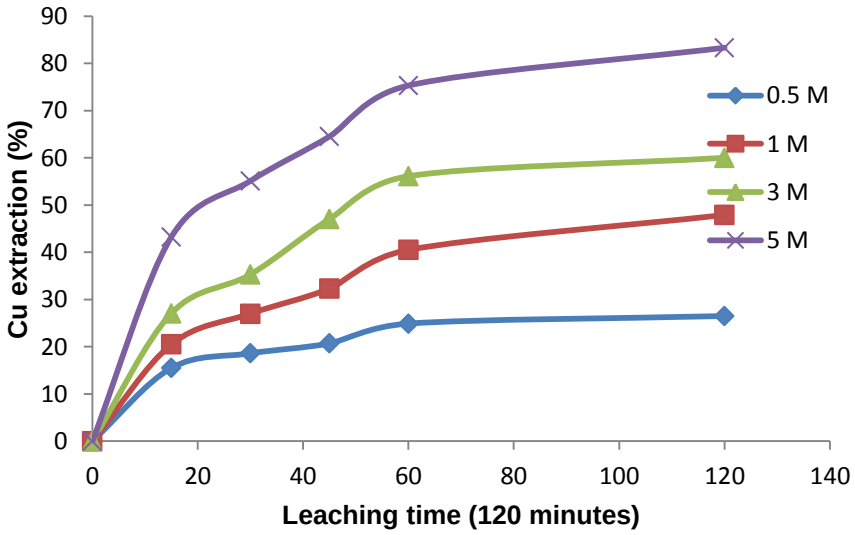

Figure 6.4b: Cu extraction in the product ore as function of leaching time (t), NH_4Cl concentration range 0.5 M to 5 M, stirring speed 300 rpm, particle size - 64 + 45 µm, temperature 70 ˚C, solid-to-liquid ratio 1: 250 mL

When the data of Cu extraction obtained from the experiment (Figures 6.4a and 6.4b) was fitted using the SCM (Equations 6.1 to 6.3), Figures 6.5a and 6.5b were constructed. The result of the plot indicated that the best fit was obtained

using the chemical control reaction (Equation 6.1). The rate constants $lnkr$ were obtained by plotting the natural logarithm of the slope against time, t. The linear relationship obtained from the plot of $1-(1-\alpha)^{1/3}$ versus leaching time (t) further suggests that the reaction is controlled by shrinking particle model for chemical reaction at the interface. The kinetic equations about the effect of NH_4Cl concentration is shown in equations 6.6a and 6.6b. From the values presented in the equations 6.6 and 6.7, the apparent reaction order for the dissolution of Cu from the classified ore was estimated to be 0.47 and 0.43 with respect to $[H^+]$ concentration for the middling and the product. With the same reaction order mechanism obtained, it is probable that the reaction leading to Cu extraction in the ore follows a similar pattern. This is expected, since the Cu was found to be present in the mineral matrix in the same manner. The only difference is the variation in Cu content and other mineral gangue content.

$$lnkr = 0.47\ ln[NH_4Cl] - 7.8 \quad (6.6)$$

$$lnkr = 0.43\ ln[NH_4Cl] - 6.7 \quad (6.7)$$

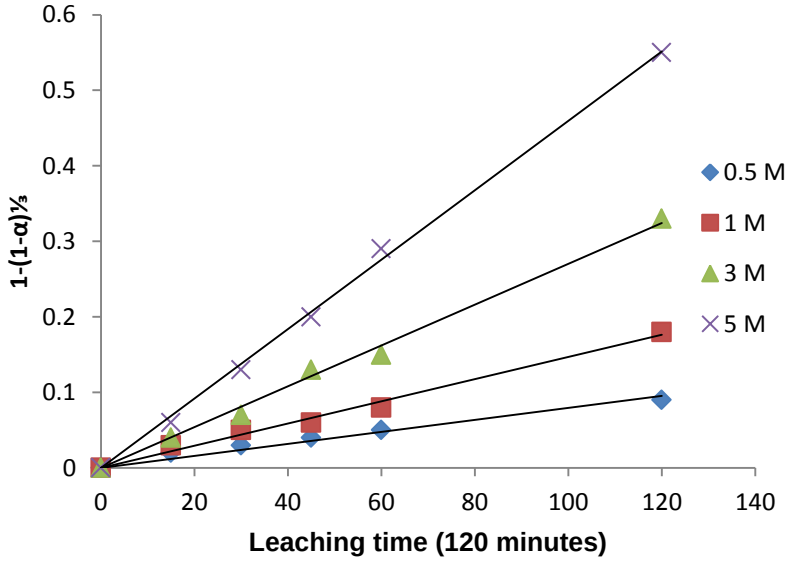

Figure 6.5a: Plot of $1-(1-\alpha)^{1/3}$ versus leaching time, t for middling

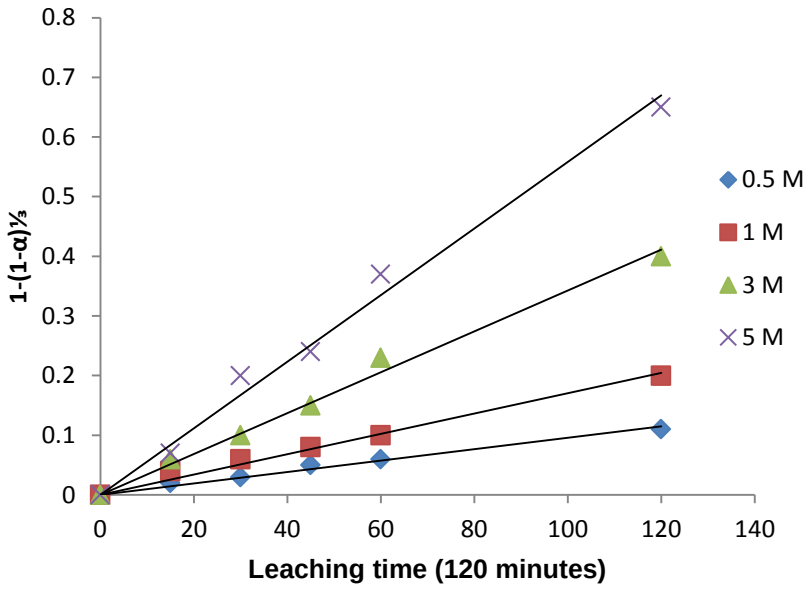

Figure 6.5b: Plot of $1-(1-\alpha)^{⅓}$ versus leaching time, t for product

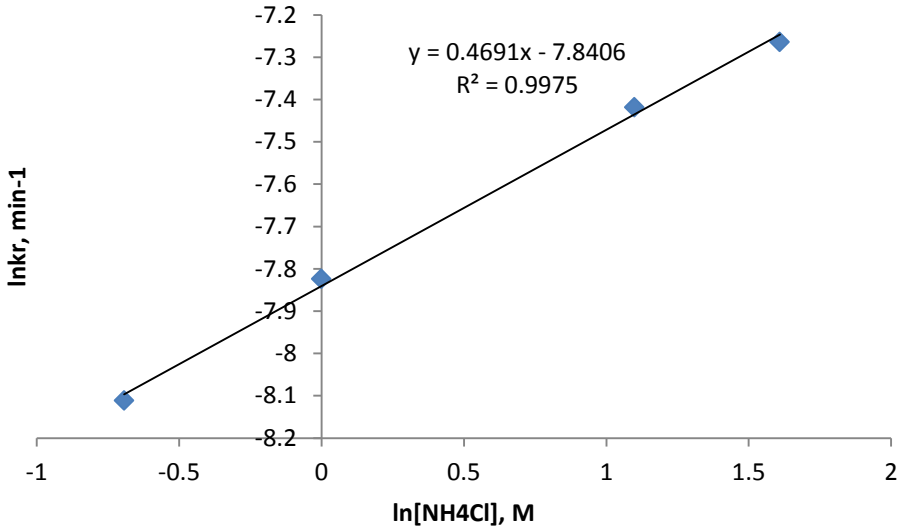

Figure 6.6a: Plot of $lnkr$ versus ln[NH_4Cl] for determination of reaction order, middling

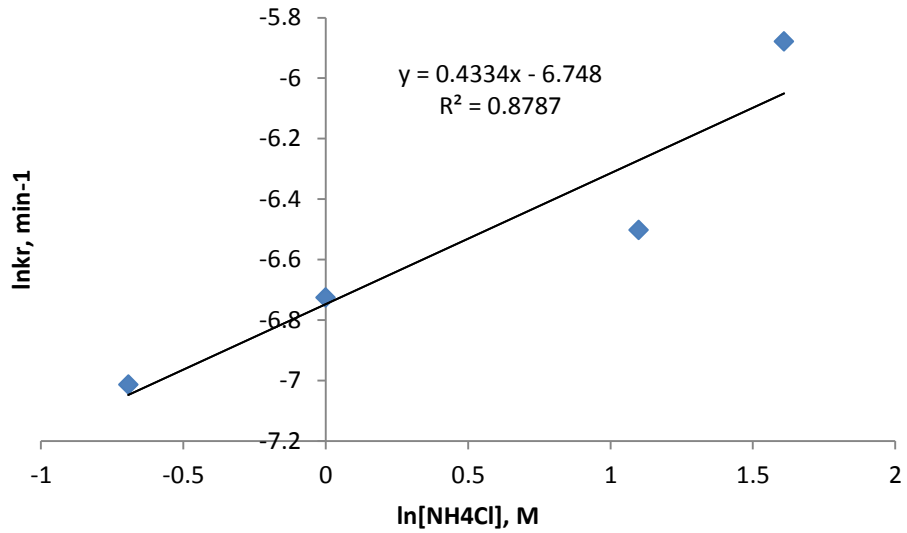

Figure 6.6b: Plot of $lnkr$ versus ln[NH_4Cl] for determination of reaction order, product

6.3.3. Effect of particle size

Figures 6.7a and 6.7b show the effect of particle size on Cu extraction for the middling and product, respectively. The experiment was performed using – 63 + 45 μm, - 90 + 63 μm and -125 + 90 μm particle size fractions (Table 6.1). Optimization of the leaching process was undertaken by keeping NH_4Cl concentration, solid-to-liquid ratio, temperature, and stirring speed constant (Appendix 6.1). The results show that the effectiveness of rate of leaching and rate of Cu extraction increases with decreasing particle sizes from – 63 + 45 μm to - 90 + 63 μm and -125 + 90 μm. The trend in dissolution was observed to follow the same pattern in the classified ore, with the rate of dissolution steadily increasing over time. The result agrees with Awe (2013) and Baba et al. (2014) who indicated that the finer the sizes of particles of copper ores the better the leaching results and also the faster the leaching reaction. This is an indication that surface area of the ore increases with a decrease in particle size, thus the chance of more particles to react is very high. Awe (2013) found that with decreasing particle size the rate of mass-transfer coefficient appears to increase. This supports the theory that the change of ratio of solid to liquid per volume relates to geometric properties of ore, such as sphericity, which affects rate of chemical reaction. The observed behaviour is interpreted using the SCM model.

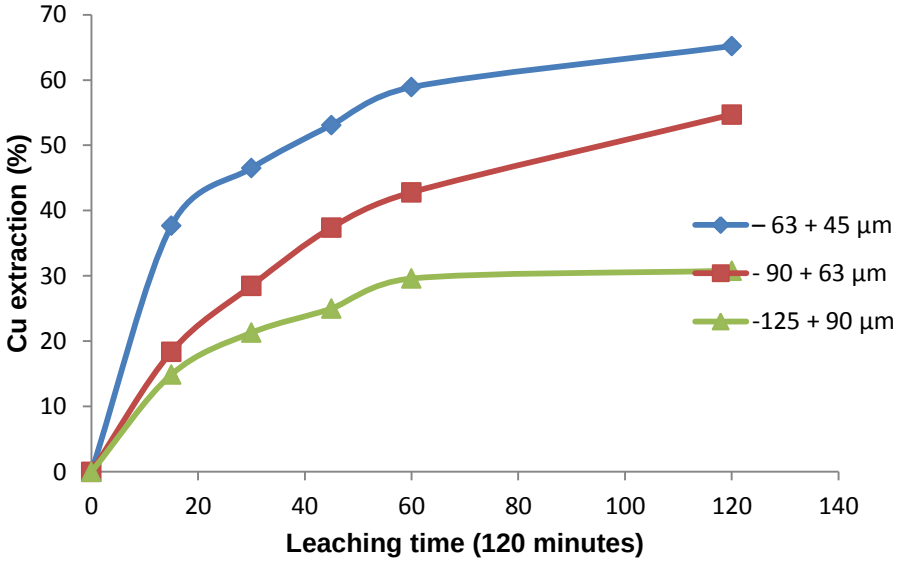

Figure 6.7a: Cu extraction in the middling as a function of leaching time (t), Particle sizes - 64 + 45 µm, - 90 + 63 µm and -125 + 90 µm, NH_4Cl concentration 5 M, stirring speed 300 rpm, , temperature 70 ˚C, solid-to-liquid ratio 1: 250 mL

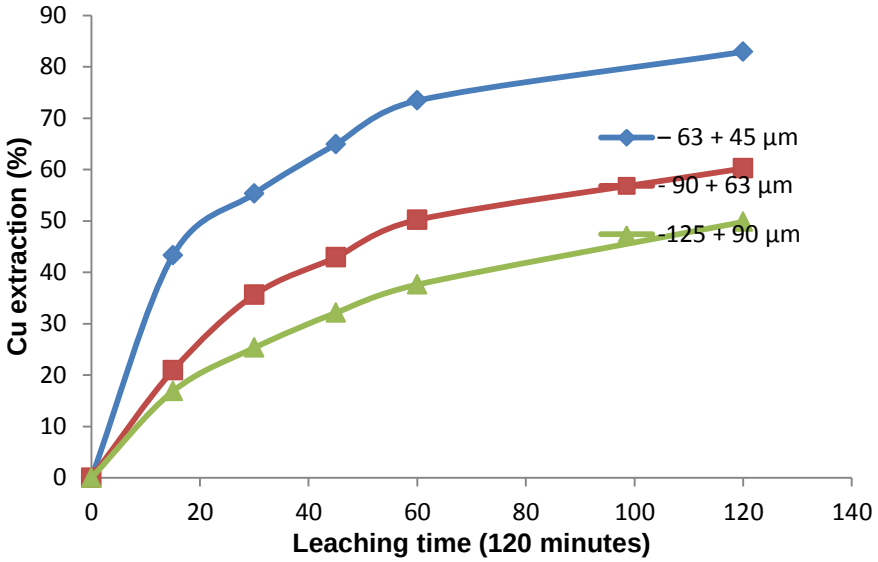

Figure 6.7b: Cu extraction in the product as a function of leaching time (t), Particle sizes - 64 + 45 µm, - 90 + 63 µm and -125 + 90 µm, NH_4Cl concentration 5 M, stirring speed 300 rpm, , temperature 70 ˚C, solid-to-liquid ratio 1: 250 mL

According to the SCM model used for evaluating leaching results, if the leaching process is chemically-controlled then the rate constants would be inversely proportional to the particle size. The experimental data was tested to determine the dependence of leaching on particle size by fitting the data into the SCM. The plot of $1-(1-\alpha)^{1/3}$ versus leaching time, t is shown in Figures 6.8a and 6.8b while the results of the plot of the rate constant $lnkr$ versus inverse of initial

particle size ($\frac{1}{ro}$) is presented in Figures 6.9a and 6.9b. The inverse of particle size ($\frac{1}{ro}$) is obtained from the geometric averages of the particles determined using the relationship in equation 6.8 after Baba et al. (2013) and Baba et al. (2014).

$$r_O = \sqrt{\frac{(f1+f2)}{2}} \qquad (6.8)$$

The results of the plot indicated a linear dependence of leaching on particle size since the plot of rate constants versus ($\frac{1}{ro}$) increases. As can be seen in the plots shown in Figures 6.9a and 6.9b the linear line passing through the origin is in conformity that the leaching is chemical reaction controlled. This observation agrees with Baba et al. (2013) and Baba et al. (2014) on the dependence of leaching on particle size controlled by surface chemical reaction.

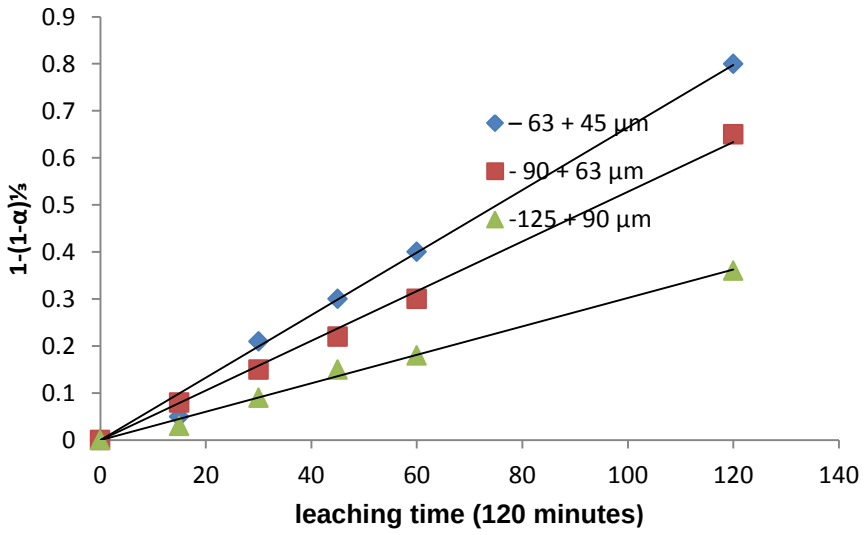

Figure 6.8a: Plot of 1-(1-α)^{⅓} versus leaching time, t for the middling

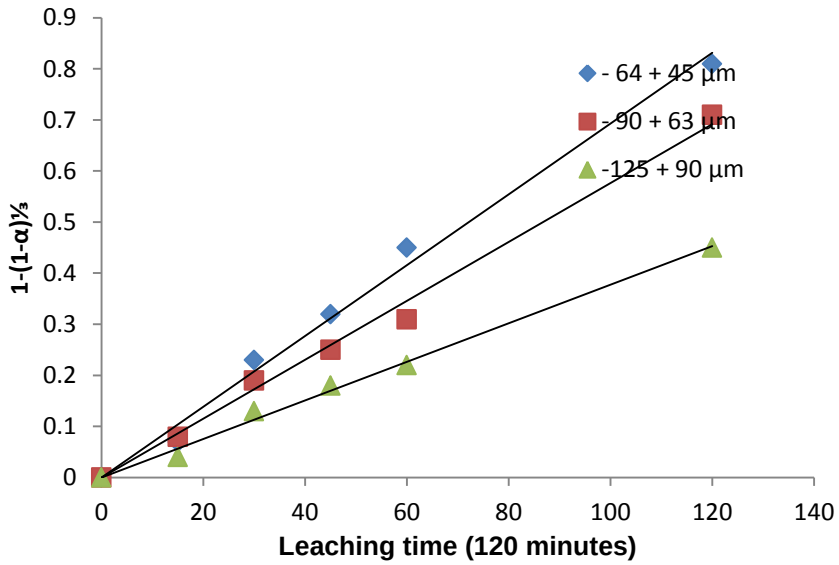

Figure 6.8b: Plot of $1-(1-\alpha)^{⅓}$ versus leaching time, t for the product

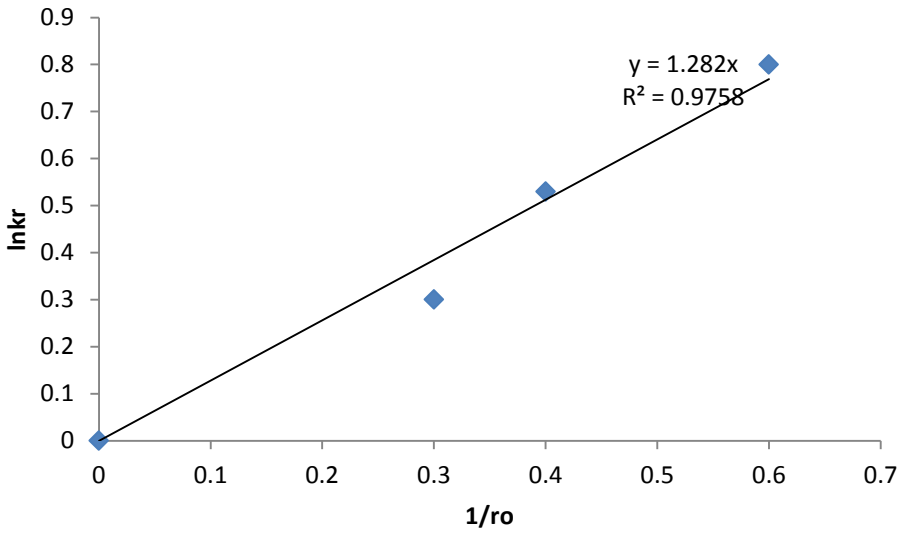

Figure 6.9a: Plot of apparent rate constant versus inverse of particle sizes, for the middling

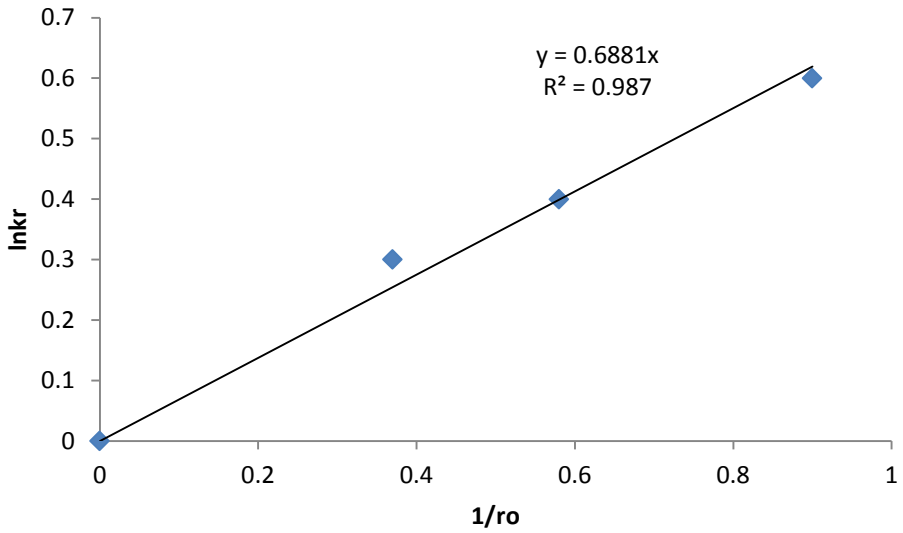

Figure 6.9b: plot of apparent rate constant versus inverse of particle sizes, product

6.3.4. Effect of stirring speed

The effect of stirring speed on Cu dissolution from the classified ore was determined to provide information with respect to the prevailing leaching mechanism. Experiments were carried out on - 64 + 45 µm size fraction, in 5 M NH_4Cl at 70 ˚C, solid-to-liquid ratio of 1 g: 250 mL, leaching time 2 h with stirring speed from 300 rpm to 800 rpm. The agitation speed was varied over three stirring rates (300, 500 and 800 rpm) while the other variables were kept constant. The result of agitation speed is presented in Figures 6.10a and 6.10b, for the middling and the product respectively. The result shows that the rate of Cu extraction decreases with increasing stirring speed from 300 rpm to 500 rpm and 800 rpm. Excessive agitation prevents the effective contact between the reagent and the ore particles. The lack of dependence of leaching on high agitation speed is characteristic of chemically controlled reactions.

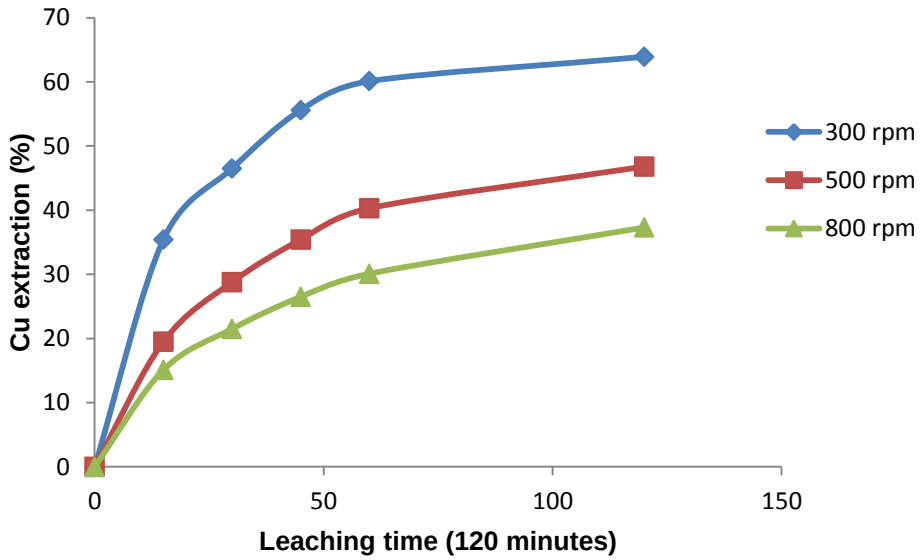

Figure 6.10a: Cu extraction in the middling as a function of leaching time (t), Particle sizes - 64 + 45 µm, 5 M NH_4Cl concentration, stirring speed 300 rpm – 800 rpm, temperature 70 ˚C, and solid-to-liquid ratio 2: 250 mL

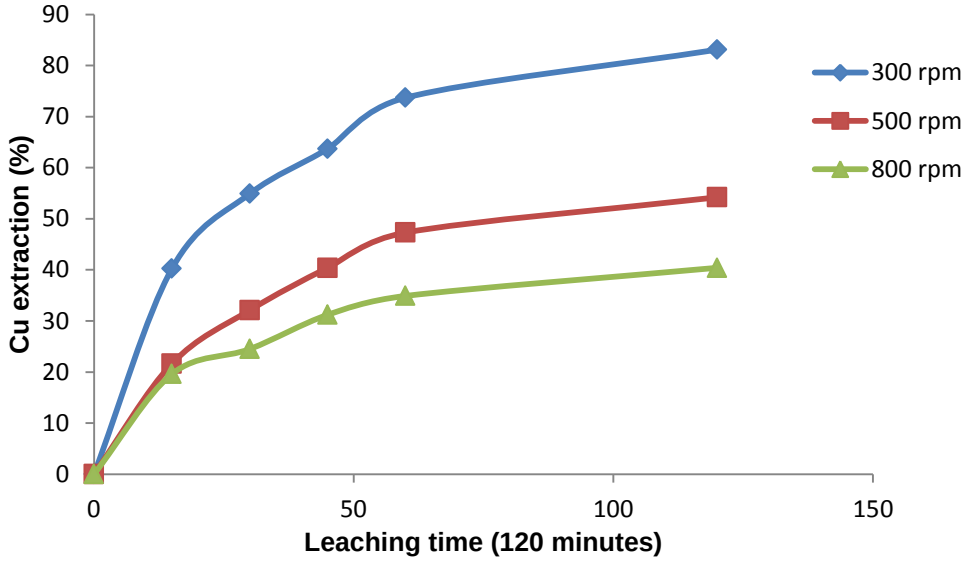

Figure 6.10b: Cu extraction in the product as a function of leaching time (t), Particle sizes - 64 + 45 µm, 5 M NH_4Cl concentration, stirring speed 300 rpm to 800 rpm, temperature 70 ˚C, and solid-to-liquid ratio 2: 250 mL

6.3.5. Effect of solid-to-liquid ratio

The effect of the solid-to-liquid ratio in the first batch of experiments was investigated for four solid-to-liquid ratios (Appendix 6.1). Further discussion on the effect of solid-to-liquid ratio is made under discussions on the second batch of experiments. During the experiments the liquid volume and other parameters presented in Appendix 6.1 were kept constant, while the solid was varied. According to results shown in Figures 6.11a and 6.11b, the rate of Cu extraction

as a function of weight of solid/volume of liquid was significantly affected by the changes in the solid-to-liquid ratio. The dissolution of Cu increases significantly with decrease in solid-to-liquid ratio. The pattern of Cu extraction appears to be the same in the classified ore. The trend where the leaching of Cu extraction decreases is due to an increase in the solid amount in the reaction mixture. This observation is similar to that by Bingöl and Canbazoğlu (2004) and Bingöl et al. (2005) on the dissolution kinetics of malachite in sulphuric acid and ammonia/ammonium carbonate. Since the rate of Cu extraction appears to increase with decreasing solid to liquid amount in the pre-concentrated ore, a balanced solid weight to liquid volume is essential to achieve optimum Cu leaching. This factor does not suffice to imply that the Cu extraction is based entirely on this parameter. However, it is an essential requirement for constructing a compatible leaching reactor with capacity for handling a specific mass/ volume at a given ratio. For better output a consideration of this is done in tandem with concentration of lixiviant and time of leaching.

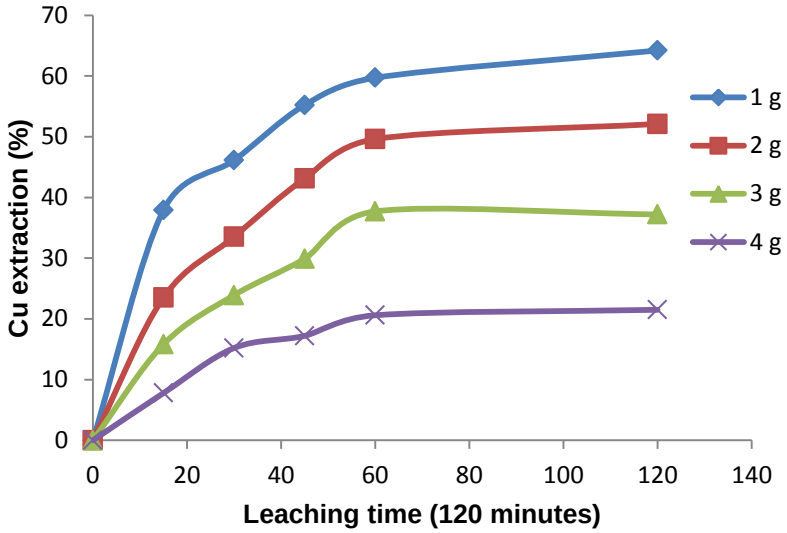

Figure 6.11a: Cu extraction in the middling as a function of leaching time (t), solid-to-liquid ratio 1 to 4 g/ constant volume of 250 mL, particle sizes - 64 + 45 µm, 5 M NH_4Cl concentration, stirring speed 300 rpm, and temperature 70 ˚C.

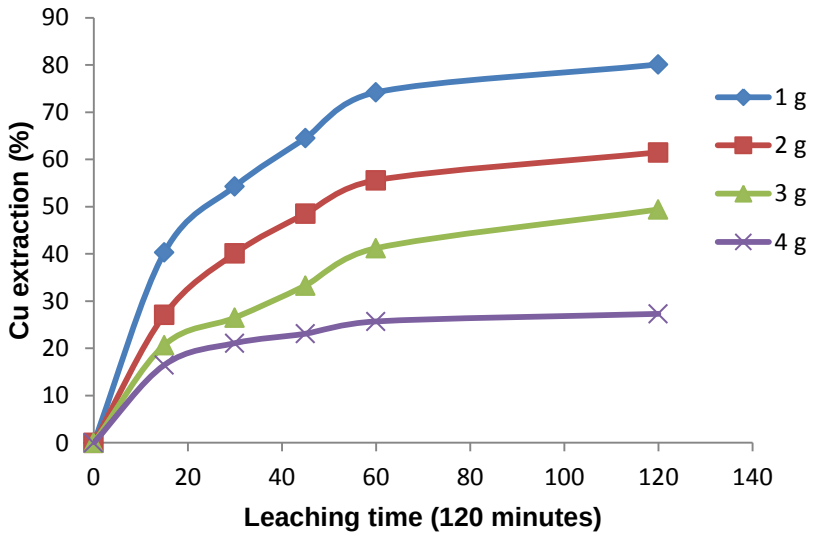

Figure 6.11b: Cu extraction in the product as a function of leaching time (t), solid-to-liquid ratio 1 to 4 g/ 250 mL Particle sizes - 64 + 45 µm, 5 M NH_4Cl concentration, stirring speed 300 rpm, and temperature 70 ˚C

6.4. Validation of leaching and process parameters

The second batch of the experiment was conducted to validate the optimized variables in the first batch of the leaching experiments. The process focussed on the determination of the effect of leaching time, solid-to-liquid ratio and NH_4Cl concentration on the extent of Cu extraction. This is a follow up to the experiment in the first batch which was principally to find out the optimum conditions that are fundamental toward obtaining an improved result. Since the results in the first batch indicated that temperature, NH_4Cl concentration, solid to liquid amount and particle sizes have a positive influence on the leaching behaviour of the pre-concentrated copper ores. These parameters, which were optimised in the first batch of experiments, were further extended (Table 6.2). The optimized variables and conditions are presented in appendix 6.2. In each case the leaching process was carried out in order to determine the effectiveness of the parameters studied or otherwise on the extent of Cu extraction. The results obtained are illustrated in Figures 6.12a, 6.12b, 6.13a and 6.13b. It can be seen that despite the NH_4Cl concentration being kept low, the rate of Cu extraction continues to increase due to the increase in temperature with extended leaching time. The dissolution increased from 40 % to 71.5 % and 45 % to 87.75 % at 6 g solid weight to liquid volume in the middling and product. Under these experimental conditions the effect of leaching time was seen to be effective. This is an indication of the effectiveness of time, NH_4Cl, solid-to-liquid ratio, and temperature to the rate of Cu extraction. Another point to note is that all the variables appear to be interdependent. Based on this result it is notable that the leaching of the classified ore is effective under both experimental conditions determined in the first and second

batch leaching tests. But in the case of the second batch experiment, doubling the leaching time is probably a factor complimenting the effect of NH_4Cl concentration. However, for better results and economic consideration of these operating parameters it is important to consider factors such as the cost of NH_4Cl and the grinding cost. These are important factors for the leaching process.

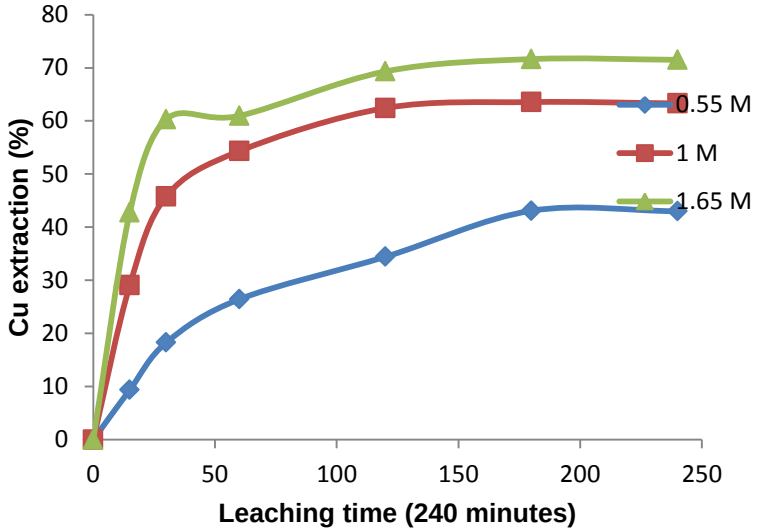

Figure 6.12a: Cu extraction in the middling as a function of extended leaching time (t), at 0.55 M to 1.65 M NH_4Cl concentration, Particle size - 64 + 45 µm, temperature 80 ˚C, solid-to-liquid ratio 6 g/ 250 mL and stirring speed 300 rpm

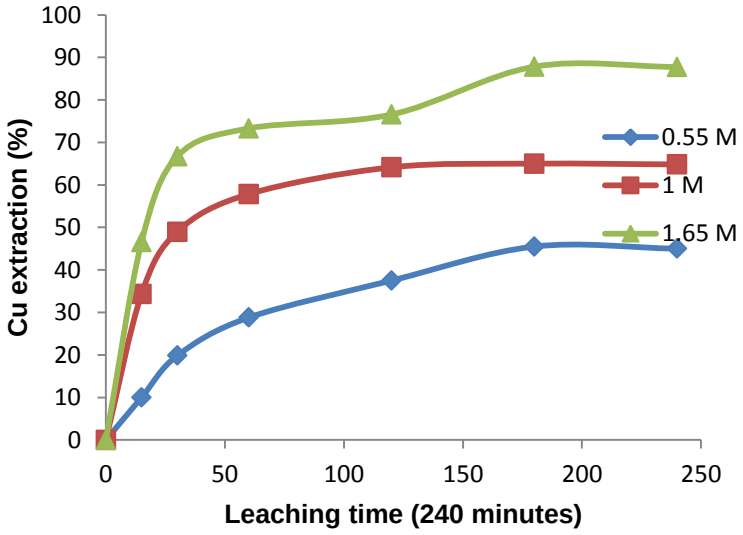

Figure 6.12b: Cu extraction in the product as a function of extended leaching time (t), at 0.55 M to 1.65 M NH_4Cl concentration, Particle size - 64 + 45 µm, temperature 80 ˚C, solid-to-liquid ratio 6 g/ 250 mL and stirring speed 300 rpm

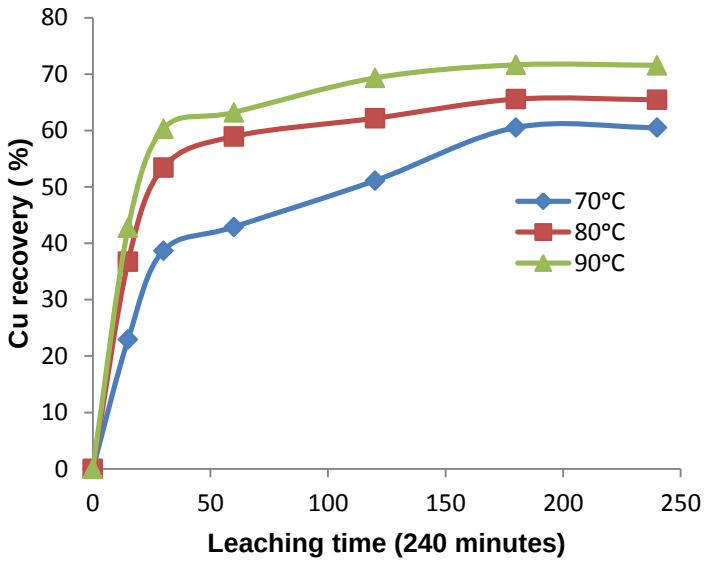

Figure 6.13a: Cu extraction in the middling as a function of extended leaching time (t), 1.65 M NH_4Cl concentration, Particle size - 64 + 45 µm, temperature range 70 ˚C to 90 ˚C, solid-to-liquid ratio 6 g/ 250 mL and stirring speed 300 rpm.

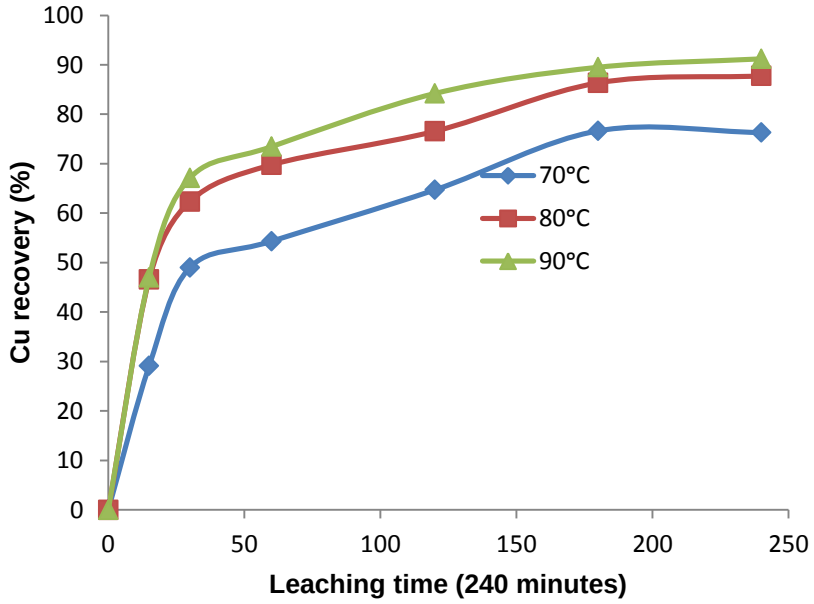

Figure 6.13b: Cu extraction in the product as a function of extended leaching time (t), 1.65 M NH_4Cl concentration, Particle size - 64 + 45 µm, temperature range 70 ˚C to 90 ˚C, solid-to-liquid ratio 6 g/ 250 mL and stirring speed 300 rpm

The temperature dependence of the reaction was investigated and the mechanism controlling the leaching process was determined. The experimental data in the second batch of leaching experiments were also tested using the SCM as previously stated. Analysis of the data using the SCM and kinetic analysis are presented. Figures 6.14a and 6.14b are the graphical illustration of

these results for the middling and product, respectively. It was found that the activation energy of the process was 45.9 and 47.5 KJ/mol for the product and the middling. These values are similar and within the range obtained in the first batch of leaching experiments especially for the activation energy found for the product. This is a validation of the earlier finding that the mechanism controlling the leaching process is chemical-controlled through the reaction at the particle surface.

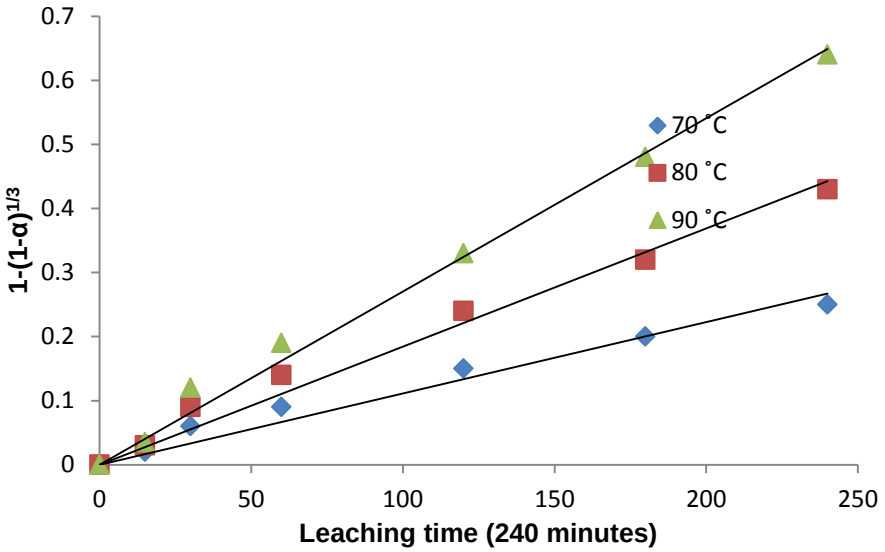

Figure 6.14a: Plot of $1-(1-\alpha)^{⅓}$ versus leaching time, t for the middling

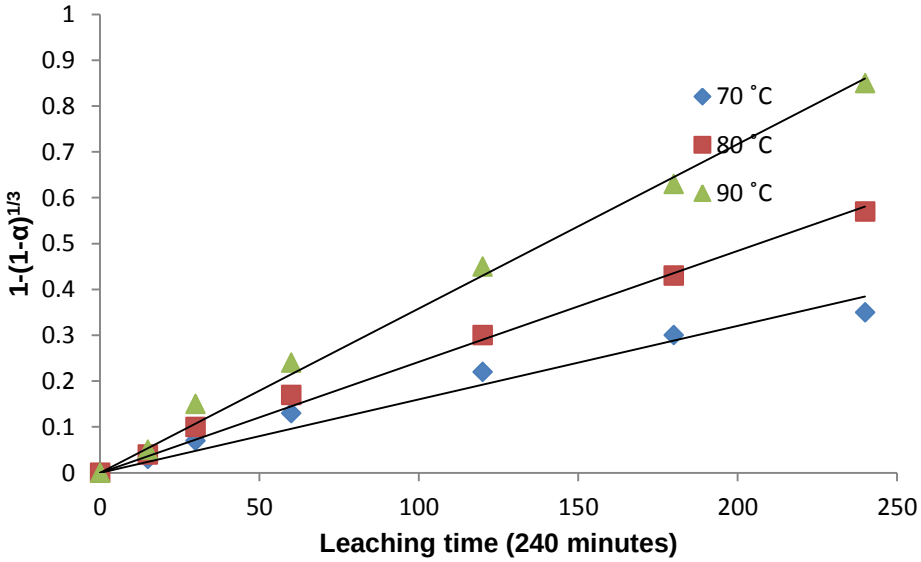

Figure 6.14b: Plot of $1-(1-\alpha)^{⅓}$ versus leaching time, t for the product

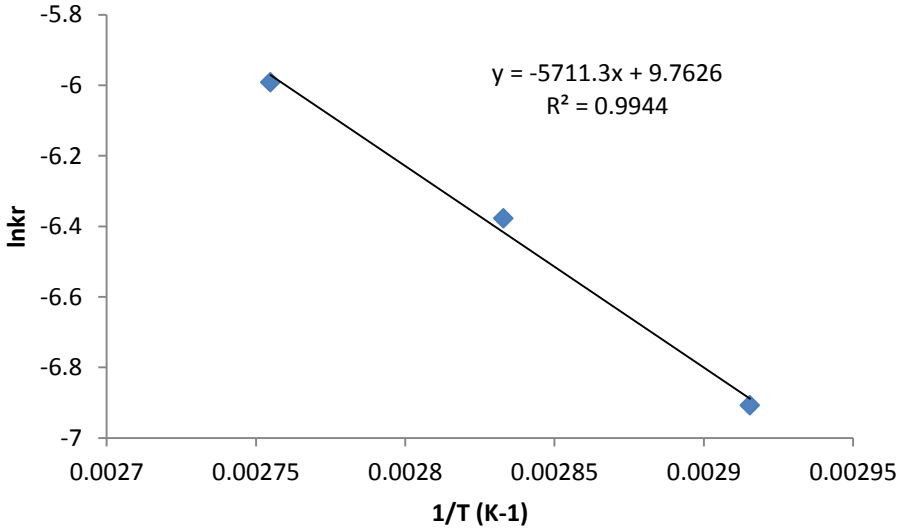

Figure 6.15a: Arrhenius plot of ln k_r versus 1/T (K^{-1}) for middling

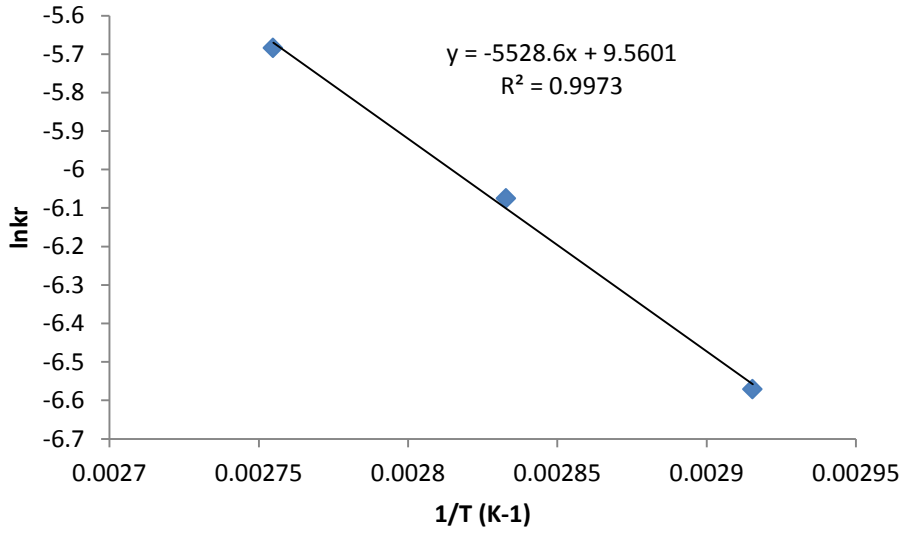

Figure 6.15b: Arrhenius plot of ln k_r versus 1/T (K^{-1}) for product

6.5. Determination of co-extraction of Mn, Co, Ni and Zn (ppm)

The determination of the percentage of co-extraction of Mn, Co, Ni and Zn was investigated from the leachate obtained from the second batch leach experiment. The leachate obtained after leaching with two different NH_4Cl concentrations of 0.55 M and 1.65 M at a constant particle size of – 63+45 μm, stirring speed of 300 rpm, temperature of 90 ˚C and at a solid weight of 6 g and constant volume of 250 mL were analysed. The essence of the determination of the metals is to assess the level of their co-extraction with Cu in the leachate for effectiveness and selectivity of the reagent for Cu extraction in the ore. Results

of the metals extraction is presented in Figures 6.16a and 6.16b for the middling and the product, respectively. It was found that the level of extraction of these metals varies considerably with the NH_4Cl concentration. The rate and extent of co-extraction of these metals differs significantly in the classified ore. The rate of metal concentration in the leachate increases with an increase in concentration of the reagent from 0.55 M and 1.65 M. The level of extraction of the metals in the middling was more than that of the product. The highest rate of extraction was obtained for Mn followed by Ni, Co and Zn. Co and Zn extraction were very poor, mostly at time intervals between 45 and 240 minutes, and the extraction rates were found to be insignificant (> 0.02 %). It should be noted that the metals extraction which were not represented in the plot at some time intervals were found to have concentration of below 0.03 %. The extraction rate increases in the first 30 minutes and then starts decreasing towards a low value after 240 minutes of leaching. The rate of extraction of these metals in the classified ore followed a similar pattern. When the rate of Cu extraction in the ore presented in the preceding sections is compared with that of Mn, Ni, Co and Zn in Figures 6.16a to 6.17b, it can be observed that Cu extraction in the classified ore was very significant. This suggests that NH_4Cl leaching of the ore was selective for Cu. This selectivity is is attributed to the affinity of NH_4Cl reagent toward Cu. This observation is in line with that indicated by Sabba and Akretche (2006) and Chmielewski et al. (2009) on the selective extraction of Cu by ammonia. The potential of the use of an alkaline reagent for Cu leaching such as ammonium carbonate and ammonium chloride/ ammonium carbonate for selective leaching of Cu from high gangue ore, such as the one in this work, have been established by other workers (Bingöl et al., 2005, Liu et al., 2010, Künkül et al., 2013, Ochromowicz et al., 2014).

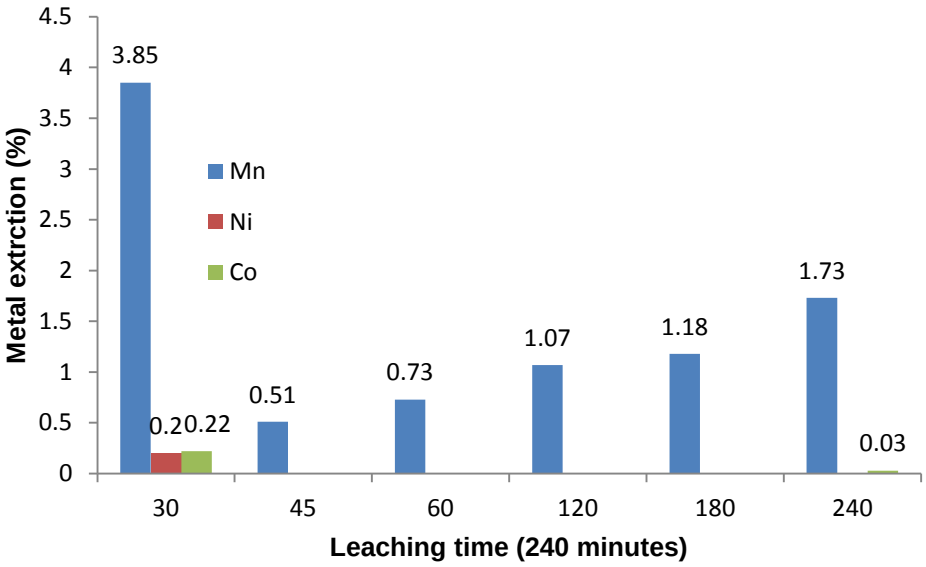

Figure 6.16a: Mn, Ni, and Co extraction in the middling as a function of leaching time and constant 0.55 M NH_4Cl, – 63+45 μm particle size, temperature 90 ˚C, stirring speed 300 rpm, solid-to-liquid ratio 6 g /250 mL

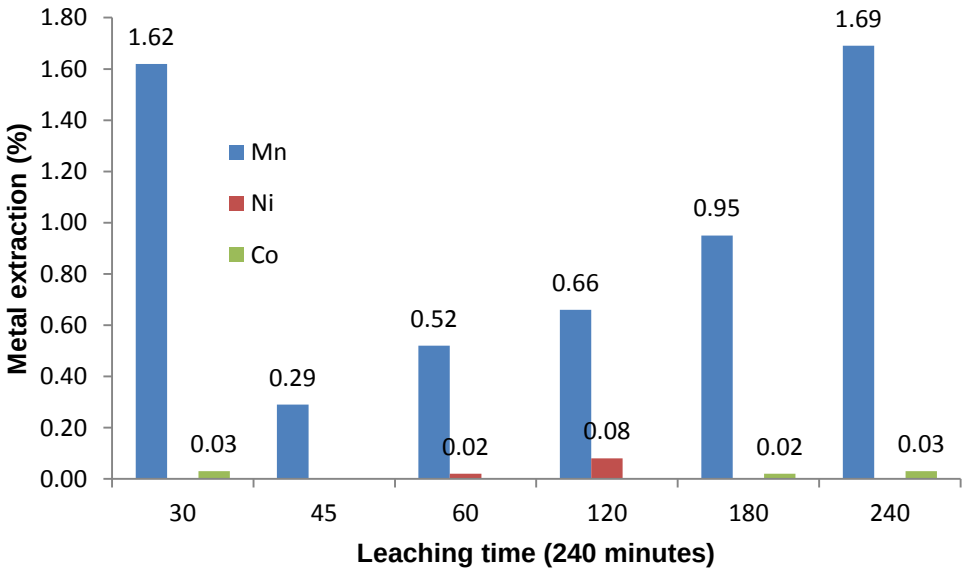

Figure 6.16b: Mn, Ni, and Co extraction in the product as a function of leaching time and constant 0.55 M NH_4Cl, – 63+45 μm particle size, temperature 90 ˚C, stirring speed 300 rpm, solid-to-liquid ratio 6 g/250 mL

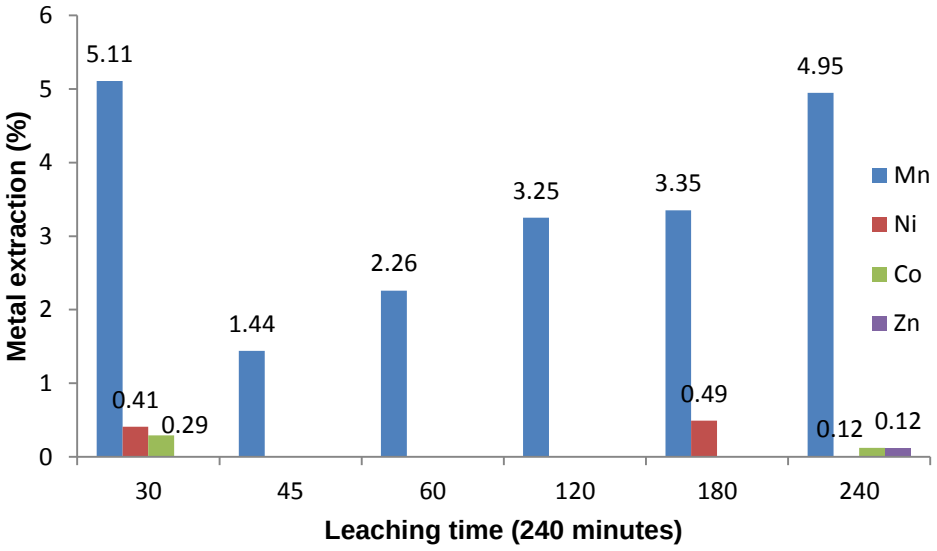

Figure 6.17a: Mn, Ni, and Co extraction in the middling as a function of leaching time and constant 1.65 M NH_4Cl, – 63+45 μm particle size, temperature 90 ˚C, stirring speed 300 rpm, solid-to-liquid ratio 6 g /250 mL

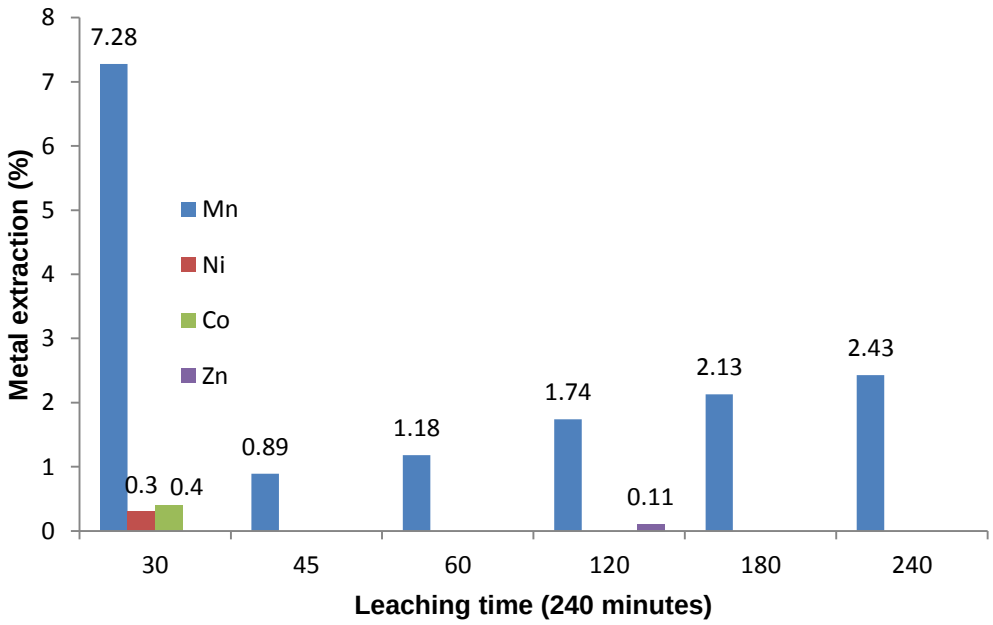

Figure 6.17b: Mn, Ni, and Co extraction in the product as a function of leaching time and constant 1.65 M NH_4Cl, – 63+45 μm particle size, temperature 90 ˚C, stirring speed 300 rpm, solid-to-liquid ratio 6 g /250 mL

6.6. Comparison of Cu extraction in oxalic acid and ammonium chloride

As previously stated, the most important aspect of hydrometallurgy is the efficiency of the leaching reagent for metal recovery from an ore. Another new lixiviant was tested for leaching of the classified ore in order to verify the potential of the lixiviant as a substitute for Cu extraction and possible application. Hence the discussion in this section is focussed on 'oxalic acid' leaching of the ore and comparison with NH_4Cl. A third batch of leaching was concerned with oxalic acid and ammonium chloride leaching under the same experimental conditions. The conditions and parameters applied are presented in Table 6.3. Apart from the concentration of the reagents all other parameters were kept constant throughout the experiments. The concentration of the oxalic acid could not be extended beyond 0.8 M in order to avoid difficulty in making up the standard solution due to the formation of precipitates which could affect the leaching results. Since one of the aims of this research is developing an environmentally friendly process for copper leaching, this informed the choice of this lixiviant for comparison.

6.6.1. Leaching with oxalic acid

The rate of Cu extraction in the classified ore with oxalic acid was investigated at time intervals of 15, 30, 60, 120, 180 and 240 minutes. Figure 6.18 and 6.19 show the percentage extractions of Cu with oxalic acid at concentrations of 0.25 M to 0.75 M. Contrasting results were found with the lixiviant; the pattern of Cu extraction in the presence of $H_2C_2O_4$ was different. In general, the rate of

extraction during the entire leaching time was poor compared to that of the ammonium chloride. The low extraction of copper may be a result of the formation of insoluble precipitate of copper oxalates which tend to inhibit the leaching process, slowing the extraction process. The extraction rates varied after 240 minutes in the two ore fractions, as was found in the middlings and the product. Higher rates of extraction were obtained in the product fraction than in the middling. The difference in Cu content is responsible for the difference in the rate of extraction between the two pre-concentrated ore fractions. However, the increase in the rate of Cu extraction with increasing oxalic acid concentration is consistent with the observation in the preceding sections. The initial higher rates of extraction within the first 15 minutes is a sharp contrast to that observed for the NH_4Cl lixiviant, thus it is possible that the mechanism controlling the leaching process is different. According to Stuurman et al. (2014) the leaching of metals by organic acid differs from other reagents because it occurs via protonation, chelation and ligand exchange reactions. Since metal-ligand complexes could be formed at solid-solution interface, this results in the weakening of the cation-oxygen bond as the reaction progresses with time. The observation in the experiment agrees with that of Stuurman et al. (2014).

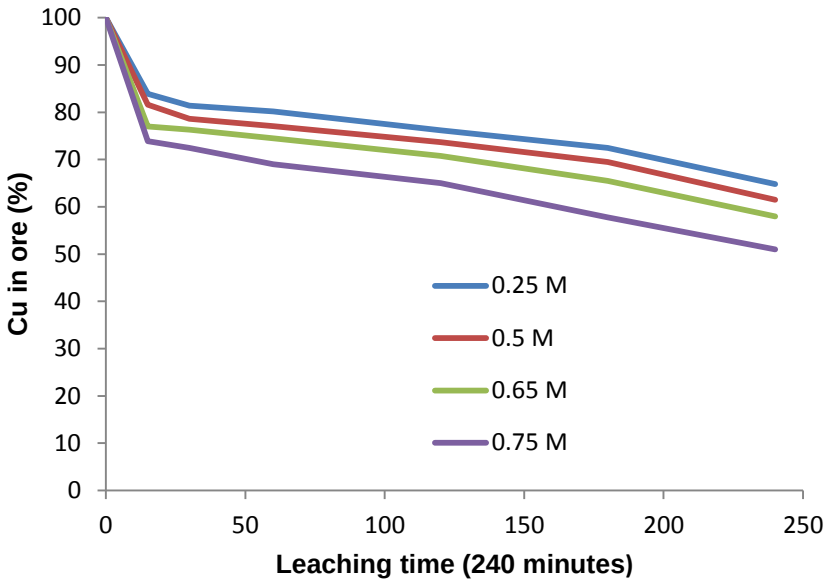

Figure 6.18: Cu extraction in the middling as a function of leaching time, oxalic acid concentration 0.25 M to 0.75 M, particle size -63 + 45 μm, temperature 80 ˚C, and stirring speed 300 rpm

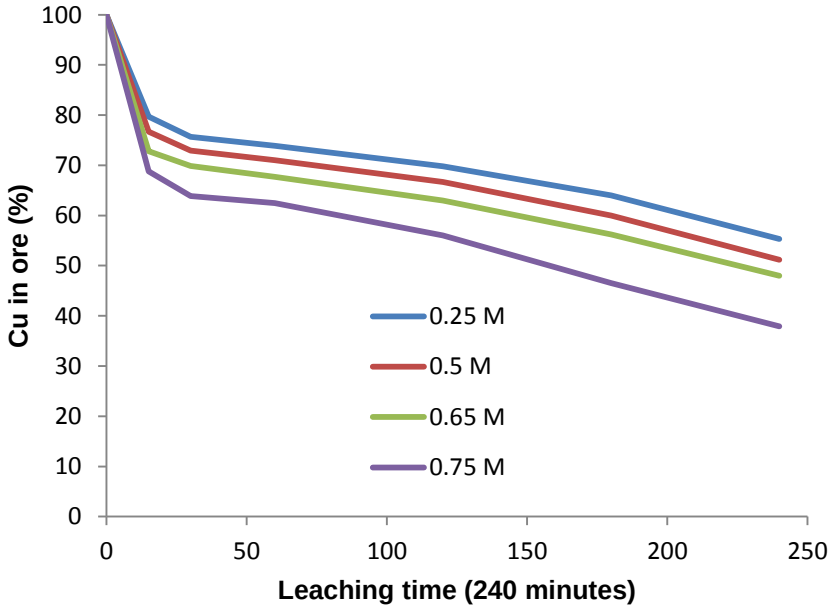

Figure 6.19: Cu extraction in the product as a function of leaching time, oxalic acid concentration 0.25 M - 0.75 M, particle size -63 + 45 μm, temperature 80 ˚C, and stirring speed 300 rpm

6.6.2. Leaching with ammonium chloride

Figures 6.20 and 6.21 presents the rate of Cu extractions with ammonium chloride lixiviant under the same experimental conditions discussed in the preceding section. It can be seen that the Cu extraction was higher than that obtained with oxalic acid. The rate of extraction increases with an increase in concentration from 0.5 M to 0.75 M. Unlike the oxalic acid, the opposite was observed in this case, as the rate of extraction was consistent with increasing leaching time from 15 minutes to 240 minutes. It was also found that the Cu extraction in ammonium chloride was greater than oxalic acid throughout the concentration ranges. This is a clear indication that the lixiviant this more efficient for Cu leaching than the oxalic acid. The results in these experiments correlate with that obtained in the two previous batches (first and second batch). Based on these results the electrochemical analysis of the copper-ammonia complexes formed with ammonium chloride is required to understand the electrowinning process as presented in the next chapter. However, for better understanding of the leaching process an economic analysis of the two reagents for cost effectiveness is required before application. Thus, calcite versus copper grade in the three fractions is discussed in chapter 8 as the basis for adopting the current strategy in this research for technological consideration for an effective leaching design.

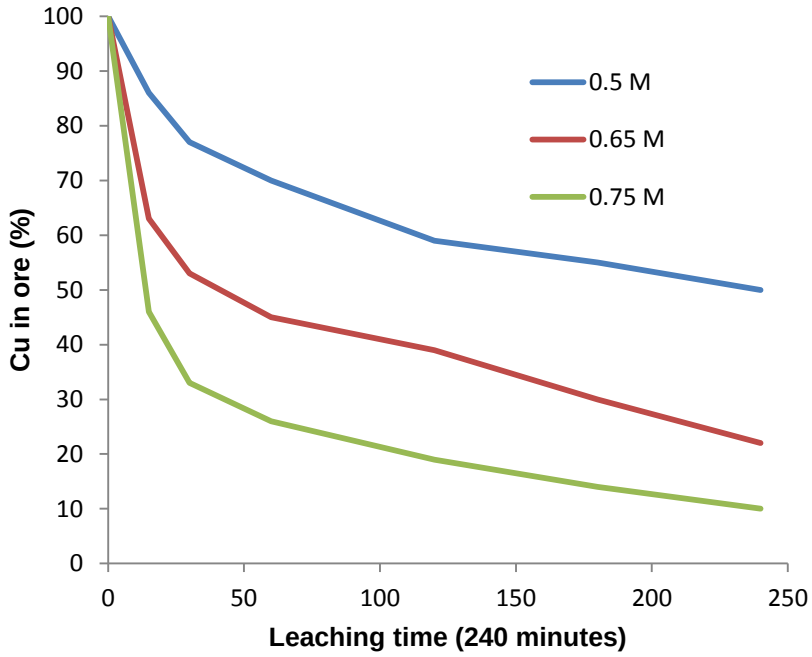

Figure 6.20: Cu extraction in the middling as a function of leaching time, ammonium chloride concentration 0.25 M to 0.75 M, particle size -63 + 45 μm, temperature 80 ˚C, and stirring speed 300 rpm

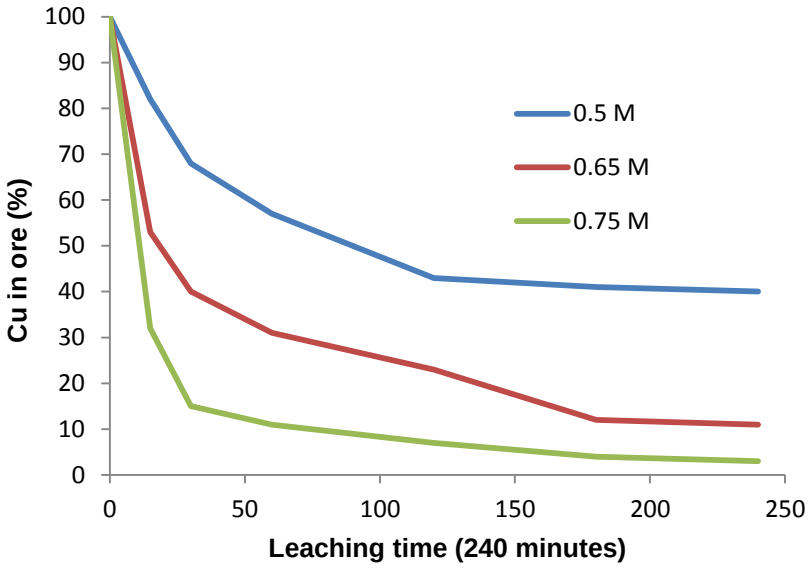

Figure 6.21: Cu extraction in the product as a function of leaching time, ammonium chloride concentration 0.25 M to 0.75 M, particle size -63 + 45 μm, temperature 80 ˚C, and stirring speed 300 rpm

6.7. Residue characterization

6.7.1. ICP-MS analysis of residue

At the end of the leaching experiments, where the Cu extraction was greater than 70 % in NH_4Cl solution and 40 % in $H_2C_2O_4$, these were selected for analysis. The leachate was filtered and four of the leach residues were selected for elemental analysis (two from the product and two from the middling). The analysis aimed at determining the amount of elements unreacted and to also assess the percentage recovery and selectivity of the reagents for Cu in the pre-concentrated ore. Secondly, to compare the amount of metals in the residue after leaching in the NH_4Cl and the $H_2C_2O_4$ lixiviants. The results of the ICP-MS analysis are presented in Tables 6.4 and 6.5 for NH_4Cl and $H_2C_2O_4$, respectively. It was found that both lixiviants appear to be strongly selective toward Cu during the leaching process. The percentage of Cu recovery was determined by comparing the amount of elements in the feed grade and the leach residue. The relationship in equation 6.9, after Liu et al. (2011) was used to assess the leaching efficiency:

$$J\ (\%) = \frac{W_m \times Cu_a - W_r \times Cu_r}{W_m \times Cu_a} \times 100 \quad (6.9)$$

Where J is the percentage recovery of Cu, Wm is the weight of ore material before leaching, Cu_a is the Cu content of the raw ore before leaching, W_r is the weight of the residue after leaching, and Cu_r is the Cu content of the residue after leaching.

It was found that the percentage extraction of Cu from the NH_4Cl leaching solution was above 90 % in the product and 80 % in the middling when the residue was examined. This is an indication that the level of Cu extraction with NH_4Cl in the product was more than that of the middling. In the case of $H_2C_2O_4.2H_2O$ only 59.4 % and 45.6 % recovery was obtained in the product and middling, respectively. This observation is an indication that the $H_2C_2O_4.2H_2O$ was not as effective as the NH_4Cl reagent. However, considering the percentage of Cu recovery from the raw ore and amount of metals in the residue after leaching, it is clear that the leaching was beyond average. This is an indication that the leaching process was selective to a large extent especially in NH_4Cl. A similar observation was obtained by Awe et al. (2013) for antimony recovery from Sb-bearing ore. For a better understanding of the selectivity towards Cu and efficiency of the lixiviants, the residues were subjected to mineralogical characterization using XRD. The results of the characterization with XRD are presented in the next section.

Table 6.4 Elemental concentration of the feed and residue after leaching in NH_4Cl

Metal→ Ore category↓	Cu (Wt.%)	Zn (ppm)	Mn (ppm)	Co (ppm)	Ni (ppm)
Product feed	1.79	0.02	0.06	0.03	0.01
Middling feed	1.01	0.03	0.02	0.03	0.02
Product residue	0.17	0.012	0.052	0.02	0.00
Middling residue	0.13	0.024	0.013	0.02	0.015

Table 6.5 Elemental concentration of residue after leaching in $H_2C_2O_4$

Metal→ ore category↓	Cu (wt.%)	Zn (ppm)	Mn (ppm)	Co (ppm)	Ni (ppm)
product	0.13	< 0.02	< 0.02	0.00	0.00
middling	0.16	0.01	<0.03	0.00	0.00

6.7.2. X-Ray Diffraction (XRD) characterization of residue

The solid residues produced after leaching described in the preceding section were investigated using X-ray diffraction to obtain information regarding the mineralogical transformation that took place in the raw ore and phase composition of the leach residue. Another consideration of the residue was to observe the identification of any new phase that may have formed during the leaching process. Qualitative analysis was carried out on both samples (middling and product) leached in NH_4Cl and $H_2C_2O_4.2H_2O$. Details of the XRD technique and mineralogical analysis of the raw ore can be found in chapter 3 and 4, respectively. The results of major elements analysis in the residue is presented in Figures 6.22 to 6.25. The mineralogical compositions of the residues shown in the figures were compared with the profile of the original ore presented in Figures 4.11 and 4.12 (Chapter 4). Table 6.6 presents the mineral species found in the residue. It can be seen from Table 6.6 that the mineral species identified in each residue sample (product and middling) were similar, with the only differences being in their concentration. It is interesting to note that the variation in concentration appears to correlate with the mineralogical concentrations obtained in the classified ore in chapter 4. The result, however, showed that the concentrate undergoes a number of transformations caused by the leaching process. The results indicated that a substantial amount of chrysocolla hosting Cu was leached due to the disappearance of the rise in baselines caused by amorphous chrysocolla mineral phases in the classified ore. It should be noted that the high rise in the baseline in the product (Figure 4.11) was suggestive of the abundance of chrysocolla in the product than in the

middling. Expectedly, the variations observed in the raw ore accounted for the observed trend in residue profiles between the product and the middling. The calcite peaks detected in the raw ore were completely absent, which suggests that calcite has reacted during the extended leaching process. This confirms the earlier prediction of calcite reactive nature with chemical reagents. However, as seen from the results in the Figures 6.22 to 6.25 for the residues, hematite, microcline, muscovite and quartz were not leached. Since these minerals were not leached, it is appropriate to state that they were unreactive toward both lixiviants. It is probable that the rate at which these gangues react is slow toward the reagents, thus limiting the process of their leaching. This confers the advantage of these lixiviants for Cu extraction, especially in high amount of gangue minerals ores compared to other inorganic acid. This is in line with the observation by Bingöl et al. (2005), Wang et al. (2009) and Liu et al. (2010). The results in this study indicate the consistency in the selective leaching of Cu in chrysocolla mineral from the classified ores.

Table 6.6 Comparison of mineral species identified in the raw ore and residue by XRD (-63 + 45 μm size fraction)

Raw ore category	minerals	Residue category	minerals
product	microcline, calcite, clinochlore, hematite, quartz, muscovite, chrysocolla	product	quartz, hematite, clinochlore, muscovite, orthoclase, microcline
middling	quartz, calcite, hematite, microcline, muscovite, chrysocolla	middling	quartz, hematite, clinochlore, muscovite, orthoclase

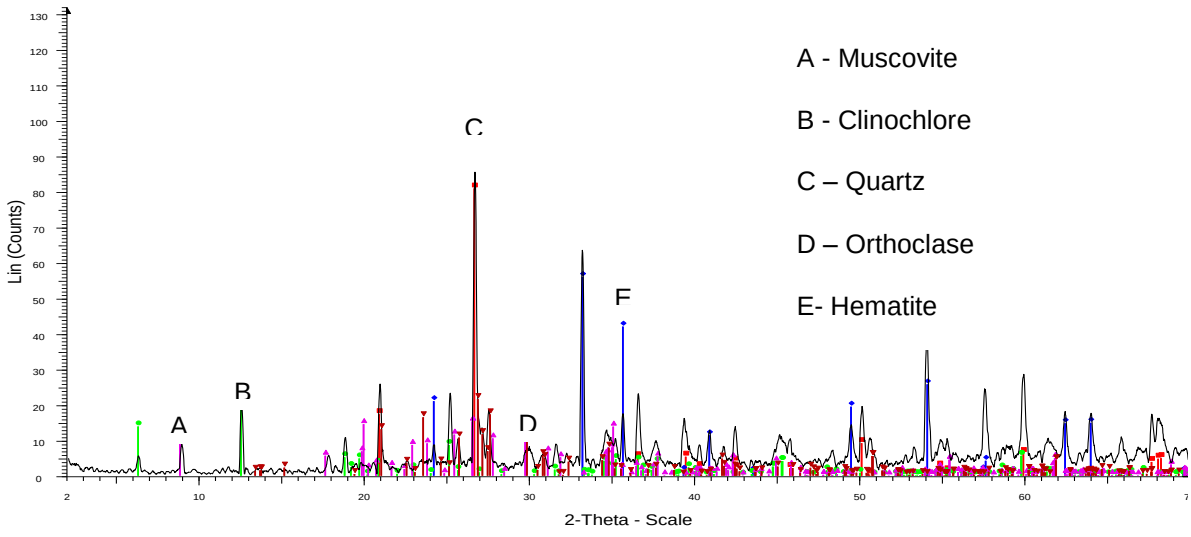

Figure 6.22: XRD pattern of the middling leach residue using NH_4Cl lixiviant

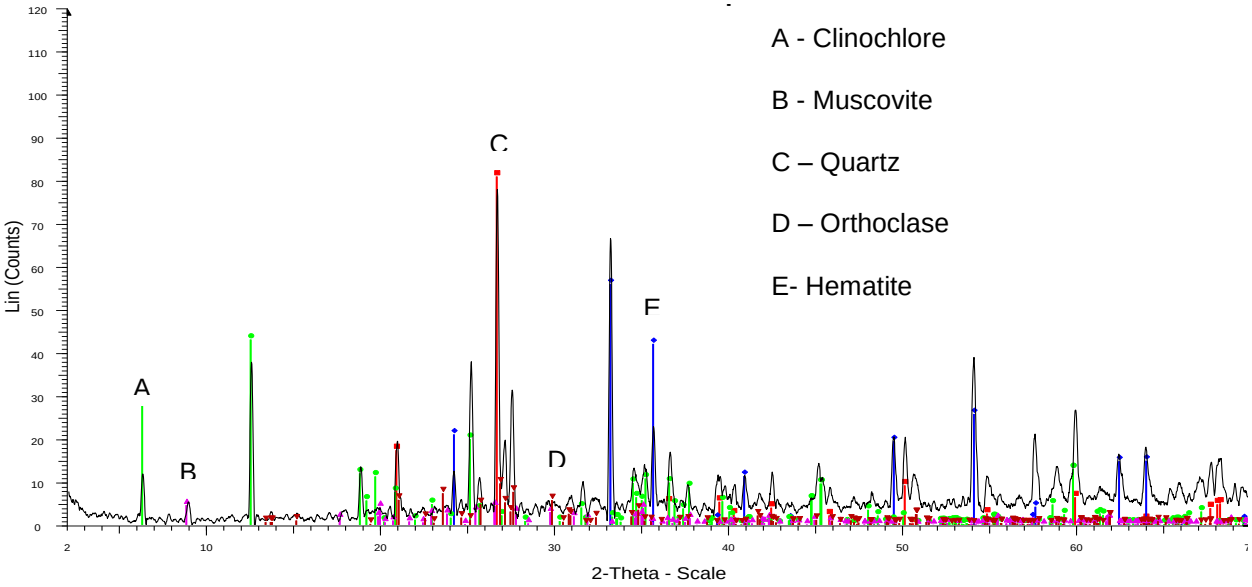

Figure 6.23: XRD pattern of the product leach residue using NH_4Cl

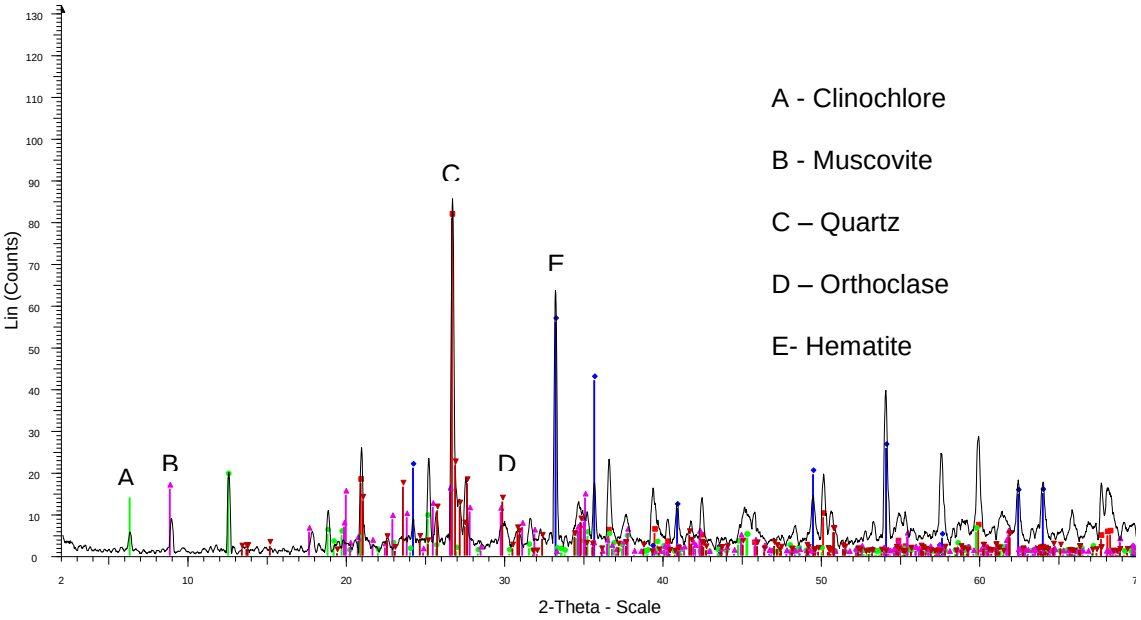

Figure 6.24: XRD pattern of the middling leach residue using $H_2C_2O_4.2H_2O$

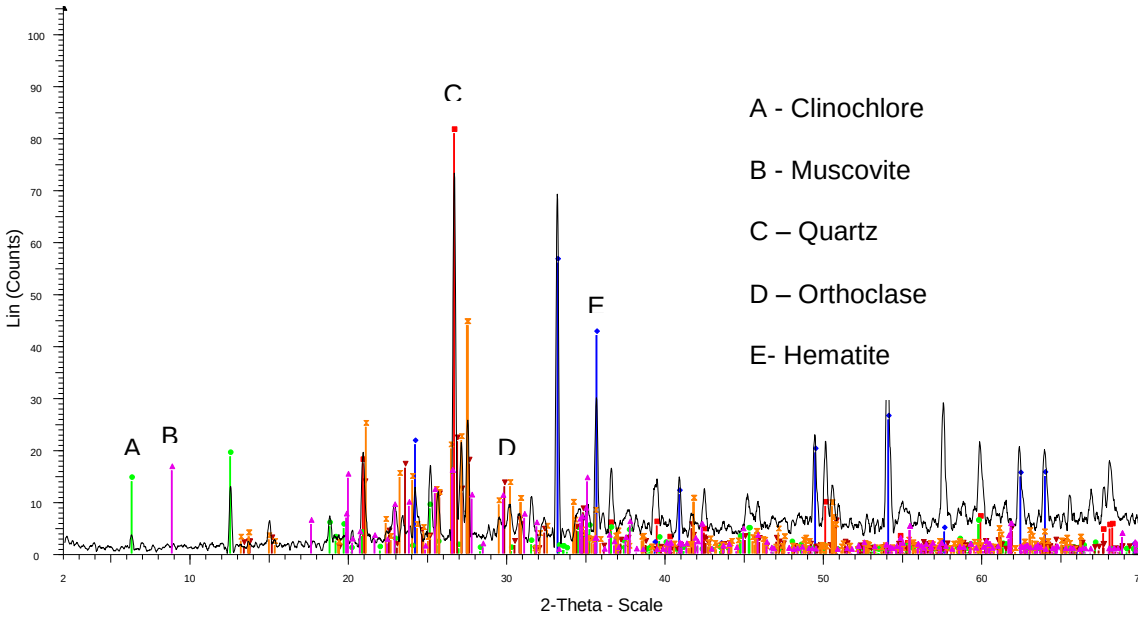

Figure 6.25: XRD pattern of the middling leach residue using $H_2C_2O_4.2H_2O$

6.8. Conclusion

Leaching studies of near infrared pre-concentrated and classified copper ore fractions were presented in this chapter. The studies were performed by conducting three batches of experiments ranging from optimization of the process to validation and comparison of Cu extraction in NH_4Cl and $H_2C_2O_4$ acid. The effects of varying process variables on the rate of Cu extraction were investigated. The variables (parameters) studied were NH_4Cl concentration, $H_2C_2O_4$ acid concentration, particle size, temperature, solid-to-liquid ratio, stirring speed and leaching time.

It was found that increasing the temperature of the leaching system from 40 ˚C to 70 ˚C and 70 ˚C to 90 ˚C resulted in increases in the rate of Cu extraction. The trend in Cu extraction was the same in the classified ore. However, the rate of extraction is higher in the product than in the middling due to variation in Cu content between these two. Since the rate of Cu extraction increases with temperature, increase it is proper to conclude that the reaction between the ore and the lixiviant is temperature sensitive. The concentration of the lixiviants significantly affected the rate of Cu extraction in all three batches of experiments. As expected, the increase in extraction rate corresponds to available Cu for leaching in the particle size fractions processed. In the case of particle size, higher extraction rate was achieved using finer size fraction of – 63 + 45 μm. Generally, the rate of extraction increases with decreasing particle sizes from – 125 + 90 μm to – 90 + 63 μm and – 63 + 45 μm. On the other hand, the stirring speed was found to have a weak effect on Cu extraction. The rate of Cu extraction was observed to decrease with increasing stirring speed from 300 rpm to 500 rpm and 800 rpm. With solid-to-liquid ratio, the result indicated that a balanced ratio of solid weight to liquid volume is essential for

better Cu extraction. It was also found that the rate of Cu extraction increases with decreasing solid-to-liquid ratio. Besides these variables, increasing of leaching time from 2 to 4 h was found to be more effective with Cu extraction increasing even at low concentration of NH_4Cl. The mechanism of the leaching process was investigated using the shrinking core model by fitting the experimental data into three models. The results indicated that the data fitted well into the chemically-controlled model which satisfactorily explains the leaching reaction to occur through the particle surface. With activation energy (Ea) of 48 kJ/mol and 71 kJ/mol obtained for the product and the middling, respectively during the first batch experiments and a value of 45.9 kJ/mol and 47 kJ/mol in the second batch experiments clearly show that the leaching process is chemically-controlled.

Analysis of leachate for co-extraction of Mn, Co, Ni and Zn with Cu revealed that their concentration in the leachate was very low compared to that of Cu. Of all these metals (Mn, Co, Ni, and Zn) Mn appears to have the highest rate of co-extraction with a value of 7.28 % while for the rest of the metals it is below 0.05 %. The insignificant concentration of these metals in the leachate suggests that the leaching process was selective for Cu. It was determined that the percentage recovery of over 90 % and 80 % upward in the product and middling can be achieved with NH_4Cl reagent. Analysis of selected residue obtained after optimal leaching conditions with ICP-MS and XRD indicated that the lixiviant was efficient for Cu leaching in the classified ore while for $H_2C_2O_4$ the rate of Cu extraction is lower than that of NH_4Cl. Based on the leaching results of the two lixiviants, NH_4Cl is considered more efficient for the classified ore leaching. XRD mineralogical composition of the original ore and residue indicated that a substantial amount of chrysocolla (Cu-bearing mineral) was leached while hematite, microcline, muscovite, and quartz were not leached. This is in line with the earlier assertion on the selective extraction of Cu from the ore. The disappearance of the calcite peaks in the residue is suggestive of their consumption during the process.

Chapter 7

Electrochemical studies

7.1. Introduction

The recovery of high-purity copper metal from ore leachate at a competitive production cost is increasingly challenging due to the decline in ore grade. The presence of impurities can be a major challenge due to their negative impact, especially due to the increasing cost of electrowinning as a result of the dissolution of impurities into the leachate solution. Therefore, a selective leaching process was used to minimise the effect of this problem during electrowinning. To enhance the efficiency in the copper processing in this current study a strategy of integrated methods has been adopted, involving the use of pre-concentration of copper ores, classification and selective leaching processes. However, the strategy is only efficient with an electrowinning stage. As such for a complete integrated hydrometallurgical processing, a downstream electrowinning process is essential. Now the aim is to test the appropriateness of the leaching method by carrying out electrowinning of the leachate. This chapter focuses on copper recovery processes from the ore leachate. The use of a cyclic voltammetry technique is adopted here to understand the reactions occurring during electrowinning, resulting in the copper deposition processes. Experimentally, voltammetry can be used to record the half wave potentials of both reduction waves for Cu(II)-complex to Cu(I)-complex and Cu(I)-complex to C(0) metal (Meng and Bard, 2015).

Therefore, it is imperative to study copper electrodeposition from the resultant leachate obtained using the pre-concentrated ore. It is anticipated that the electrochemical study of the leachate will give an insight into the reduction and electrodeposition processes of copper-ammonia complexes formed in the solution. Cyclic voltammetry is used because of it robustness in revealing electrochemical reactions over a wide potential range (Popescu et al., 2013). This chapter aims to understand the copper recovery process by way of electrochemical analysis of the ore leachate and comparing the results with that of synthetic copper ammonium sulphate [$Cu(NH_3)_4SO_4$] solution. In order to achieve this target, the potential electrochemical reactions occurring on a platinum electrode at different scan rates are studied to understand the reduction and electrodeposition behaviour of the two different complexes in the two solutions. The electrowinning is undertaken by considering the effect of scan rates and potentials on the copper deposition and its behaviour at the cathode and electrolytic oxidation at the anode. Since the ability of copper to exist in a particular oxidation state in solution depends on the material composition. The two solutions may contain copper in different oxidation forms and as such the electrodeposition process may differ. In view of this, the comparison between the two solutions is an ideal way of understanding the

processes of copper deposition from an ore leachate. This is considered a true solution containing copper-ammonia complexes, requiring copper recovery by electrowinning while the synthetic solution is pure solution of copper synthesised using pure copper sulphate.

The overall aim is to establish whether there is any relationship between the two solutions in terms of electro-reduction and electro-deposition behaviour and to also observe the effect of scan rate on the electrodeposition processes. In summary both the reduction and oxidation processes at the cathode and anode are compared. The mechanisms controlling the electrodeposition of copper in both solutions are described. The relationship between the two solutions containing complexes, the effect of scan rate and current density are also discussed.

7.2. Electrochemical analysis

In order to develop a fundamental procedure for the electrodeposition of copper and kinetic analysis in this research, the ore was subjected to series of steps. Figure 7.1 presents the work flow detailing the strategy adopted for the electrochemical analysis. The electrodeposition process was investigated by carrying out voltammetric measurement using 100 mL leachate in a cell. The steps outlined depict some essential hydrometallurgical processes for copper recovery from copper ores. The near infrared spectroscopy sensor-based sorted copper ores were first crushed, ground, homogenised and sieved into different fractions as presented in Figure 5.1.

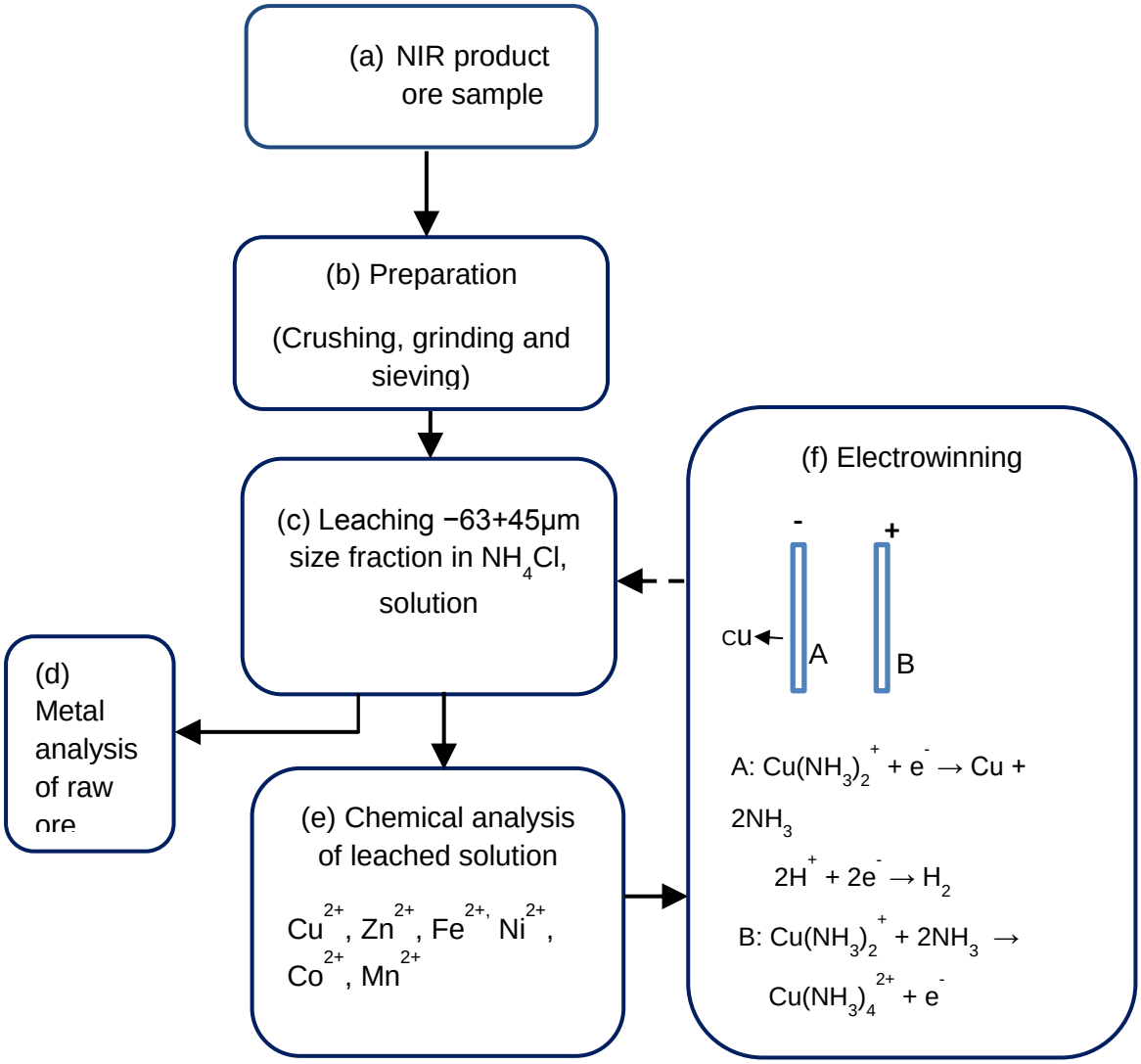

Figure 7.1 Flow diagram of the strategy for electrochemical studies.

It should be noted that the dashed line in the figure indicates there is potential for recycling of the solution after electrowinning. This would reduce the requirement for fresh leaching reagent and hence the cost of processing.

The product fraction was advanced for leaching and electrochemical experiments by subjecting them to different processes in order to generate relevant information needed at every step (Figure 7.1).The maximum amount of copper available for leaching was determined by dissolving the -125+90 µm, -90+63 µm and -65+45 µm product fraction size fractions in Aqua Regia (75% conc. HCl, 25% conc. HNO_3) and was analysed by ICP-MS according to the method described in section 3.5.2. The result of metal grades available for leaching is presented in Table 5.2. For clarity the result of only the size fractions of the product considered for leaching and electrochemical studies is shown in Table 7.1.

Table 7.1 Metal grades of product size fractions for leaching experiments

NIR sample	Size fraction	Cu	Ni	Co	Mn
		(Wt. %)	(ppm)	(ppm)	(ppm)
Product	−125+90 µm	1.04	0.00	0.00	0.05
	−90+63 µm	1.70	0.00	0.00	0.05
	−63+45 µm	1.97	0.02	0.03	0.06

Table 7.1 shows that the -63+45 µm size fraction had higher copper content than the other fractions, so the prospect for copper dissolution and recovery from that fraction is better compared to the other fractions. Similarly, the product has a higher copper grade than the middling and the waste (Tables 5.1 and 5.2). On that basis for better electrochemical results, the -63+45 µm fraction in the product category was subjected to leaching in 1M NH_4Cl solution for 120 min, stirring speed of 300 rpm and temperature of 55 ˚C using solid-to-liquid ratio of 2:125. Next, 5 mL of the leachate was withdrawn and filtered using Whatman 540 filter paper for metal grade determination with ICP-MS according to the method described in chapter 3. Another 100 mL of leachate was filtered and used for cyclic voltammetry studies without further purification. The pH of the leachate was determined to be 6.5 after leaching. The 0.5 M synthetic solution was prepared using $CuSO_4.2H_2O$ and ammonia solution and de-ionised water. The pH of the $Cu(NH_3)_4SO_4$ synthetic solution was adjusted to match with that of the leachate before cyclic voltammetry studies (CVs).

Typical results of the percentage of copper and other metals extracted from the product size fraction can be found in chapter 6. ICP-MS analysis indicates that over 50% of the available copper is leached, while Co and Zn are also leached in comparison to Ni and Mn. The leaching of these metals is conditional on the formation of stable ammine complexes.

7.3. Copper electrodeposition from ore leachate

Figure 7.2 shows the cyclic voltammogram measured with a positive starting potential of 0.8 V to a negative end potential of – 1.0 V at scan rates of 20, 50, 100, and 200 mV/s in the cathodic and anodic directions. The scan reveals two reduction peaks (peak A and peak B) at cathodic potentials between – 0.10 V and – 0.23 V. Similarly, in the reverse scan (anodic) direction, two peaks (peak C and peak D) were also observed at anodic potential of – 0.10 V and 0.39 V.

7.3.1. Cathodic process of Cu deposition from ore leachate

The two distinct cathodic peaks A and B are a result of electrodeposition of divalent copper ammonia complex formed as a result of the leaching of the ore

with an alkaline ammonium chloride lixiviant. The divalent copper formed undergoes reduction to the monovalent copper complex as shown in peak A. The monovalent copper in Peak A further undergoes reduction to copper metal (Peak B). As can be seen in peak B, the depth of the peak increases, which is an indication that electrodeposition of copper takes place at a negative potential as evidenced by a shift of cathodic peak as the scan rate increases. The two-step reduction process occurring in peaks A and B is expressed in Equations 7.1 and 7.2, respectively. It is clear from Fig. 7.2 that electrodeposition consisted of two reversible electrochemical processes.

$$Cu(NH_3)_4^{2+} + e^- \leftrightharpoons Cu(NH_3)_2^{+} + 2NH_3 \quad (7.1)$$

$$Cu(NH_3)_2^{+} + e^- \leftrightharpoons Cu + 2NH_3 \quad (7.2)$$

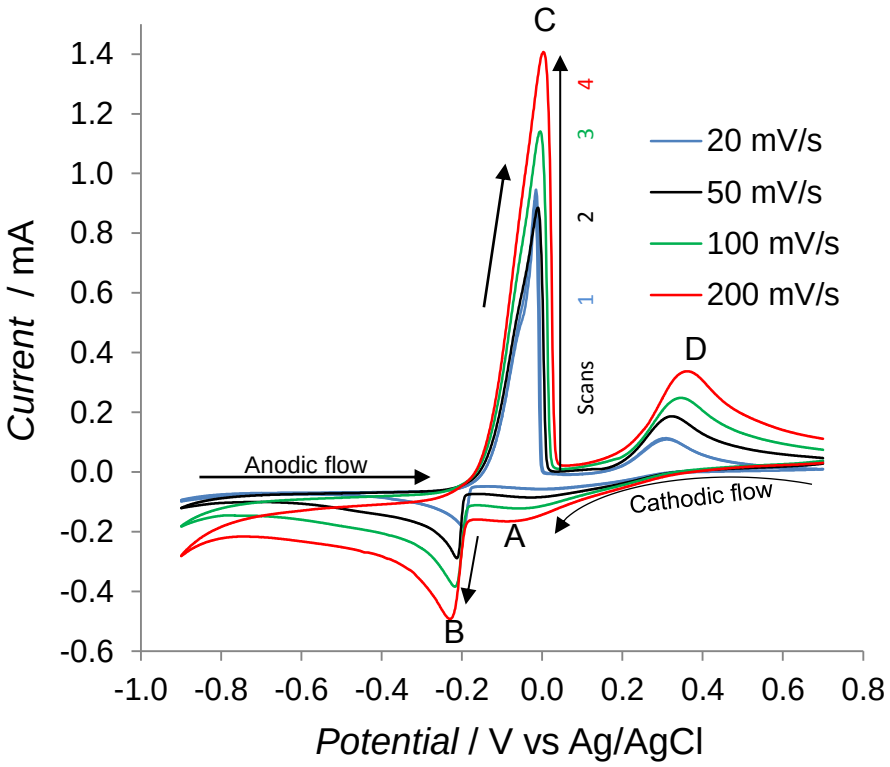

Figure 7.2 Cyclic voltammogram of NIR sensor- based sorted ore in ammonium chloride leached solution at different scan rate (Reference electrode: Ag/AgCl vs. 3 M KCl).

The $Cu(NH_3)_4^{2+}/Cu(NH_3)_2^{+}$ and $Cu(NH_3)_2^{+}/Cu$ corresponds to Cu(II)/Cu(I) and Cu(I)/Cu(0) redox couples. The potential of the reduction of these couples is dependent on the nature of electrode/electrolyte interface. It is also found that the cathodic peak potential varies with sweep rates (Figure 7.2). This suggests that it involves a fast electron transfer process. Thus, this further confirmed that copper deposition on the platinum electrode occurs by electrodeposition of Cu(II) ions through a two-stage mechanism, though the cathodic and anodic peak potentials and currents are significantly different. Majidi et al. (2009) have

shown that the conventional copper electrodeposition occurs via a two stage-electrochemical reaction as shown in Equations 7.3 and 7.4:

$$Cu^{2+} + e^{-} \leftrightharpoons Cu^{+} \text{ slow} \quad (7.3)$$

$$Cu^{+} + e^{-} \leftrightharpoons Cu \text{ fast} \quad (7.4)$$

The above expression (Equations 7.3 and 7.4) is similar with that shown in Equations 7.1 and 7.2. It is observed also from Equations 7.1 and 7.2, that the number of ammonia ligands co-ordinated to the Cu(II) and Cu(I) ions are different. This suggests a decoordination in the number of ammonia ligands during the reduction process, which is an indication that the overall redox reaction (Equation 7.1) consists of several steps. The difference in the number of ammonia ligands in the two peaks A and B (Equations 7.1 and 7.2) corresponding to [Cu(II)/Cu(I)] redox couple indicates that the reaction involves the decoordination of ammonia ligands from the $Cu(NH_3)_4^{2+}$ to $Cu(NH_3)_2^{+}$ complex in the leachate before copper metal is electrodeposited.

The findings in this research corroborates that of Shumilov et al. (1983) and Brown and Wilmott (1985), who showed that the reduction of copper occurs on the Cu(I)-ammonia complex species ($Cu(NH_3)_2^{+}$ and $Cu(NH_3)_3^{+}$). Darchen et al.(1997) and Aravinda et al.(2000) observed that the electronation of divalent copper(II) solution containing complexing agents occur by a stepwise process with ammonia and a number of ammine and nitrogen-containing heterocyclic compounds given rise to copper metal. Giannopoulou et al.(2009), Popescu et al.(2013) and Meng and Bard (2015) also confirm the two-step reduction of Cu(II) and Cu(I) species to be a cathodic reduction process to obtain Cu(0) metal from their copper complexes. The observation in this study indicated that ore leaching led to the formation of copper ammonia complexes in the leachate and the electrochemical reduction of copper from the complex proceeds via a stepwise process.

7.3.2. Anodic process of Cu deposition from ore leachate

Copper (I) systems are unstable and are readily oxidised by dissolved oxygen to a more stable state by a disproportionation reaction. This takes place by reduction of Cu^{2+} to Cu at the cathode and the oxidation of Cu to Cu^{2+} at the anodic direction as shown in Equations 7.5 and 7.6 (Majidi et al.,2009).

$$Cu^{2+} + 2e^{-} \leftrightharpoons Cu \quad (7.5)$$

$$Cu \leftrightharpoons Cu^{2+} + 2e^{-} \quad (7.6)$$

During the reverse scan in the anodic direction, the shift in anodic peak potential had a more positive value. The electrochemical regeneration of the copper ammonia complex ($Cu(NH_3)_4^{2+}$) takes place by the dissolution of copper and the formation of monovalent copper ammonia complex in the presence of

the complexing agent in the anode. Two anodic peaks (C and D) observed in Figure 7.2 have a different width to the forward scan peaks (A and B). It is observed that the Cu electrodeposited in the cathodic scan (peak B) dissolves to form Cu^{+}. The ammonia ions react with the Cu^{+} ions on the anodic surface and enter the solution to form $Cu(NH_3)_2^{+}$ which is converted to $Cu(NH_3)_3^{+}$ ions in the presence of more ammonia (peak C). The species in solution are then oxidised to form $Cu(NH_3)_4^{2+}$ (peak D). The process is dependent on the cathodic reaction process and the relative concentration of species in solution. Equation 7.7 shows the oxidative dissolution and reaction of copper in the presence of ammonia (peak C):

$$Cu + 2NH_3 \leftrightharpoons Cu(NH_3)_2^{+} \qquad (7.7)$$

The monovalent copper (I) ammonia complex in Equation 7.7 is unstable and undergoes oxidation into the stable copper (II) ammonia complex. This oxidation is facilitated by oxygen as indicated by the sharp anodic stripping peak D and by the high value of peak current. Equation 7.8 depicts the anodic oxidation reaction occurring in peak D:

$$Cu(NH_3)_2^{+} + 2NH_3 + \tfrac{1}{2}O_2 + H_2O + e^{-} \rightarrow Cu(NH_3)_4^{2+} + 2OH^{-} \qquad (7.8)$$

The increase in the wave peak C height as a function of scan rate reflects that the reduction of the copper (I) ammonia complex occurred as a reversible electrochemical process while peak D corresponds to a single electron transfer process. The clear difference in the peak areas of anodic peak C and cathodic peak A suggest that the reaction is partially reversible. Thus the closeness in the current of peaks (A and D) attributed to the reversible reaction suggest that the redox couple $Cu(NH_3)_4^{2+}/Cu(NH_3)_2^{+}$ is a reversible system.

Taking into account the peaks behaviour in Fig. 7.2 above, it is evident that the electrodeposition of copper from the copper ammonia complex is a reversible electrochemical reaction taking place via disproportionation of the Cu(II) and Cu(I) species. During the electrodeposition and electrodissolution of the species, it is observed that the increase in scan rates led to an increase in both cathodic and anodic peaks (B and C) which coincide to Cu(I) reduction to Cu metal [Cu(I) $\leftrightharpoons$ Cu(0)]. Thus, the reduction peaks (A and B) have associated oxidation peaks (C and D) which relate to the Cu(0)/Cu(I) and Cu(I)/Cu(II) reactions, respectively. This is line with the observation by Popescu et al. (2013).

7.3.3. Effect of scan rate

The effect of scan rate on electrodeposition of copper was observed at different scan rates of 20 mV/s, 50 mV/s, 100 mV/s and 200 mV/s respectively, (Figure 7.2). It was found that the current density increased with increasing scan rate. The remarked increase in ΔE_p with increasing scan rate is depicted by peak

depths. The dependence of the peak depth increase with increasing scan rate suggests the involvement of an electrodeposition reaction. It is likely that copper deposition first proceeded through Equation 7.1. The observation is in response to the current density at the scan range of between 20 mV/s to 200 mV/s and at a potential of 0.8 V to – 1.0 V from positive to negative scan direction. The cathodic peak potential (peak B), for the reaction given by Equation 7.2, is – 0.20, - 0.21, - 0.22, - 0.23 V. The increase in peak depth with scan rate suggests that the reaction that has taken place (Equation 7.2) is probably under mass transfer-diffusion control under the experimental conditions. Thus the scan rate had an effect on the positions of peaks and copper electrodeposition.

As shown in peak B, the reduction current appeared at a negative potential. It was very interesting to find that the peak depths increased dramatically with increasing scan rate corresponding to the current density. This result indicates that something was deposited on the electrode. Based on this observed, it is obvious that elemental copper deposited on the cathode electrode increases with the scan rate. So, at a potential lower than – 0.8 V vs. Ag/AgCl the cathodic reaction leading to copper deposition from (peak A→ peak B) can be expressed as:

$Cu(NH_3)_2^+ + e^- \leftrightharpoons Cu + 2NH_3$ E^o = - 0.20 V occurs at a scan rate of 20 mV/s (7.9)

$Cu(NH_3)_2^+ + e^- \leftrightharpoons Cu + 2NH_3$ E^o = - 0.21 V occurs at a scan rate of 50 mV/s (7.10)

$Cu(NH_3)_2^+ + e^- \leftrightharpoons Cu + 2NH_3$ E^o = -0.22 V occurs at a scan rate of 100 mV/s (7.11)

$Cu(NH_3)_2^+ + e^- \leftrightharpoons Cu + 2NH_3$ E^o = - 0.23 V occurs at a scan rate of 200 mV/s (7.12)

Comparison of the observed electrochemical behaviour of the ore leachate in Figure 7.2 is made with that of a synthetic solution of copper ammonium sulphate in Fig. 7.3. The discussion in the next section is about the electrochemical analysis of the synthetic solution and comparison between the electrolytic solutions to establish whether there is any similarity in electro-deposition behaviour between the two or otherwise. It should be noted that the synthetic solution does not contain: Mn, Ni, Co and Zn determined in the ore leachate before and after leaching.

7.4. Copper electrodeposition from copper ammonium sulphate

The electrodeposition behaviour of $Cu(NH_3)_4SO_4$ was investigated under the experimental conditions of: Scan rate 20 mV/s, 50 mV/s, and 100 mV/s and

positive potential of 0.8 V to a negative potential of – 1.0 V. The scan was initiated from the positive cathodic direction to the negative anodic direction (Figure 7.3). The cyclic voltammogram of the synthetic $Cu(NH_3)_4SO_4$ shows a distinct behaviour. A pair of redox peaks is observed for the complex, corresponding to Cu/Cu^{2+} redox couple as indicated by the cathodic and anodic peaks (E and F). The appearance of two peaks instead of four in Figure 7.2 is an indication that the electrodeposition behaviour is different.

7.4.1. Cathodic process of Cu deposition from copper ammonium sulphate

The scans in the cathodic direction revealed a single peak (E) which increases with scan rates. The appearance of the peak suggests that the electroactive copper (II) metal in the complex is reduced to a copper (I)-ammonia complex species (Equation 7.13):

$$Cu(NH_3)_4^{2+} + e^- \leftrightharpoons Cu(NH_3)_4^{+} \qquad (7.13)$$

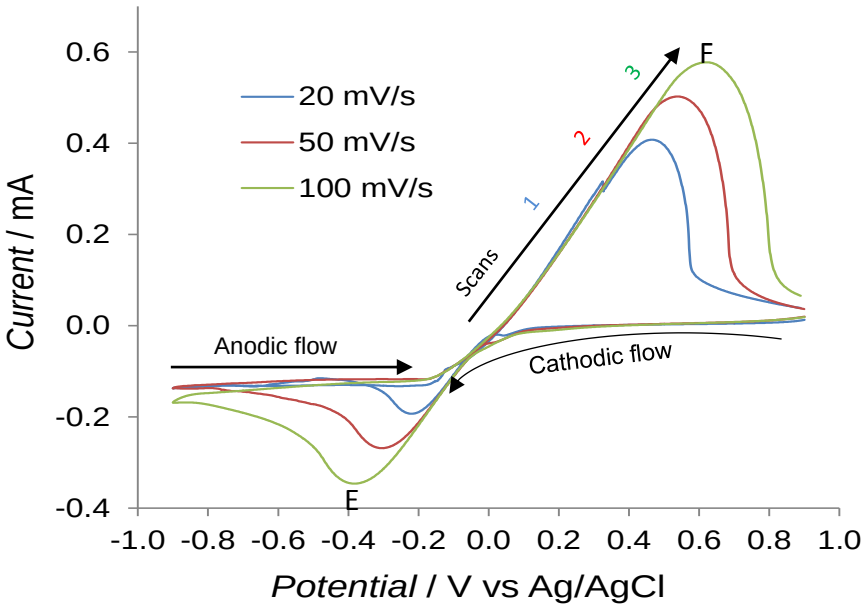

Figure 7.3 Cyclic voltammogram of synthetic $Cu(NH_3)_4SO_4$ electrolyte at different scan rates (Reference electrode Ag/AgCl vs.3 M KCl).

7.4.2. Anodic process of Cu deposition from copper ammonium sulphate

It was found that the anodic scans revealed a single peak (F), signifying the dissolution of copper electrodeposited during the forward potential scan. The observed behaviour is an indication that the copper (II) metal reduced undergoes electron transfer predominantly from the copper ammonia complex. Thus the reduction of Cu^{2+} to Cu metal during the cathodic scan and its oxidation in the reversal potential scan in the anodic direction is a reversible electrochemical reaction as shown in Equation 7.14:

$$Cu(NH_3)_4^{+} + e^{-} \leftrightharpoons Cu + 4NH_3 \quad (7.14)$$

The unique behaviour observed in Figure 7.3 shows that as copper metal is electrodeposited after reduction in peak E, there is also the disappearance of copper in unison in peak F. This behaviour suggests a quasi-reversible deposition/dissolution response of Cu^{+} ions.

Equations 7.13 and 7.14 suggest that $Cu(NH_3)_4^{+}$ is an intermediate species during the reduction of $Cu(NH_3)_4^{2+}$ to copper metal, which proceeds through a ligand-coupled electron transfer reaction and involved the loss of the ammonium ion. This observation corroborates that of Darchen et al. (1997), and Grujicic and Pesic (2005). They observed that the electrochemical reduction of copper can take place without the formation of Cu^{+} complex as in intermediary during the reduction process but involves electron transfer reaction. Pecequilo and Panossian (2010) also used the cyclic voltammetry technique to understand the electrodeposition mechanism of copper from a strike alkaline bath and showed that Cu^{2+} reduction to Cu from HEDP electrodeposition occurs via a direct reduction without formation of a Cu^{+} intermediate. Meng and Bard (2015) stated that the electrochemical reduction of complexes can occur via ligand-coupled electron transfer with loss of ion. This is in line with the observation in this study (Figure 7.3). However, since the synthetic solution contains pure copper, it is suggested that it could be the major cause of the observed electrodeposition behaviour.

7.4.3. Effect of scan rate

As shown in Figure 7.3, it was found that the electrodeposition of copper from a $Cu(NH_3)_4SO_4$ complex occurred at cathodic peak potentials of -0.22 V, -0.30 V, and –0.38 V at scan rates of 20 mV/s, 50 mV/s and 100 mV/s respectively, (peak E). The peak depth and width increased with increasing scan rates as observed for the leachate in Fig. 7.2. This is an indication that the scan rates have a positive effect on the electrodeposition processes. It can be seen also in peak E that the reduction current appeared at a negative potential as it was observed for the ore leachate. This is an indication that the copper metal deposited at the cathode increases with scan rates corresponding to the current density. The cathodic reaction (peak E) leading to copper electrodeposition can be expressed as shown in Equations 7.15 to 7.17:

$Cu(NH_3)_4^{+} + e^{-} \leftrightharpoons Cu + 4NH_3$ E^{o} = -0.22 V occurs at a scan rate of 20 mV/s (7.15)

$Cu(NH_3)_4^{+} + e^{-} \leftrightharpoons Cu + 4NH_3$ E^{o} = -0.30 V occurs at a scan rate of 50 mV/s (7.16)

$Cu(NH_3)_4^{+} + e^{-} \leftrightharpoons Cu + 4NH_3$ E^{o} = -0.38 V occurs at a scan rate of 100 mV/s (7.17)

7.5. Stability of complexes

The stability of the Cu(I) and Cu(II) complex species is responsible for their perceived electrochemical reactions. As such the fundamental reactions of these complex species with regards to the Cu(II)/Cu(I) and Cu(I)/Cu(0) redox chemistry, concentrations and kinetics is dependent on the stability of their complexes and other factors such as pH (Nila and González, 1996a and 1996b). Though this work is not focussed on the stability of complexes, the study involves the analysis of solutions containing copper-complexes. As such their effect on the electrochemical studies was observed not to be of any consequence. It was observed in Chapter 6 that the concentrations of other metals (e.g. Mn, Co, Ni, and Zn) in the leachate were not significant enough to interfere with copper electro-deposition processes. It should be noted that the electrochemical experiment involved sulphate and chloride ions which can form complexes with copper species, which could affect the stability of the Cu(I) and Cu(II)-ammonia species. However, the concentrations of sulphate or chloride ions were much lower than the concentration of ammonia, which readily forms more stable copper complexes than sulphate and chloride ions. Hence, the effect of sulphate and chloride ions on the experiment is considered negligible. This is in line with previous studies by Senanayake (2004) and Black (2006); their investigation indicated that the sulphate and chloride ions in a solution of Cu(I)-ammonia species do not take part in the formation of complexes, but remain as uncomplexed ions while with Cu(II)-ammonia species these ions can form $Cu(NH_3)_4SO_4^0$ and $Cu(NH_3)_4Cl^+$ complexes which share the same λ_{max} with $Cu(NH_3)_4^{2+}$ complex. Therefore, they concluded that it is appropriate to refer to these anions as ion pairs rather than complexes as they do not affect the stability of the Cu(II)-ammonia complex species.

7.6. Electrochemical kinetics

Figures 7.4 and 7.5 can be used to infer the electrodeposition kinetics. The cyclic voltammograms obtained from various scans show that the behaviour of ore leachate and synthetic solution are distinct. The separation between the cathodic peak potential (ΔE_p) peaks B (Figure 7.2), for the reaction given by the Equations 7.9 to 7.12, only increased slightly with the scan rate. The gradual shift of peak potential in cathodic and anodic directions is evidence of reversibility of electrochemical process, as observed for the cathodic peak potential Cu(I)/Cu(0) to a more negative values with increasing scan rates. The cathodic and anodic peak currents from the reversible electrochemical processes were plotted against the square root of potential scan rate and a good linear correlation was obtained. The exhibition of a linear relationship is a clear indication that the reduction of Cu^{2+} to Cu is mainly under diffusion control (Figure 7.4). The higher peak currents and smaller peak width provides further evidence of a highly reversible reaction. Also, the height of the cathodic peaks

(B) and anodic peaks (C) for Cu(I) ⇋ Cu(0) process is directly proportional to the potential scan rate.

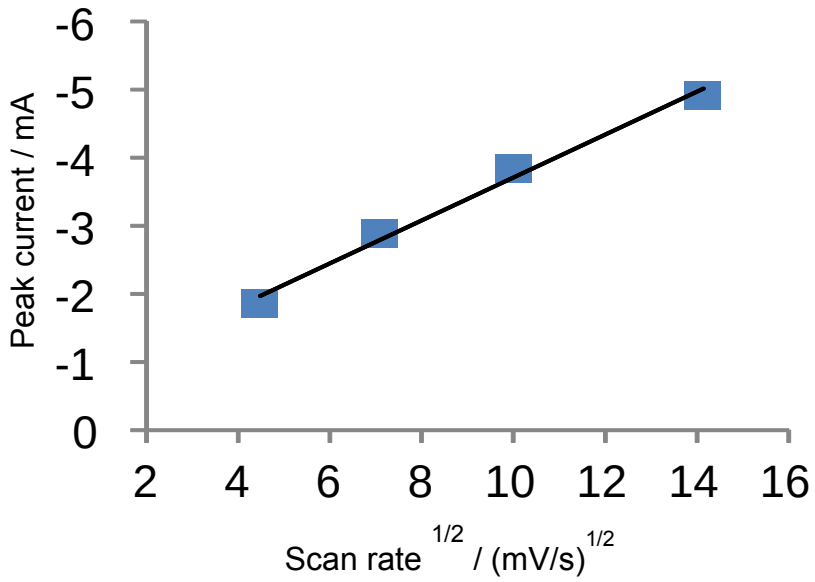

Figure 7.4 Plot of cathodic peak current vs. square root of scan rate for ore leachate

The cathodic and anodic peaks (E and F) for a synthetic solution of $Cu(NH_3)_4SO_4$, which correspond to Cu/Cu^{2+} redox couple as shown in Equations 7.15 to 7.17, appear at -0.22 V, - 0.30 V, and – 0.38 V at the scan rate of 20 mV/s, 50 mV/s, and 100 mV/s respectively, (Figure 7.3). The separation between the cathodic and anodic peak potentials increased with the scan rate, which is characteristic of slow electron transfer kinetic. A linearity dependence on the cathodic current versus square root of scan rate was obtained from a plot of cathodic and anodic peak current versus square root of scan rate (Figure 7.5). The linear relationship between the peak current and the square root of the scan rate is an indication that the reduction of Cu^{2+} ion to copper metal is also a diffusion controlled process. The observation in this study is similar with the one by Grujecic and Pesic (2005), Majidi et al. (2009) and Popescu et al. (2013) which have also shown that the cathodic peak current linearity dependence on the square root of the scan rate is a proof that copper electro-reduction is a diffusion controlled electrochemical process.

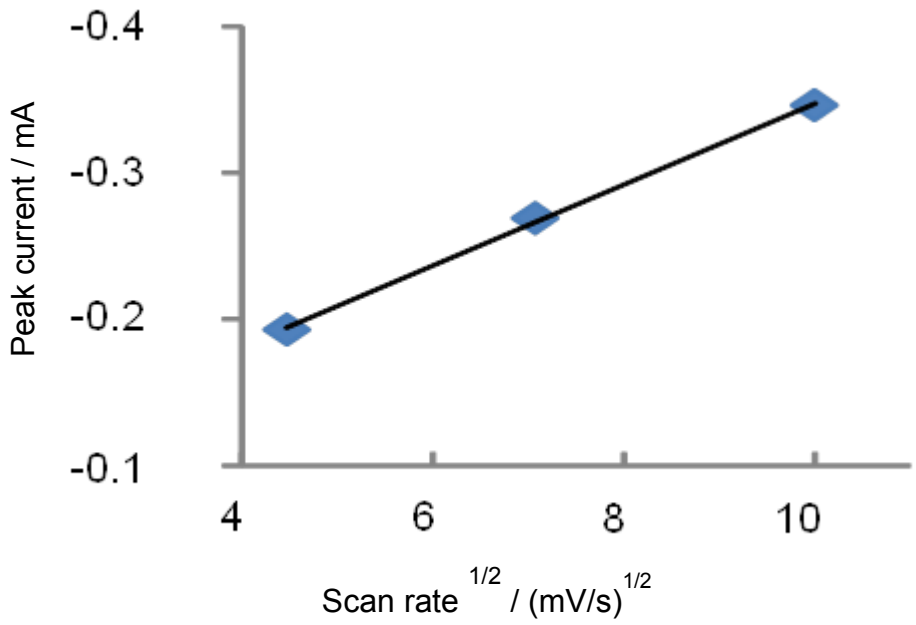

Figure 7.5 Plot of cathodic peak current vs. square root of scan rate for $Cu(NH_3)_4SO_4$ synthetic solution

Therefore, comparison between the two experiments shows that the Cu/Cu^{2+} redox couple in the synthetic solution is a sluggish electron transfer process due to the large separation between the cathodic and anodic peaks while the $Cu/Cu(NH_3)_4^{+}$ redox reaction couple in the ore leachate is more reversible, with fast electron transfer. While only one pair of redox peaks are observed for the $Cu(NH_3)_4SO_4$ solution, this suggests two separate electron transfer reactions attributed to simultaneous cathodic deposition of ionic Cu^{2+} to copper and anodic dissolution of copper to Cu^{2+}. With two pairs of redox peaks observed for the ore leachate, is an indication that reduction of $Cu(NH_3)_4^{+}$ to Cu has higher rate constant compared to the reduction of Cu^{2+} to Cu. As a result, when the peak C increases, peak A which corresponds to the reduction of Cu(II) to Cu(I), also increase continuously (Figure 7.2).

7.7. Conclusion

The cyclic voltammograms provide insight into the electrochemical behaviour of ore leachate after leaching in ammonium chloride solution and synthetic solution of copper ammonium sulphate ($Cu(NH_3)_4SO_4$). The electrodeposition process consists of two reversible electrochemical reactions. The observed behaviour depends on the potential sweep rates as shown in Figures 7.2 and 7.3. From the voltammetric scans, it is clear that the copper reduction and electrodeposition is a stepwise process involving two steps, with the electronation of Cu^{2+} in solution containing the complexing agent. The electrodeposition is an equilibrium reversible electrochemical process whereby

the free Cu^{2+} concentration is in equilibrium with Cu^{+} concentration. It was found that the deposition of copper metal from the ore leachate solution is a two-step process while that of the copper ammonium sulphate proceeds as two separate sequential, single-electron transfer processes. The $Cu/Cu(NH_3)_4^{2+}$ redox reaction taking place during the deposition of copper from the leachate is fast compared to that of the Cu/Cu^{2+} redox reaction in the $Cu(NH_3)_4SO_4$ synthetic solution. The scan rate and oxygen have a positive effect on copper deposition: Oxygen contributes indirectly to the cathodic reaction by regenerating the copper ammine species. It was also shown that the electrochemical reaction on the cathode is based on the potential at which the cathodic current appeared in the cathode, which indicated that the reactions are diffusion controlled. The linearity with the square root of the scan rate obtained for the kinetic analysis is an indication that the electrowinning of copper from the ore leachate and synthetic solution is diffusion controlled mass transfer processes. Although the presence of impurities in the leachate was not significant during the experiment, their presence must be taken into consideration in the development of a hydrometallurgical process with solution recycling to raise the prospect of recovering high purity copper. This could serve as a guide towards determining accurate potentials for copper electrowinning from copper ammonia complexes. The potential for recycling of the leaching solution after electrowinning will reduce the requirement for fresh leaching reagent and hence the cost of processing.

Chapter 8

Application

8.1. Introduction

The development of novel techniques that allow for optimal extraction of low grade ores from their associated gangues has continued to receive attention (Awe, 2013). Ultimately, the target of any processing hydrometallurgist is to explore the application of potential techniques with cost benefits in order to improve copper extraction and its supply to the market. This is because for any processing method to be considered economically viable it has to be one that allows for copper processing at low cost with low complexity in the processing technology and a realistic application for optimal production with increase in the economic value of Cu. In order to reduce the cost of energy during ore crushing and grinding, enhance Cu recovery from leachate as well as mitigate challenges arising from emission of noxious gases during copper processing, a novel copper processing method was adopted in this present research. It is based on the application of selective leaching of Cu from high gangue pre-concentrated and classified ores, and electrochemical analysis of ore leachate for electrowinning. Although quite a number of copper processing technologies are already in existence, the impetus of this research is to improve existing techniques in order to attain sustainable and optimum copper processing.

Successful implementation of the current copper processing technology based on NIR pre-concentration and classification of ores, selective leaching and electrowinning will lead to economic improvement in copper processing from high gangue and low grade copper ores. The major problem of processing low grade ores stems from the high cost of reagent chemicals and the leaching of undesirable metals into the leachate, which usually add more cost in the downstream Solvent Extraction (SX) stage. Since the process of copper recovery depends on so many processes ranging from ore pre-concentration, crushing, grinding, sieving, leaching and electrowinning, an integrated process is considered noteworthy. The pre-concentration process and alkaline leaching of classified ore in copper processing has some advantages. Some of the benefits include reduced reagent cost and efficient processing of copper from high calcite and silicate ores. In addition, since copper ores containing valuable minerals have to be liberated to release the valuable metal, the balance between the best size fraction for leaching and grinding cost has to be made. This is on the basis that crushing and grinding takes about half of the cost of processing (Wills, 2011). It should be noted that if the copper minerals are interlocked with gangue in the ore, this will interfere with leaching as was observed in Figure 4.21. One of the best approaches is to determine the texture of the minerals, size, and shape and liberation sizes in order to optimise the leaching process. This can only be achieved through crushing, grinding and

sieving to the optimum size fractions to improve the leaching kinetics. Against this backdrop, this chapter aims to discuss the application of the processes adopted in this study for copper processing ranging from NIR pre-concentration and classification, selection of appropriate lixiviant for leaching and implication of calcite toward chemical consumption in the classified ore.

There is a constant search for an improved flowsheet. The hydrometallurgical flow sheet developed from this research work is based on three routes identified for leaching of the classified ore, with different approaches identified for reducing the cost of leaching chemicals at different stages of processing on the basis of the copper and gangue content in each category. In summary, the application considers pre-concentration, particle size requirement for leaching and implications of calcite in the classified ore.

8.2. Process description and selection process criteria for flow sheet development

The aim of any copper processing, regardless of the method, is to separate copper ore into valuable product and waste (Wills and Napier-Munn, 2006). It is important to assess the economic viability of every stage of copper processing. This is essential before any consideration can be made particularly with regards to the process parameters and process design. Marsden (2008) highlighted some of the factors for the selection process to include: copper ore mineralogy, associated gangue types, copper ore grade, metal recovery (copper and by-products), processing cost, throughput and environmental concerns. In this research the hydrometallurgical flow sheet is designed to meet the requirement for agitation leaching because this is considered suitable for processing of the classified ore based on the results presented in chapters 4, 5, 6 and 7.

A number of critical processing stages considered important for good projection of the process design have been selected. Results of all the operating parameters and process analysis of all the different stages of the classified ore processing, ranging from ore crushing, grinding, leaching and electrochemical studies, were considered for a proper analysis and accurate estimation of the cost advantages of the proposed hydrometallurgical flow sheet. The advantages and in some instances the considerations of the processing stages such as ore crushing and reagent effectiveness are discussed. The bases of consideration of processes include calcite consumption by chemicals as well as the benefits of integration of pre-concentration. In order to arrive at the process development, a wide range of tests and analyses were carried out to provide information about the relationship between parameters such as particle size versus copper extraction and time. Optimization of variables discussed in the preceding chapters is a requirement for better extraction of copper during leaching as considered in the flow sheet design. It should be noted that the economic recovery of copper is not limited to only the cost of chemicals but on

other variables such as grinding cost, and the amount of gangue in the ore. Hence, the flowsheet is geared towards improving the processing of copper from low-grade Cu ore. The following selection criteria are discussed as part of the process analysis and development: NIR pre-concentration, grinding and chemical consumption by calcite.

8.2.1. Pre-concentration process

Pre-concentration of copper is an evolving method used for discrimination gangues from ore minerals, where waste material is rejected prior to further processing (Murphy and Damingo, 2012).The aim of copper processing, regardless of the method, is to separate copper from copper ore into valuable product and gangue waste (Will and Napier-Munn, 2011). The ore samples used in this work have been pre-concentrated and classified by Iyakwari (2014). The process is considered vital in this research as one of the steps towards upgrading the ore and reducing the quantity of overall waste material prior to the leaching stage. Details of the pre-concentration and classification process can be found in Iyakwari (2014). It was observed that the classification of the ore was responsible for the variation in copper leaching obtained. Based on that the waste category could not be leached as it would lead to wastage and high consumption of chemicals, in other words there may not be the need to subject the waste to subsequent stages of crushing and grinding and leaching. The benefits of this to the leaching stage are that the cost of grinding undesired portion is minimised if not completely removed. Because each category of the ore classified can be treated or considered on the basis of economic importance for leaching with regards to acid consumption. As such only samples that will lead to high copper recovery with minimal acid consumption are considered realistic (product and potentially middling). Integration of the pre-concentration stage where ore is classified according to gangue and copper content into the design for leaching application is considered a very important requirement toward minimizing the cost of leaching chemicals. By extension, three processing routes have been identified which when applied separately for leaching and solvent extraction of the product, middling and waste categories of the classified ore, result in optimum Cu extraction.

It is imperative to state that the application of the classified ore processing starts with NIR pre-concentration and classification. Thus, each category is considered separately. The application of this technology for copper processing cannot be carried out without integrating other components such as comminution before copper leaching. The mineralogical and chemical analysis of the classified ore allows for the development of this concept. As earlier discussed in chapter 4, the classified copper ores have varying concentration of copper and other metals as well as gangue contents. The contrasting leaching behaviour in the pre-concentrated ores was what informed the basis of developing three routes for application. The variation in the rate of copper

extraction in the three categories is an indication of the variation in leaching chemical requirement. Implementation of three routes for treating the ore means effectively reducing the amount of acid-consuming gangue and other unwanted materials thus extending the amount of chemicals for leaching.

8.2.2. Comminution requirement

Crushing and grinding stage is considered one of the most critical aspects in copper processing. The comminution process constitutes the highly cost-intensive stage of hydrometallurgy (Wills, 2003). However, despite the cost implications of this operation, it is the pivotal preparation stage for downstream ore treatment (Baum and Ausburn, 2011). The need to maximise the best output from copper processing in the present work necessitated the implementation of eco-comminution across the entire hydrometallurgical processing chain. This was carried out by finding a balance between the best size fraction for efficient leaching and the chemical requirement. In addition the implementation of comminution, leaching, solvent extraction and electrowinning as complimentary processes covers for the lost which may be incurred at any particular processing stage. Essentially, employing the best comminution process that offer good liberation size with sufficient surface area for leaching with better copper recovery, while at the same time maintaining a balanced economic process was adopted. It involved rigorous tests on different particle size fractions. According to Dhawan et al. (2012) it is essential to have a balanced particle size analysis before arriving at the most economical size required for better extraction.

A flow diagram depicting a comminution process employed (after Stephen, 2015) before arriving at the desired size fraction for leaching is presented in Figure 8.1.

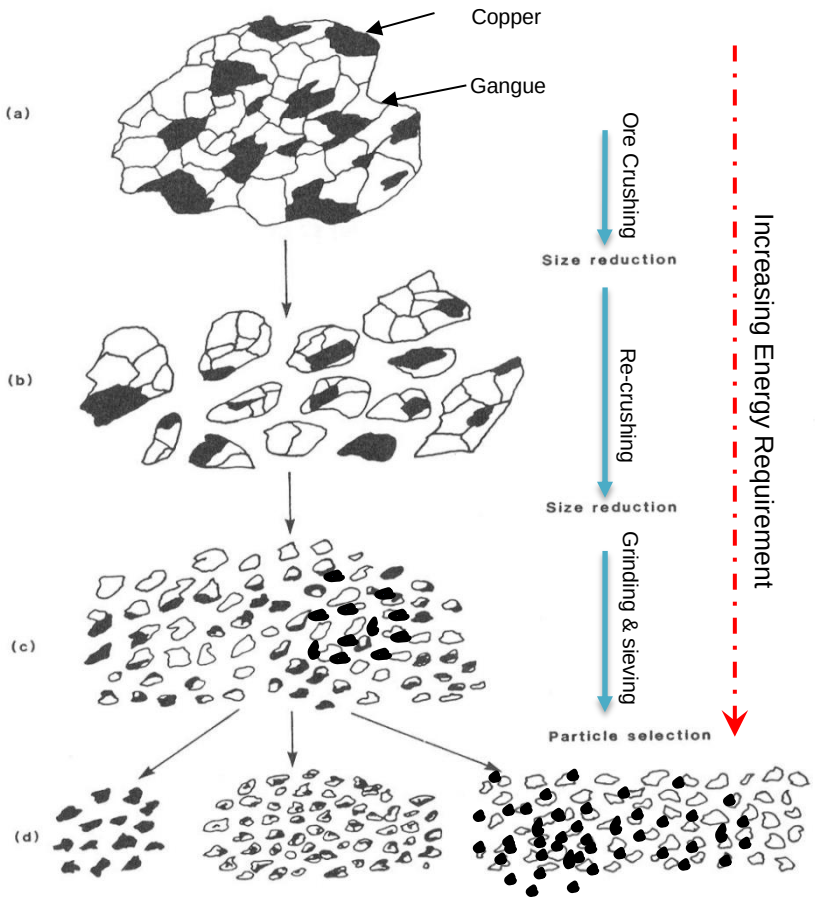

Different size fractions containing copper

Figure 8.1 Flow diagram of copper comminution process, a) bulk ore, b) crushed ore, c) ground ore d) sieved ore (Modified after Stephen, 2015)

It should be noted that the same comminution process was adopted for each category of the classified ore. The implementation of this strategy was based on the information obtained from the scanning electron microscope in chapter 4 which revealed the disseminated nature of Cu in the ore minerals. Based on the results, Cu from copper particles in the ore can only be effectively exposed from the ore matrix by crushing and grinding to fine sizes before subjecting the fractions to leaching. Several tests were conducted with size fractions described in chapter 5 and 6. By optimizing the leaching parameters described in chapter 5 and 6 an economic size fraction was chosen. Since the energy requirement for grinding increases with decreasing particle size during comminution (Figure 8.1), the choice of the fraction that is considered economic in each of the ore categories for leaching was critical for a balanced economic process. As noted in Chapter 6, the finer the size fractions, the better the surface areas for leaching, in this case the -63 + 45 µm fraction. However, finer particle sizes have relatively poor wetting properties, which reduce the leaching efficiency (Awe, 2013). Dhawan et al. (2012) stated that the selection of particle size

fraction that will lead to copper recovery at minimal energy consumption and/or reduced capital expenditure should be considered for application.

Details of the size fraction analysis and development strategy can be found in chapter 5 while details of the optimization process of the parameters stated in the preceding section can be found in chapter 6. Following the results of the leaching on different size fractions described in Chapter 6, the -63+45 µm fraction is considered more economical to leach in the present study because it gave optimum copper leaching in the classified ore. With the same pattern of leaching observed for the classified ore for any successful hydrometallurgical leaching process, it is important to grind the ore to release copper from the ore matrix. It should be noted that finer grinding to lower fractions than -63+45 µm may lead to faster leaching kinetics. With 50% energy cost expended on comminution excluding leaching, and solvent extraction and electrowinning, further crushing to finer size fraction is not required. This corroborates with Wills (2006) and Wills and Napier-Munn, 2011), on comminution cost analysis and implications for copper ore processing. Aside from the process cost associated with the grinding it has been found that finer grinding can lead to slime or dispersion of particles on the surface which may be incurred as losses. Although grinding is considered the most expensive stage due to the intensive energy consumption, the choice of -63+45 µm fraction meets a balanced economic process under the experimental conditions in this research.

Grinding to fractions finer than -63+45 µm could lead to additional cost of processing. Von Essen and Ricks (1999) suggests that grinds coarser than 65 mesh tend to cause excessive abrasion and wear due to the degree of agitation required for suspending the coarser particles. It should be noted that the size fraction considered optimum in this research was based on copper recovery, and as such does not infer or suggest that it is the standard particle size for any agitation leaching design. Therefore, the choice of particle size for analysis or leaching depends on a wide range of factors outlined in the preceding sections.

8.2.3. Leaching

Liberation of copper-containing minerals described in the preceding section was necessary to allow for successful implementation of the third phase (leaching stage). Agitation leaching was considered efficient for the pre-concentrated ore under the experimental conditions in the preceding chapters. For effectiveness of leaching, it was found that agitation leaching is better compared to other leaching methods for extracting copper from the pre-concentrated ore with the aid of the stirrer and aqueous lixiviants. Since leaching the waste is not economical on the basis of the reagent consuming gangue minerals, an alternative method (heap or dump) leaching is suggested. Optimization of the leaching process indicated that apart from the effect of stirring, other parameters have an influence on leaching. Details of influence of the leaching

parameters have already been discussed in chapter 6. Since the mechanism of the process was found to be chemically controlled, the effect of temperature is present. Though the mechanism of leaching in the product and middling was the same, the temperature requirement for the middling is higher. The temperature requirement should be in the range of between 70 to 90 ˚C with moderate stirring speeds of 300 rpm or less. Higher temperatures may lead to excessive heat and loss of liquids and higher cost of energy. As discussed in chapter 6, the rate of copper leaching increases with time. Obviously, due to the nature of the classified ores, ammonium chloride (alkaline lixiviants) is considered to have greater potential for leaching than oxalic acid as was found during the leaching process. The process will be enhanced by longer leaching times.

8.2.4. Calcite versus copper grade in ore fractions and implications for leaching

The relationship between copper grade, calcite and other gangues in the ore fractions was utilised as a criteria for adopting leaching strategy used for treating the ore in this research (Figure 8.3). For any successful leaching operation the choice of the appropriate reagent and amount of reagent required is critical. The choice of NH_4Cl reagent was intended to avoid acid consumption by calcite and the dissolution of other metals during leaching. Ammonium chloride led to efficient copper extraction from the ore. The variation of copper in the three ore fractions and calcite was the major determinant of the choice of selective leaching process. The product is more interesting for leaching than it is for middling and waste fractions due to its higher copper grade. Ammonium chloride is readily recyclable and meets environmental standard regulations on waste disposal, thus reducing costs.

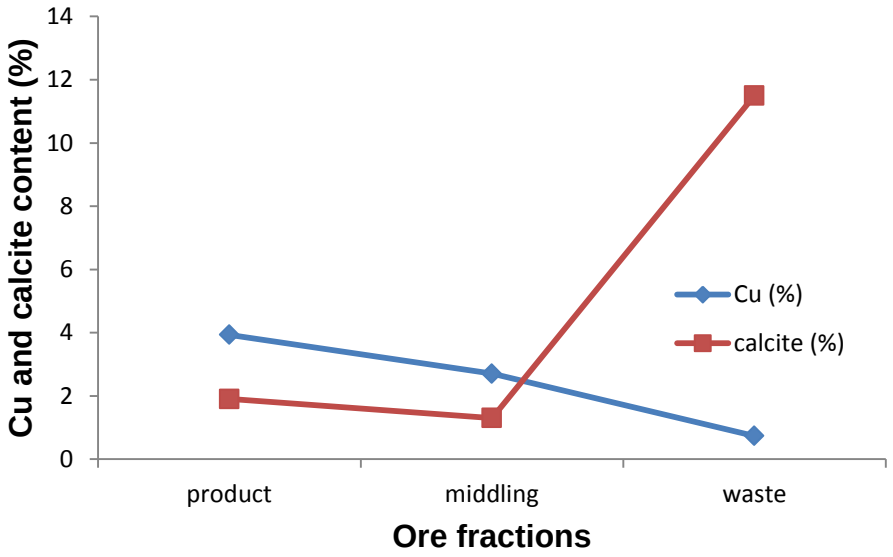

Figure 8.2 Relationship between copper and calcite content in ore fractions

Since, H_2SO_4 is shown to be unselective toward copper it is expected that the application of H_2SO_4 leaching for this ore will be unfavourable from the point of calcite consumption. Besides this, huge cost is also required in running and sustenance of plants operated with sulphuric acid due to corrosion of equipment (Liu et al., 2012). Further to this leaching of the ore with the acid will amount to higher cost of chemicals in the downstream processing due to poor selectivity of the reagent toward copper, which usually leads to the dissolution of other undesirable impurities to the leachate (Liu et al. 2010), as will be discussed in the next section. On the other hand the ammoniacal system has been found to be more selective and efficient for copper extraction (Chmielewski et al. 2009, Künkül et al., 2013).

Another method has been considered for extracting copper from the waste as will be discussed in the next section. Therefore copper would be better extracted from the classified ore fractions using different routes approach and or techniques in order to minimise cost of processing.

8.3. Flow sheet design for leaching application and copper recovery

The hydrometallurgical flowsheet for the processing of the pre-concentrated classified copper ores is presented in Figure 8.3. Discussion in this section is focussed on some selected hydrometallurgical unit operations. The development of the flow sheet is informed based on results obtained in the preceding chapters. The process is a novel technique integrating copper processing units ranging from: NIR pre-concentration of copper ores, classification of the ores, leaching processes of the product and middling and alternative method for processing the waste, solvent extraction of the leachate and electrowinning to obtain copper metal as the final product. Gupta (2003) found that the leaching of soluble copper ores such as chrysocolla can be carried out under Atmospheric Leaching (AL) conditions, with better recovery when compared to High-Pressure Acid Leaching (HPAL).

Habashi (2009) suggested that, for efficient and fast leaching kinetics in AL, the feed grade should have significant copper assay of 0.6 %. With a lower content of other metals (Mn, Zn, Pb, Co), the product fraction was considered for leaching using route 1 in a separate tank because the reagent requirement for both leaching and solvent extraction will be lower compared to the middling and waste fractions. For the middling, the significant content of Fe in hematite and other metals from associated gangues compared to the product results in leaching using route 2, in a separate tank, and as expected the chemical requirement for leaching and solvent extraction will be more significant especially during the solvent extraction stage where removal of co-extracted metals (Fe, Mn, Co, Zn) is required to a higher extent compared to the product, as was found in chapter 6. The waste was very high in both calcite and other associated metals apart from the insignificant copper content, and is considered

problematic for agitation leaching thus an alternative process (heap or dump leaching) is suggested for treating the waste using route 3. The consideration of the waste for processing using heap leaching technique is because it is most suitable method for processing of ores with low copper and high gangue content due to its slow leaching kinetics. Besides that, the waste has a significant proportion of quartz and silicate gangue minerals which can be another source of concern due to the dissolution of silicon from the ore and other fine silica particles. Leaching of ores with significant quartz in alkaline media is better due to the less aggressive nature of the lixiviant; as a result the dissolution of silica is quit slow in alkaline environment (Raghavan and Gajam, 1986). Crushing of the waste ore is not required before heap leaching as such energy cost is minimised.

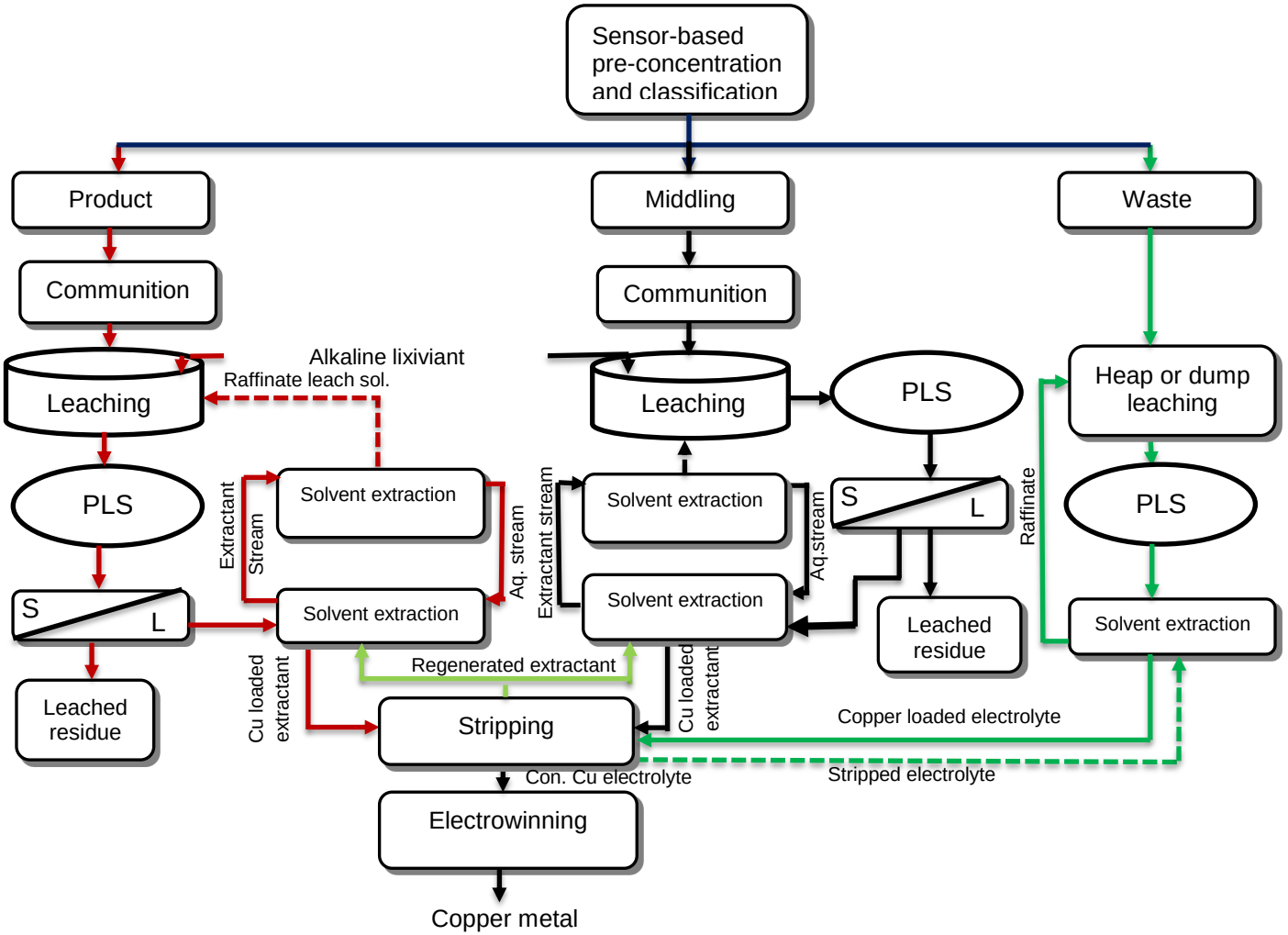

Figure 8.3 Hydrometallurgical flow sheet for treating NIR pre-concentrated classified copper ore

The presence of silica in the copper leach solution can cause difficulties in the downstream solvent extraction circuit. This difficulty may arise from the formation of slime which stabilizes emulsion thereby slowing down phase separation and or the dissolved particles which precipitate and polymerizes as chains of colloidal siloxane according to Equation 8.1 after Littlejohn (2007):

$$Si(OH)_4 + (H_4SiO_4)_{n-1} \rightarrow (H_4SiO_4)_n \quad (8.1)$$

With the NH_4Cl lixiviant the silica content, undesirable metals, calcite and other gangues that would have impacted on the other components of processing were minimised. The leaching results indicated that ammoniacal alkaline is better suited for processing the ores due to their advantages such as environmental friendliness, low consumption by calcite and amenability to electrowinning and regeneration as was found in this study. The benefits of these lixiviants is their selectivity for copper as indicated from the examination of the residue where the undesirable metals were only detected in trace amounts when compared to the head grade (chapter 6). Limpo et al. (1992) indicated the possibility of regeneration of ammonia from pregnant leachate as was obtained in the present study. As found in chapter 6, for effective and efficient leaching of copper from the pre-concentrated ore, it is necessary to grind the ore to fine particle sizes before subjecting them to leaching. This is in line with observation by Awe (2013) and Baba et al. (2014). It is important to state that the leaching rate can be improved greatly in the circuit with adequate supply of temperature while increasing the temperature is necessary to maintain high extraction of copper as was found from the kinetic analysis (chapter 6). One of the novelties of the design is that copper ores can be leached according to copper grades, followed by solvent extraction separately with a common integrated electrowinning stage for copper recovery. This will allow optimal extraction of Cu with cost benefits.

8.3.1. Implication of undesirable elements at the solvent extraction stage

The application of the leaching strategy adopted in this work is effective in reducing the co-dissolution of metals with copper. The discussion in this section explores the implications of some metals in the downstream processing after leaching and to further understand why it is necessary to have them removed or minimised by adopting the strategy of selective leaching. Hematite and other iron bearing minerals such as chlorites are a rich source of iron. Especially ferric iron has a negative impact during solvent extraction (Jansen and Taylor, 2003). The authors indicated that acid consumption is proportional to the wt-% of the metals leached with the consumption increasing over longer leaching period.

Leaching experiments revealed that, in terms of co-extraction of Mn, Ni, Co and Zn in the leachate, the middling had higher concentration than the product. With a slightly higher concentration of the metals in the middling, leaching will require

more solvent extraction and chemicals during the process. It has been found by Liu et al. (2011) that the co-extraction of Fe and Mn presents severe problems during downstream processing of a mixed pregnant solution. Co-deposition of Fe, Mn and other metals with Cu usually leads to the production of inferior-quality cathode (Ntengwe et al, 2010). The result found in chapter 4 indicated very significant concentrations of the Fe metal in the middling due to high hematite content. Therefore the pregnant leach solution from the three processing stages (product, middling and waste leaching) has to be subjected to one or more separation steps to remove elements (Fe, Mn, Ni, Co, Zn) prior to electrowinning.

The control of Fe/Mn and other metals during leaching and solvent-extraction before the electrowinning (SX-EW) circuit is necessary to avoid, oxidation of the metals in the electrolyte to a higher valence state. For instance, Mn (II) can be oxidized to Mn (III), Mn (IV), and or Mn (VII)). The oxidation process usually leads to lower current efficiency of the EW operation. Apart from the loss of energy the side reactions are also responsible for the lowering of the conductivity of the electrolyte (Littlejohn, 2007). This will not only lead to a poor copper cathode but an increasing cost of electrowinning (Awe, 2013). Although the selective leaching process adopted in this research was efficient in minimising the passage of these metals and silica to the solvent extraction stage owing to their poor reactivity with the reagent. There is the need to remove their traces in the leachate in the solvent extraction stage. With the variation in concentration of dissolved metals in the leachate (chapter 6), the separation process will differ in terms of reagent requirement and process recovery. Since, this was not carried out in this present study the discussion is for clarity and further recommendation for economic copper recovery.

Several authors (Ferron, 2002; Jha et al., 2001; Ismael and Carvalho, 2003; Zhang and Cheng, 2007) indicated that precipitation of most of these metals ions, M^{n+}, from leachate can be carried out in alkaline media using sodium hydroxide, as described in Equation 8.2:

$$M^{n+} + nOH^{-} \rightarrow M(OH)_n\ (s) \qquad (8.2)$$

The use of a separate precipitation/solvent extraction circuit for the classified ore will improve the extraction efficiency. Thus, the quality of the electrolyte and final copper metal will be improved in a cost-effective manner at the electrowinning stage. It is on this basis that the flow sheet designed in Figure 8.3 was developed to accommodate the leachabilities of copper in the classified ore, on the basis of Gangue Acid Consumption (GAC) and mineralogical difference in the ores so as to improve preferential leaching of copper and reduction in leaching significant amount of other metals in the process.

8.3.2. Electrowinning

Perhaps this is the final and one of the most important stages of copper hydrometallurgical processing that is concerned with the recovery of copper. Obviously the quality of the final copper metal obtained at this stage is dependent on the entire processing chain starting from pre-concentration, leaching and solvent extraction and purification stages. The result of electro-deposition studies for copper from copper ammonia complexes in chapter 7 indicated that the leaching process was successful with the possibility of recovering copper metal in the leachate. For successful electrowinning of copper from the leachate, the current density and concentration of copper in the leachate are very important. As was found in chapter 7, the deposition process depends on scan rates and current density. The most interesting thing to note from the experimental approach adopted is the minimal interference of undesirable elements during electro-deposition process as a result of insignificant concentration of these undesirable elements in solution. Based on these results, the best approach to obtaining high quality copper cathode is application of integrated approach: NIR sensor-based pre-concentration and classification, comminution (-63 + 45 μm fraction), ammonium chloride selective leaching, solvent extraction for efficient electrowinning. It is worth noting that, in this application, the purified electrolytes obtained after stripping from the three different solvent extractions (product, middling and waste) are connected to a source electrowinning plant where high purity copper metal is recovered. This shows the advantage of reducing the cost of using many electrowinning plants for recovering copper from the three different processing units.

8.4. Merit of the process

For optimal and economic copper ore processing the use of three different routes but that are complimentary for treating the classified ore will ultimately reduce the chemical cost of copper processing (Figure 8.3). Since the hydrometallurgical flow sheet is aimed at mitigating cost at different stages of ore processing, a common stripping plant for handling copper loaded solvent obtained after solvent-extraction from the three routes is proposed to reduce the cost of installing three different stripping plants.

The advantage of leaching the waste using an alternative method is that the process can be integrated with other leaching circuits as outlined for the product and middling (Figure 8.3).

Economic consideration of processes such as crushing and grinding and implication of calcite suggests that the application of the process has the potential for improved copper processing.

The flowsheet is a simplified process for economic copper processing that can be carried out within a time scale. The downstream processing stage further

gives impetus of the simplification in the process due to the integrated unit which can be used to handle or process materials from the three different processing stages. Other advantages of the process include:

1. It is a process design that can be used to handle or process low grade copper ore of different mineralogies with varying concentration of copper and gangue content
2. It is a fast and selective copper leaching process with minimal dissolution of other metals such as Fe, Mn, Zn, Co, Ni which may pose difficulties in the downstream (solvent-extraction and electrowinning) processing.
3. The process is efficient for obtaining high purity electrolyte containing copper for electrowinning.
4. The process has environmental benefits due to the non-emission of noxious gases into the environment and low ecological damage in terms of disposal of the chemicals after usage.
5. Ability to handle difficult impurities and low grade copper ores especially when the ore is a complex one requiring complex chemistry for extraction.
6. It requires low capital cost because it can be implemented at a smaller scale with high prospect of copper production over other processes.
7. The ability to recycle chemicals will serve as a potential source of lixiviants as a cost effective way of leaching of the ore .
8. The leaching of copper according to the pre-concentration and classification has advantages of effectively extracting copper as well as presenting different options depending on the available techniques. The solvent extraction can also be carried out according to leaching route adopted and the amount of undesirable metals in the leachate handled.

However, the process requires careful consideration in these areas:

1. It is limited to NIR pre-concentrated and classified ore and may not be suitable for other types of copper ores.
2. Requires a sensor-based pre-concentration and classification before application of leaching strategy which may not easily or readily be available.
3. Can only be carried out on ores with variable copper grades and gangue contents.

4. Since it requires NIR pre-concentration and classification the application may be limited because of the technology involved.

8.5. Conclusion

A novel integrated process for processing sensor-based pre-concentrated classified copper ores has been developed. Results of the leaching and electrochemical analysis indicated that the process has huge potential benefits for processing of the classified ore at a reduced economic cost. The process depends on prior pre-concentration of the ore before leaching, solvent extraction and electrowinning to obtain high-purity copper metal at the electrowinning stage. The application was informed by the mineralogical and chemical analysis of the ore, which suggests contrasting results in the classified ore. On this basis, the technology considers the metal grades in the ore, calcite and concentrations of other metals in the different classified ore as criteria for developing the strategy. The use of two different chemicals for leaching of the ore indicated that ammoniacal alkaline leaching is the most favoured method that will lead to high recovery of copper and, at the same time, reduces the environmental impact. Though organic acid leaching may be considered, the leaching results obtained with this reagent are poor. The selectivity of the ammoniacal reagent toward copper and the amenability of the reagent for recycling is an advantage because it will lead to reduction in the cost of processing chemicals.

The benefit of the process is that much copper can be leached within low capital operational costs. Similarly, the application of different leaching circuit or tanks would no doubt reduce the cost of chemicals. While the adoption of a separate method for the waste will complement the other processes. The use of a chelating ligand for selective leaching in the design is considered a better option for copper extraction. The process has the capacity to reduce the concentration of some metals such as Fe, Mn, Zn, Co, As, Ni and other ions which would have been found in the recirculation unit that always find their way into the electrowinning process (EW), causing current efficiency loss or poor quality of copper deposit (Badilla and Haussmann, 2013). Another advantage of the use of ligand complex forming agent for leaching is that the process can lead to the control of the effect of some metals such as antimony, arsenic and bismuth whose concentration in significant amounts in leachate solution is known to cause problems in the SX-EW, due to the gradual built up to aqueous entrainment which can affect the quality of the final cathode. Littlejohn (2007) demonstrated that ligand systems have great potentials for maintaining the purity of electrolyte containing these metals.

The concept of having different leaching tanks is informed by the variation in factors such as copper grade, gangue content, acid consumption and impurities contents in the pregnant leach solution (especially iron). It is recommended that

the removal of iron from the leachate be carried out first with much regard to the middling due to their significant concentration in the ore. Some authors (Ferron, 2002; Sole et al., 2005; Hu et al., 2010) have suggested that the removal can be effected by precipitation or alternatively the metal can be removed by solvent extraction. The pregnant leach solution can be subjected to further alkaline precipitation, sulphide precipitation and/or solvent extraction for removal of other metallic components (Zhang and Cheng, 2007; Agarwal et al., 2010). The entire process lies solely on the cost of reagent with efficient capacity for copper leaching. The application of the strategy in this research is only limited to leaching processes as other aspects such as the energy cost of powering equipment were not considered. Further recommendations will be made.

Chapter 9: Discussion

9.1. Introduction

This research was focussed on the chemical investigation of the leaching behaviour of near infrared sensor-based pre-concentrated copper ores. The pre-concentration and classification after Iyakwari (2014) were subsequently investigated using different analytical techniques (PXRF, ICP-MS, SEM and XRD) before subjecting them to series of analysis: titrimetric analysis, leaching studies and electrochemical studies. In each case, the sample categories (product, middling and waste) were investigated separately and collectively, and results evaluated and in some instances compared to account for the variation in behaviour across categories or within size fractions. The research is aimed at seeking alternatives to sulphuric acid leaching by developing a selective process for extracting copper from the classified ore in an environmentally friendly fashion. Finally, it also aimed at identifying a low cost process with minimal chemical costs for leaching the classified ore, as for any hydrometallurgical copper processing the major concern is how to minimise the cost of processing. The basic requirement for efficient and low cost processing of the classified ore has been identified and outlined in this work. It is based on an integrated approach: NIR pre-concentration and classification, selective extraction of Cu in the classified ore, and electrowinning of Cu from the leachate.

9.2. Ore mineralogical and chemical characterization

The classified ore samples were crushed, ground and sieved to obtain different size fractions. Each size fraction was subjected to characterization processes to evaluate both the mineralogical and chemical content using techniques mentioned in the preceding sections. All the results compared well, suggesting a positive correlation in the methods and high precision. The results of the mineralogical and chemical analysis was adapted to ensure better understanding of the ore and to avoid ambiguity during interpretation of results of leaching in chapters 5 and 6. The results indicated variation in both the Cu and gangue contents of the classified ore. Since the product category was found to have a higher copper content than the middling and waste, it was concluded this was probably due to the pre-concentration and classification according to Iyakwari (2014). Hence the findings were expected. The high hematite content of the middling was found to have a masking effect on Cu while the waste fraction, whose content of gangue was significant, was found to correlate with the low Cu content in the fraction. The examination of the ore for liberation analysis revealed that Cu was disseminated in the ore matrix, and in some cases masked by hematite and K-feldspars. Due to the dissemination of Cu in the ore, efficient leaching of the classified ore required it to be crushed and ground to fine particle sizes to expose the metal from the grains. In terms of

the degree of liberation for efficient leaching and Cu extraction, the category with least Cu content is considered more probable. In this case the trend followed the pattern waste > middling > product.

9.3. Laboratory study

To develop an efficient leaching strategy the different classified ore fractions were subjected to a pilot study to investigate the effect of elemental concentration, and to assess the available Cu for leaching in the size fractions by complexometric titration, according to the methods described by Rao et al. (1969), Rao et al.(1994) and Copper determination (2015). The investigation using different particle size fractions of the classified ore indicated that for each of the size fractions the dissolution behaviour differs. The rate of Cu-EDTA complex formed was in consonance with the amount of available Cu for reaction to occur. A higher rate of dissolution was obtained in the – 90 + 63 μm size fraction, this observation suggests that the finer the particle size the higher the rate of Cu dissolution hence better extraction rate. Since the amount of Cu-EDTA complex formed increases with increasing concentration of the chelating reagent with decreasing solid-to-liquid ratio, this shows a correlation in dissolution property of the ores with these parameters. Results of PXRF indicated that the variation of the concentration of metal contents across the different size fractions increases sharply according to the classification from waste to middling to product, as expected. For Cu concentration the increase was from product to middling to waste while for Ca the inverse was observed. The same was noted for Ni and Co elements. Whereas for Mn, K, Si, and Ti the middling have least concentration than the product while the waste have the highest. In general, the Cu content increases with increasing particle sizes from -63 + 45 μm to -180 + 125 μm in the three ore categories. The value of these metals was found to be a reflection of the mineralogy of the minerals bearing them. This compares well with the findings by Glassman and Close (2007) on ore analysis using XRF. A contrasting result was found the analysis with ICP-MS. In this case the metal content appears to increase with decreasing particle size fraction which was consistent throughout the classified ore. Since this technique requires digestion of samples in acids, the rate of metals in solution expectedly was found to relate to the concentration of acids used and target metals made available for determination. In this case, it was the finer size fraction of -45 μm. This agrees with Fletcher (2013) and Jarvis and Jarvis (1992). The results suggest that the variations could be caused by the difference in methods of preparation and measurements. However, a comparative assessment of the results showed high degree of comparison for both analyses.

It is worthy of mention that the results allow for the prediction of the solubility and expected leaching behaviour of Cu with regards to Cu content in the size

fractions. This was considered useful on account of the analytical consideration for the ore leaching studies. A rigorous complexometric test based on these results was carried out bearing in mind that chrysocolla, the major copper bearing mineral, is soluble in both acid and alkaline reagents. Na_2EDTA was used as a titrant over the copper fractions in solution. As stated in the preceding section the calculated values of Cu-EDTA complex formed for each fraction across each category was different on the basis of variation in Cu content. The contrasting result is suggestive of the difference in the rate of copper-EDTA complex formation probably due to available Cu content, particle sizes and concentration of Na_2EDTA titrant. This result is in line with the mineralogical results found for the ores. The ability of Cu to be determined using the complexing agent was based on the reduction of Cu^{2+} state of the metal to Cu+ and Cu^0 by the masking agent, which is in accordance with the findings by Narayana et al. (2000). The variation of the results of Cu-EDTA complex formation in the product, middling and waste compares with the observation by Ata et al. (2001) on factors responsible for Cu dissolution in ores, which include mineralogical difference and metals available for reaction. The increasing rate of Cu-EDTA complex formation with decreasing particle size fractions is believed to be proportional to the Cu content available for reaction with the titrant. This is to be expected since the Cu content in the size fractions and grain sizes differs: hence the chances of Cu-complex formation differed with the classified ore. The difference with size fractions accounted for the differences in dissolution of Cu as a function of reagent concentration. Olubambi et al. (2007) and Crundwell et al. (2013) reported similar observations when considering the dynamics of particle size distribution towards Cu dissolution. Since the least amount of Cu was determined in the waste fractions this was attributed to the high volume of gangue to Cu content compared to the product and middling. High gangue contents in ores are capable of interfering with the dissolution of target metal in ores during leaching, as was the case in the waste category. It was noted that the reactions leading to the formation of Cu-EDTA are surface reaction-controlled: as such gauges in the surface are responsible for reducing the access of reagent by limiting the contact of Na_2EDTA with the Cu found in the ore matrix. This is in accordance with the SEM findings which revealed the fine disseminated property of Cu in the ore. This agrees with Daoud and Karamaner (2006) on the gangue limiting effect on Cu rate of dissolution.

The complexometric analysis was considered indicative for Cu concentration under the experimental conditions investigated. Due to the requirement of readjusting pH and heating, some difficulties were encountered especially with regards to pH adjustment. The same was reported by other researchers, Narayana et al. (2000) and Junar (2014). For a comprehensive understanding of the leaching behaviour of the classified ore only two categories (product and middling) fractions were subjected to further leaching studies to determine the rate of Cu extraction with variation in operating variables. This was based on

the findings on complexometric analysis where the waste was found to show poor results.

9.4. Leaching studies

The leaching studies were focussed on the determination of the effect of operating variables (parameters) on the rate of Cu extraction. The parameters considered include: concentration of NH_4Cl and $H_2C_2O_4$, temperature, particle sizes, solid-to-liquid ratio, and stirring speed. It was found that all the parameters were interdependent. In each case when the effect of one parameter was investigated the others were kept constant. The experiments were initiated in batches ranging from optimization, validation and comparative leaching of the classified ore with two lixiviants. It was found that the leaching process was temperature sensitive because when the temperature was increased from 40 ˚C up to 90 ˚C the rate of Cu extraction consistently increased in all the experiments and in both the ore categories. This underscores the importance of temperature for the leaching process. This observation compared well with the findings by Baba et al. (2013), Awe (2013), Alafara et al. (2015), and Prada et al. (2015). As stated in chapter 6, higher values of Cu extraction were obtained in the product than the middling. The mechanism controlling the leaching process was investigated using the shrinking core model. Results obtained indicated that of all the three models the chemically-controlled model shows a higher correlation coefficient and it was concluded that the reaction was under chemical control. High values of activation energy E_a of 45.9 and 48 kJ/mol determined for the product and 47 and 71 kJ/mol for the middling shows that the rate of reaction was surface reaction controlled. This agrees with results obtained by Alafara et al. (2015) and Prada et al. (2014) thus suggesting that the reaction is probably not under a boundary layer ionic diffusion mechanism. Other researchers, Awe (2013), Baba et al. (2014), also indicated that for leaching of copper ores, where activation energies of higher than 12 kJ/mol are determined, this indicates that the leaching process is chemically-controlled. The variation in E_a value between the product and middling suggests the difference in amount of reagent, temperature or probably variation in interfacial mass transfer during leaching may be due to variation in gangue contents.

Increasing the concentration of NH_4Cl or $H_2C_2O_4$ shows a consistent increase in the rate of Cu extraction at a time of between 2 h to 4 h. The increase in the rate of Cu dissolution reveals the dependence of the process on the concentration of the reagents. Since the rate of extraction was found to follow a similar pattern in both the product and middlings, which is consistent as was also found in the pilot study, it was observed that the behaviour was due to the available Cu for extraction with increasing strength of the reagent. The SCM concept used to investigate the experimental data revealed that the leaching

reaction was the same due the similarity in the rate constants. This was revealed from a plot of the rate constants vs concentration where the dependence of leaching on NH_4Cl was determined. Awe (2013) found a similar trend on the leaching of Sb-bearing Cu ores with estimated rate constants of 2 for two ores investigated under the same experimental conditions.

When the effect of stirring speed was evaluated, more insight into the prevailing leaching mechanism was obtained. A decrease in Cu extraction was observed when the stirring was increased from 300 rpm to 500 rpm and 800 rpm. Since increasing stirring speed is found not increase Cu extraction, the reaction is considered to purely be under a chemically-controlled process. Based on this finding of the effect of stirring speed, it is appropriate to state that intensive stirring is not required for the leaching of the classified ore. The result of this finding agrees with that by Jansz (1984) on the effect of agitation speed on the chloride leaching of zinc-lead sulphide ore.

The results for the effect of particle sizes on leaching showed that Cu extraction increases with decreasing particle size fractions. This is because the crushing of the classified ore to finer size fractions will provide a large surface area for leaching with reagents. The trend was found to be similar in the classified ore. The linearity in the plot of rate constant versus average radius of the particle is an indication of surface chemical reaction. This is considered to be in conformity with the mechanism determined for the leaching process. This observation is in accordance with Baba et al. (2013) and Awe (2013). With solid-to-liquid ratio the increasing rate of Cu extraction appears to correlate with the weight of solid to volume used. However, in each case a balanced solid-to-liquid ratio is required for better leaching of the ore.

The insignificant concentration of these metals: Mn, Co, Ni and Zn determined in the leachate are an indication that the leaching process was selective for Cu thus revealing the potential of the reagent for selective extraction of Cu in the ore. Of all the metals investigated Mn appears to have a higher rate of extraction which correlates to the minerals hosting it. Although higher concentrations of the metals were determined in the middlings, the results show the relationship of the mineralogy of the classified ore and metals concentration. The rate of extraction of metals was found to increase with increasing NH_4Cl concentration. Only a low concentration of other (non-Cu) metals was dissolved in the leachate.

Investigation of the efficiency of NH_4Cl and $H_2C_2O_4$ for Cu extraction and their potential for leaching applications shows contrasting results, with an indication that the rate of Cu extraction in NH_4Cl was much higher than $H_2C_2O_4$. The trend in Cu extraction in $H_2C_2O_4$ revealed that the reagent is less efficient when compared with NH_4Cl. Since the analysis was on the basis of comparison under the same conditions the application of $H_2C_2O_4$ lixiviant is considered unrealistic

and of less potential compared to that of the alkaline lixiviant under the experimental conditions investigated. On this note the focus is on the application of NH_4Cl for the leaching of the classified ore because of its prospect. The better results obtained with NH4Cl is attributed to the presence of chlorides, which are known to be aggressive leaching reagents for Cu and ammonium ion which continuously provides adequate supply of protons as well as producing ammonia needed for copper ammonia complex formation (Limpo et al., 1992). The perceived advantage of the lixiviant is a demonstration of its potentials indicated by Ek et al. (1982). Assessments of the leaching efficiency further revealed that NH_4Cl is a better lixiviant compared to the $H_2C_2O_4$. A percentage extraction of above 45.6 % and 67.3 % possible in the classified ore in the two lixiviants under the experimental conditions investigated, shows that improved Cu extraction can be obtained. Mineral analysis of the residue by XRD showed that the lixiviants appears to be selective for Cu leaching in the classified ore. Most of the minerals were found to be unleached. For example when the profiles of the raw ore and that of the residue were compared the following minerals: quartz, clinochlore, hematite muscovite, orthoclase, and microcline were found to be in abundance even after leaching. Since quartz and hematite were mostly unaffected, this may probably be connected to their poor reactivity toward the lixiviants. A similar observation was made by Baba et al. (2013) on the leaching of copper ore containing abundance of these minerals.

9.5. Electrochemical studies

Electrochemical studies of the copper ammonia complexes formed in the leachate after leaching in ammonium chloride was investigated using the Cyclic Voltammetry (CV) technique and a platinum electrode to understand the reduction and electrodeposition behaviour of the Cu as a potential way of determining the electrowinning potential of Cu in the leachate. A leachate solution obtained after leaching of the products is considered representative of the classified ore due to high Cu content in the fraction. The choice of the product was on the account of the higher Cu extraction rate. Elucidation of the leachate was carried out by first determining the concentrations of metals before subjecting it to CVs analysis. Basically the analysis revealed the half wave potentials of the reduction process of $Cu(NH_3)_4^{2+}$ to Cu occurred step wise according to two step conventional Cu deposition steps. This complies with the results by Majidi et al. (2009) and Beukes and Badenhorst (2009) on the theoretical requirement of Cu electrowinning. Since the rate of Cu deposition was found to increase with an increase in potential (scan rates) across the leachate. It is very clear that the major determinant of the rate of Cu deposition was the change in potential (ΔEp). With each reduction or oxidation step occurring separately, it was found that each of the steps corresponds to a single electron transfer reaction. As for the remarked increase in ΔEp with response to

Cu deposition, this is suggestive of the dependence of Cu electrowinning on the potential as was also found by Koyama et al. (2006). Comparison of the results with that on the electrodeposition of $Cu(NH_3)_4SO_4$ revealed a contrasting electrodeposition behaviour. Unlike the $Cu(NH_3)_4^{2+}$ deposition process from the ore leachate, the $Cu(NH_3)_4SO_4$ deposition process revealed one pair of peaks, although the deposition was also found to occur via a similar two-step process. However, in the case of the $Cu(NH_3)_4SO_4$, it was more of a ligand-coupled electron transfer reaction. The observed peak behaviour indicated a disappearance in Cu deposition due to quasi-reversible deposition/dissolution of Cu ions. This corroborates the finding by Meng and Barth (2015) on the ligand – coupled transfer reactions involving complexes. Pecequilo and Panossian (2010) also indicated the occurrence of reduction of Cu without the formation of Cu+ as an intermediate. This compares well with the results in this study. The perceived behaviour of complexes in solution is in tandem with their stability as described by Nila and Gonzàlez (1996a) and (1996b).

By conducting a cathodic and anodic current plot of the reverse electrochemical reactions against the square root of the potential scan rate, the mechanism of the electrodeposition reaction was obtained. The results of the plot exhibited a linear relationship with a good linear correlation. The linear dependence of the cathodic current versus the square root of the scan rate indicated that the reduction and electrodeposition of Cu from the complexes was diffusion controlled. This compares well with Grijicic and Pesic (2005), Majidi et al. (2009) and Popescu et al. (2013) who indicated that the linearity dependence on the square root of the scan rate on cathodic current density suggests a diffusion-controlled reaction, leading to Cu deposition from copper ammonia complexes. The Cu/Cu^{2+} redox couples in the synthetic solution show a large separation between the cathodic and anodic peaks, indicating it is a sluggish electron transfer process. The $Cu(NH_3)_4^{2+}$ complex in the ore leachate shows smaller separations between the peaks, which are caused by fast electron transfer. This suggests that the likelihood of the electrochemical reaction occurring is higher with complexes in ore leachate than with synthetic complexes. With only one pair of redox peaks in the $Cu(NH_3)_4SO_4$ voltammogram, two separate one electron transfer reactions have taken place during the deposition process, due to simultaneous cathodic deposition of ionic Cu^{2+} to Cu and reversal of the process. As for the $Cu(NH_3)_4^{2+}$, the two pairs of redox peaks are indications that the two complementary reduction/electrodeposition reactions involve two separate single electron reactions.

9.6. Application

Based on the results of the investigation in this research and the analysis of calcite concentration versus copper grade in the ore fractions, a hydrometallurgical flow sheet has been designed with three routes identified for

treating the classified ore according to the differences in Cu and gangue content. Route 1 is designed for processing the product category, route 2 for processing the middling category and route 3 for processing the waste category. The application of eco-comminution agrees with Baum and Ausburn (2011) and Dhawan et al. (2012) as a means of reducing the cost of crushing and grinding.

A lot of research on copper leaching has been carried out with alkaline lixiviants such as NH_3-NH_4Cl, $(NH_4)_2CO_3$, $(NH4)_2SO_3$, $C_2H_3O_2NH_4$, NH_4Cl, NH_4NO_3, Na_2S and NH_3-$(NH_4)_2SO_4$ by Mena and Olson (1985), Ekmekyapar et al. (2003), Bingöl et al. (2005), Wei et al. (2009), Zhao and Liuc (2010), Liu et al. (2012), Ekmekyapar et al. (2012), Haque et al. (2012), Künkül et al. (2013) and Parada et al. (2014). The findings show that the alkaline leaching process leads to less consumption of calcite with minimal co-extraction of metals. However, the drawback is the slow leaching kinetics of the process. Despite the progress made so far no work was found on electrowinning analysis of leachate obtained from pre-concentrated ore in alkaline lixiviant. Also, a review of the literature indicated that the evaluation of sensor-based pre-concentrated copper ores and leaching behaviour of copper according to variation in gangue and copper grade has not being carried out. The novelty of this current work is the leaching of pre-concentrated copper ores and electrochemical analysis of leachate for potential of copper electrowinning. The work is concluded by drawing a hydrometallurgical flowsheet for treating the pre-concentrated ore according to three routes on the basis of variation in of copper grade and calcite content.

It is expected that ammoniacal leaching of secondary copper deposits can also be carried out using the technique developed in this research under certain experimental conditions, stated by Limpo et al. (1999). It was found that the high solubilizing power of chloride is an advantage for its hydrometallurgical treatment of sulphide ores, particularly for complex sulphides. This can be achieved by the addition of chloride-based reagents such as calcium chloride or sodium chloride. NH_4Cl lixiviant used in this research provided adequate supply of chloride ion and NH_4^+ for proton generation required for driving the leaching reaction. This agrees with Limpo et al. (1999) on the potential application of NH_4Cl lixiviant. For effective leaching, the reaction can be carried out in oxidizing leach in a chloride media with oxygen as a oxidizing agent. This is in line with the finding by Baba et al. (2014) on the leaching of complex sulphide ore in an oxygen pressure system.

Complex forming agents such as EDTA and other alkaline reagents have been successfully utilised for the leaching of secondary copper sulphides and primary copper minerals such as chalcopyrite (Tomášek and Neumann, 1982). It is expected that the leaching process developed in this study will be suitable for leaching of other types of ore deposits. However, the leaching rate may be very slow compared to that of porphyry copper oxide deposits which are readily soluble in most solvents due to their hydrophilic nature.

Chapter 10

Conclusions and recommendations

10.1. Conclusions

Investigations of the alkaline leaching of NIR pre-concentrated and classified ore samples have been performed. The mineralogical and chemical content as well as the leaching behaviour of each category (product, middling and waste) was determined separately for evaluation of the rate of Cu extraction and electrodeposition of Cu from the ore leachate. This was achieved using the fraction containing the higher concentrations of Cu after leaching with ammonium chloride (NH_4Cl) as the lixiviant.

Evaluation of the classified ore indicated contrasting behaviour in terms of the mineralogical and chemical content. The product showed a higher content of Cu, consequently the rate of Cu extractions was found to be higher in the product than the middling and the waste. The result was consistent according to the Cu content in the ore category. Generally, the concentration of Cu and rate of extraction with Na_2EDTA is product > middling > waste while with NH_4Cl and $H_2C_2O_4$ it was found to be product > middling. Although the leaching pattern in the product and middling is found to be the same the chemical and temperature requirements were different.

The use of ammonium chloride and oxalic acid for leaching Cu ore was found to be selective for Cu extraction, with low consumption of gangue minerals. Of the three classified ore categories, the product and middling's can be leached using the agitation leaching method whereas the waste can be treated using either heap or a dump leaching method. The agitation leaching can be carried out under a mild stirring speed of between 300 rpm or less. In the presence of increased temperature, the rate of Cu extraction was found to increase. Other useful parameters which led to enhanced rate of Cu extraction include increasing the reagent concentration with decreased particle sizes and a balanced liquid to solid ratio. However, at extended leaching times and low reagent concentration, it is possible to have improved Cu extraction rates. The nature of the ore is responsible for the observed behaviour. Gangue contents of the classified ore led to a decrease in the Cu extraction rate, which varies with concentration in the classified ore composition. To improve the leaching of Cu in the ore gangues and overcome Cu dissemination within the ore matrixes, the classified ore was ground to a size fraction of – 63 + 45 μm.

Comparison of the leaching potential of ammonium chloride and oxalic acid showed that NH_4Cl is a better lixiviant for the extraction of Cu from the classified ore than $H_2C_2O_4$.

Electrochemical studies of the leachate obtained from NH_4Cl leaching revealed the formation of copper ammonia complexes $[Cu(NH_3)_4^{2+}]$. The analysis indicated that the reduction and electrodeposition of Cu from the copper ammonia complexes in the leachate is in accordance with the two step conventional electrowinning of Cu from solution. Comparison of the reduction/electrodeposition behaviour with that of synthetic copper ammonium sulphate $[Cu(NH_3)_4SO_4]$ complex solution suggests different electrochemical behaviour, although the kinetics of reduction and electrodeposition processes in the two complexes are both diffusion controlled. This provided insight into the electrowinning potential of Cu from the ore leachate.

For efficient leaching and the economic enhancement of Cu processing at minimal cost requires the implementation of different strategies to reduce the cost in the different stages: pre-leaching and post-leaching stages. Three processing routes have been developed for processing of the classified ore according to the classification on the basis of chemical requirement for leaching and downstream processing.

1. Route 1: For processing of the product category due the high Cu content, low gangues and concentration of other metals in the ore

2. Route 2: For processing the middling with moderate Cu content, high hematite, metal concentration and gangues

3. Route 3: For processing the waste with higher concentration of gangues, metals and least Cu content.

The three routes for treating the classified ore are complimentary: the leaching stages can be operated independently with a common plant for stripping the Cu loaded extractant and a final stage where the electrowinning of the Cu is carried out. This will lower the financial requirement for establishing multiple plants for handling the different ore categories (product, middling and waste). However, the design is only suitable for processing pre-concentrated and classified ore with variation in Cu and other metal concentrations as well as gangue contents.

10.2. Key findings

The key findings in this research are summarised as follows:

- ✓ The pattern and leaching behaviour of Cu in the classified ore differs according to Cu concentrations in the ores. The rate of Cu extraction correlates with the mineralogical and chemical concentration of each ore category.
- ✓ Low agitation speed, fine particle sizes, increasing temperature, increasing reagent concentration, balanced solid-to-liquid ratio and extended leaching

time are essential requirement for improved Cu extraction in the classified ore.

- ✓ The evaluation of the implication of calcite in the ore fractions for leaching in terms of acid consumption indicated that NH_4Cl is a potential lixiviant both in terms of leaching efficiency and selectivity for copper. When the three fractions are compared, the waste is most unsuitable due the higher calcite and other gangue content.

- ✓ The leaching of Cu from the classified ore using NH_4Cl or $H_2C_2O_4$ indicated that the extraction of Cu was selective and the rate of co-extraction of Mn, Co, Ni and Zn was insignificant. This will greatly reduce the cost of downstream processing of Cu from the leachate.

- ✓ Electrochemical studies of copper ammonia complex $[Cu(NH_3)_4^{2+}]$ in the ore leachate after leaching in NH_4Cl indicated that the electrowinning of Cu from the leachate is possible. The reduction/deposition of Cu from the leachate is in accordance with the conventional two-step electrowinning process. Similar observation was found when compared with synthetic copper ammonium sulphate $[Cu(NH_3)_4SO_4]$.

- ✓ The electrodeposition processes of Cu from the complexes were under diffusion controlled process.

- ✓ Three stages where the cost of processing of the classified ore can be mitigated have been identified: during the crushing stage, leaching stage and post leaching stage.

- ✓ A hydrometallurgical process consisting of three routes for efficient processing of the classified ore at low economic cost have been developed. Each of the processing routes is designed for handling the ores on the basis of variation in Cu and gangue content.

10.3. Recommendations

The following recommendations are made:

- ✓ The leaching studies were carried out on a small scale laboratory test. Therefore, rigorous analysis on extended leaching should be carried out in large scale industrial settings to assess the suitability of the process for Cu extraction from classified ore.

- ✓ More detailed analysis of the ore leachate containing copper ammonia complex after leaching in ammonium chloride should be carried out to investigate further the effect of $Cu(NH_3)_4^{2+}$ concentration, and effect of temperature on the electrodeposition of Cu and constant current

experiments to determine the exact electrowinning current for Cu deposition in the ore leachate.

- ✓ Analysis on the aspect of solvent extraction of Cu from the ore leachate and chemical requirement is recommended.
- ✓ Further leaching tests and analysis is recommended to assess the leaching potential of $H_2C_2O_4$ and Cu electrodeposition process from the leachate and the kinetics of the process.
- ✓ The use of electrodes other than platinum to examine the electrodeposition of Cu is recommended to observe the differences in behaviour.
- ✓ Practical implementation of the design on a large scale is recommended with emphasis on cost analysis of crushing and grinding, and operational cost of the process is recommended.
- ✓ Experiments on the effect of stirring speed lower than 300 rpm should be carried out to further investigate rate of Cu extraction.
- ✓ The flowsheet for processing the classified ore be investigated in a large scale. Attention should also be geared towards identifying solvents with high selectivity for extracting Cu from leachate in the solvent extraction stage.
- ✓ The leaching process with oxalic acid should be investigated further to determine the mechanism controlling copper extraction.

References:

Agarwal, S., Ferreira, A. E., Santos, S. M., Reis, M. T. A., Ismael, M. R. C., Correia, M. J. N., & Carvalho, J. M., 2010. Separation and recovery of copper from zinc leach liquor by solvent extraction using Acorga M5640. *International Journal of Mineral Processing*, *97* (1), 85-91.

Alafara, A. B., Kuranga, I. A., Rafiu, B. B., & Folahan, A. A., 2015. Quantitative leaching of a Nigerian chalcopyrite ore by nitric acid. *Bayero Journal of Pure and Applied Sciences*, *7* (2), 115-121.

Alamiry, M. A., Harriman, A., Mallon, L. J., Ulrich, G., & Ziessel, R., 2008. Energy-and Charge-Transfer Processes in a Perylene–BODIPY–Pyridine Tripartite Array. *European Journal of Organic Chemistry*, *2008* (16), 2774-2782.

Allen, H. E., & Chen, P. H., 1993. Remediation of metal contaminated soil by EDTA incorporating electrochemical recovery of metal and EDTA. *Environmental Progress*, *12* (4), 284-293.

AmmLeach, 2009. Amenability testing of copper oxide ores for First Quantum Minerals Ltd.

An, J. W., Jung, B. H., Lee, Y. H., Tran, T., Kim, S. J., & Kim, M. J., 2009. Production of high-purity molybdenum compounds from a Cu–Mo acid-washed liquor using solvent extraction. Part 2: Pilot and plant operations. *Minerals Engineering*, *22* (12), 1026-1031.

Anderson, J.C.O., Rollinson, G.K., Snook, B., Herrington, R., Fairhurst, J.R., 2009. Use of QEMSCAN® for the characterization of Ni-rich and Ni-poor goethite in laterite ores. *Miner Eng,* 22: 1119-1129

Anderson, K. F. E., 2014. Geometallurgical evaluation of the Nkout (Cameroon) and Putu (Liberia) iron ore deposits, Doctoral dissertation, University of Exeter.

Antonijević, M. M., Dimitrijević, M. D., Stevanović, Z. O., Serbula, S. M., & Bogdanovic, G. D., 2008. Investigation of the possibility of copper recovery from the flotation tailings by acid leaching. *Journal of hazardous materials*,*158*(1), 23-34.

Aravinda, C. L., Mayanna, S. M., & Muralidharan, V. S., 2000. Electrochemical behaviour of alkaline copper complexes. *Journal of Chemical Sciences 112* (5), 543-550.

Arbiter, N., & McNulty, T., 1999. Ammonia leaching of copper sulfide concentrates. *Copper 99 Vol. IV–Hydrometallurgy*, 197-212.

Arbiter, N., & Fletcher, A. W., 1994. Copper hydrometallurgy- evolution and milestones. *Mining Engineering*, *46* (2), 118-123.

Ata, O. N., Çolak, S., Ekinci, Z., & Çopur, M., 2001. Determination of the optimum conditions for leaching of malachite ore in H_2SO_4 solutions. *Chemical engineering & technology*, *24* (4), 409-413.

Awe, S. A., 2010. Hydrometallurgical upgrading of a tetrahedrite-rich copper concentrate. Luleå tekniska universitet.

Awe, S. A., 2013. Antimony recovery from complex copper concentrates through hydro-and electrometallurgical processes. Doctoral thesis, Luleå University of technology, SE-97187 Luleå, Sweden.

Awe, S. A., & Sandström, Å., 2010. Selective leaching of arsenic and antimony from a tetrahedrite rich complex sulphide concentrate using alkaline sulphide solution. *Minerals Engineering 23* (15), 1227-1236

Awe, S. A., & Sandström, Å., 2013. Electrowinning of antimony from model sulphide alkaline solutions. *Hydrometallurgy*, *137*, 60-67.

Aydogan, S., Aras, A., & Canbazoglu, M., 2005. Dissolution kinetics of sphalerite in acidic ferric chloride leaching. *Chemical Engineering Journal*,*114* (1), 67-72.

Baba, A. A., & Adekola, F. A., 2010. Hydrometallurgical processing of a Nigerian sphalerite in hydrochloric acid: Characterization and dissolution kinetics. *Hydrometallurgy*, *101* (1), 69-75.

Baba, A. A., Ayinla, K. I., Adekola, F. A., Bale, R. B., Ghosh, M. K., Alabi, A. G., ... & Folorunso, I. O., 2013. Hydrometallurgical application for treating a Nigerian chalcopyrite ore in chloride medium: Part I. Dissolution kinetics assessment. *International Journal of Minerals, Metallurgy, and Materials,20* (11), 1021-1028.

Baba, A. A., Omipidan, A. O., Adekola, F. A., Job, O., Alabi, A. G., Baral, A., & Samal, R., 2014. Optimization study of a Nigerian dolomite ore dissolution by hydrochloric acid. *Journal of Chemical Technology and Metallurgy*, *49* (3), 280-287.

Badilla, S. J., and Haussmann, F. J., 2013. Recovery of improvements in copper heap leaching by using EMEW® technology, proceedings of copper, Santiago, Chile

Baum, W., & Ausburn, K., 2011. HPGR comminution for optimization of copper leaching. *Minerals and Metallurgical Processing*, *28* (2), 77.

Beukes, N. T., & Badenhorst, J., 2009. Copper electrowinning: theoretical and practical design. *The Journal of The Southern African Institute of Mining and Metallurgy*, *109*, 343.

Bhatti, N. K., Subhani, M. S., Khan, A. Y., Qureshi, R., & Rahman, A., 2006. Heterogeneous Electron Transfer Rate Constants of Viologen Monocations at a Platinum Disk Electrode. *Turkish Journal of Chemistry*, *30* (2), 165.

Black, S. B., 2006. The Thermodynamic Chemistry of the Aqueous Copper-ammonia Thiosulfate System, Doctoral dissertation, Murdoch University.

Bingöl, D., & Canbazoğlu, M., 2004. Dissolution kinetics of malachite in sulphuric acid. *Hydrometallurgy*, *72* (1), 159-165.

Bingöl, D., Canbazoğlu, M., & Aydoğan, S., 2005. Dissolution kinetics of malachite in ammonia/ammonium carbonate leaching. *Hydrometallurgy*, *76* (1), 55-62.

Biswas, A. K., & Davenport, W. G., 2013. Extractive Metallurgy of Copper: International Series on Materials Science and Technology. Elsevier.

Brown, O. R., Wilmott, M. J., 1985. A kinetic study of the $Cu(NH_3)_4^{II}/Cu(NH_3)_2^{I}$ redox couple at carbon electrodes. *Journal of Electroanalytical Chemistry and Interfacial Electrochemistry,* 191 (1), 191-199.

Cao, Z. F., Zhong, H., Liu, G. Y., Zhao, S. J., 2009. Techniques of copper recovery from Mexican copper oxide ore. *Mining Science and Technology China 19* (1), 45-48.

Chander, S., 1991. Electrochemistry of sulfide flotation: growth characteristics of surface coatings and their properties, with special reference to chalcopyrite and pyrite. *International journal of mineral processing*, *33* (1), 121-134.

Chase, K.C., 1980. Leaching and recovering of copper from As-mined materials, Las Vegas Symposium, Las Vegas, 94-103

Chmielewski, T., 2012. Hydrometallurgy in Kghm Polska Miedz SA–Circumstances, Needs and Perspectives of Application. *Separation Science and Technology*, *47* (9), 1264-1277.

Chmielewski, T., Wódka, J., and Iwachów, Ł., 2009. Ammonia pressure leaching for lubin shale middlings. *Physicochemical Problems of Mineral Processing*, *43*, 5-20.

Christian, G. D., 2004. Analytical chemistry. John Wiley and sons.

Cifuentes, G., Hernández, J., & Guajardo, N., 2014. Recovering Scrap Anode Copper Using Reactive Electrodialysis. *American Journal of Analytical Chemistry*, *5*(15), 1020.

Complex formation, 2015. [Online]. Available: http://www.cffet.net/cons/7_Complexes.pdf retrieved [Accessed 12/04/2015]

Copper determination., 2015. [Online]. Available: http://atsherren.faculty.noctrl.edu/chm210/CUEDTA.htm [Accessed 25/03/2013]

Crane, M. J., Sharpe, J. L., & Williams, P. A., 2001. Formation of chrysocolla and secondary copper phosphates in the highly weathered supergene zones of some Australian deposits. *RECORDS-AUSTRALIAN MUSEUM*, *53* (1), 49-56.

Crundwell, F. K., du Preez, N., & Lloyd, J. M., 2013. Dynamics of particle-size distributions in continuous leaching reactors and autoclaves. *Hydrometallurgy*,*133*, 44-50.

Dalm, M., Buxton, M. W., van Ruitenbeek, F. J., & Voncken, J. H., 2014. Application of near-infrared spectroscopy to sensor based sorting of a porphyry copper ore. *Minerals Engineering*, *58*, 7-16.

Darchen, A., Drissi-Daoudi, R., & Irzho, A., 1997. Electrochemical investigations of copper etching by Cu (NH3) 4Cl2 in ammoniacal solutions. *Journal of applied electrochemistry*, *27* (4), 448-454.

Daoud, J., & Karamanev, D., 2006. Formation of jarosite during Fe^{2+} oxidation by Acidithiobacillus ferrooxidans. *Minerals Engineering*, *19* (9), 960.

Davenport, W.G., King, M., Schlensinger, M., Biswass, A.K., 2002. Extractive Metallurgy of Copper, Fourth edition, Elsevier Science Ltd., Oxford, UK.

Demirkıran, N., 2008. A study on dissolution of ulexite in ammonium acetate solutions. *Chemical Engineering Journal*, *141* (1), 180-186.

Dhawan, N., Safarzadeh, M. S., Miller, J. D., Rajamani, R. K., & Moats, M. S., 2012. Insights into heap leach technology. In *SME Annual Meeting*, 967.

Dixon, S., 2004. Definition of economic optimum for the leaching of high acid-consuming copper ores. *Minerals and Metallurgical Processing*, *21*(4), 198-201.

Dorin, I., Diaconescu, C., & Topor, D. I., 2014. The Role of Mining in National Economies. *International Journal of Academic Research in Accounting, Finance and Management Sciences*, *4* (3), 155-160.

Dreisinger, D., & Abed, N., 2002. A fundamental study of the reductive leaching of chalcopyrite using metallic iron part I: kinetic analysis. *Hydrometallurgy*,*66*(1), 37-57

Durance, P., Jowitt, S. M., & Bush, K., 2014. An assessment of portable X-ray fluorescence spectroscopy in mineral exploration, Kurnalpi Terrane, Eastern Goldfields Superterrane, Western Australia. *Applied Earth Science (Trans. Inst. Min. Metall. B)*, *123* (3), 150-163.

Ek, C., Frenay, J., & Herman, J. C., 1982. Oxidized copper phase precipitation in ammoniacal leaching—the influence of ammonium salt additions. *Hydrometallurgy*, *8* (1), 17-26.

Ekmekyapar, A., Oya, R., & Künkül, A., 2003. Dissolution kinetics of an oxidized copper ore in ammonium chloride solution. *Chemical and biochemical engineering quarterly*, *17* (4), 261-266.

Ekmekyapar, A., Demirkıran, N., & Künkül, A., 2008. Dissolution kinetics of ulexite in acetic acid solutions. *Chemical Engineering Research and Design*,*86*(9), 1011-1016.

Ekmekyapar, A., Tanaydin, M., Demirkiran, N., 2012. Investigation of copper cementation kinetics by rotating aluminum disc from the leach solutions containing copper ions. Physicochem. Probl. Miner. Process. 48 (2), 355-367.

Ekmekyapar, A., Aktaş, E., Künkül, A., & Demirkiran, N., 2012. Investigation of leaching kinetics of copper from malachite ore in ammonium nitrate solutions. *Metallurgical and Materials Transactions B*, *43* (4), 764-772.

Electrochemical analyser, 2015. [Online]. Available: https://www.google.co.uk/?rct=j#q=electrochemical+analyser+model+660D [Accessed 25/08/2015]

El-Taher, A., 2012. Elemental analysis of granite by instrumental neutron activation analysis (INAA) and X-ray fluorescence analysis (XRF). *Journal of applied radiation and isotopes,* 70, 350-354

Elsherief, A. E., 2002. The influence of cathodic reduction, Fe< sup> 2+</sup> and Cu< sup> 2+</sup> ions on the electrochemical dissolution of chalcopyrite in acidic solution. *Minerals Engineering*, *15* (4), 215-223.

Engelken, R. D., & Van Doren, T. P., 1985. Ionic Electrodeposition of II–VI and III–V Compounds I. Development of a Simple, Butler-Volmer Equation-Based Kinetic Model for Electrodeposition. *Journal of The Electrochemical Society*, *132* (12), 2904-2909.

Ettel, V. A., Gendron, A. S., & Tilak, B. V., 1975. Electrowinning copper at high current densities. *Metallurgical and Materials Transactions B*, *6* (1), 31-36.

Feeney, R., & Kounaves, S. P., 1999. Determination of heterogeneous electron transfer rate constants at microfabricated iridium electrodes. *Electrochemistry communications*, *1* (10), 453-458.

Ferron, C. J., 2002. The Control of Manganese in Acidic Leach Liquors, with Special Emphasis to Laterite Leach Liquors. Perth, Australia: ALTA.

Filik, H., Çetintaş, G., Avan, A. A., Koç, S. N., & Boz, İ., 2013. Electrochemical sensing of acetaminophen on electrochemically reduced graphene oxide-nafion composite film modified electrode. *Int. J. Electrochem. Sci*, *8*, 5724-5737.

Filippou, D., St-Germain, P., Grammatiko poulos, T., 2007. Recovery of metal values from copper-arsenic minerals and other related resources. Mineral Processing and Extractive Metallurgy Review. 28, 247-298.

Fletcher, W. K., 2013. Analytical Methods in Geochemical Prospecting. Elsevier.

Frantz, R. F., & McNulty, T. P., 1973. Leaching of copper silicate ore with aqueous ammonium carbonate. In *International Symposium on Hydrometallurgy*(pp. 627-644). AIME New York, NY.

Francois-Xavier, P., 2013. Kansanshi mixed ore treatment: Development and optimization. MSc dissertation, University of Exeter, Camborne School of Mines, UK

Fu, W., Chen, Q., Hu, H., Niu, C., & Zhu, Q., 2011. Solvent extraction of copper from ammoniacal chloride solutions by sterically hindered β-diketone extractants. *Separation and Purification Technology*, *80* (1), 52-58.

Gaydon J.W., 2011. The application of a near-infrared sensor to the sorting of minerals. Doctoral thesis Camborne School of Mines, University of Exeter, Penryn Campus.

Gharabaghi, M., Irannajad, M., & Noaparast, M., 2010. A review of the beneficiation of calcareous phosphate ores using organic acid leaching. *Hydrometallurgy*, *103* (1), 96-107.

Giannopoulou, I., Panias, D., & Paspaliaris, I., 2009. Electrochemical modeling and study of copper deposition from concentrated ammoniacal sulfate solutions. *Hydrometallurgy*, *99* (1), 58-66.

Gill, R., 2014. Modern Analytical Geochemistry*:* An introduction to quantitative chemical analysis techniques for Earth, environmental and materials scientists. Routledge.

Glanzman, R. K., & Closs, L. G., 2007. Field portable X-Ray fluorescence geochemical analysis-its contribution to onsite real-time project evaluation. In *Proceedings of Exploration*, Vol. 7, pp. 291-301.

Gordon, R. B., Bertram, M., & Graedel, T. E., 2006. Metal stocks and sustainability. *Proceedings of the National Academy of Sciences of the United States of America*, *103* (5), 1209-1214.

Gordon, R. B., Bertram, M., & Graedel, T. E., 2007. On the sustainability of metal supplies: A response to Tilton and Lagos. *Resources Policy*, *32*(1), 24-28.

Gottlieb, P., Wilkie, G., Sutherland, D., Ho-Tun, E., Suthers, S., Perera, K., Jenkins, B., Spencer, S., Butcher, A., & Rayner, J., 200. Using quantitative electron microscope for process mineralogy applications. *JOM,*52(4): 24-25.

Grujicic, D., & Pesic, B., 2002. Electrodeposition of copper: the nucleation mechanisms. *Electrochimica Acta*, *47* (18), 2901-2912.

Grujicic, D., & Pesic, B., 2005. Reaction and nucleation mechanisms of copper electrodeposition from ammoniacal solutions on vitreous carbon. *Electrochimica acta*, *50* (22), 4426-4443.

Gupta, C. K., 2006. Chemical Metallurgy: Principles and Practice. John Wiley & Sons.

Gupta, C. K., & Mukherjee, T. K., 1990. Hydrometallurgy in Extraction Processes (Vol. 2). CRC press.

Haarberg, G. M., & Keppert, M., 2009. Diffusion Kinetics for the Electrochemical Reduction of Fe (III) Species in Molten NaCl-FeCl3. *ECS Transactions*, *16* (49), 309-315.

Habbache, N., Alane, N., Djerad, S., & Tifouti, L., 2009. Leaching of copper oxide with different acid solutions. *Chemical Engineering Journal*, *152* (2), 503-508.

Habashi, F., 1997. Handbook of Extractive Metallurgy, Volume *2*. Wiley-VCH.

Habashi, F., 1998. Principles of Extractive Metallurgy, Volume 4*.* Amalgam & Electrometallurgy. Métallurgie Extractive Québec.

Habashi, F., 1999. A Textbook of Hydrometallurgy. Métallurgie Extractive Québec.

Habashi, F., 2009. Recent trends in extractive metallurgy. *Journal of Mining and Metallurgy, Section B: Metallurgy*, *45* (1), 1-13.

Haque, N., Bruckard, W., & Cuevas, J., 2012. A techno-economic comparison of pyrometallurgical and hydrometallurgical options for treating high-arsenic copper concentrates. In *XXVI International Mineral Processing Congress, New Delhi, India*.

Havlík, T., 2014. Hydrometallurgy: Principles and Applications. Elsevier.

Hayes, P. C., 2003. Process principles in minerals and materials production, 3rd edition, Hayes Publishing Co., Brisbane, Queensland, Australia

Helle, S., & Kelm, U., 2005. Experimental leaching of atacamite, chrysocolla and malachite: relationship between copper retention and cation exchange capacity. *Hydrometallurgy*, *78* (3), 180-186.

Holliday, R. I., & Richmond, W. R., 1990. An electrochemical study of the oxidation of chalcopyrite in acidic solution. *Journal of Electroanalytical Chemistry and Interfacial Electrochemistry*, *288* (1), 83-98.

Hu, H. P., Liu, C. X., Han, X. T., Liang, Q. W., & Chen, Q. Y., 2010. Solvent extraction of copper and ammonia from ammoniacal solutions using sterically hindered β-diketone. *Transactions of Nonferrous Metals Society of China*, *20* (10), 2026-2031.

Humar, M., Pohleven, F., & Šentjurc, M., 2004. Effect of oxalic, acetic acid, and ammonia on leaching of Cr and Cu from preserved wood. *Wood Science and Technology*, *37* (6), 463-473.

Ikehata, K., Notsu, K., & Hirata, T., 2008. In situ determination of Cu isotope ratios in copper-rich materials by NIR femtosecond LA-MC-ICP-MS. *Journal of Analytical Atomic Spectrometry*, *23* (7), 1003-1008.

International Copper Study Group, 2015. Production trend of copper metal [Online].Available:https://www.google.co.uk/?gfe_rd=cr&ei=nzKoVZHGFObt8wefr4GoDw#q=World+copper+demand [Accessed 17/02/2015].

Ismael, M. R. C., & Carvalho, J. M. R., 2003. Iron recovery from sulphate leach liquors in zinc hydrometallurgy. *Minerals Engineering*, *16* (1), 31-39.

Iyakwari, S., Glass, H. J., & Kowalczuk, P. B., 2013. Potential for near infrared sensor-based sorting of hydrothermally-formed minerals. *Journal of Near Infrared Spectroscopy*, *21*(3), 223-229.

Iyakwari S., 2014. Application of near infrared sensors to minerals pre-concentration. Doctoral thesis Camborne School of Mines, University of Exeter, Penryn Campus

Iyakwari, S. and Hylke, J., 2015. Mineral preconcentration using near infrared sensor-based sorting. *Physicochem. Probl. Miner. Process*, *51*(2), 661-674.

Jansz, J. J. C., 1984. *Chloride hydrometallurgy for pyritic zinc-lead sulfide ores: the non-oxidative leaching route*. Doctoral dissertation, TU Delft, Delft University of Technology.

Jansen, M., & Taylor, A., 2003. Overview of gangue mineralogy issues in oxide copper heap leaching. In *Copper 2003 Conference* p.2.

Jarvis, I., & Jarvis, K. E., 1992. Inductively coupled plasma-atomic emission spectrometry in exploration geochemistry. *Journal of Geochemical Exploration*,*44* (1), 139-200.

JOEL, 1993. Scanning Electron Microscope Instruction Manual (5400LV)

Jha, M. K., Kumar, V., & Singh, R. J., 2001. Review of hydrometallurgical recovery of zinc from industrial wastes. *Resources, conservation and recycling*,*33* (1), 1-22.

John, E.D., 1999. Chemistry of copper leaching. [Online]. Available: http://jedreiergeo.com/copper/article1/Chemistry_of_Copper_Leaching.html. [Accessed 11/05/2015]

Junar Adnan, I. M., 2014. Spectrophotometric determination of some metal ions via complex formation with carboxylated tris (2-amino ethyl) amine chelating agent, MSc thesis Faculty of graduate studies, An-Najah National University, Nablus-Palestine.

Kappes, D. W., 2002. Precious metal heap leach design and practice. *Kappes, Cassiday & Associates, Reno, Nevada*.

Kelm, U., & Helle, S., 2005. Acid leaching of malachite in synthetic mixtures of clay and zeolite-rich gangue. An experimental approach to improve the understanding of problems in heap leaching operations. *Applied clay science*, *29*(3), 187-198.

Khang, S. J., & Levenspiel, O., 1973. The suitability of an nth-order rate form to represent deactivating catalyst pellets. *Industrial & Engineering Chemistry Fundamentals*, *12*(2), 185-190.

Kilbride, C., Poole, J., Hutchings, T. R., Rodriguez-Walters, O., Sinnett, D., & Brunt, A., 2008. Field portable X-ray fluorescence (FPXRF): A rapid and low cost alternative for measuring metals and metalloids in soils. *CL: AIRE Research Bulletin*, (7).

King, M. J., Sole, K. C., & Davenport, W. G., 2011. Extractive metallurgy of copper. Elsevier.

Kordosky, G. A., 2002. Copper recovery using leach/solvent extraction/electrowinning technology: forty years of innovation, 2.2 million tonnes of copper annually. *Journal of the South African Institute of Mining and Metallurgy*, *102* (8), 445-450.

Koyama, K., Tanaka, M., Miyasaka, Y., & Lee, J. C., 2006. Electrolytic copper deposition from ammoniacal alkaline solution containing Cu (I). *Materials transactions*, *47* (8), 2076-2080.

Künkül, A., Gülezgin, A., & Demirkiran, N., 2013. Investigation of the use of ammonium acetate as an alternative lixiviant in the leaching of malachite ore.*Chemical Industry and Chemical Engineering Quarterly*, *19*(1), 25-34.

Lamping, B. A., & O'Keefe, T. J., 1976. Evaluation of zinc sulfate electrolytes by cyclic voltammetry and electron microscopy. *Metallurgical Transactions B*, *7* (4), 551-558.

Lamya, R. M., 2007. A fundamental evaluation of the atmospheric pre-leaching section of the nickel-copper matte treatment process. Doctoral thesis, Stellenbosch, University of Stellenbosch.

Larouche, P., 2001. Minor elements in copper smelting and electrorefining. Master thesis, Mining and Metallurgical Engineering, McGill University, Montreal, Canada.

Levenspiel, O.,1999. Chemical reaction engineering. *Industrial & engineering chemistry research*, *38* (11), 4140-4143.

Liew, F. C., 2015. [Online]. Available: http://www.tes-amm.com.au/downloads/TES-AMM_analysis_pyrometallurgy_vs_hydrometallurgy.pdf, [accessed 6/05/2015]

Limpo, J. L., Figueiredo, J. M., Amer, S., & Luis, A., 1992. The CENIM-LNETI process: a new process for the hydrometallurgical treatment of complex sulphides in ammonium chloride solutions. *Hydrometallurgy*, *28* (2), 149-161.

Littlejohn, P., 2007. Technical Review–Copper Solvent Extraction in Hydrometallurgy.

Liu, W., Tang, M. T., Tang, C. B., He, J., Yang, S. H., & Yang, J. G., 2010. Dissolution kinetics of low grade complex copper ore in ammonia-ammonium chloride solution. *Transactions of the Nonferrous Metals Society of China*,*20* (5), 910-917.

Liu, Z. X., Yin, Z. L., Hu, H. P., & Chen, Q. Y., 2012a. Leaching kinetics of low-grade copper ore containing calcium-magnesium carbonate in ammonia-ammonium sulfate solution with persulfate. *Transactions of Nonferrous Metals Society of China*, *22* (11), 2822-2830.

Liu, J., Wen, S., Liu, D., Lv, M., & Liu, L, 2011. Response surface methodology for optimization of copper leaching from a low-grade flotation middling. *Minerals and Metallurgical Processing*, *28* (3), 139.

Liu, Z. X., Yin, Z. L., Hu, H. P., & Chen, Q. Y., 2012b. Leaching kinetics of low-grade copper ore with high-alkality gangues in ammonia-ammonium sulphate solution. *Journal of Central South University*, *19*, 77-84.

Lou, H. H., & Huang, Y., 2005. Encyclopedia of chemical processing, Doctoral thesis, ed. S. Lee, Taylor & Francis, USA.

Lu, Z. Y., Jeffrey, M. I., & Lawson, F., 2000. An electrochemical study of the effect of chloride ions on the dissolution of chalcopyrite in acidic solutions. *Hydrometallurgy*, *56* (2), 145-155.

Majidi, M. R., Asadpour-Zeynali, K., & Hafezi, B., 2009. Reaction and nucleation mechanisms of copper electrodeposition on disposable pencil graphite electrode. *Electrochimica Acta*, *54* (3), 1119-1126.

Marcus, R., 1968. Electron transfer at electrodes and in solution: Comparison of theory and experiment. *Electrochimica Acta*, *13* (5), 995-1004.

Marsden, J. O., 2008. Energy efficiency and copper hydrometallurgy. *Hydrometallurgy*, 29-42.

Mathews, K.M., 2013. Development of a feasible flowsheet for ammonia leaching of the kansashi high gangue acid consuming copper oxide Ore. Master's thesis Camborne School of Mines, University of Exeter

Meech, J. A., & Paterson, J. G., 1980. The economics of beneficiating copper oxide ores prior to leaching. *Engineering and Mining Journal*, *181*(8), 71-77.

Mena, M., & Olson, F. A., 1985. Leaching of chrysocolla with ammonia-ammonium carbonate solutions. *Metallurgical Transactions B*, *16* (3), 441-448.

Meng, X., & Han, K. N., 1996. The principles and applications of ammonia leaching of metals—a review. *Mineral Processing and Extractive Metullargy Review*, *16* (1), 23-61.

Meng, Y., & Bard, A. J. (2015). Measurement of Temperature-Dependent Stability Constants of Cu (I) and Cu (II) Chloride Complexes by Voltammetry at a Pt Ultramicroelectrode. *Analytical chemistry*, *87*(6), 3498-3504.

Meritxell, S. B., 2009. Recovery of copper from electronic waste, Master of Science thesis, Chalmers University of Technology, Göteborg, Sweden

Merritt, R. C.,1971. Extractive metallurgy of uranium.

Moore, D. M., & Reynolds, R. C., 1989. *X-ray Diffraction and the Identification and Analysis of Clay Minerals* (Vol. 378). Oxford: Oxford university press.

Moskalyk, R.R., Alfantazi, A.M., 2003. Review of copper pyrometallurgical practice: Today and tomorrow, *Minerals Engineering 16*, 893-919.

Murphy, B., van Zyl, J., & Domingo, G., 2012. Underground pre-concentration by ore sorting and coarse gravity separation. In *Narrow Vein Mining Conference.* pp. 26-27.

Nacer, S. N., & Lanez, T., 2013. Calculation of Diffusion Coefficients and Layer Thickness for Oxidation the Ferrocene Derivative in Organic Medium from Rotating Disk Electrode Data. Research & Reviews*: Journal of Chemistry*, *2* (2), 28-32.

Narayana, B., Bhat, N. G., Bhat, K. S., Nambiar, C. H. R., Ramachandra, B., & Joseph, A., 2000. Selective complexometric determination of copper in ores and alloys using 2, 2′-bipyridyl as masking agent. *Microchemical Journal*, *64* (3), 221-225.

Neighbour, M., 2010. Tantalum and niobium mineralogy and recovery from Kaolinised Cornish granite, Doctoral thesis Camborne School of Mines, University of Exeter.

Ni, Y., & Wu, Y., 1997. Simultaneous determination of mixtures of metal ions by complexometric titration and multivariate calibration. *Analytica chimica acta*,*354* (1), 233-240.

Nila, C., & González, I., 1996a. Thermodynamics of Cu H 2 SO 4 Cl− H 2 O and Cu NH 4 Cl H 2 O based on predominance-existence diagrams and Pourbaix-type diagrams. *Hydrometallurgy*, *42* (1), 63-82.

Nila, C., & González, I., 1996b. The role of pH and Cu (II) concentration in the electrodeposition of Cu (II) in NH_4Cl solutions. *Journal of Electroanalytical Chemistry*, *401* (1), 171-182.

Noren, D. A., & Hoffman, M. A., 2005. Clarifying the Butler–Volmer equation and related approximations for calculating activation losses in solid oxide fuel cell models. *Journal of Power Sources*, *152*, 175-181.

Ntengwe, F. W., 2010. The leaching of dolomitic-copper ore using sulphuric acid under controlled conditions. *Open Mineral Processing Journal*, *3*, 60-67.

Ntengwe, F. W., Mazana, N., & Samadi, F., 2010. The Effect of Impurities and Other Factors on the Current Density in Electro-Chemical Reactors. *International Journal of ChemTech Research*, *2* (2).

Ochromowicz, K., Jeziorek, M., & Wejman, K., 2014. Copper (ii) extraction from ammonia leach solution. *Physicochem. Probl. Miner. Process*, *50* (1), 327-335.

Oishi, T., Koyama, K., Konishi, H., Tanaka, M., & Lee, J. C., 2007. Influence of ammonium salt on electrowinning of copper from ammoniacal alkaline solutions. *Electrochimica Acta*, *53* (1), 127-132.

Olubambi, P. A., Ndlovu, S., Potgieter, J. H., & Borode, J. O., 2007. Effects of ore mineralogy on the microbial leaching of low grade complex sulphide ores.*Hydrometallurgy*, *86*(1), 96-104.

Olubambi, P. A., Ndlovu, S., Potgieter, J. H., & Borode, J. O., 2008. Mineralogical characterization of Ishiagu (Nigeria) complex sulphide ore. *International Journal of Mineral Processing*, *87*(3), 83-89.

Oudenne, P.D. and Olson, F.A., 1983. Leaching kinetics of malachite in ammonium carbonate solutions. Metall. Trans., 14B: 33-40.

Osman, A., Nezungai, D., Crundwell, F. K., & Lloyd, J., 2013. Analysis of the Effects of Changes in Operating Conditions on the Agitated Leaching of Copper. The Southern African Institute of Mining and Metallurgy Base Metals Conference.

Padilla, R., Vega, D., & Ruiz, M. C., 2007. Pressure leaching of sulfidized chalcopyrite in sulfuric acid–oxygen media. *Hydrometallurgy*, *86* (1), 80-88.

Padilla, R., Pavez, P., & Ruiz, M. C., 2008. Kinetics of copper dissolution from sulfidized chalcopyrite at high pressures in H_2SO_4–O_2. *Hydrometallurgy*, *91* (1), 113-120.

Padilla, R., Rodríguez, G., & Ruiz, M. C., 2010. Copper and arsenic dissolution from chalcopyrite–enargite concentrate by sulfidation and pressure leaching in H 2 SO 4–O 2. *Hydrometallurgy*, *100* (3), 152-156.

Park, S. M., & Yoo, J. S., 2003. Peer reviewed: electrochemical impedance spectroscopy for better electrochemical measurements. *Analytical chemistry*,*75* (21), 455-A.

Parker, G. K., 2005. Spectroelectrochemical investigation of chalcopyrite leaching. Doctoral thesis Faculty of Science, Griffith University.

Parker, G. K., & Hope, G. A., 2010. A Raman spectroscopic investigation of pyrite oxidation and flotation reagent interaction. *ECS Transactions*, *28* (6), 39-50.

Parker, G. K., Woods, R., & Hope, G. A., 2003. Raman investigation of sulfide leaching. In *Proceedings Electrochemical Society,* Vol. 18, pp. 181-192.

Parada, F., Jeffrey, M. I., & Asselin, E., 2014. Leaching kinetics of enargite in alkaline sodium sulphide solutions. *Hydrometallurgy*, *146*, 48-58.

Peacey, J., & Robles, E., 2004. Copper hydrometallurgy--current status, preliminary economics, future direction and positioning versus smelting. *Trans.Nonferrous Met.Soc. China*, *14* (3), 560-568.

Peacey, J., Xian-jian, G. U. O., & Robles, E., 2004. Copper hydrometallurgy—current status, preliminary economics, future direction and positioning versus smelting. *Transactions of Nonferrous Metals Society of China*, *14* (3), 560-568.

Pecequilo, C. V., Panossian, Z., 2010. Study of copper electrodeposition mechanism from a strike alkaline bath prepared with 1-hydroxyethane-1, 1-diphosphonic acid through cyclic voltammetry technique. Electrochimica Acta 55 (12), 3870-3875.

Pirrie, D., & Rollinson, G.K., 2011. Unlocking the applications of automated mineral analysis. *Geology Today* 27(6), 226-235

Pletcher, D., and Walsh, F. C., 1993. Industrial Electrochemistry, 2nd edition, Blackie Academic and Professional, Glasgow, UK

Popov, K. I., Djokić, S. S., & Grgur, B. N., 2002. Electrodeposition at a Periodically Changing Rate. *Fundamental Aspects of Electrometallurgy*, 145-174.

Popescu, A. M., Cojocaru, A., Donath, C., & Constantin, V., 2013. Electrochemical study and electrodeposition of copper (I) in ionic liquid-reline. *Chemical Research in Chinese Universities*, *29* (5), 991-997.

(Raghavan, S., & Gajam, S. Y., 1986. Application of an enlarging pore model for the ammoniacal leaching of chrysocolla. *Hydrometallurgy*, *16*(3), 271-281).

Ramatsa, I. M., 2012. An investigation into the leaching behaviour of nickel-copper bearing matte, Doctoral thesis.

Rao, T. H., Rao, B. V., & Acharyulu, S. L. N., 1969. Rapid determination of copper in copper ores.

Rao, B. M., Narayana, B., & Bhat, K. S., 1994. Complexometric determination of copper (II) in ores, alloys and complexes using 2-mercaptoethanol as indirect masking reagent. *Microchimica Acta*, *117* (1-2), 109-115.

Reed, S. J. B., 2005. Electron microprobe analysis and scanning electron microscopy in geology. Cambridge University Press.

Revathi, M., Saravanan, M., Chiya, A. B., & Velan, M., 2012. Removal of copper, nickel, and zinc ions from electroplating rinse water. *CLEAN–Soil, Air, Water*, *40* (1), 66-79.

Robben, M., Wotruba, H., Balthasar, D., and Rehrmann, V., 2015. [Online]. Available: http://www.germancolorgroup.de/html/Vortr_09_pdf/b13_robben_farbbv.pdf [Accessed 21/04/2015

Roldan, P. S., Alcântara, I. L., Padilha, C. C., & Padilha, P. M., 2005. Determination of copper, iron, nickel and zinc in gasoline by FAAS after sorption

and pre-concentration on silica modified with 2-aminotiazole groups. *Fuel*, *84* (2), 305-309.

Rubi, J. M., & Kjelstrup, S., 2003. Mesoscopic nonequilibrium thermodynamics gives the same thermodynamic basis to Butler-Volmer and Nernst equations. *The Journal of Physical Chemistry B*, *107* (48), 13471-13477.

Sabba, N., & Akretche, D. E., 2006. Selective leaching of a copper ore by an electromembrane process using ammonia solutions. *Minerals engineering*,*19* (2), 123-129.

Sawada, K., 2014. Competitive world copper concentrate market and implications for Japanese copper industry chain. Conference of Metallurgist Proceedings ISBN: 978-1-926872-24-7

Senanayake, G., 2004. Analysis of reaction kinetics, speciation and mechanism of gold leaching and thiosulfate oxidation by ammoniacal copper (II) solutions. Hydrometallurgy, 75 (1), 55-75.

Seo, S. Y., Choi, W. S., Kim, M. J., & Tran, T., 2013. Leaching of a Cu-Co ore from Congo using sulphuric acidhydrogen peroxide leachants. *Journal of Mining and Metallurgy, Section B: Metallurgy*, *49* (1), 1-7.

Setterfield-Price, B. M., 2013. Electrochemical Reduction of Carbon Dioxide. Doctoral thesis submitted to the University of Manchester, Faculty of Engineering and Physical Sciences

Schwartz, M., 1994. Deposition from aqueous solutions: an overview.*Handbook of Deposition Technologies for Films and Coatings—Science, Technology and Applications, William Andrew Publishing, Noyes*, 506.

Shabani, M. A., Irannajad, M., & Azadmehr, A. R., 2012. Investigation on leaching of malachite by citric acid. *International Journal of Minerals, Metallurgy, and Materials*, *19* (9), 782-786.

Shumilov, V. I., Kucherenko, V. I., Flerov, V. N.,1983. Cathodic reduction of copper (II) ions in concentrated chloride solutions of copper ammonia complexes. Soviet Electrochemistry 19 (12), 1477-1479.

Sokić, M. D., Marković, B., & Živković, D., 2009. Kinetics of chalcopyrite leaching by sodium nitrate in sulphuric acid. *Hydrometallurgy*, *95* (3), 273-279.

Soldenhoff, K. H., 1987. Solvent extraction of copper (II) from chloride solutions by some pyridine carboxylate esters. *Solvent Extraction and Ion Exchange*, *5* (5), 833-851.

Sole, K. C., Feather, A. M., & Cole, P. M., 2005. Solvent extraction in southern Africa: An update of some recent hydrometallurgical developments. *Hydrometallurgy*, *78* (1), 52-78.

Stevanović, Z., Antonijević, M., Jonović, R., Avramović, L., Marković, R., Bugarin, M., Trujić, V., 2009. Leach-SX-EW copper revalorization from overburden of abandoned copper mine Cerovo, Eastern Serbia. *Journal of Mining and Metallurgy, Section B: Metallurgy 45* (1), 45-57.

Stephen, G., 2015. Institute for Mineral and Energy Resources, University of Adelaide.

Stuurman, S., Ndlovu, S., & Sibanda, V., 2014. Comparing the extent of the dissolution of copper-cobalt ores from the DRC Region. *Journal of the Southern African Institute of Mining and Metallurgy*, *114* (4), 347-349.

Tasior, M., Gryko, D. T., Shen, J., Kadish, K. M., Becherer, T., Langhals, H., ... & Flamigni, L., 2008. Energy-and Electron-Transfer Processes in Corrole− Perylenebisimide− Triphenylamine Array. *The Journal of Physical Chemistry C*, *112* (49), 19699-19709.

Tilton, J. E., & Lagos, G., 2007. Assessing the long-run availability of copper.*Resources Policy*, *32* (1), 19-23.

Torma, V., Vidoni, O., Simon, U., & Schmid, G., 2003. Charge-Transfer Mechanisms between Gold Clusters. *European Journal of Inorganic Chemistry*, *2003* (6), 1121-1127.

Tomášek, J., and Neumann, L., 1984. Dissolution of secondary copper sulphides using complex forming agents. (EDTA, EDA). Part I: Covellite dissolution in EDTA and EDA. International journal of mineral processing, 9, 23-40

Townsend, A. T., Miller, K. A., McLean, S., & Aldous, S., 1998. The determination of copper, zinc, cadmium and lead in urine by high resolution ICP-MS. *Journal of Analytical Atomic Spectrometry*, *13* (11), 1213-1219.

Urbano, G., Meléndez, A. M., Reyes, V. E., Veloz, M. A., & González, I., 2007. Galvanic interactions between galena–sphalerite and their reactivity. *International Journal of Mineral Processing*, *82* (3), 148-155.

Uses of Copper, 2015. International Copper Study Group [Online]. Available: https://www.google.co.uk/?gfe_rd=cr&ei=nzKoVZHGFObt8wefr4GoDw#q=World+copper+demand [Accessed 15/02/2015].

Van Der Merwe, R., & Kasaini, H., 2011. Leaching characteristics of copper refractory ore in sulfate media. *Minerals and Metallurgical Processing*, *28*(4), 208-214.

von Essen, J. A., & Ricks, B., 1999. Design agitated slurry storage tanks to minimize costs. *Chemical engineering progress*, *95*(11), 51-55.

Vračar, R. Ž., Vučković, N., & Kamberović, Ž., 2003. Leaching of copper (I) sulphide by sulphuric acid solution with addition of sodium nitrate. *Hydrometallurgy*, *70*(1), 143-151.

Wang, X., Chen, Q., Hu, H., Yin, Z., & Xiao, Z., 2009. Solubility prediction of malachite in aqueous ammoniacal ammonium chloride solutions at 25 *Hydrometallurgy*, *99*(3), 231-237.

Watling, H. R., 2006. The bioleaching of sulphide minerals with emphasis on copper sulphides—a review. Hydrometallurgy 84 (1), 81-108.

Wei, L. I. U., TANG, M. T., TANG, C. B., Jing, H. E., YANG, S. H., & YANG, J. G., 2010. Dissolution kinetics of low grade complex copper ore in ammonia-ammonium chloride solution. *Transactions of Nonferrous Metals Society of China*, *20*(5), 910-917.

Wieszczycka, K., Kaczerewska, M., Krupa, M., Parus, A., & Olszanowski, A., 2012. Solvent extraction of copper (II) from ammonium chloride and hydrochloric acid solutions with hydrophobic pyridineketoximes. *Separation and Purification Technology*, *95*, 157-164.

Will, B.A., 2003. Mineral Processing technology Burlington, Butterworth-Heinmann.

Williamson, B.J., Rollinson, G. and Pirrie, D., 2013. Automated mineralogical analysis of PM10: new parameters for assessing PM toxicity. *Environmental science & technology*, *47*(11), pp.5570-5577.

Wills, B. A., & Napier-Munn, T., 2006. Mineral processing technology: An Introduction to the practical aspects of ore treatment and mineral. Maryland heights, MO: Elsevier science & technology books.

Wills, B. A., 2011. Mineral processing technology: An introduction to the practical aspects of ore treatment and mineral recovery. Butterworth-Heinemann.

World copper demand, 2015. International copper study group, [Online]. Available:https://www.google.co.uk/?gfe_rd=cr&ei=nzKoVZHGFObt8wefr4GoDw#q=World+copper+demand [Accessed 15/02/2015].

World Copper Producers, 2015. United States Geological Survey. [Online]. Available: http://www.copper.org/resources/market_data/pdfs/annual_data.pdf [Accessed 16/02/2015].

Yartaşi, A., & Çopur, M., 1996. Dissolution kinetics of copper (II) oxide in ammonium chloride solutions. *Minerals Engineering*, *9* (6), 693-698.

Yao, S., and Jiang, C., 2014. Modern copper smelting and converting technology applications, development and improvement in China copper industry. Conference of Metallurgist Proceedings ISBN: 978-1-926872-24-7.

You-Cai, L., Wei, Y., Jian-Gang, F., Li-Feng, L., & Dong, Q. (2013). Leaching kinetics of copper flotation tailings in aqueous ammonia/ammonium carbonate solution. *The Canadian Journal of Chemical Engineering*, *91*(4), 770-775.

Youcai, L., Hong, Z., & Zhanfang, C., 2009. Molybdenum removal from copper ore concentrate by sodium hypochlorite leaching. *Mining Science and Technology (China)*, *21*(1), 61-64.

Zhao, G. D., Wu, H. S., Zhang, Y., LIU, Q., 2004. Ammonia leaching of tailings from a copper mine. Nonferrous Metals-Beijing 56 (3), 54-56.

Zhao, G. D., & Liuc, Q., 2010. Leaching of copper from tailings using ammonia/ammonium chloride solution and its dynamics. In *Chemistry and Chemical Engineering (ICCCE), 2010 International Conference on* (pp. 216-220). IEEE.

Zhang, W., & Cheng, C. Y., 2007. Manganese metallurgy review. Part II: Manganese separation and recovery from solution. *Hydrometallurgy*, *89*(3), 160-177.

Zoski, C. G., 2007. Handbook of Electrochemistry. Elsevier. (Ed.)

Appendix 3.1

Step-by-step method for samples preparation and analysis with ICP-MS

A. Head grade and residue analysis

1. 1 g of each particle size fractions – 63 + 45 μm, - 90 + 63 μm or 125 + 90 μm of the classified ore was weight into a 50 ml polyethylene tube.

2. The sample was subjected aqua regia extraction by adding (mixture of 6 mL conc. HCl and 2 ml conc. HNO_3) to the sample. The content was left for 15 minutes at room temperature, followed by boiling in a Digi prep block digester at a temperature of 90 ˚C for 60 minutes. The digested samples were left to cool at room temperature. After cooling, the sample is made up to 50 ml with deionised water and allowed to stand for three days.

3. 1 mL of solution was then taken using a micropipette and a further dilution of 1: 50 was made in 5 % HNO_3 (1 ml sample solution and 49 ml HNO_3)

4. The solutions were then analysed for Cu, Mn, Ni, Co and Zn with an Agilent Technology, model 7700 × ICP-MS.

B. Leaching

1. The sample was weight into a 250 ml reactor containing the lixiviant of pre-determined temperature.

2. The content is heated in thermostatically electric heating mantle equipped with a mechanical stirrer for a time of between 2 h and 4 h. At time intervals of 15, 30, 45, 60, 120, 180, and 240 minutes, 5 ml sample was withdrawn and filtered using Whatman 540 filter paper to obtain filtrate. 5 mL fresh lixiviant was replaced into the reactor immediately to maintain a constant volume of the solution.

3. 1 ml of the filtrate in (2) was taken and 1:50 dilution was made using 50 % HNO_3. The solution were then analysed for percentage extraction of the following metals: Cu, Mn, Ni, Co and Zn from the sampled solution for all the leaching times with ICP-MS Agilent Technology, model 7700.

4. The analyses were conducted at different temperatures. In each case the analyses was repeated for different reagent concentrations, particle size fractions, solid-to-liquid ratio, and stirring speed as discussed in chapter 6.

Appendix 3.2

Step by step method of preparation of standard solutions and complexometric analysis

A. Preparation of 0.01 M, 0.05 M Na_2EDTA and H_2SO_4/HCl aqua regia of standard solutions

1. 3.722 g of Na_2EDTA was accurately weight and dissolved in 1000 ml distilled water to obtained a standard solution of 0.01 M

2.18.6.15 g of Na_2EDTA was also accurately weight and dissolved in 1000 ml distilled water to obtain 0.05 M standard solution

3. Equimolar concentration of 1 M solution of aqua regia, ratio 1: 1(56 ml of H_2SO_4 and 83 ml of HCl acids) were prepared by mixing the two acids.

B. Determination process

1. 1g to 2 g of solid copper ore sample of different size fractions (-90 + 63 μm, -125 + 90 μm or – 180 + 125 μm) was accurately weight and transferred into a 250 ml Erlenmeyer conical flask

2. 20 mL solution of aqua regia mixture in A (3) in the ratio 1: 1 (H_2SO_4 + HCl) was added and the mixture was heated on a hot plate at time of between 20 to 30 minutes.

3. The contents in (2) above was allowed to cool after heating and made to up to 100 ml using distilled water. The solution was rewarmed again for another 10 minute before it was finally cooled to room temperature.

4. After the cooling process was finished the solution in (3) was filtered using Whatman 540 grade filter paper to obtain filtrate for determination of copper

5. 25 ml aliquot of the filtrate was taken and NH_4Cl/NH_3 buffer solution was added in drop-wise until the solution completely turns blue and precipitates which first formed dissolved at a pH range of between 7 to 9.

6. Murexide indicator (2 to 3) drops was added and the content in (5) titrated using EDTA disodium until colour changes from yellow (green) to deep violet. The percentage copper dissolved in the classified ore fraction was calculated using the value of the molarity of Na_2EDTA described in section 3.5.6

Appendix 4.1

Modal mineralogy and result of classified ore

Mineralogical data presented in Appendix 4.1and 4.2 indicated that the main copper-bearing mineral in the ore is chrysocolla, a silicate mineral of secondary origin. Crane et al. (2001) indicated that the mineral chrysocolla is an amorphous (cryptocrystalline) while Mena and Olson (1985) suggested that the hydrous silicate mineral is found in the upper oxidation zones of copper deposits. Mineralogical analysis revealed that the main-copper mineral occurs in association with other copper-bearing minerals such as cuprite and malachite, both of which are present in minute concentration (below 2 wt %). In some of the samples their concentration was found to be below detection limit (0.001 wt %). As suggested by John (1999), the abundance of chrysocolla in the silicate copper deposit may be due to its relative stability in the ore deposits compared to other copper minerals at conditions of oxidizing-moderate pH, where the solubility of silica is near its limit. The stable nature of chrysocolla relative to other secondary copper silicate minerals is predicated largely by the substitution of Mn, Al, Fe and other cations in the chrysocolla structure. In some cases the oxidized copper ore could replace the copper carbonates such as malachite and azurite (Crane et al., 2001).

Contribution of minerals by volume

In terms of contribution by volume, the following samples, 5, 9,14, 15, 16, 17, 18, 19, 20, 21, 22, 23, 25, 26, 27,29, 30, 31 and 32 accounted for the high quartz contents with each having quartz content of above 20% volume per sample. With K-feldspars the significant contribution is from samples 1, 2, 3, 6, 7, 8, 10, 11, 14, 20, 24, 27 and 28 each having concentration above 17%.

Appendix 4.1 Modal mineralogy of Mantoverde copper ore samples (mass %) measured by QEMSCAN®, < 0.01% = not detected (after Iyakwari, 2014)

		Silicates									Oxides	Carbonates			Phosphates	Others (Trace phases)	Total
		Cu-bearing	Non-Cu-bearing									Cu-bearing	Non-Cu-bearing				
		Non-Iron-bearing			Iron-bearing			Non-Iron-bearing			Iron-bearing	Non-Iron-bearing			Iron-bearing	Non-Iron-bearing		
Sample ID	NIR Classification	Chrysocolla	Muscovite	Kaolinite	Biotite	Tourmaline	Chlorite	Quartz	K-feldspar	Plag-feldspar	Hematite	Cuprite	Malachite	Calcite	Ankerite	Apatite		
1	Products	8.33	5.95	0.01	15.54	0.39	8.87	17.69	25.54	0.07	16.63	0.01	0.00	0.01	0.02	0.18	0.76	100.00
2		19.05	3.79	0.01	8.32	0.30	6.68	14.96	26.21	0.03	19.90	0.02	0.00	0.01	0.04	0.27	0.41	100.00
3		21.11	2.96	0.05	4.53	0.04	3.08	18.16	17.87	0.02	31.77	0.01	0.31	0.00	0.00	0.00	0.09	100.00
4		5.14	3.28	0.68	7.30	0.72	5.13	6.84	15.50	0.06	55.32	0.01	0.00	0.00	0.00	0.00	0.02	100.00
5		3.29	5.34	0.00	8.38	0.55	24.87	37.88	13.11	0.17	3.72	0.01	1.00	0.02	0.05	0.73	0.88	100.00
6		1.09	1.00	0.00	15.32	0.13	6.64	9.86	32.42	1.16	10.37	0.04	0.01	17.17	2.88	0.13	1.78	100.00
7		0.15	1.55	0.00	13.01	0.48	8.74	7.46	38.83	0.03	29.03	0.00	0.00	0.01	0.06	0.33	0.32	100.00
8		5.58	0.22	0.00	5.96	0.10	15.76	4.91	38.01	0.00	28.47	0.01	0.00	0.01	0.02	0.16	0.79	100.00
9		7.78	1.62	0.00	5.86	0.13	4.47	15.13	1.32	0.01	62.04	0.03	1.55	0.00	0.01	0.01	0.04	100.00
10	Middlings	9.31	2.67	0.33	5.46	0.18	4.66	13.13	20.65	0.08	43.17	0.00	0.00	0.00	0.00	0.00	0.36	100.00
11		6.92	3.55	0.43	4.90	0.27	3.47	11.19	19.44	0.05	49.74	0.00	0.00	0.00	0.00	0.00	0.04	100.00
12		0.00	2.31	0.02	3.33	0.06	2.99	18.37	11.74	0.30	53.44	0.00	0.00	5.08	2.03	0.00	0.33	100.00
13		1.19	3.73	1.16	6.71	2.40	13.43	16.14	11.15	0.82	43.06	0.00	0.00	0.10	0.05	0.00	0.06	100.00
14	Wastes	0.40	0.12	0.00	9.42	0.06	15.16	38.98	34.25	0.00	0.63	0.00	0.01	0.01	0.00	0.29	0.67	100.00
15		0.45	9.90	0.00	17.70	0.30	5.37	20.54	16.95	1.16	7.13	0.00	0.00	16.28	2.45	0.25	1.52	100.00
16		0.81	1.67	0.00	10.10	0.36	36.47	38.26	10.07	0.05	0.98	0.01	0.14	0.03	0.00	0.24	0.81	100.00
17		0.05	0.05	0.00	1.78	1.13	33.81	57.69	3.13	0.20	0.89	0.00	0.00	0.03	0.01	0.21	1.02	100.00
18		0.36	0.10	0.00	3.36	0.47	17.66	51.90	4.50	0.30	0.51	0.00	0.00	18.81	0.45	0.38	1.20	100.00
19		3.26	4.14	0.00	8.47	0.40	26.35	36.34	14.00	0.15	4.13	0.01	1.20	0.02	0.04	0.46	1.03	100.00
20		0.00	10.55	0.03	5.08	0.44	2.22	25.81	18.98	3.80	0.18	0.00	0.00	28.89	0.27	0.25	3.50	100.00
21		1.64	0.00	0.01	0.84	0.80	35.08	57.24	0.10	0.50	1.03	0.01	0.62	0.05	0.01	0.96	1.11	100.00
22		0.21	14.84	0.02	3.06	0.51	1.27	20.72	11.64	3.51	1.22	0.00	0.00	38.82	0.81	0.27	3.10	100.00
23		0.27	1.62	0.00	5.93	0.36	45.02	30.31	10.25	0.12	4.02	0.00	0.00	0.05	0.03	0.86	1.16	100.00
24		0.00	11.26	0.14	16.28	0.17	5.24	10.64	40.11	0.98	3.05	0.00	0.00	8.01	2.13	0.05	1.94	100.00
25		0.22	0.04	0.00	1.69	0.25	36.54	56.91	2.32	0.05	0.26	0.00	0.00	0.05	0.01	0.35	1.31	100.00
26		2.98	1.65	0.00	7.24	0.06	19.10	21.38	10.43	0.26	3.08	0.23	0.85	27.02	4.10	0.53	1.09	100.00
27		0.02	0.54	0.00	12.15	0.06	16.30	30.12	34.50	0.07	0.73	0.00	0.00	3.78	0.12	0.18	1.43	100.00
28		0.82	0.08	0.00	15.69	0.02	43.83	0.40	35.92	0.00	1.72	0.00	0.00	0.01	0.00	0.21	1.30	100.00
29		0.89	0.06	0.00	1.59	0.94	19.61	72.21	3.80	0.05	0.02	0.00	0.00	0.01	0.00	0.06	0.76	100.00
30		0.27	6.12	0.00	11.81	0.34	4.56	20.31	11.18	1.79	0.43	0.00	0.00	40.52	0.56	0.26	1.85	100.00
31		0.15	0.21	0.00	3.14	0.06	40.72	41.10	1.71	0.05	0.35	0.00	0.00	10.11	0.25	0.65	1.50	100.00
32		0.13	8.37	0.06	3.91	1.82	4.86	31.37	8.74	7.32	0.95	0.00	0.00	25.81	0.51	0.19	5.96	100.00

Appendix 4.2

Modal mineralogy of classified ore functional groups

Functional group is a portion of a molecule that is responsible for the chemical reactivity and characteristic reaction of a compound. Identifications of minerals in a compound can be done by using near infrared spectroscopy (Robben et al., 2015). This is achieved as a result of interactions of the functional groups with absorbed radiation at different frequencies (Zornoza et al., 2008, Iyakwari et al., 2014 and Dalm et al., 2014).

The cumulative average of the functional groups in the minerals in the three categories (product, middling and waste) and calculated values of iron and copper are presented in Appendix 4.2.

Table 4.2 Modal mineralogy of functional groups (after Iyakwari, 2014)

Sample ID	NIR Classification	Hydroxyls								Carbonates			Oxides	Cumulative -OH	Cumulative CO_3^{2-}	Iron	Copper
		Percentage functional groups															
		8.53% -OH	7.84% -OH	26.34% -OH	22.85% -OH	6.61% -OH	20.71% -OH	3.34% -OH	15.38% -OH	27.13% CO_3^{2-}	59.95% CO_3^{2-}	58.14% CO_3^{2-}					
		Muscovite	Biotite	Kaolinite	Chlorite	Tourmaline	Chrysocollla	Apatite	Malachite		Calcite	Ankerite	Hematite				
1	Products	0.51	1.22	0.00	2.03	0.03	1.73	0.01	0.31	0.00	0.01	0.01	16.63	5.82	0.02	13.74	2.83
2		0.32	0.65	0.00	1.53	0.02	3.95	0.01	0.46	0.00	0.00	0.03	19.90	6.94	0.03	15.29	6.46
3		0.25	0.35	0.01	0.70	0.00	4.37	0.00	0.62	0.08	0.00	0.00	31.77	6.31	0.08	22.88	7.33
4		0.28	0.57	0.18	1.17	0.05	1.06	0.00	0.77	0.00	0.00	0.00	55.32	4.08	0.00	39.88	1.75
5		0.46	0.66	0.00	5.68	0.04	0.68	0.02	0.92	0.27	0.01	0.03	3.72	8.46	0.31	6.16	1.70
6		0.09	1.20	0.00	1.52	0.01	0.23	0.00	1.08	0.00	10.29	1.67	10.37	4.12	11.97	9.51	0.41
7		0.13	1.02	0.00	2.00	0.03	0.03	0.01	1.23	0.00	0.01	0.03	29.03	4.45	0.04	22.25	0.05
8		0.02	0.47	0.00	3.60	0.01	1.16	0.01	1.38	0.00	0.00	0.01	28.47	6.64	0.02	22.16	1.90
9		0.14	0.46	0.00	1.02	0.01	1.61	0.00	1.54	0.42	0.00	0.01	62.04	4.78	0.43	44.32	3.55
Cumulative Average														5.73	1.43	21.80	2.89
10	Middling	0.23	0.43	0.09	1.06	0.01	1.93	0.00	1.69	0.00	0.00	0.00	43.17	5.44	0.00	31.12	3.15
11		0.30	0.38	0.11	0.79	0.02	1.43	0.00	1.85	0.00	0.00	0.00	49.74	4.89	0.00	35.55	2.34
12		0.20	0.26	0.01	0.68	0.00	0.00	0.00	2.00	0.00	3.04	1.18	53.44	3.15	4.22	38.28	0.00
13		0.32	0.53	0.31	3.07	0.16	0.25	0.00	2.15	0.00	0.06	0.03	43.06	6.78	0.09	32.51	0.40
Cumulative Average														5.07	1.08	34.37	1.47

Appendix 4.2 Modal mineralogy of functional groups (after Iyakwari, 2014)

Sample ID	NIR Classification	Hydroxyls								Carbonates			Oxides	Cumulative -OH	Cumulative CO_3^{2-}	Iron	Copper
		Percentage functional groups															
		8.53%	7.84%	26.34%	22.85%	6.61%	20.71%	3.34%	15.38%	27.13% CO_3^{2-}	59.95% CO_3^{2-}	58.14% CO_3^{2-}					
		-OH	-OH	-OH	-OH	-OH	-OH	-OH	-OH								
		Muscovite	Biotite	Kaolinite	Chlorite	Tourmaline	Chrysocolla	Apatite	Malachite		Calcite	Ankerite	Hematite				
14	Waste	0.01	0.74	0.00	3.46	0	0.08	0.01	2.31	0	0	0	0.63	6.62	0.01	2.83	0.14
15		0.84	1.39	0	1.23	0.02	0.09	0.01	2.46	0	9.76	1.42	7.13	6.04	11.18	7.2	0.15
16		0.14	0.79	0	8.33	0.02	0.17	0.01	2.61	0.04	0.02	0	0.98	12.08	0.06	5.68	0.36
17		0	0.14	0	7.72	0.07	0.01	0.01	2.77	0	0.02	0.01	0.89	10.73	0.02	4.88	0.02
18		0.01	0.26	0	4.04	0.03	0.07	0.01	2.92	0	11.28	0.26	0.51	7.35	11.54	2.79	0.12
19		0.35	0.66	0	6.02	0.03	0.68	0.02	3.08	0.33	0.01	0.02	4.13	10.83	0.36	6.59	1.81
20		0.9	0.4	0.01	0.51	0.03	0	0.01	3.23	0	17.32	0.16	0.18	5.08	17.47	0.82	0
21		0	0.07	0	8.02	0.05	0.34	0.03	3.38	0.17	0.03	0.01	1.03	11.89	0.21	5.02	0.92
22		1.27	0.24	0.01	0.29	0.03	0.04	0.01	3.54	0	23.27	0.47	1.22	5.43	23.74	1.41	0.07
23		0.14	0.46	0	10.29	0.02	0.06	0.03	3.69	0	0.03	0.02	4.02	14.69	0.05	8.53	0.09
24		0.96	1.28	0.04	1.2	0.01	0	0	3.85	0	4.8	1.24	3.05	7.33	6.04	4.17	0
25		0	0.13	0	8.35	0.02	0.05	0.01	4	0	0.03	0.01	0.26	12.56	0.04	4.62	0.07
26		0.14	0.57	0	4.36	0	0.62	0.02	4.15	0.23	16.2	2.38	3.08	9.86	18.82	5.54	1.71
27		0.05	0.95	0	3.73	0	0	0.01	4.31	0	2.26	0.07	0.73	9.04	2.33	3.23	0.01
28		0.01	1.23	0	10.02	0	0.17	0.01	4.46	0	0	0	1.72	15.89	0	7.36	0.28
29		0.01	0.12	0	4.48	0.06	0.18	0	4.61	0	0.01	0	0.02	9.47	0.01	2.57	0.3
30		0.52	0.93	0	1.04	0.02	0.06	0.01	4.77	0	24.29	0.33	0.43	7.34	24.61	1.74	0.09
31		0.02	0.25	0	9.3	0	0.03	0.02	4.92	0	6.06	0.15	0.35	14.55	6.21	5.27	0.05
32		0.71	0.31	0.02	1.11	0.12	0.03	0.01	0	0	15.47	0.3	0.95	2.3	15.77	1.86	0.04
Cumulative Average														9.43	7.29	4.32	0.33

Appendix 6.1 Optimized operating parameters and conditions for first batch experiment + = optimized parameter

Parameters/conditions	Stirring speed	Temperature	Sol- to-liq. ratio	NH4Cl conc.	Particle size
NH_4Cl (0.5 M)	300 rpm	70 ˚C	1-4g/ 250 ml		−63µm + 45 µm
NH_4Cl (1 M)	+	+	+		+
NH_4Cl (3 M)	+	+	+		+
NH_4Cl (5 M)	+	+	+		+
Solid- to-liquid ratio (1 to 4 g/250 mL	+	70 ˚C		5 M	+
Temperature (40 ˚C to 70 ˚C)	+		1 g/ 250 ml	5 M	+
Particle size (−63µm + 45 µm)	+	+	1 g/ 250 ml	5 M	
Particle size (−90 + 63 µm)	+	+	1 g/ 250 ml	5 M	
Particle size (−125 + 90 µm)	+	+	1 g/250 ml	+	
Stirring speed (300, 500, 800 rpm)		70 ˚C	1 - 4g/ 250 ml	5 M	−63µm + 45 µm

Appendix 6.2 Optimized operating parameters and conditions for second batch experiment + = optimized parameter

Parameters/conditions	Stirring speed	Temperature	Solid-to-liquid ratio	NH4Cl Con.	Particle size
NH_4Cl Con. (0.55 M)	300 rpm	90 ˚C	6 g/250 ml		-63 + 45 µm
NH_4Cl Con. (1 M)	+	+	+		+
NH_4Cl Con. (1.65 M)	+	+	+		+
Solid-to-liquid ratio	+			1.65 M	+
Temperature (70 ˚C to 90 ˚C	+		6 g/250 ml	+	+
Stirring speed		90 ˚C	+	+	+
Particle size	300 rpm	+	+	+	